THE ADIABATIC, EVAPORATING, TWO-PHASE FLOW OF STEAM AND WATER IN HORIZONTAL PIPE

A THESIS

Presented to the

Faculty of the Graduate Division

by

Ralph Webster Pike, Jr.

In Partial Fulfillment

of the Requirements for the Degree

Doctor of Philosophy

in the School of Chemical Engineering

Georgia Institute of Technology

July, 1962

"In presenting the dissertation as a partial fulfillment of the requirements for an advanced degree from the Georgia Institute of Technology, I agree that the Library of the Institution shall make it available for inspection and circulation in accordance with its regulations governing materials of this type. I agree that permission to copy from, or to publish from, this dissertation may be granted by the professor under whose direction it was written, or, in his absence, by the dean of the Graduate Division when such copying or publication is solely for scholarly purposes and does not involve potential financial gain. It is understood that any copying from, or publication of, this dissertation which involves potential financial gain will not be allowed without written permission.

_____

_____

5Δ
12T

THE ADIABATIC, EVAPORATING, TWO-PHASE FLOW OF STEAM AND WATER IN HORIZONTAL PIPE

Approved:

Henderson C. Ward

William M. Newton

Charles W. Gorton

Date Approved by Chairman: August 13, 1962

To my wife

Patricia

for her love, encouragement

and real help.

ACKNOWLEDGMENTS

The author is grateful to his thesis advisor, Dr. Henderson C. Ward for his suggestion of the research work and his helpful suggestions and constructive criticisms as it progressed. The advice given by Dr. William M. Newton and Dr. Charles W. Gorton in their reading of this work is also appreciated.

The invaluable suggestions and aid given the author by Mr. Bert Wilkins, Jr. in the development of the void fraction measurement is gratefully acknowledged. The author appreciates the help of Dr. William F. Atchison and the staff of the Rich Electronic Computer Center for the large amount of computer time used in this study, and to the members of the Chemical Engineering Special Problems Courses who aided in the collection and processing of certain portions of the data.

The author also wishes to express his appreciation to Dow Chemical Company for the Dow Fellowship in Chemical Engineering during the academic years of 1959-1960 and 1960-1961.

TABLE OF CONTENTS

LIST OF TABLES

Tables

LIST OF FIGURES

Figures Page

Figures Page

SUMMARY

Interest in gas-liquid, two-phase flow is evidenced by nine separate literature surveys (3,5,6,7,8,9,10,11,12) of the subject. They cover a spectrum of topics which include flow of nuclear reactor coolants, flow of petroleum in long pipe lines, flow of liquid rocket propellants fuels, and any situation when a liquid and a gas flow cocurrently. At present the only correlations that are available to compute the flow parameters are empirical in nature and provide little insight into the mechanisms which are involved in the flow.

In the general area of two-phase flow, the specific area of interest in this study is adiabatic, evaporating flow of a pure fluid. The two presently accepted methods of predicting two-phase flow pressure drops are the Martinelli-Nelson method (13) and the Homogenous Flow model (14). The accuracy of both these methods is of the order of ± 40 per cent. Attempts have been made to modify these two models individually and also to combine them to better correlate the data in the literature. These attempts have met with only slightly better success than the original models. Also, the data in the literature are meager for adiabatic, evaporating flow. For detailed discussions of this area and two-phase flow correlations in general, refer to the literature surveys by Gresham, et al., (5), Ward, et al., (6), Isben, et al., (3), and Bennett (7).

To consider the adiabatic, evaporating flow of one component, the continuity, momentum and energy equations were written on a differential element of annular, two-phase flow in a manner first suggested by Linning

(27). The annular flow type considers the vapor flowing in the core with the liquid in the annulus between the vapor core and the tube wall. This type of flow was chosen as its occurrence is the most probable. The result of considering this type of flow was a system of nonlinear differential equations which included different phase velocities, fluid acceleration, wall shear forces, interface shear forces, and mass and energy transfer between the phases. The equations are classified as compressible, one-dimensional equations. The basic assumptions used in deriving these Annular Flow equations were that thermodynamic equilibrium exists at all stages of the expansion and that the wall shear force could be described by the liquid friction factor--Reynolds number relation based on the tube diameter and the liquid velocity.

Due to the complexity of the equations, a numerical solution was necessary. The method of Runge-Kutta (62) provided an accurate numerical method for the solution. The solution was obtained by programming the equations in ALGOL (63) for the Burroughs 220 Data Processing System. The initial conditions for the solution were the mass flow rate and inlet pressure. From the solution of the equations the liquid velocity, vapor velocity, quality, relative velocity factor, void fraction, pressure, temperature, maximum and minimum liquid velocities, and Reynolds number were obtained as functions of distance along the tube axis from the point of initial vaporization to the tube exit.

Experimental data for the system steam-water were obtained in a range where no data are presently available. These data were used to establish the validity of the equations, and the assumptions that were a basis

for the equations. A total of twenty eight runs was made and the range of the data was: mass flow rates - 445 to 864 lb_m/ft^2-sec, inlet pressures - 32.4 to 66.5 psia and discharge pressures - 25.9 to 56.5 psia. The test section of the experimental system consisted of a 0.930 inch I D thin walled stainless steel tube approximately twenty feet long. Temperatures were measured with thermocouples at sixteen equally spaced points along the tube. Pressures were measured with pressure transducers at the entrance, center and exit of the tube and at an expansion section. The void fraction of the two-phase flow was measured at various tube cross sections by traversing across the tube with a one-sixteenth inch diameter beam of radiation from a 45 Kvp X-ray tube.

Analysis of the data showed that the basic assumption of thermodynamic equilibrium was approached for thirteen of the twenty eight runs. For these runs the computed void fraction was within the Probable Error of the measured void fraction. The average per cent deviation of the computed tube length from the measured tube length was ± 5.2% for equal pressure drops. This close agreement served to establish the validity of the equations when the basic assumptions were met.

For the remaining fifteen runs thermodynamic equilibrium at the cross section of the tube was not approached, as determined by comparing the measured temperatures with the saturation temperatures which corresponded to the measured pressures. For these runs the rates of heat and mass transfer were controlling and the measured void fractions were less than the computed void fractions for equal pressure drops. Also the computed tube lengths were an average of 29.5 per cent less than the measured tube lengths, since the liquid velocity did not increase as rapidly with

distance along the tube as it would have had thermodynamic equilibrium been approached.

Design charts are presented for the system steam-water for inlet pressures of 30 to 150 psia in intervals of 20 psia based on the numerical solution of the Annular Flow equations. These charts permit estimation of two-phase flow pressure drops and corresponding L/D ratios for specified inlet pressures and mass flow rates up to and including the critical conditions.

All the data which are available in the literature for the adiabatic flow of steam and water are reported to be for critical flow. Comparisons were made of the critical outlet pressure predicted by the Annular Flow equations with the experimental values reported in the literature. The predicted values were 20.6 per cent higher than the six experimental values reported by Benjamin and Miller (14) for an inlet pressure range from 20.0 to 35.8 psia. The predicted value was 61.5 per cent higher than the one experimental value reported by Bottomley (19) at an inlet pressure of 41 psia. For the nine runs reported by Burnell (29), the predicted values for four runs were 57.2, 53.7, 30.8, and -8.8 per cent higher than the experimental values for inlet pressures of 158, 114, 52.4 and 24.0 psia. No comparison could be made for Burnell's five other runs for inlet pressures of 14.3 psia and less as the outlet temperatures were less than the lower limit of accuracy for the least squares polynomials fitted to the thermodynamic properties. Isben (46) found similar deviations from the previously mentioned investigators data when he compared his experimental data with their data. For Linning's data in an inlet pressure range from 20.8 to 29.8 psia, the average per cent

deviation of the predicted values from the measured values was ± 21.4 per cent. Isben (46) found Linning's values 40 to 50 per cent less than his experimental values. Isben correlated his critical outlet pressure data by a log-log plot of $(W/A)/P_c^{0.96}$ versus exit quality. A comparison was made based on the correlation for the critical outlet pressures computed from the Annular Flow equation used in the design charts. Unfortunately, only a few points were obtained from the solution of the equations that lie in the range of the empirical correlation. The other points indicate that the extension of the correlation curve would be lower than indicated by Isben.

Based on this study the following conclusions were reached:

1. The adiabatic, two-phase flow of steam and water in a horizontal tube from the point of initial vaporization to the exit of the tube was successfully described by the Annular Flow equations when the basic assumptions of thermodynamic equilibrium at all stages of the expansion and constant temperature across any section normal to the flow were approached. The accuracy in computing the two-phase flow pressure drop by the Annular Flow equations for a specified mass flow rate, inlet pressure and tube length was ±10 per cent when these basic assumptions were met.

2. When the basic assumptions of thermodynamic equilibrium at all stages of the expansion and of constant temperature across any section normal to the flow were not approached, the pressure drop which was predicted from the Annular Flow equations was from 15 to 45 per cent greater than the measured pressure drop.

3. The solution of the Annular Flow equations required that only

the initial conditions of mass flow rate and inlet pressure be known along with the tube length or outlet pressure. Further information concerning the flow variables at some point downstream from point of initial vaporization was not required to obtain a solution for the flow variables as a function of distance along the tube. All previous flow models have required additional information about the flow variables at some point downstream from the point of initial vaporization or that a simplifying assumption be made to obtain a solution.

4. The use of an X-ray tube as a source of monoenergetic gamma radiation was developed for the measurement of the void fraction in two-phase steam-water flow. The accuracy of the measurement was established to be within the Probable Error.

NOMENCLATURE

The symbols in this list do not include any computer program symbols; for these refer to Table 36 and Table 38.

A	tube cross sectional area	ft^2
a_g	cross sectional area of vapor phase	ft^2
a_ℓ	cross sectional area of liquid phase	ft^2
B	parameter defined in equation (1.603)	ft/sec
b_1	parameter defined in equation (2.401)	ft/sec
b_2	parameter defined in equation (2.401)	ft/sec
b_3	parameter defined in equation (2.401)	ft/sec
C	velocity of sound	ft/sec
C	constant from Table I for equation (4.208)	dimensionless
c	parameter defined in equation (1.603)	dimensionless
D	tube diameter	ft
E	total energy	BTU/lb_m
e	error in local void fraction	dimensionless
e_{avg}	error in average void fraction	dimensionless
F	function defined by equation (4.501)	ft/°F
F_p	interface shear force	lb_f
F_w	wall shear force	lb_f
f	friction factor	dimensionless
G	mass flow rate per unit area	$lb_m/ft^2\text{-sec}$
g_c	gravitational constant 32.174	$ft\text{-}lb_m/sec^2\text{-}lb_f$

H	enthalpy of vapor	BTU/lb_m
h	enthalpy of liquid	BTU/lb_m
h_i	heat transfer coefficient	$BTU/hr\text{-}ft^2\text{°}F$
I	intensity of gamma radiation	counts/min
I_F	intensity of radiation passing through the tube full of water	counts/min
I_{MT}	intensity of radiation passing through the empty tube	counts/min
I_{TP}	intensity of radiation passing through the tube containing two-phase flow	counts/min
I_o	intensity of radiation before passing through the tube	counts/min
K	thermal conductivity	$BTU/hr\text{-}ft^2\text{-}°F/ft$
k	relative velocity factor	dimensionless
L	tube length	ft
L/D	tube length to diameter ratio	dimensionless
$(L/D)_c$	critical tube length to diameter ratio	dimensionless
ℓ	chord length of steam phase in two-phase flow	ft
m	chord length of tube	ft
P	pressure	psia
Pr	Prandtl number	dimensionless
Q	total heat transfer	BTU
q	rate of heat transfer	BTU/hr
R	tube radius	ft
r	distance along the tube radius	ft
r_1	Martinelli-Nelson model parameter defined by equation (1.407)	ft^3/lb_m
r_2	Martinelli-Nelson model parameter defined by equation (1.408)	ft^3/lb_m

Re	Reynolds number	dimensionless
R_g	fraction of tube filled by vapor	dimensionless
R_ℓ	fraction of tube filled by liquid	dimensionless
T	temperature	°F
T_e	exit temperature	°F
T_o	inlet temperature	°F
t	tube wall thickness	ft
U_i	overall heat transfer coefficient	BTU/hr-ft^2-°F
V	velocity	ft/sec
V_g	vapor velocity	ft/sec
V_ℓ	liquid velocity	ft/sec
V_p	interface velocity	ft/sec
v	specific volume	ft^3/lb$_m$
v_g	specific volume of vapor	ft^3/lb$_m$
v_ℓ	specific volume of liquid	ft^3/lb$_m$
W	total mass flow rate	lb$_m$/sec
W_g	mass flow rate of vapor	lb$_m$/sec
W_ℓ	mass flow rate of liquid	lb$_m$/sec
W/A	total mass flow rate per unit area	lb$_m$/ft^2-sec
x	quality	dimensionless
y	reduced diameter	dimensionless
z	distance along tube axis	ft

GREEK SYMBOLS

α	local void fraction	dimensionless
α_{avg}	average void fraction	dimensionless
θ	angle formed by the tube axis and the vapor-liquid interface	radians

μ_ℓ	liquid viscosity	centipoise
ρ	density	lb_m/ft^3
ρ_g	vapor density	lb_m/ft^3
ρ_ℓ	liquid density	lb_m/ft^3
σ	mass attenuation coefficient	cm^2/gm
σ_{air}	mass attenuation coefficient air	cm^2/gm
σ_s	mass attenuation coefficient for steel	cm^2/gm
σ_w	mass attenuation coefficient for water	cm^2/gm
$\Phi_{\ell tt}$	Martinelli parameter defined by equation (1.401)	dimensionless
X_{tt}	Martinelli parameter defined by equation (1.402)	dimensionless
Δ	forward difference operator	dimensionless

SUBSCRIPTS

a	momentum pressure drop
air	air
avg	average
c	critical
e	exit conditions
F	full
g	vapor
ℓ	liquid
MT	empty
o	initial conditions or all liquid flow
p	interface
s	steel
TP	two-phase
w	water

CHAPTER I

INTRODUCTION

Areas of Interest

The cocurrent transport of a liquid and a gas is of interest in many technical endeavors. This interest has grown from that of Barbet (1) who in 1914 was working with a vertical tube evaporator and observed two-phase flow patterns to the spectrum of present day interest. Some of the topics of interest will be discussed briefly.

The petroleum industry must critically design pipe lines to carry two-phase, gas-crude oil mixtures, especially when these pipe lines are laid on ocean floors to transport the two-phase mixtures from off-shore wells to on-shore storage facilities, or when they are laid in the remote regions of the world where petroleum deposits occur (2).

The design of water cooled and moderated nuclear reactors presents different and difficult areas of design (3). The geometry of the reactor is of prime importance to insure proper operation, but flow channels must be designed to provide necessary cooling capacity and moderation to maintain the reactor materials at safe operating temperatures under the conditions of very high heat fluxes. These two design criteria are generally not compatible, and a considerable amount of research effort has gone into overcoming this difficulty.

The partial vaporization of aircraft fuel in jet aircraft fuel systems is detrimental to the proper operation of the fuel system (4). The two-phase flow phenomena is extremely difficult to evaluate in these

situations due to the number of variables involved, such as the change in altitude, length and complexity of fuel lines, composition and temperature of the fuel, flow rate of the fuel, and the amount of dissolved gas in the fuel.

The rapid and accurate transport of liquid fuels, usually at cryogenetic temperatures, to rocket motors presents another series of two-phase flow problems. Also film cooling in the rocket motor itself is another two-phase flow problem.

Other situations where two-phase flow occurs are in boilers, stills, condensers, expansion valves, restrictor tubes of refrigeration units, and air or gas lifts.

Literature Survey

The amount of technical endeavor which has taken place in the field of two-phase flow is summarized in the nine literature surveys of the field.

Gresham, et al., (5) surveyed the literature for all references in the area of gas-liquid, two-phase flow through June 1955. A summary and review of 180 papers are presented. The discussion covered the areas of flow patterns and methods of calculating two-phase pressure drops for fluids flowing without mass transfer in horizontal and vertical pipes, for fluids and condensing vapors in horizontal and vertical flow. Ward, et al., (6) brought the previously mentioned survey to date as of August 1959 with abstracts of 393 additional papers.

Isben, et al., (3) surveyed the literature through November 1954, and summarized the current knowledge and limitations of the present

methods for estimating two-phase pressure drops, specifically, as applied to steam-water flows. The report considered the present status of two-phase pressure drop calculation methods, flow patterns, flow models, and flow stability. A total of 89 references is listed.

Bennett (7) presented a review of the published literature concerning two-phase, gas-liquid flow approximately to December 1957. The topics reviewed were flow patterns, methods and accuracy in predicting two-phase pressure drops with and without mass transfer, flow models, critical flow phenomena, and experimental techniques. A total of 113 references is listed.

Charvonia (8) reviewed the literature with emphasis on the "annular" flow pattern. The annular flow pattern was defined as the liquid flowing in an annulus around the inner circumference of the pipe while the gas flows through the core, with the interface smooth or rough. Previous correlations were examined, and experimental investigations were reviewed and categorized depending upon whether film thickness measurements were made or were not made. Interest in "film cooling" of rocket motors was expressed. A total of 55 references was cited.

Rodabaugh's survey (9) was divided into the areas of two-phase flow and acoustic phenomena and was intended as background information of possible value in designing an acoustical measuring instrument. The survey was not intended to be comprehensive. A total of 127 references was reported.

Other literature surveys were made by Jens and Leppert (10), Shell Pipeline Company (11), and Ambrose (12). Jens and Leppert presented a

review with seventy references which covered heat transfer and pressure drop. The Shell Pipeline Company's survey reported 154 references of general interest to the petroleum industry. Ambrose surveyed the literature for flow patterns associated with two-phase flow and cited 15 references.

Adiabatic, Evaporating Two-Phase Flow Models

The topic of interest in two-phase flow for this study is the adiabatic, evaporating flow of water in horizontal pipes.

At present there are two generally accepted methods or models for estimating flow parameters in adiabatic, evaporating, two-phase flow in horizontal pipes. These are the Martinelli-Nelson method (13), and Homogenous Flow Model or Friction Factor method (14). Since the original papers were presented, there has been much interest in modifying these models to give better correlations for particular cases, especially the case of heat transfer with boiling. Actually, the adiabatic case is a special case of the Martinelli-Nelson method as it is normally used for the prediction of pressure drop during forced-circulation boiling of water.

The Homogenous Flow model derived its name from the fact that basic assumptions of the model were that the liquid and its vapor flowed at the same average velocity, and that the physical properties of the fluid could be taken as an average of those of the liquid and the vapor. This is sometimes also referred to as "fog" or "frothing" flow. Benjamin and Miller (14) developed this model to describe the flow of steam and water in cascade drain lines of power plants.

Modifications of these models have been described in detail by Gresham, et al., (5) and Isben, et al., (3). Investigators who have published work after these literature surveys were made are Davis (16), Hatch and Jacobs (17) and Buthod (18). Davis modified the Lockhart Martinelli X parameter used in the Martinelli-Nelson method to show the effect of the Froude number. Hatch and Jacobs considered the Martinelli-Nelson model in connection with the flow of hydrogen and trichloromonofluoromethane with and without heat transfer. Buthod considered the Homogenous Flow model in connection with the thermodynamics of two-phase flow in furnace tubes and transfer lines.

A third model will also be discussed--the Linning model. This model considered more of the flow variables than any previous one.

Martinelli-Nelson Model.--Martinelli and Nelson (13) made the following assumptions as a basis for the derivation of their equations:

1. A turbulent--turbulent flow pattern exists for all practical purposes in any normal forced circulation boiler design.

2. The pressure drop resulting from the flow of the boiling mixture, where the pressure drop across the tube is small compared to the absolute pressure, is made up of two parts:

   (a) the pressure drop due to frictional forces, and

   (b) the pressure drop resulting from the increase of momentum of the mixture as it flows through the tube and vaporizes.

3. The curve of $\Phi_{\ell,tt}$ versus X_{tt} which was obtained for the flow of air and various other liquids by Lockhart and Martinelli (15) is applicable to boiling water. $\Phi_{\ell,tt}$ is defined by

$$\left(\frac{\Delta P}{\Delta L}\right)_{TPF} = \left(\frac{\Delta P}{\Delta L}\right)_{\ell} \Phi^2_{\ell,tt} \tag{1.401}$$

where $\left(\frac{\Delta P}{\Delta L}\right)_{TPF}$ is the frictional pressure drop due to two-phase flow $\left(\frac{\Delta P}{\Delta L}\right)_{\ell}$ is the frictional pressure drop resulting if only liquid were flowing in the pipe, and $\Phi_{\ell,tt}$ is a parameter obtained experimentally. $\Phi_{\ell,tt}$ was correlated by means of the dimensionless parameter X_{tt} where

$$X_{tt} = \left(\frac{v_\ell}{v_g}\right)^{0.571} \left(\frac{\mu_\ell}{\mu_g}\right)^{0.143} \left(\frac{1}{x} - 1\right) \tag{1.402}$$

4. Thermodynamic equilibrium exists at each point along the tube.

5. The quality, x, is a linear function of pipe length.

Combining equation (1.401) with the relation

$$\left(\frac{dP}{d\ell}\right)_{\ell} = \left(\frac{dP}{dL}\right)_o \left(\frac{W_\ell}{W}\right)^{1.75} = \left(\frac{dP}{dL}\right)_o (1-x)^{1.75} \tag{1.403}$$

gives

$$\frac{\left(\frac{dP}{dL}\right)_{TPF}}{\left(\frac{dP}{dL}\right)_o} = (1-x)^{1.75} \Phi^2_{\ell,tt} \tag{1.404}$$

where $\left(\frac{dP}{\Delta L}\right)_o$ is the pressure gradient for the flow of 100% liquid. This equation relates the two-phase flow pressure drop with the pressure drop for 100% liquid and with the quality at any point along the pipe.

If the liquid flow rate, exit quality and physical properties are known, the two-phase pressure drop can be computed. For various exit

qualities and mean pressures the authors have evaluated the integral of the above relation expressed as

$$\frac{\Delta P_{TPF}}{\Delta P_o} = \frac{1}{x_e} \int_o^{x_e} \left[\frac{\left(\frac{dP}{dL}\right)_{TPF}}{\left(\frac{dP}{dL}\right)_o} \right] dx \qquad (1.405)$$

and plotted the results for rapid computations.

In order to obtain the total pressure drop, the pressure drop due to the momentum change, i.e., acceleration of the fluid, must be added to the pressure drop due to friction. The pressure drop due to change in momentum was expressed as

$$\Delta P_a = \frac{W_\ell V_\ell}{g_c A} + \frac{W_g V_g}{g_c A} - \frac{W V_o}{g_c A} \qquad (1.406)$$

As the authors point out, equation (1.406) is extremely difficult to evaluate. However, they considered two extreme cases: (1) the liquid and vapor flow with equal velocities (fog flow), and (2) the liquid and vapor are completely separated and the phase velocities are dependent upon the fraction of the pipe volume occupied by each phase.

The pressure drop for the first case is given by

$$\Delta P_a = \frac{G^2}{g} \left[(1-x) + x\left(\frac{v_g}{v_\ell}\right) - 1 \right] v_\ell = r_1 \frac{G^2}{g_c} \qquad (1.407)$$

where G is the mass flow rate per unit area.

The pressure drop for the second case is given by

$$\Delta P_a = \frac{G^2}{g} \left[\frac{(1-x)^2}{R_\ell} + \frac{x^2}{R_g}\left(\frac{v_g}{v_\ell}\right) - 1 \right] v_\ell = r_2 \frac{G^2}{g_c} \qquad (1.408)$$

where R_ℓ and R_g are the fractions of the pipe volume filled by the liquid and vapor respectively.

The equations (1.407) and (1.408) are conveniently expressed using multipliers r_1 and r_2 to relate the pressure drop due to the change in momentum with the total mass flow rate per unit area G. It can be seen that the multiplier r_1 is a function of the quality and specific volumes of the phases, and the multiplier r_2 is an additional function of R_ℓ and and R_g. The multiplier r_2 was evaluated from experimental data and plotted as a function of pressure with exit quality as a parameter for rapid computations.

The total pressure drop, $(\Delta P)_{TP}$ can now be expressed as,

$$(\Delta P)_{TP} = \Delta P_o \left(\frac{\Delta P_{TPF}}{\Delta P_o} \right) + r \frac{G^2}{g_c} \qquad (1.409)$$

The authors recommend evaluating both r_1 and r_2, but usually no significant difference is found.

In general the accuracy for this method is ± 40%. A glance at the previously mentioned literature surveys will show the wide acceptance for this method of predicting two-phase flow pressure drops and the attempts to improve and employ it over a wide range of applications. One advantage appears to be the general independence of flow pattern, and another is the fact that the method correlates two-phase flow data over wide ranges within reasonable limits.

Homogenous Flow Model.--Benjamin and Miller (14) made the following assumptions in the derivation of the equations for the Homogenous Flow model:

1. The liquid and vapor flow with equal velocities.

2. The thermodynamic equilibrium is attained at any plane normal to the pipe cross-section.

3. The physical properties of the mixture are an average of the liquid and vapor properties

4. A single-phase friction factor can be used for the two-phase mixture flow.

Benjamin and Miller (14) wrote the momentum equation over a differential length of horizontal pipe as

$$vdP + \frac{VdV}{g_c} + f\,\frac{V^2}{2g_c}\,\frac{dz}{D} = 0 \qquad (1.501)$$

where v is the specific volume of the two phase mixture, V is the linear velocity of the two-phase mixture, P is the pressure at any point normal to the flow and is constant over the pipe cross-section, D is the pipe diameter, f is the friction factor, and z is the distance measured along the pipe axis.

According to the continuity equation

$$V = \frac{Wv}{A} = Gv \qquad (1.502)$$

where W is the total mass flow rate, A is the cross-sectional area of the pipe and G is the mass flow rate per unit area.

If equation (1.502) is substituted into equation (1.501), the result is

$$\frac{dP}{v} + \frac{G^2}{g_c}\,\frac{dv}{v} + f\,\frac{G^2}{2g_c}\,\frac{dz}{D} = 0 \qquad (1.503)$$

If the above equation is integrated over the length of pipe from L_1 to L_2, the result is

$$\int_{P_1}^{P_2} \frac{dP}{v} + \frac{G^2}{g_c} \ln \left(\frac{v_2}{v_1} \right) + f_{avg} \frac{G^2}{2g_c} \frac{(L_2-L_1)}{D} = 0 \qquad (1.504)$$

The friction factor is assumed constant over the interval $(L_2 - L_1)$. Bottomley's measurements (19) suggested the use of a constant friction factor. Benjamin and Miller (14) showed that the friction factor varies ± 20% from Bottomley's measurements.

For adiabatic flow, both isentropic and isenthalpic conditions have been assumed to evaluate v in the integral $\int \frac{dP}{v}$. If the kinetic energy is significant, the isenthalpic condition is not correct; and if frictional losses are present, the isentropic assumption is also in error. In many cases, very little difference is found between the use of isenthalpic and isentropic for flashing steam-water mixtures. Dusinberre (20) has prepared a plot of volume versus entropy for a family of saturation pressures. Bridge (21) has evaluated the integral $\int \frac{dP}{v}$ for isenthalpic expansions for initial saturation pressures up to 600 psia. Allen (22) gave an analytical expression for isenthalpic expansion.

The general procedure for a solution of equation (1.504), having the mass flow rate, up-stream pressure, and pipe length specified, is to evaluate the integral $\int \frac{dP}{v}$ numerically for an assumed downstream pressure. At each step, the unknowns involve the specific volume of the mixture, $v = v_\ell(1 - x) + v_g x$ and the saturation pressure. By trial and error the pressure is changed and the integral evaluated until the equation is satisfied. The accuracy of this calculation is generally ± 40%.

Other friction-factor methods (23), (24), (25), have been reported.

Isben (26) refers to Mixed Models. These are models having features based on both the Martinelli-Nelson and Homogenous models. These models have had, at best, only slightly better success in describing two-phase flow parameters.

In general the problems in describing two-phase flow are descriptions of (1) the transport phenomena at the interface i.e., mass, momentum, and energy transfer across the interface; (2) the interface surface characteristics; (3) the approach to thermodynamic equilibrium; (4) the velocity profiles in the liquid and vapor; and (5) the wall shear stresses.

Linning Model.--Linning in his paper developed models to describe annular flow, stratified flow, and fog or frothing flow, of which the Annular Flow model is of interest here. The Stratified Flow model was said to serve to indicate the type of experimental work necessary to evaluate the fraction of the wall wetted by each phase. The Frothing Flow model is the previously discussed Homogenous Flow model. The Annular Flow model is of interest because it includes wall shear forces, interface shear forces, different phase velocities, mass acceleration, and mass and energy transfer between the phases.

In deriving equations for his Annular Flow model, Linning assumed that:

1. The pressure and temperature are constant across any section normal to the flow.

2. The fluid is in thermodynamic equilibrium at all stages of an expansion.

3. The velocities on the bases of continuity, momentum and energy, are equal.

4. Steady state conditions exist.

5. The pipe is of constant cross-sectional area and is horizontal.

Linning wrote the following equations for his Annular Flow model for an elemental length of horizontal pipe, dz. Continuity equations for each phase are

$$a_\ell V_\ell = W(1-x)v_\ell \qquad (1.601)$$

and

$$a_g V_g = Wxv_g \qquad (1.602)$$

where a_ℓ and a_g are the cross-sections of the pipe occupied by the liquid and vapor respectively.

Putting $\frac{V_g}{V_\ell} = k$, $\left(\frac{x}{1-x}\right)\frac{v_g}{v_\ell} = c$, and $\left(\frac{W}{A}\right)(1-x)\,v_\ell = B$

equations (1.601) and (1.602) yield

$$V_\ell = B(1+c/k) \qquad (1.603)$$

To determine the quality at any point in the system, the following approximate relation was derived from the total energy equation

$$x = \frac{h_o - h + Q}{\Delta H} \qquad (1.604)$$

Although Linning was concerned with adiabatic flow, he included the heat

transferred to the surroundings term, Q, in the above equation to account for the small heat loss from his uninsulated pipe. Q, expressed in BTU/lb, was determined experimentally as a function of tube length.

The momentum equation for the complete fluid was written as

$$-dF_w - AdP = \frac{1}{g_c} d\left[W(1-x)V_\ell + WxV_g\right] \qquad (1.605)$$

where F_w is the wall shear force. The momentum equation for the liquid phase was written as

$$dF_w - dF_p + a_\ell dP + \frac{W(1-x)}{g_c} dV_\ell = 0 \qquad (1.606)$$

where F_p is the shear force at the interface and a_ℓ is the cross-sectional area occupied by the liquid phase. The energy equation for the vapor phase was written as

$$Wx\left[dH + V_g \frac{dV_g}{g_c}\right] + V_p dF_p + \frac{V_g^2 - V_\ell^2}{2g_c} Wdx = 0 \qquad (1.607)$$

where V_p is the interface velocity, defined as the mean velocity of the fluid particles lying on the line traced by the liquid-vapor interface perphery on a plane perpendicular to the pipe axis.

Eliminating dF_p and dF_w from equations (1.605), (1.606) and (1.607) yields

$$\frac{Wx}{g_c}(dH + V_g dV_g) - V_p\left[\frac{WxdV_g}{g_c} + \frac{(V_g - V_\ell)Wdx}{g_c} + a_g dP\right] + \frac{V_g^2 - V_\ell^2}{2g_c} = 0 \qquad (1.608)$$

The equations were nondimensionalized using the expressions for k, c, B, equation (1.603), and $n = V_p/V_\ell$. The result, for a differential length of pipe or a differential change in temperature assuming B constant, is

$$\frac{kdH}{nv_g} - dP + \left(\frac{W}{A}\right)^2 \left(1 + \frac{k}{c}\right) \frac{v_\ell(1-x)}{2g_c} \left\{ 2x \left(\frac{k}{n} - 1\right)(dc + dk) + \left(1 + \frac{c}{k}\right)\left[\frac{k^2-1}{n} - 2(k-1)\right] dx \right\} = 0 \qquad (1.609)$$

Equation (1.609) is a function of k, dk, n and temperature.

Linning assumed that the wall shear stress term in the momentum equation could be expressed as

$$\frac{dF_w}{dT} = \frac{F\pi D}{8g_c v_\ell} V_\ell^2 \frac{dz}{dT} \qquad (1.610)$$

and that the friction factor f could be evaluated from single-phase liquid data with the Reynolds number based on the pipe diameter.

If equation (1.605) is combined with equation (1.610) and the definitions for k and B, the result is

$$-\frac{f\pi DV_\ell^2}{8g_c v_\ell} \frac{dz}{dT} - \frac{AdP}{dT} - \frac{W}{g_c}\left\{(1-x)\frac{dV_\ell}{dT} + (k-1)\frac{dx}{dT} + xk\frac{d(kV_\ell)}{dT}\right\} = 0 \qquad (1.611)$$

Differentiating equation (1.603), the result is

$$\frac{dV_\ell}{dT} = \frac{B}{k^2}\left(k\frac{dc}{dT} - c\frac{dk}{dT}\right) \qquad (1.612)$$

Thus knowing the experimental temperature distribution, dz/dT,

Linning was able to obtain a numerical solution for k as a function of T and z using equations (1.611) and (1.612). Then by using the solution for k he was able to evaluate n as a function of T by using equation (1.609). Linning represented his results by the following empirical relation

$$n = 1 + 0.2\ (T_o - T)^2/(T_o - T_c)^2 \qquad (1.613)$$

where T_o is the temperature at the commencement of evaporation, T_c is the outlet temperature at the critical flow rate, and T is the temperature at any point in the expansion.

Using a momentum balance Linning was able to determine experimentally the value of k at the pipe exit. The comparison of the values of k from his theoretical equations with his experimental values had an average per cent deviation of ± 13.1% for eight of twelve tests with water for a tube inside diameter of 0.1285 inches, for mass flow rates of 250 to 500 lb_m/ft^2-sec and for inlet pressures from 20.8 to 29.8 psia. All discharge pressures were atmospheric.

A critical flow criterion was developed for the Annular Flow model. The critical flow predictions from the Annular Flow model were, in general, within the experimental error of the data. Linning compared his theoretical results for critical flow with the experimental data of Burnell (29) and showed that his theoretical values were, in general, within the experimental error of Burnell's data, except for one run in a 1.5 inch diameter tube with a mass flow rate of 500 lb_m/ft^2-sec, where his theoretical results were 24 per cent higher than the experimental results.

A critical flow criterion was developed for the Frothing Flow

model also. The theoretical results for the Frothing Flow model were, in general, within the experimental error of Linning's experimental data. Although one investigator (28) reported critical flow phenomena for Freon 12, Linning was not able to obtain any quantitative experimental results from this investigation to compare with his work.

Thus, to use the Linning model i.e., the annular flow equations as written by Linning, the necessary information which is required to compute the length of pipe for a specified mass flow rate, inlet pressure and pressure drop is:

1. The temperature corresponding to the saturation pressure at the tube outlet for the critical flow rate for equation (1.613).

2. A boundary condition for k for equation (1.609) at a point in the expansion, preferably at the tube exit or entrance.

3. The thermodynamic and physical property data of the fluid. This information permits a tedious numerical solution of equation (1.609) to relate k with temperature. The friction factor relation, equation (1.610), relates the variables with distance down the pipe.

Linning found that he obtained excellent experimental verification of his theoretical equations over a limited range, but further experimental data is required to determine the usefulness of the model to describe the two-phase flow variables over a wide range. The assumptions that may prove restrictive are that thermodynamic equilibrium is approached at all stages in the expansion, and that the temperature is constant across any section normal to the flow.

It should be noted that Linning was not clear on the method he used to obtain a solution to his annular flow equations and the boundary

conditions he used in the solution. Also Linning did not make any statements concerning the methods that were used to obtain the derivatives of the thermodynamic properties, and a statement was not made about the size of the interval which was required to obtain an accurate solution to the equations.

Void Fraction

The average void fraction α_{avg} is defined as the ratio of the cross-sectional area occupied by the gas phase to the cross-sectional area of the pipe i.e.,

$$\alpha_{avg} = \frac{a_g}{A} \tag{1.701}$$

The void fraction is a useful parameter in studying two-phase flow. The following development will illustrate its use.

The continuity equation for the liquid phase is

$$V_\ell = \frac{W_\ell v_\ell}{a_\ell} \tag{1.702}$$

The continuity equation for the vapor phase is

$$V_g = \frac{W_g v_g}{a_g} \tag{1.703}$$

The area relation is

$$a_g + a_\ell = A \tag{1.704}$$

The quality is defined as

$$x = \frac{W_g}{W_g + W_\ell} = \frac{W_g}{W} \tag{1.705}$$

where $W = W_g + W_\ell$.

By combining equations (1.701), (1.702), (1.704) and (1.705), the continuity equation for the liquid phase may be written as

$$V_\ell = \frac{W}{A} \frac{(1-x)}{(1-\alpha_{avg})} v_\ell \tag{1.706}$$

By combining equations (1.701), (1.703), (1.704) and (1.705), the continuity equation for the vapor phase may be written as

$$V_g = \left(\frac{W}{A}\right)\left(\frac{x}{\alpha_{avg}}\right) v_g \tag{1.707}$$

Equation (1.706) and (1.707) show the use of the void fraction in the determination of the mean velocities of the liquid and the vapor phases in two-phase flow. The fact that each phase flows at a different velocity has been realized for a considerable length of time (14), but the determination of the void fraction has been the major difficulty in quantitatively evaluating the mean velocity of each phase. The total mass flow rate per unit area can be readily measured, and the quality can be determined to a sufficient degree of accuracy by assuming isenthalpic or isentropic expansion in the case of adiabatic two-phase flow or by an energy balance in the case of two-phase flow with heat transfer.

Various experimental techniques have been used to measure the void fraction in two-phase flow. Some investigators such as Martinelli, Boelter, Taylor, Thompson, and Morrin (30); and Govier and Omer (31) used quick closing valves to measure the volume fraction of the liquid in the

pipe which is referred to as the hold-up. This method of quick closing valves was particularly useful for time dependent changes in the void fraction as occur in slug flow and plug flow. Krasiakova (32) measured the conductivity of the liquid film. Johnson (33) measured the volumetric flow rate of the vapor to the volumetric flow rate of the liquid by a concentration method. Dengler and Addoms (34) in a heat transfer study measured the volumetric fraction of the liquid over a short section of tube by a radioactive tracer technique.

The most generally used method of determining the void fraction for annular flow has been gamma-ray attenuation. Isben and co-workers have used a narrow columinated beam of high intensity radiation from the radioisotopes selenium-175 (35) and thulium-170 (36). The technique has also been used at Argonne National Laboratory with thulium-170 by Marchaterre (37), Richardson (38), Cook (39), Hooker and Popper (40) and Petrick (41). Thulium-170 essentially radiates a 0.08 MEV gamma photon. Other investigators who used the same technique but used the radioisotope iridium-192 were Schwartz (42), and Zmola and Bailey (43).

Critical Flow Phenomena

The critical flow rate is defined as the maximum flow rate that occurs for a given upstream pressure and length of pipe, when the downstream pressure is reduced until no further increase in flow rate takes place. There has been considerable experimental evidence of critical flow occurring in one-component, two-phase flow with and without heat transfer. Investigators such as Bottomley (19), Benjamin and Miller (14), Burnell (29), Allen (22), Linning (27), Isben (46) and Waters (47) have observed the two-phase critical flow behavior in adiabatic studies.

Investigators such as Harvey and Foust (48), Schweppe and Foust (49) and Stein et al., (50) reported critical flow behavior in studies with heat transfer.

Shapiro (44) derived the following relation for the velocity of sound in a single phase fluid

$$C = \sqrt{\left(\frac{\partial P}{\partial \rho}\right)_s} \qquad (1.801)$$

where C is the velocity of sound in the fluid and $\left(\frac{\partial P}{\partial \rho}\right)_s$ is the partial derivative of pressure with respect to density at constant entropy. Steitz (51) applied equation (1.801) to adiabatic two-phase flow of water, and used a digital computer to calculate flow parameters such as the critical pressure ratio as a function of inlet conditions, and a factor K versus inlet conditions, where the factor K multiplied by inlet pressure produces the desired value of the critical flow. Steitz does not compare his solution with any experimental data and his equations assume that the liquid and vapor phase flow with equal velocities.

Isben (46) obtained critical outlet pressure data as a function of mass flow rate per unit area by flowing adiabatically a mixture of steam and water through four test sections three feet long and from 1/4 inch to 1 inch nominal pipe diameter. A theoretical critical mass flow rate per unit area, G_{th}, was defined as

$$G_{th}^2 = -g_c \left(\frac{dp}{dv}\right)_s \qquad (1.802)$$

where v is the mixture specific volume and is equal to $(1-x)v_\ell + xv_g$. A plot of per cent deviation $(G_{ob} - G_{th})\,(100)/G_{ob}$ versus exit quality is

presented. G_{ob} is the observed critical mass flow rate per unit area. Isben compared his data with the data of Benjamin and Miller (14) and Bottomley (19), and found that this data was significantly lower than his data. Both Benjamin and Miller's data and Bottomley's data were closely approximated by the Homogenous Flow model. Isben found the data of Burnell (29) to agree within ± 10 per cent in the pressure range from 6 to 15 psia and were 20 to 35 per cent lower for a pressure range of 25.4 to 58.5 psia. Isben found the values reported by Linning were 40 to 50 per cent less than his data.

Bridge (21) calculated the critical flow rate per unit area based on the Homogenous Flow model. Charts are given for mass flow rates per unit area versus L/D ratio with parameters of inlet pressure. Linning (27) prepared a plot based on his Annular Flow model of critical outlet pressure versus mass flow rate per unit area with inlet pressures as parameters.

Karplus (45) calculated the velocity of sound in steam containing water droplets and plotted the results as the velocity of sound versus steam quality with pressure as a parameter. For qualities of 10 per cent or less and pressures from 10 to 1000 psia, the velocity of sound was of the order of 100 to 350 ft/sec. These results were to be applied to the continuous monitoring of the quality in water cooled nuclear reactors.

In summary, a critical flow phenomena occurs in two-phase flashing flow. The critical flow velocity can be said to be of the order of hundreds of feet per second rather than thousands of feet per second as is the case in single component flow. Although the critical flow rate is not difficult to produce experimentally, the mathematical models to treat

the problem have not been too successful in describing the flow. This statement could also be made concerning two-phase flow in general.

The Objectives of the Present Investigation

In view of the previous discussion, more fundamental knowledge of two-phase flow variables is needed. The present investigation will consider the adiabatic, evaporating, two-phase flow of a pure fluid, with the following objectives.

1. The equations of motion for annular, two-phase flow will be written in the manner first suggested by Linning, since the preceding critical review of the literature showed the Linning model considered more of the flow variables than any other flow model. The boundary conditions will be sought at the point of initial vaporization and the accuracy of the numerical method which will be required to solve the equation will be established.

2. Experimental data will be obtained to permit:

   (a) A comparison with the theoretical equations, particularly in a range where no data is available.

   (b) The examination of the assumptions of constant temperature across any section normal to the flow and of thermodynamic equilibrium at all stages of the expansion, as these assumptions have been made previously in all of the accepted flow models. The assumption of thermodynamic equilibrium at all stages in the expansion is, in general, not always true as pointed out in the previously mentioned paper by Hatch and Jacobs (17).

The system steam-water is chosen for this investigation. The accurate and complete thermodynamic property data for the system available in the Thermodynamic Properties of Steam by Keenen and Keyes (52) will eliminate inaccuracies which might be introduced into the model for lack of this essential data.

CHAPTER II

THEORETICAL DEVELOPMENT OF ANNULAR FLOW MODEL

Statement of the Physical Problem

The case of the adiabatic flow of a single component in a horizontal pipe of constant cross-section will be considered. The liquid will be considered to enter the pipe at a temperature slightly lower than the saturation temperature corresponding to the inlet pressure. As the pressure decreases along the pipe, a point will be reached at which the temperature of the liquid is equal to the saturation temperature at that pressure, and a fraction of the liquid will be vaporized. This point will be called the point of initial vaporization. Two-phase flow will occur, and as the pressure continues to decrease more liquid will be vaporized. As a result of the large change in specific volume of the small fraction of liquid that has been vaporized, the effective flow area of the liquid phase will be reduced. The liquid velocity will necessarily increase due to this reduction in cross-sectional area, and also as a result of the drag forces on the interface by the vapor which is now moving at a higher velocity than the liquid phase. Due to this higher relative velocity of the vapor phase, it has been observed that the vapor travels in a core surrounded by the liquid in the annulus between the vapor core and the pipe wall, thus the term annular flow.

The transfer phenomena that takes place in the previously described flow are mass transfer of the liquid into the vapor, energy transfer as the liquid is cooled to supply energy for the latent heat of vaporization

and momentum transfer at the pipe wall and interface of the liquid and vapor.

The description of this adiabatic, vaporizing two-phase flow will be written as the equations describing annular flow in the manner suggested by Linning (27). The model will include different phase velocities, fluid acceleration, wall and interface shear forces, mass and energy transfer between the phases.

Assumptions

The following assumptions will be made (after Linning, (27)).

1. The pipe is of constant cross sectional area and is horizontal.

2. Steady state conditions exist.

3. The mean velocity of each phase is the same whether derived on the basis of continuity, momentum or energy. (This does not mean that the velocities of the phases are equal.)

4. The pressure and temperature are constant across any section normal to the flow.

5. The fluid is near thermodynamic equilibrium at all stages in the expansion.

Derivation of Continuity, Momentum and Energy Equations for the Annular Two-Phase Flow Model

Continuity Equation.--With reference to Figure 1 (a) the continuity equation for the liquid phase is

$$W (1 - x) v_{\ell} = a_{\ell} V_{\ell} \qquad (2.301)$$

and for the vapor phase the continuity equation is

$$W \times v_g = a_g V_g \tag{2.302}$$

The quality, x, is defined as

$$x = W_g/W \tag{2.303}$$

where $W = W_g + W_\ell$.

Momentum Equations.--Newton's Second Law in the z-direction may be expressed as the algebraic sum of the forces acting on a control volume is equal to the time rate of change of the momentum within the control volume minus the flux of momentum into the control volume plus the flux of momentum out of the control volume. The mathematical statement (54) is

$$\sum F_z = \frac{\partial}{\partial t} (mV_z)_{c.v.} + \int_{c.v.} V_z dW_{out} - \int_{c.v.} V_z dW_{in} \tag{2.304}$$

At steady state the time rate of change of the momentum in the control volume is zero. Referring to Figure 1 (b) and considering the liquid in a differential length of pipe, dz, as the control volume, the momentum equation for the liquid phase gives

$$a_\ell dP + \cos\theta\, dF_p - P da_g - a_\ell P - d(a_\ell P) - dF_w = 0 + W(1-x)V_\ell + d\left[W(1-x)V_\ell\right] + W dx V_\ell - W(1-x)V_\ell$$

Simplifying

$$W(1-x)dV_\ell + a_\ell dP - \cos\theta\, dF_p + dF_w = 0 \tag{2.305}$$

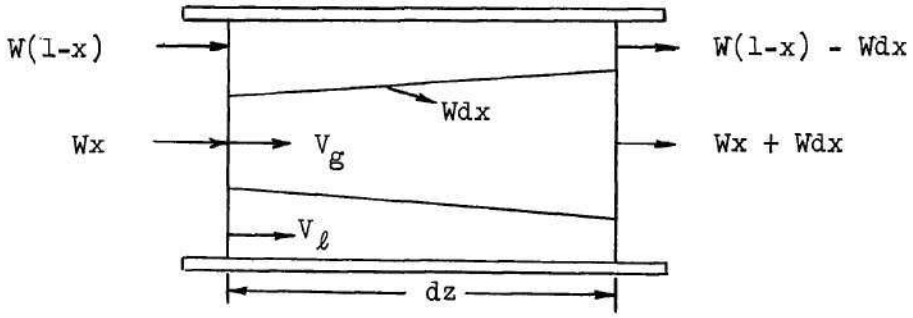

a. Continuity

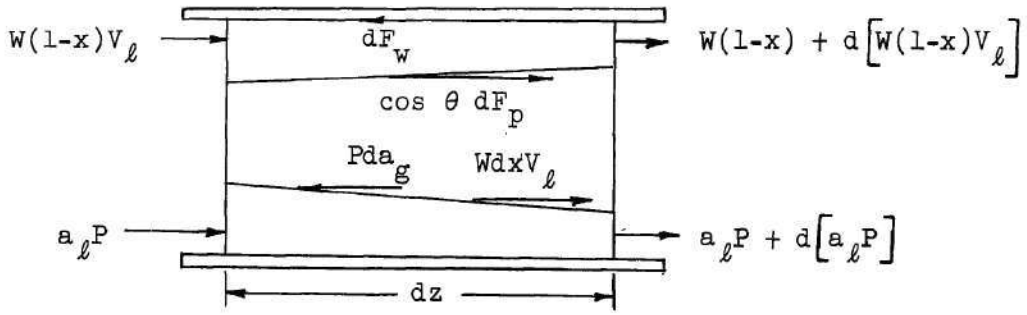

b. Liquid Momentum

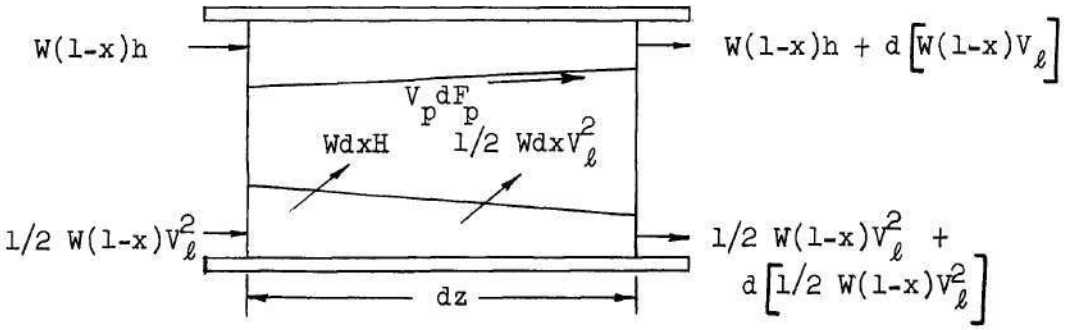

c. Liquid Energy

Figure 1. Diagrammatic Sketch of a Section of Fluid During Annular Flow.

The corresponding momentum equation for the vapor phase is

$$WxdV_g + W(V_g - V_\ell)\, dx + a_g dP + \cos\theta\, dF_p = 0 \qquad (2.306)$$

The total momentum equation can be obtained by adding equations (2.305) and (2.306) to yield

$$d\left[WxV_g + W(1-x)V_\ell\right] + AdP + dF_w = 0 \qquad (2.307)$$

Energy Equations.--The First Law of Thermodynamics for the adiabatic case may be expressed as the time rate of change of the total energy within the control volume is equal to the flux of total energy into the control volume minus the flux of total energy out of the control volume minus the rate of work done by fluid in the control volume. The total energy E is the sum of the enthalpy, kinetic energy and potential energy. The sign convention for the work term is that work done by the fluid in the control volume is positive and work done on the fluid in the control volume is negative (55). The mathematical statement for the First Law of Thermodynamics (56) for the adiabatic case is,

$$\left(\frac{\partial E}{\partial T}\right)_{c.v.} = \int_{c.v.} EdW_{in} - \int_{c.v.} EdW_{out} - \mathcal{W} \qquad (2.308)$$

At steady state the time rate of change of energy in the control volume is zero. Referring to Figure 1 (c) and considering the liquid in a differential length of pipe, dz, as the control volume, the energy equation for the liquid phase gives

$$0 = \left[W(1-x)h + \frac{W(1-x)V_\ell^2}{2} \right] - \left[W(1-x)h + d\left[W(1-x)h\right] + \frac{W(1-x)V_\ell^2}{2} \right.$$

$$\left. d\left(\frac{W(1-x)V_\ell^2}{2}\right) + HWdx + \frac{WdxV_\ell^2}{2} \right] + V_p dF_p$$

Simplifying

$$W\,\Delta H dx + W(1-x)dh + W(1-x)V_\ell dV_\ell - V_p dF_p = 0 \qquad (2.309)$$

The corresponding energy equation for the vapor phase is

$$WxdH + WxV_g dV_g + \frac{(V_g^2 - V_\ell^2)}{2} Wdx + V_p dF_p = 0 \qquad (2.310)$$

The total energy equation can be obtained by adding equations (2.309) and (2.310) to yield

$$d\left(HxW\right) + d\left[W(1-x)h\right] + d\left[\frac{WxV_g^2}{2}\right] + d\left[\frac{W(1-x)V_\ell^2}{2}\right] = 0 \qquad (2.311)$$

The total energy equation can be written as

$$d\left[HxW + hW(1-x) + \frac{WxV_g^2}{2} + \frac{W(1-x)V_\ell^2}{2} \right] = 0$$

For a particular mass flow rate W, the above equation can be integrated with the lower limit taken as the point of initial vaporization where

1. $z = 0$
2. $V_\ell = V_o = W\, v_o/A$

3. $x = 0$

4. $T = T_o$, $h = h_o$, $H = H_o$

5. V_g is finite

and the upper limit taken as any point downstream in the two-phase flow. The result is

$$HWx + hW(1-x) + \frac{WxV_g^2}{2} + \frac{W(1-x)V_\ell^2}{2} - h_oW - \frac{WV_o^2}{2} = 0$$

If the preceding equation is solved for the quality x, the result is

$$x = \frac{h_o - h + 1/2\ (V_o^2 - V_\ell^2)}{\Delta H + 1/2\ (V_g^2 - V_\ell^2)} \qquad (2.312)$$

where ΔH is the latent heat of vaporization and is equal to $(H - h)$. If the kinetic energy terms are neglected in equation (2.312), the expression for the quality is that of an isenthalpic expansion and is given by

$$x = (h_o - h)/\Delta H \qquad (2.313)$$

Summary.--The following is a summary of the important equations derived in this section. Similar equations were obtained by Linning (27).

Continuity:

liquid $\quad W(1-x)v_\ell = a_\ell V_\ell \qquad (2.301)$

vapor $\quad Wxv_g = a_g V_g \qquad (2.302)$

Momentum:

liquid $\quad W(1-x)dV_\ell + a_\ell dP - \cos\theta\, dF_p + dF_w = 0 \qquad (2.305)$

vapor $\quad WxdV_g + W(V_g - V_\ell)dx + a_g dP + \cos\theta\, dF_p = 0 \qquad (2.306)$

Energy:

$$\underline{\text{liquid}} \qquad W\Delta H dx + W(1-x)dh + W(1-x)V_\ell dV_\ell - V_p dF_p = 0 \qquad (2.309)$$

$$\underline{\text{vapor}} \qquad WxdH + WxV_g dV_g + \frac{(V_g^2 - V_\ell^2)}{2} Wdx + V_p dF_p = 0 \qquad (2.310)$$

$$\underline{\text{total}} \qquad x = \frac{h_o - h + 1/2\ (V_o^2 - V_\ell^2)}{\Delta H + 1/2\ (V_g^2 - V_\ell^2)} \qquad (2.313)$$

By a change of variable in the preceding differential equations, the temperature T may be considered as the independent variable rather than distance along the axis of the pipe z. Thus, there are seven independent relations: three algebraic relations from continuity and area relations and a system of four nonlinear differential equations. The variables are V_ℓ, V_g, V_p, a_ℓ, a_g, F_w, F_p, x, T, and thermodynamic properties H, h, ΔH, v_ℓ, v_g, and P which are functions of T only. Parameters are the mass flow rate W and cos θ where cos θ is assumed to depend only on the L/D ratio.

It will be necessary for the present to assume that the quality x is a function of temperature only, and that the interface velocity can be expressed in terms of the other variables by an independent relation. Thus for the system of differential equations the dependent variables are V_ℓ, V_g, F_w and F_p; the independent variable T. For convenience, the system of differential equations may be written in matrix form as

$$\begin{bmatrix} W(1-x) & 0 & -\cos\theta & 1 \\ 0 & Wx & \cos\theta & 0 \\ W(1-x)V_\ell & 0 & -V_p & 0 \\ 0 & WxV_g & V_p & 0 \end{bmatrix} \begin{bmatrix} dV_\ell \\ dV_g \\ dF_p \\ dF_w \end{bmatrix} = \begin{bmatrix} -a_e dP \\ -a_g dP - W(V_g - V_\ell)dx \\ -W(1-x)dh - W\Delta H dx \\ -WxdH - 1/2(V_g^2 - V_\ell^2)Wdx \end{bmatrix}$$

Applying Cramer's Rule to the above system of differential equations, the following four relations are obtained

$$\frac{dV_\ell}{dT} = \frac{-1}{V_\ell}\left\{dh + \frac{\Delta H dx}{(1-x)} + \frac{x}{(1-x)(\cos\theta\, V_g/V_p - 1)}\left[\frac{(V_g-V_\ell)^2 dx}{2x} + V_g dP - dH\right]\right\} \tag{2.314}$$

$$\frac{dV_g}{dT} = \frac{\cos\theta\, x\, dH + 1/2\cos\theta\, dx\,(V_g^2-V_\ell^2) - xv_g dP V_p/V_g - V_p(V_g-V_\ell)dx}{x(V_p - \cos\theta\, V_g)} \tag{2.315}$$

$$\frac{dF_p}{dT} = \frac{W\left[x\, v_g dP - xdH + 1/2\, dx\,(V_g-V_\ell)^2\right]}{(V_p - \cos\theta\, V_g)} \tag{2.316}$$

$$\frac{dF_w}{dT} = \frac{W}{V_\ell(V_p - \cos V_g)}\left\{(V_p - \cos\theta\, V_g)\left[\Delta H dx + (1-x)dh\right]\right. \tag{2.317}$$

$$+ (V_p - \cos\theta\, V_\ell)\left[xdH - 1/2(V_g-V_\ell)^2\, dx\right] +$$

$$\left.\left[\frac{\cos\theta\, V_\ell V_g}{W} - \frac{xv_g + (1-x)v_\ell}{A} V_p\right] AdP\right\}$$

where derivatives indicated on the right of the above differential equations are with respect to temperature.

If equations (2.301) and (2.302) are combined using the result is

$$V_g = \frac{Wxv_g V_\ell}{AV_\ell - W(1-x)v_\ell} \tag{2.318}$$

Equation (2.314) is a function of V_ℓ, V_p, V_g, x, thermodynamic properties and T. V_g can be expressed in terms of V_ℓ by equation (2.318).

The thermodynamic properties and quality are functions of T only. Thus the derivative of the liquid velocity with temperature dV_ℓ/dT, as given by equation (2.314), becomes a function of V_ℓ, V_p and T. Also equations (2.315), (2.316) and (2.317) become functions of V_ℓ, V_p and T.

To relate the vapor velocity V_g and the liquid velocity V_ℓ with temperature T for given values of the parameters W and cos θ it is necessary to solve equations (2.314) and (2.318) with the proper boundary conditions at the point of initial vaporization. Once a simultaneous solution of equations (2.314) and (2.318) is obtained, equation (2.317) can be solved with proper boundary conditions to relate wall shear force F_w with temperature. The wall shear forces F_w can then be related to distance along the pipe axis z by use of a friction factor--Reynolds number relation. This, in turn, will relate all other flow variables with distance along the pipe axis z. The solution of these equations is discussed in detail in the next chapter.

Boundary Conditions.--At the point of initial vaporization the following boundary conditions can be specified.

1. $T = T_o$
2. $V_\ell = V_o = W v_o/A$
3. $V_p = V_o$
4. $x = 0$
5. $\left(\frac{dF_w}{dT}\right)_{T=T_o} = - A \left(\frac{dP}{dT}\right)_{T=T_o}$, which comes directly from equation (2.317).
6. Thermodynamic properties and derivatives of the thermodynamic properties with respect to temperature are finite.

A difficulty arises from the fact that the point of initial vaporization $T = T_o$ is a singular point for the differential equations. Equations (2.314), (2.315), and (2.318) have the form zero divided by zero i.e., the derivative of the liquid velocity with respect to temperature (dV_ℓ/dT) and the vapor velocity V_g are not defined as T approaches T_o. This difficulty is one of the reasons that it is desirable to have information about the flow at some point downstream from the point of initial vaporization. The way this point is circumvented is discussed in the following chapter, and a solution of the differential equations is obtained with the boundary conditions being taken at the point of initial vaporization.

CHAPTER III

SOLUTION OF THE ANNULAR FLOW EQUATIONS

The equations which relate the important variables are

$$\frac{dV_\ell}{dT} = -\frac{1}{V_\ell}\left\{dh + \frac{\Delta H dx}{(1-x)} + \frac{x}{(1-x)\left(\frac{\cos\theta\, V_g}{V_p} - 1\right)}\left[\frac{(V_g-V_\ell)^2 dx}{2x} + v_g dP - dH\right]\right\} \quad (2.314)$$

$$V_g = \frac{W x v_g V_\ell}{AV_\ell - W(1\ x)v_\ell} \quad (2.318)$$

$$\frac{dF_w}{dT} = \frac{W}{V_\ell(V_p - \cos\theta\, V_g)}\left\{(V_p - \cos\theta\, V_g)\left[\Delta H dx + (1-x)dh\right]\right. \quad (2.317)$$
$$+ (V_p - \cos\theta\, V_\ell)\left[x dh - 1/2(V_g-V_\ell)^2 dx\right] + \left[\frac{\cos\theta\, V_\ell V_g}{W}\right.$$
$$\left.\left. - \frac{xv_g + (1-x)v_\ell}{A} V_p\right] AdP\right\}$$

and the available boundary conditions at the point of initial vaporization are

1. $T = T_o$
2. $V_\ell = V_o = W\, v_o/A$
3. $V_p = V_o$
4. $x = 0$

5. $\left(\frac{dF_w}{dT}\right)_{T=T_o} = - A \left(\frac{dP}{dT}\right)_{T=T_o}$

6. Thermodynamic properties and their derivatives are finite.

Other relations that are needed are:

1. The thermodynamic properties and the derivatives of the thermodynamic properties with respect to temperature conveniently represented for computer work.

2. A relation to relate the wall shear force with distance along the tube axis z.

3. A relation for the interface velocity V_p in terms of the other variables.

If the boundary conditions are to be specified at the point of initial vaporization, any numerical procedure that is used will require that the slope of the liquid velocity V_ℓ versus temperature T curve be specified at the point of initial vaporization T_o. This is necessary to start the numerical procedure and obtain the particular solution of the differential equation as specified by the given boundary conditions. The difficulty that is encountered here is that $(dV_\ell/dT)_{T=T_o}$ and $V_g\Big|_{T=T_o}$ have the form zero divided by zero and are therefore not defined at T_o. T_o is a singular point for the differential equation (2.314) and equation (2.318).

In the following sections a numerical procedure, the method of Runge-Kutta, will be applied to the differential equation (2.314). Also points of singularity mentioned above will be resolved.

Thermodynamic Property Relations

Thermodynamic Properties of Steam by J. H. Keenan and F. G. Keyes (52) presents the thermodynamic properties of the saturated liquid and saturated vapor in tabular form. A detailed discussion of the results is given in the "Introduction" of this reference, along with analytical relations used to calculate the results.

For computer use tabular data is not a convenient form to use. The analytical relations given by Keenan and Keyes are unwieldy and are not in a convenient form to use. Also derivatives of the thermodynamic properties with respect to temperature are needed and this would be difficult to obtain from either the tabular data or the analytical relations.

The method that was used to obtain an accurate representation of the thermodynamic properties and their derivatives with respect to temperature was to fit the tabular data by the method of least squares in the temperature range of interest. Library Program P. L. 05 "Least Squares Curve Fitting" (57) for the I. B. M. 650 Digital Computer was used for this purpose at the Rich Electronic Computer Center on the campus of the Georgia Institute of Technology. This library program will find equations of polynomials of degree one through four which best fit (in the least square sense) a given set of data points not more than 299 in number. In addition to the coefficients of the polynomials of degree one through four, this program will give values of f (x) as computed from each of the polynomials for each value of x--input data, also, means, sums of squares, standard deviations, correlations, standard errors of estimate, and "F" test for goodness of fit.

The thermodynamic properties for the saturated liquid and saturated vapor that were fit as a function of temperature T using the previously mentioned program in the range from 170° F to 368° F were pressure P, specific volume of the liquid v_ℓ, specific volume of the vapor v_g, enthalpy of the liquid h, enthalpy of vaporization ΔH, and enthalpy of the vapor H. The least squares polynomials for the thermodynamic properties are:

$$P = 2.1002138\times10^{-8}T^4 - 7.7171229\times10^{-6}T^3 + 1.6371444\times10^{-3}T^2 - 0.16258768T + 6.6913990 \quad (3.101)$$

$$v_\ell = 1.6834591\times10^{-8}T^2 - 2.2433702\times10^{-7}T + 1.6004569\times10^{-2} \quad (3.102)$$

$$v_g = 9.0089112\times10^{-8}T^4 - 1.1194411\times10^{-4}T^3 + 5.2583948\times10^{-2}T^2 - 11.150526\ T + 912.01727 \quad (3.103)$$

$$h = 1.4895535\times10^{-4}T^2 + 0.94243237\ T - 26.480936 \quad (3.104)$$

$$\Delta H = -6.7723173\times10^{-4}T^2 - 0.34243090\ T + 1073.5792 \quad (3.105)$$

$$H = -5.3013464\times10^{-4}T^2 + 0.60103002\ T + 1046.9669 \quad (3.106)$$

where T is in degrees Fahrenheit, P is in psia, v_e is in ft^3 per lb, v_g is in ft^3 per lb, h is in BTU per lb, ΔH is in BTU per lb and H is in BTU per lb. Also the viscosity of water as a function of temperature was fit by least squares within the accuracy of the data obtained from the International Critical Tables (59). The polynomial is given as

$$\mu_\ell = -3.9703004\times10^{-9}T^4 + 4.2085671\times10^{-6}T^3 - 1.6055983\times10^{-3}T^2 + 0.24975186\ T - 10.041969 \quad (3.107)$$

where μ_ℓ is in cps/10.

In all cases the least squares fit of the data was within the accuracy of the data, except for the specific volume of the vapor v_g. In this case the difference between the value as computed by the quartic differed from the tabular values by less than 3% in the temperature range from 170° F to 330° F and less than 7% from 330° F to 364° F.

It is generally undesirable to use derivatives obtained from polynomial fits of data. In the attempt to obtain the best fit of the data the polynomial may contain maximum, minimum, and inflection points, and thus give fluctuating values for the derivatives. Finite difference methods (58) are generally preferred, but these methods can be seriously hampered by round-off error especially in computing differences of higher than the first order. An example is the data for the specific volume of the liquid. Over a two degree interval the specific volume changes one unit in the last significant figure and it would be impossible to obtain an accurate value for the derivative in the range of interest. The least squares quadratic polynomial fits the data to within the accuracy of the data with a smooth curve through the data. Thus differentiating the least squares polynomial will give more accurate values for the derivatives than finite difference methods.

A comparison was made between the derivatives which were obtained from the least squares polynomials and two finite difference methods for the data for the pressure P and the specific volume of the vapor v_g. The finite difference methods were

$$\frac{df(T_n)}{dT} \doteq \frac{1}{h}\left[\Delta n - \frac{\Delta^2 n}{2} + \frac{\Delta^3 n}{3} - \frac{\Delta^4 n}{4}\right] f(T_n)$$

and

$$\frac{df(T_n)}{dT} \doteq \frac{1}{h}\left[\frac{\Delta_n + \Delta_{n-1}}{2}\right] f(T_n)$$

where h is the interval, Δ_n is the first difference taken at T_n and is equal to $f(T_{n+1}) - f(T_n)$.

The agreement between the finite difference methods and the derivatives of the least squares polynomials was of the order of 1.0 per cent and less for the pressure, and of the order of 3 to 5 per cent for the specific volume of the vapor. Reasonable confidence may be placed in the derivatives of the data from these least squares polynomials.

In summary, the thermodynamic property data from the Steam Tables (52) were fit with least squares polynomials. In general the polynomials fit the data within the reported accuracy except as previously noted. The polynomials were examined for maximum, minimum, and inflection points in the temperature range of interest, and none were found. A comparison of the derivatives of the quartic polynomials for P and v_g with two finite difference schemes showed good agreement. The other thermodynamic properties were fit by quadratic polynomials with a smooth curve within the reported accuracy.

Wall Shear Force Relation

It is postulated that the wall shear force can be related to distance along the pipe axis, z, using the usual friction factor--Reynolds number relation, with the Reynolds number given by $DV_\ell/\mu_\ell v_\ell$. The basis for this postulate is that the fluid near the wall of the tube moves under the dual influence of a pressure gradient and shear

forces that are transmitted from the adjacent layer of fluid that travels at a higher velocity. In the case of annular two-phase flow the low velocity and relatively high density core of liquid is replaced by a high velocity and relatively low density vapor core. It is assumed that the net result of this replacement of a low-velocity high-density liquid core with a high-velocity, low-density core does not change the slope of the velocity distribution curve at the wall.

The wall shear force F_w in single-phase flow is given by

$$F_w = f \ (\pi D z)(1/2 \ \rho V^2)$$

where f is the Fanning friction factor.

The above relation can be differentiated with respect to z, noting that D and V are constant for single-phase flow, and the result can be applied to two phase flow. Using equation (2.301) and noting $A = \frac{\pi D^2}{4}$ and $a_\ell/A = 1 - \alpha_{avg}$, where α_{avg} is the void fraction, the result can be written as

$$\frac{dF_w}{dT} = 2f \frac{WV_\ell(1-x)}{D(1-\alpha_{avg})} \frac{dz}{dT}$$

Thus, if the flow variables are known as a function of temperature by the solution of equations (2.314), (2.317) and (2.318), the flow variables may then be related to z, the distance along the pipe, by integrating the previous expression from the point of initial vaporization at T_o where z = 0 to temperature T and distance z.

$$z = \int_{T_o}^{T} \left[\frac{D(1-\alpha_{avg})}{2fWV_\ell(1-x)} \frac{dF_w}{dT} \right] dT \qquad (3.201)$$

where the friction factor is based on all liquid flow for a Reynolds number which is equal to $DV_\ell/v_\ell\mu_\ell$.

A friction factor--Reynolds number relation was obtained from flow rate--pressure drop data for single phase flow in the test section of the experimental equipment and was expressed by the following relation

$$f = 0.00180 + 0.125/(Re)^{0.320} \qquad (3.202)$$

In summary, if the flow variables are known as a function of temperature from the point of initial vaporization T_o to any temperature T, the corresponding length z can be evaluated. The integral relation (3.201) will be evaluated in conjunction with equation (3.202) to compute the value of z. A numerical integration will be made using Simpson's Rule (61).

Physical Requirements on the Flow Variables and the Method to Predict Critical Flow

The following physical considerations are postulated to apply to every point other than the initial point in the expansion.

1. The vapor velocity is greater than the liquid velocity.
2. The vapor velocity is never negative or undefined.

The combined continuity equation, equation (2.318), may be written as

$$V_g = \left[\frac{Wxv_g}{AV_\ell - W(1-x)v_\ell} \right] V_\ell \qquad (2.318)$$

the bracketed part of the above equation must be greater than one, by

the first physical consideration.

$$\left[\frac{Wxv_g}{AV_\ell - W(1-x)v_\ell}\right] > 1$$

If the preceding inequality is solved for V_ℓ, the result is

$$V_\ell < \frac{Wxv_g}{A} + \frac{W(1-x)v_\ell}{A} \qquad (3.301)$$

If Wxv_g/A is defined as the superficial vapor velocity V_g^* and $W(1-x)v_\ell/A$ is defined as the superficial liquid velocity V_ℓ^*, equation (3.301) can be written as

$$V_\ell < V_g^* + V_\ell^* \qquad (3.302)$$

where $V_g^* = \frac{Wxv_g}{A}$ and $V_\ell^* = \frac{W(1-x)v_\ell}{A}$

The combined continuity equation (2.318) may be written as

$$V_g = \frac{Wxv_g V_\ell}{\left[AV_\ell - W(1-x)v_\ell\right]} \qquad (2.318)$$

The bracketed term of the continuity equation as written above must be greater than zero by the second physical consideration

$$\left[AV_\ell - W(1-x)v_\ell\right] > 0$$

If the preceding inequality is solved for V_ℓ, the result is

$$V_\ell > \frac{W(1-x)v_\ell}{A} = V_\ell^* \qquad (3.302)$$

Thus the value of the liquid velocity may be bracketed at each point other than the initial point in the expansion by the superficial liquid velocity and the superficial vapor velocity.

$$V_\ell^* < V_\ell < V_\ell^* + V_g^* \tag{3.303}$$

It should be noted that for a specified mass flow rate W and a specified cross-sectional area of pipe A, the superficial velocities are functions of temperature only. Therefore the value of V_ℓ is bounded by functions of temperature only. This fact will be useful to insure the numerical scheme gives a solution that is compatible with the physical situation.

Other physical requirements which the numerical scheme must satisfy are; first, the liquid velocity must increase from the point of initial vaporization to the critical outlet temperature. The critical outlet temperature is defined as the saturation temperature corresponding to the pressure at the pipe exit for the critical flow rate. Second, the vapor velocity must increase from the point of initial vaporization to the critical outlet temperature. Third, the relative velocity factor, defined as the ratio of the vapor velocity to the liquid velocity, must increase to the critical outlet temperature. Fourth, the slope of the liquid velocity versus temperature curve, dV_ℓ/dT, must approach zero at the critical outlet temperature. These physical requirements are to be illustrated in a following section of this chapter.

The fourth physical requirement mentioned above is the basis for the method to predict critical flow. Consider a constant mass flow rate W, a specified inlet pressure P_o and a variable length of pipe z. As the pipe length is increased to some value which is less than the critical

length of the pipe, $z_{critical}$, the pressure will decrease with z and the liquid velocity will increase with z. As z approaches $z_{critical}$, the exit pressure P approaches the critical exit pressure $P_{critical}$, and the liquid velocity approaches the critical liquid velocity. If z is extended beyond $z_{critical}$ to $z^* = z_{critical} + \delta z$ there will be an adjustment in the mass flow rate if the inlet pressure is maintained constant. The adjusted mass flow rate will correspond to the critical flow rate for the length of pipe z^* and the outlet pressure $P_{critical}$. Thus, the liquid velocity and the vapor velocity approach constant values as z approaches $z_{critical}$, and the slope, dV_ℓ/dT, approaches zero as z approaches $z_{critical}$.

Method of Runge - Kutta

Errors.--In selecting a numerical method, the accuracy of the method must be considered, as this will determine the size of the interval to be used in the method. If the method requires a relatively small interval, the calculations may be seriously affected by round-off error. An attempt to use a larger interval will result in a solution that does not approach the true solution of the differential equation. This is to say that the truncation error is large. A generally accepted method to determine if an interval gives a solution that approaches the true solution of the differential equation is to compute a solution for a specific interval; then compute a solution for an interval one half the previous interval. Compare the two solutions to determine if the two solutions lie within the limits of the required accuracy. If the comparison is not satisfactory, the interval should again be divided in half and the comparison repeated. This procedure should be repeated until a satisfactory solution

is obtained or round-off error makes the solution invalid.

In general, as the accuracy of numerical methods increase, the complexity of the numerical method increases. Thus, for a particular numerical method, there is an optimum between truncation error and round-off error.

The Method.--For this work the method of Runge-Kutta was chosen. If $dV_\ell/dT = f(V_\ell, T)$, the method of Runge-Kutta may be written as

$$V_{\ell,i+1} = V_{\ell,i} + 1/6(b_1 + 4b_2 + b_3) \qquad (2.401)$$

where

$$b_1 = h\, f(V_{\ell,i},\ T_i)$$

$$b_2 = h\, f(V_{\ell,i} + 1/2 b_i,\ T_o + 1/2\ \Delta T)$$

$$b_3 = h\, f(V_{\ell,i} + 2b_2 - b_1,\ T_i + \Delta T)$$

The error in the method of Runge-Kutta (62) is of the order of $(\Delta T)^4$, where ΔT is the interval. The method to obtain the true solution which was previously mentioned was followed in all cases.

Relation for the Interface Velocity

It is necessary to have an expression relating V_p with other flow variables. Previously, it was stated that V_p approaches V_ℓ at the point of initial vaporization. It would also be expected that the interface velocity would approach the maximum liquid velocity from the turbulent flow velocity profile when the liquid annulus is relatively thin compared to the vapor core. This is to say that $V_p = 1.2\ V_\ell$ at some point when the

liquid annulus is relatively thin as compared to the vapor core. Linning (27) experimentally determined that $V_p = 1.2\ V_\ell$ at the critical outlet conditions. He also determined the following empirical relation from his experimental data.

$$V_p = V_\ell \left[1 + 0.2 \ \frac{(T_o - T)^2}{(T_o - T_c)^2} \right]$$

where T_o is the temperature at the point of initial vaporization, T_c is the critical outlet temperature, and T is the temperature in the expansion corresponding to V_ℓ.

The relation between V_p and V_ℓ used in this study is given by

$$V_p = V_\ell \left[1 + 0.2/81 \ (T_o - T)^2 \right] \qquad (2.402)$$

Equation (2.402) is a modification of Linning's empirical relation by approximating the difference between the inlet temperature and the critical outlet temperature as 9° F. Further discussion of equation (2.402) is given in Chapter VI.

Starting the Solution

The initial slope of the liquid velocity temperature curve is not defined, as the point of initial vaporization is a singular point for the equations. If the initial slope is determined by trial and error subject to the physical considerations mentioned in the preceding section, the result will be the required solution of the annular flow equations. In general, the accuracy that is required for the initial slope is from five to eight significant figures to obtain the required solution of the liquid velocity as a function of temperature

from the temperature at the point of initial vaporization to the outlet temperature. An example is given in Figure 2.

The solution was started using the following relation

$$V_{\ell,1} = V_o + \left(\frac{dV_\ell}{dT}\right)_{T_o} \Delta T \qquad (2.403)$$

where (dV_ℓ/dT) is the initial slope, ΔT is the interval, $V_o = Wv_o/A$, and $V_{\ell,1}$ is the liquid velocity at $T + \Delta T$. The method of Runge-Kutta, equation (2.401), was used to continue the solution.

A description of the details of the computer solution and the computer program is given in Appendix G. Also a typical example of the results are given in this appendix, along with Table 38, a table of ALGOL symbols.

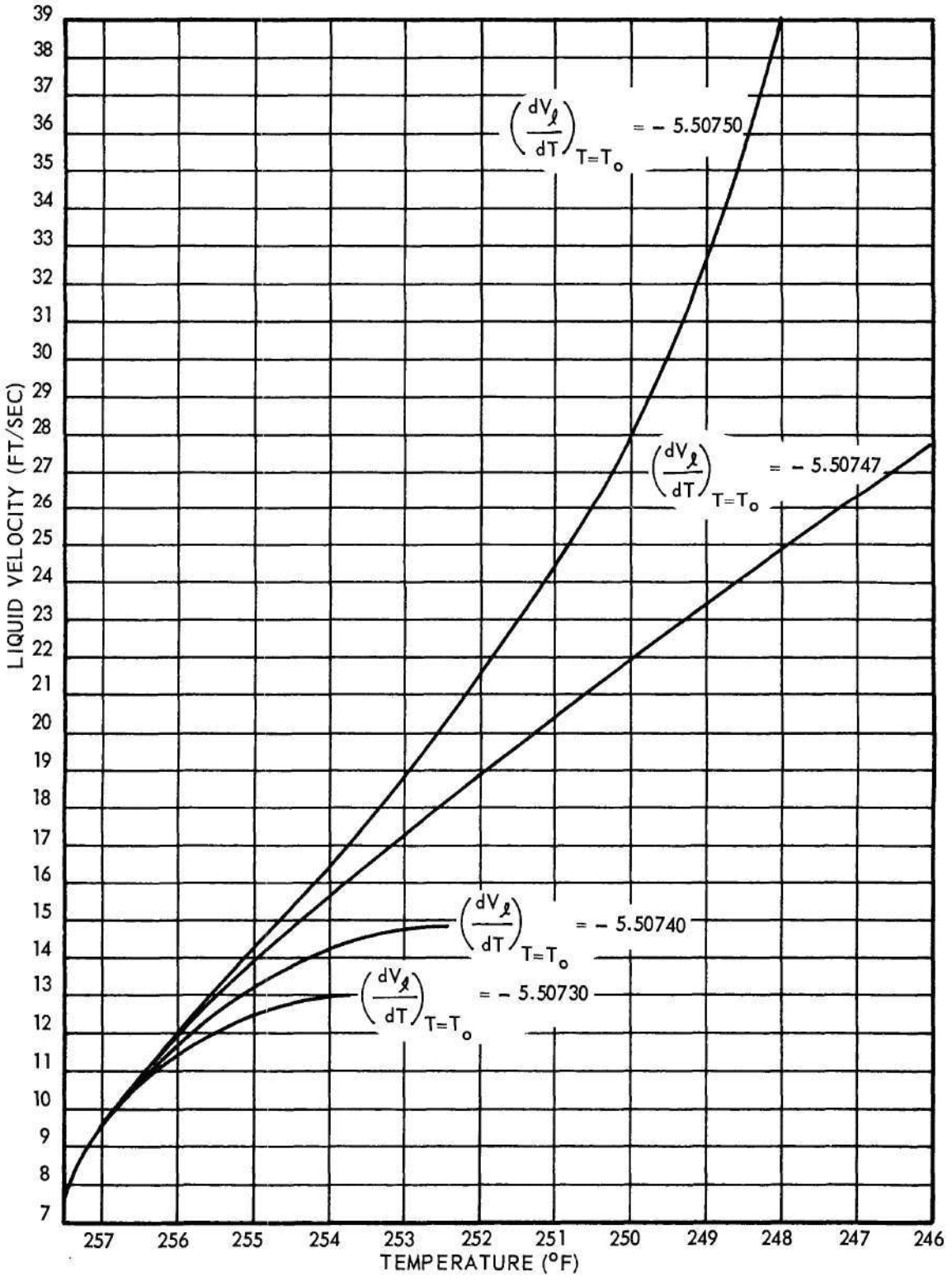

Figure 2. Effect of $(dV_\ell/dT)_{T = T_o}$ on the Solution of the Annular Flow Equations.

CHAPTER IV

THE EXPERIMENTAL SYSTEM

The experimental system was designed to obtain data on adiabatic two-phase flow of steam and water in a range where no experimental data is presently available. It was also designed to obtain the proper data which could be used in conjunction with the previously described Annular Flow model to determine the accuracy of the model as is discussed in Chapter VI. This design also included features for determining the validity of the assumptions on which the Annular Flow model was based. If the assumptions in Chapter II are reviewed, assumptions of horizontal pipe and steady state were made applicable in the design and operation of the experimental apparatus. The validity of assumptions of constant temperature at any cross-section normal to the flow and thermodynamic equilibrium at all stages of the expansion were assessed by simultaneous pressure and temperature measurements at various cross-sections of the test section. In addition to these measurements, the void fraction of the two-phase flow was to be made at various cross sections and was to be compared with the void fraction as calculated from the Annular Flow model.

The experimental system which was necessary for the above mentioned measurements will be discussed in the following paragraphs. The experimental system is shown in a schematic diagram in Figure 3, and pictorially in Figure 4 (a) and (b). It will be convenient to discuss the system in two sections. The auxiliary equipment will be discussed in the first section, and the test section with the associated instrumentation will be

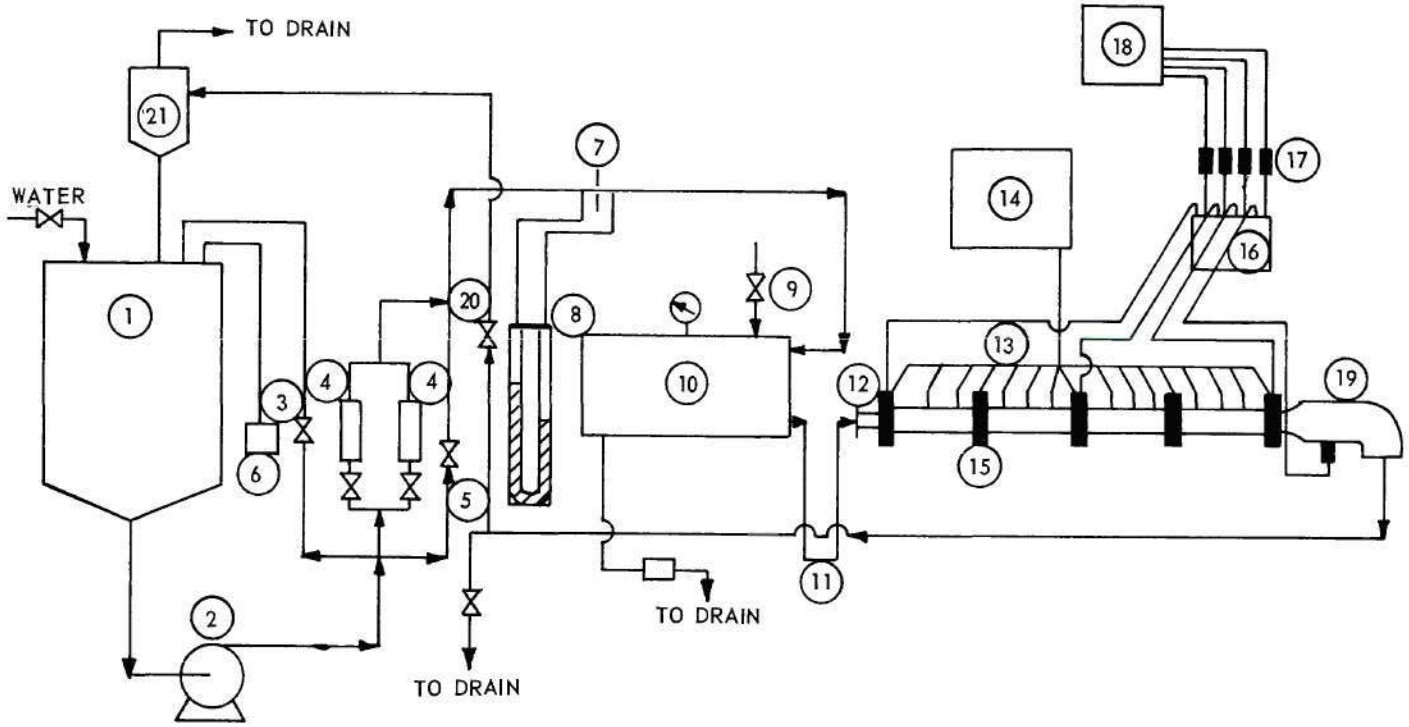

1. storage tank
2. pump
3. recycle control valve
4. rotameters
5. orifice control valve
6. potientometer
7. metering orifice
8. manometer
9. steam control valve
10. heat exchanger
11. one inch loop
12. upstream observation section
13. thermocouples
14. temperature recorder
15. piezometric rings
16. constant temperature bath
17. pressure transducers
18. pressure recorder
19. expansion section
20. downstream control valve
21. cyclone separator

Figure 3. Schematic Diagram of the Experimental System.

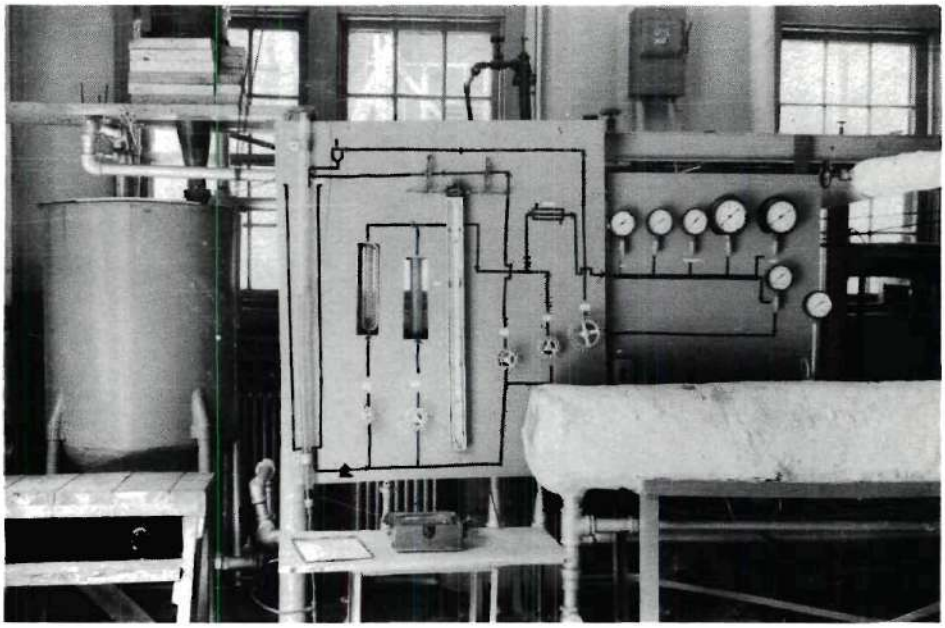

a. Supply Tank, Heat Exchanger, and Control Panel

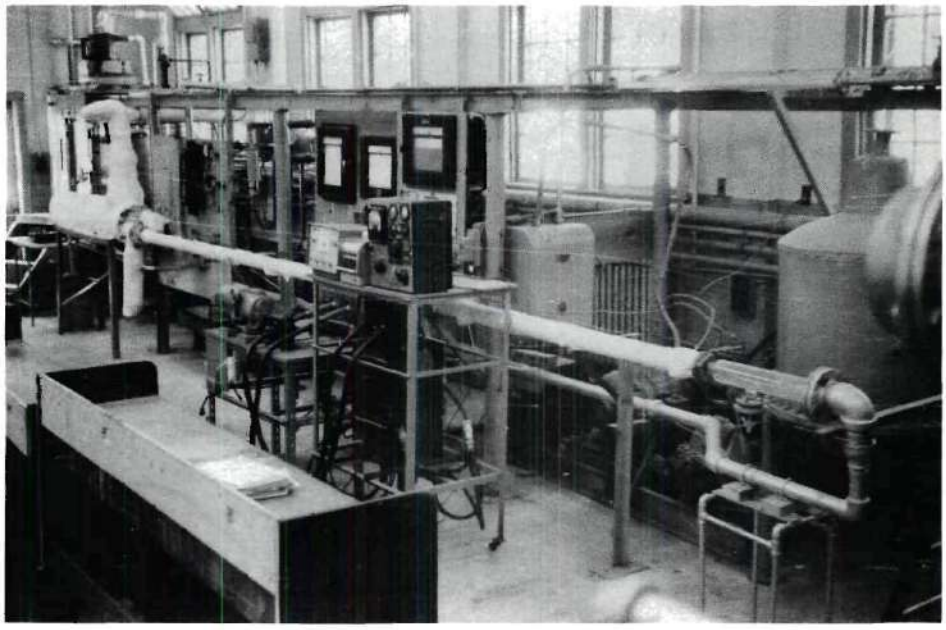

b. Overall View of the Experimental System

Figure 4. Experimental System.

discussed in the second section.

Auxiliary Equipment

With reference to Figure 3, it can be seen that the water is pumped from the storage tank through the flow metering devices and through the heat exchanger to the test section. From the test section the two-phase mixture of steam and water flows to the cyclone separator where the steam and water are separated with the water flowing back into the storage tank and the steam exhausted into the drain.

The conical bottom storage tank has a volume of about 125 gallons. Water is pumped from the bottom of the storage tank by an Ingersoll-Rand 1 CORVNL pump having a capacity of 50 GPM against a head of 205 feet of water to the flow metering devices.

The liquid leaving the pump flows through two rotameters, a recycle line, and rotameter bypass line, which are connected in parallel. The smaller rotameter was a Fisher and Porter rotameter with a maximum capacity of 2.5 GPM. The larger rotameter was a Schutte and Koerting rotameter with a maximum capacity of 11.5 GPM. The rotameter bypass line was equipped with a metering orifice for measurement of flowrates between 14 and 50 GPM. A U-tube manometer containing mercury and water measured the pressure drop across the orifice. The two rotameters and the metering orifice were calibrated in this laboratory. The recycle line was used in conjunction with the particular flow metering device used and the downstream control valve to control the inlet pressure and flow rate to the test section.

The water was raised from its initial temperature to near the saturation temperature corresponding to the pressure at the entrance of

the test section by a six-pass Taco heat exchanger, number 8612SW. The 165 psig laboratory steam was metered to the heat exchanger by a globe valve. The steam pressure in the shell was measured with a Bourdon tube-type pressure gage.

The water flowed from the heat exchanger through a three-foot loop of one-inch pipe. The loop was fitted with stainless steel screens at the entrance, center, and exit to subdivide any superheated steam bubbles which were formed as a result of boiling in the heat exchanger. A one and one-half inch inside diameter by six inches long Pyrex glass section was installed between the loop and the test section for visual observation to insure that the liquid entering the test section did not contain any steam bubbles. Also the loop was fitted with an adjustable metal strap to maintain the test section under tension and prevent the test section from buckling due to metal expansion when the temperature was increased from room temperature to the operating temperature.

The expansion section at the test section exit was a two and one-half foot section of Pyrex glass pipe of three inch inside diameter which was reduced to a one and one-half inch glass flange at one end, and this end was attached to the exit of the test section. In the center of the expansion section, a one inch glass flange was attached to permit a pressure measurement at this point.

The two-phase mixture flowed from the expansion section through the downstream control valve, a two-inch globe valve and to the cyclone separator. The cyclone separator separated the steam and the water. The water flowed back into the storage tank,and the steam was exhausted into the drain. Drain lines were also provided to drain the system of water.

Test Section and Associated Instrumentation

The test section and the associated instrumentation are discussed in the following paragraphs. The associated instrumentation included means for temperature measurement and recording, pressure measurement and recording, and void fraction measurement and recording.

Test Section.--The test section was one-inch outside diameter with 0.035 inch wall thickness, type 304 stainless steel, seamless tubing. The test section was 19.42 feet in length and was connected at the upstream end to the previously described Pyrex glass observation section. The downstream end was connected to the previously described expansion section. The test section was insulated with commercial magnesia insulation after the experimental system was pressure tested for leaks with water flowing at 100 psia and 250° F.

Pressure Measurements.--In Figure 5 (a) the pressure recorder is shown on the right; in Figure 5 (b) the pressure tap design is shown; and in Figure 5 (c) one of the pressure transducers used in the pressure measurement is shown.

Five pressure taps were installed on the test section at five foot intervals from the exit of the test section to the entrance of the test section. With reference to Figure 5 (b), three one eighth inch diameter holes were tapped in the pipe with a 60° angle between each hole in the plane of the cross-section of the tube. The holes were tapped carefully to maintain the circular cross-section of the tube, and all burrs and ragged edges were removed. The piezometric rings were machined from brass. Three holes were tapped and threaded with one-eighth inch pipe threads with a 60° angle between each hole in the plane of the

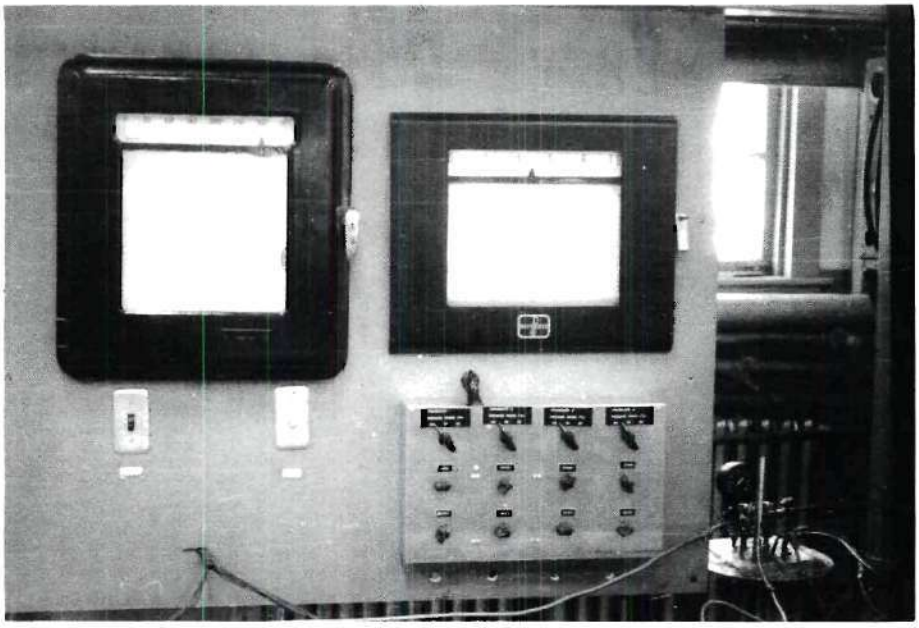

a. Temperature Recorder, Pressure Recorder, and Pressure Transducers

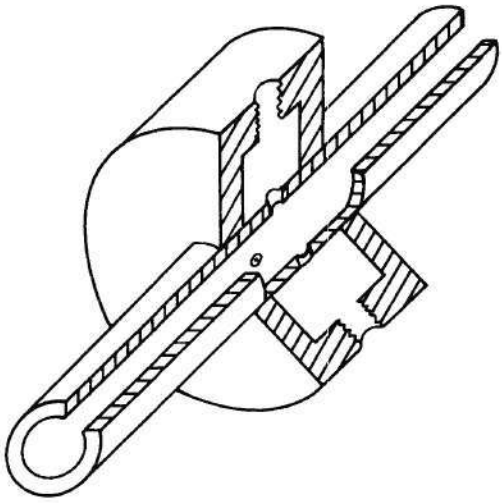

b. Pressure Tap Design

c. Pressure Transducer

Figure 5. Temperature and Pressure Measurements.

cross-section of the piezometric ring. The piezometric rings were slipped on the tube, and the holes in the piezometric ring were visually aligned with the holes in the tube. The piezometric rings were then carefully silver soldered to the tube. Thus the difficulty in attempting to attach pressure taps directly to the tube was overcome, and also three separate taps could be attached to the pipe at one point. One of these taps was used for the transducer pressure lead line, the second for a thermocouple, and the third for a pressure lead line to the Bourdon tube pressure gages used to visually monotor the pressure along the test section as shown in Figure 4 (a).

Four Consolidated Electrodynamic Corporation Type 4-312 pressure transducers with a range from 0.0 to 100.0 psig were used to measure the pressure at the entrance, center, and exit of the test section; and also at the expansion section. An eight point Bristol Dynamaster Recorder Model M 8RB560-51-T16X was used to record the output signal from the transducers. The accuracy rating of the recorder is ± 0.25 per cent of the full scale reading, and the accuracy rating of the pressure transducers is less than ± 0.5 per cent of the full scale reading or less than ± 0.5 psi. The pressure transducers were calibrated in this laboratory with a dead weight tester within the accuracy of the pressure transducer - recorder system i.e., to ± 0.5 psi. External controls were supplied between the transducers and the recorder to permit accurate zero calibration and accurate full scale calibration.

The change in temperature from room temperature to operating temperature prevented the attachment of the temperature sensitive pressure transducers directly to the piezometric rings, and it was necessary to

run pressure lead lines of one-eighth inch copper tubing from the piezometric rings, through a water bath and to the pressure transducers mounted directly above the water bath. This is shown diagrammatically in Figure 3 and pictured in Figure 5 (a). The transducers were in the same horizontal plane as the test section. The pressure lead lines were filled with oil, and the transducers were calibrated with these lead lines attached to the transducers. The lead lines were attached to the piezometric rings in a manner to prevent the oil from draining into the test section and to provide an oil-water interface at the piezometric rings which furnished a resistance to heat transfer. This method was successful as during the test runs the lead lines remained at room temperature, except for a length of two to three inches from the piezometric rings. The calibration of the pressure transducers was checked at frequent intervals during the period in which the test runs were made, and also the oil-water interface was checked at these times. The pressure lead lines did not affect the response of the transducers for the pressure fluctuations which were encountered in this work.

Temperature Measurement.--In Figure 5 (a) the sixteen point Leeds and Northrup, Micromax Recorder Model S 40000 is pictured which used iron-constantan thermocouples to measure the temperature on the test section. The temperature range measured by the recorder and thermocouples was from 0 to 350° F, and the accuracy rating of the recorder was ± 0.25 per cent of the full scale reading. The thermocouples were calibrated in this laboratory to within the accuracy of the recorder which is ± 1.0° F.

The iron-constantan thermocouples were prepared from commercial thermocouple wire cut to the proper length. The thermocouples were care-

fully attached to the pipe with a bead of solder of the order of one-eighth to one-sixteenth inch in diameter, and several turns of the thermocouple wire were taken around the tube. Referring to Figure 3, the thermocouples were spaced at 1.25 feet intervals from the exit of the pipe. Thermocouples which were attached at the piezometric rings were held with epoxy resin at a point just outside one of the holes drilled in the tube as a pressure tap. This permitted an accurate measurement of the fluid temperature but did not disturb the flow. The thermocouple calibration was checked with all liquid flowing in the test section. The temperature of the water in the tank was measured with a previously calibrated mercury thermometer as the water was recirculated through the test section. The temperatures as measured at the test section were compared with the tank temperature and found to be within the accuracy of the recorder, ± 1.0° F.

Appendix F shows the calculations which estimate the temperature drop across the tube wall to be 0.2° F. Also included in Appendix F is the calculation which shows that the heat loss from the test section to the surroundings was small, thus justifying the assumption of adiabatic flow. Also the problem of axial conduction along the tube was considered, and it was shown that axial heat flow did not affect the assumption that the temperature measured on the outside of the tube at a cross-section was equal to the fluid temperature at that cross-section.

At the startup and during the test runs, the temperature in the tank was monitored with an iron-constantan thermocouple placed in the tank. The temperature was read on a Wheelco Model 4 portable self-balancing potentiometer located at the control panel. (See Figure 4 (a).)

Void Fraction.--A review of the literature and discussion of the difficulties which are involved in the measurement of the void fraction were given in Chapter I. With reference to the necessity of having a monoenergetic gamma beam, Marchaterre (64) reported that a majority of the intensity of the gamma beam from thulium - 170 which was used in the Argonne National Laboratory work came not from the 0.08 Mev gamma beam emitted from the radioactive source, but from Bremsstrahlung radiation as a result of the 0.97 Mev beta particles impinging on the aluminum window in the source holder. Richardson (38) gave the energy spectrum for thulium - 170. This suggested that a monoenergetic source is not necessary for void fraction measurements, and a radioactive source that inherently gives a spectrum of gamma-ray energy could be used. Such a source is an X-ray tube that is operated with the difference in potential between the target and the filament at a value which is less than that required to obtain a sharp line spectrum.

From the above discussion an X-ray tube might prove suitable for the measurement of the void fraction. The suitability of the use of an X-ray tube will be ascertained with the following calculations and discussion. It will also be ascertained if a system of air and plastic will simulate the system of steam and water.

In Figure 6 the X-ray spectrum from the tungsten target of an X-ray tube operating at a peak voltage of 45Kv (65) is shown. In Figure 7 the mass attenuation coefficient for air, water, and plastic from the data of Grodstein (66) and Clark (67) are shown. Using the data from Figure 7 along with the data from Grodstein (68) for steel and considering a narrow beam of monoenergetic gamma-rays passing through the diameter of

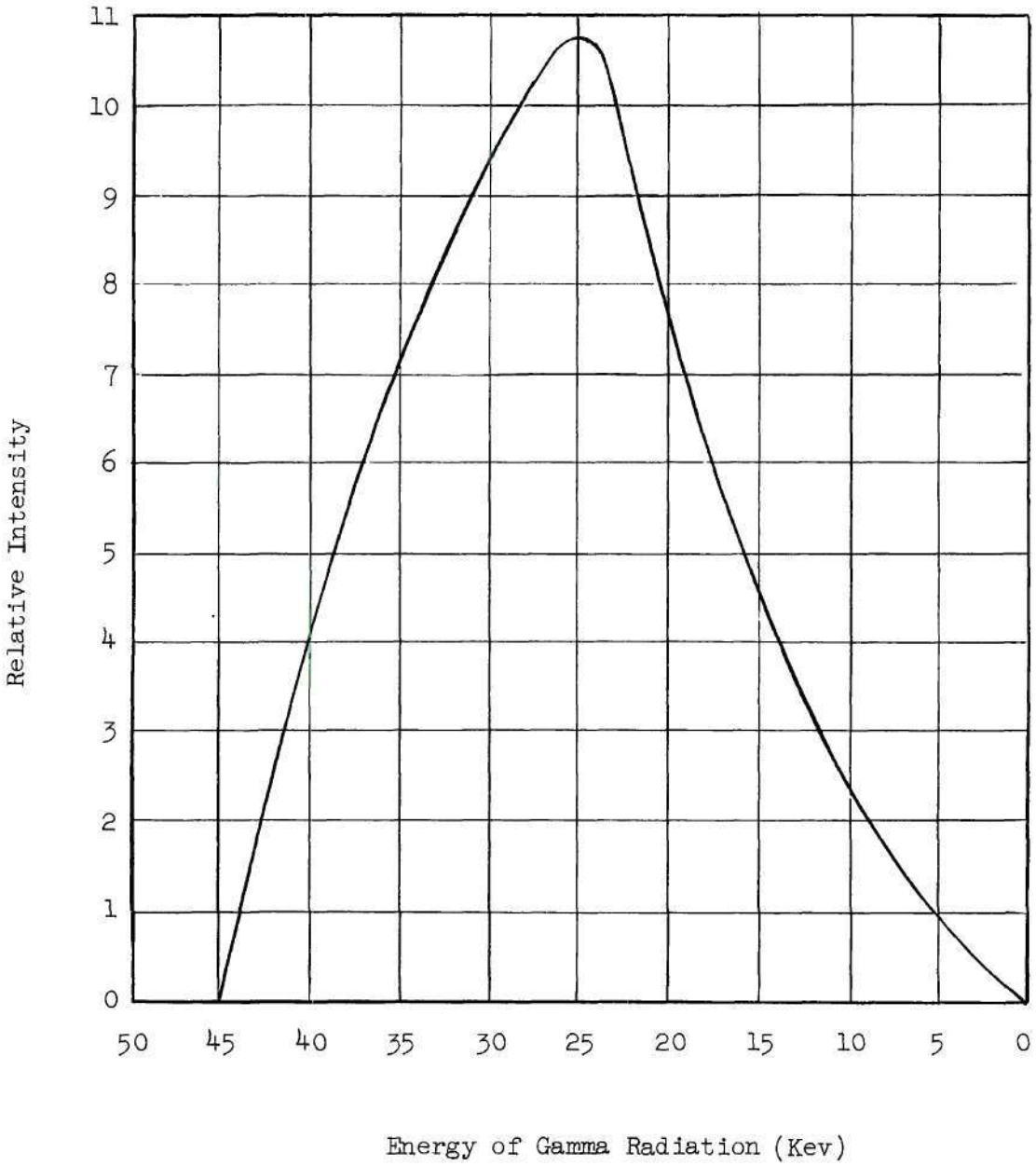

Figure 6. Energy Spectrum for a 45 KVP X-ray Tube.

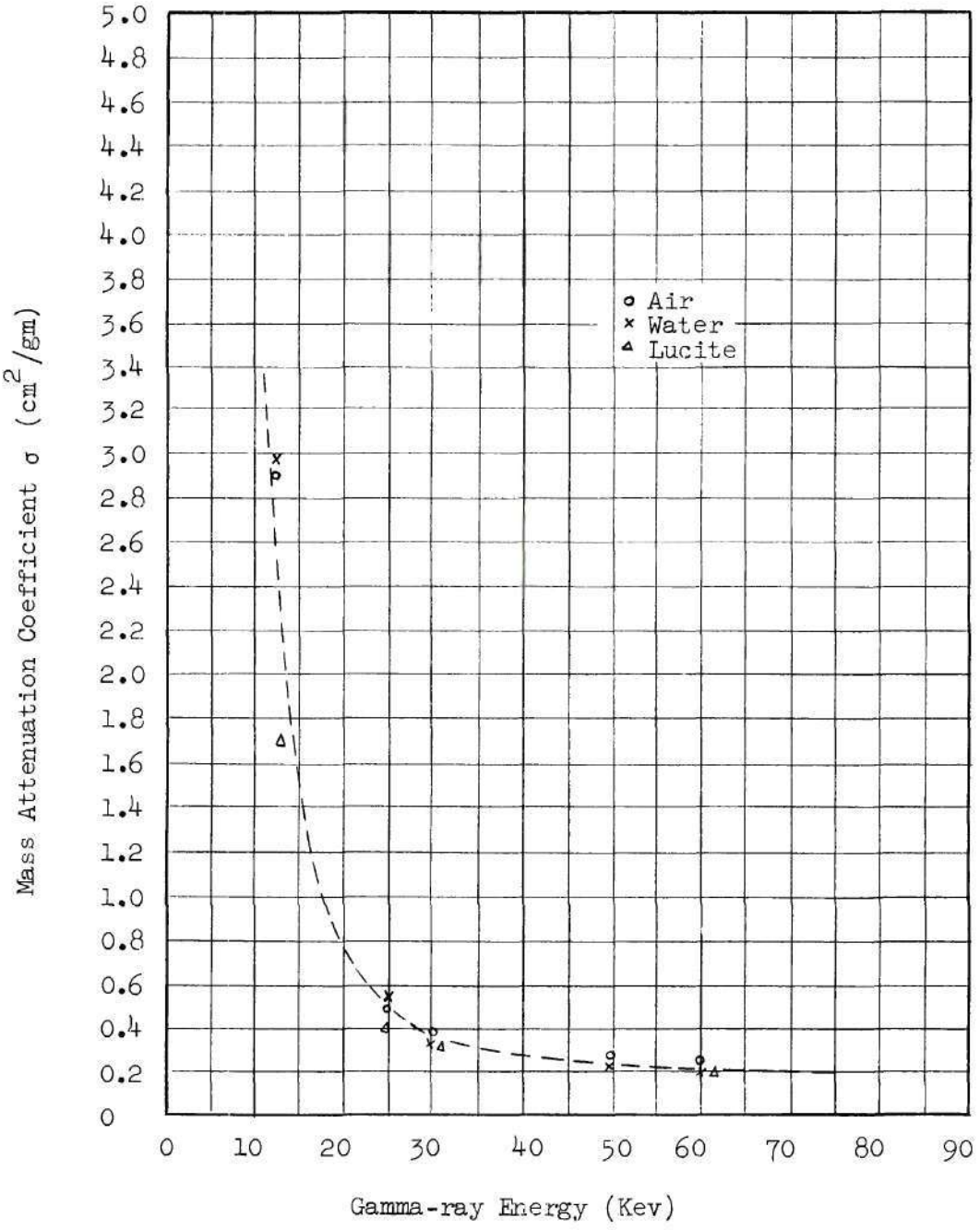

Figure 7. Attenuation Coefficients of Air, Water, and Lucite.

the one inch outside diameter tube of 0.035 inch wall thickness, the attenuation of a monoenergetic gamma beam may be calculated for the tube full of water at a given temperature. The equation which is applicable is

$$\left(\frac{I_F}{I_o}\right) = e^{-(\sigma_s \rho_s 2t_s + \sigma_w \rho_w D)} \qquad (4.201)$$

where (I_F/I_o) is the fractional change in intensity of the gamma beam as it passes through the tube full of water, σ_s and σ_w are the mass attenuation coefficients of steel and water respectively, ρ_s and ρ_w are the densities of steel and water respectively, t_s is the wall thickness of the tube and equals 0.035 inches, and D is the inside diameter of the tube and equal to 0.930 inches. The corresponding equation for the tube full of steam is,

$$\left(\frac{I_{MT}}{I_o}\right) = e^{-(\sigma_s \rho_s 2t_s + \sigma_w \rho_g D)} \qquad (4.202)$$

where ρ_g is the density of steam.

The fraction change in intensity of the pipe full of water, equation (4.201), and the fractional change in the pipe full of steam, equation (4.202) were calculated as a function of gamma ray energy from 10 Kev to 45 Kev for temperatures of 212° F (14.7 psia) and 328° F (100 psia). Also the corresponding values were calculated for air and lucite at 70° F. For a given gamma ray energy the fractional change in intensity for the tube full of water at 328° F was about 10 to 12 per cent greater than the fractional change in intensity at 212° F because

the change in the density of the water and of the steel was small over this range. The fractional change in intensity for the tube full of lucite was about 10 to 12 per cent less than the fractional change in intensity of the tube full of water at 212° F, as the density of the lucite is of the order of 1.18 gm/cm^3. With this information, the ratio (I_{MT}/I_F) was also calculated.

The Relative Intensity is defined as the ratio of the fractional change in intensity at a specific gamma-ray energy to the fractional change in intensity at 45 Kev for the tube full of steam.

$$\text{Relative Intensity} = \frac{(I/I_o)_{X\ \text{Kev}}}{(I_{MT}/I_F)_{45\ \text{Kev}}} \qquad (4.203)$$

In Figure 8 the Relative Intensity as a function of gamma ray energy for steam and water at 328° F is shown. Corresponding plots for steam and water at 212° F and lucite and air at room temperature are similar. The X-ray spectrum shown on Figure 8 was taken from Figure 6. It may be seen in Figure 8 that the Relative Intensity is essentially zero for 30 Kev and less. Thus, it may be said that the tube walls attenuate all of the beam below 30 Kev and only the photons of an energy between 45 Kev and 30 Kev pass through the tube. If the X-ray spectrum is examined with reference to the Relative Intensity, a large percentage of the photons have an energy between 33 Kev and 42 Kev. If the curve (I_{MT}/I_F) is examined, this fractional change in intensity from the tube full of water to the tube full of steam is nearly constant as a result of the fact that the attenuation coefficients are nearly constant in this range of gamma-ray energy. Thus the result of these considerations shows that:

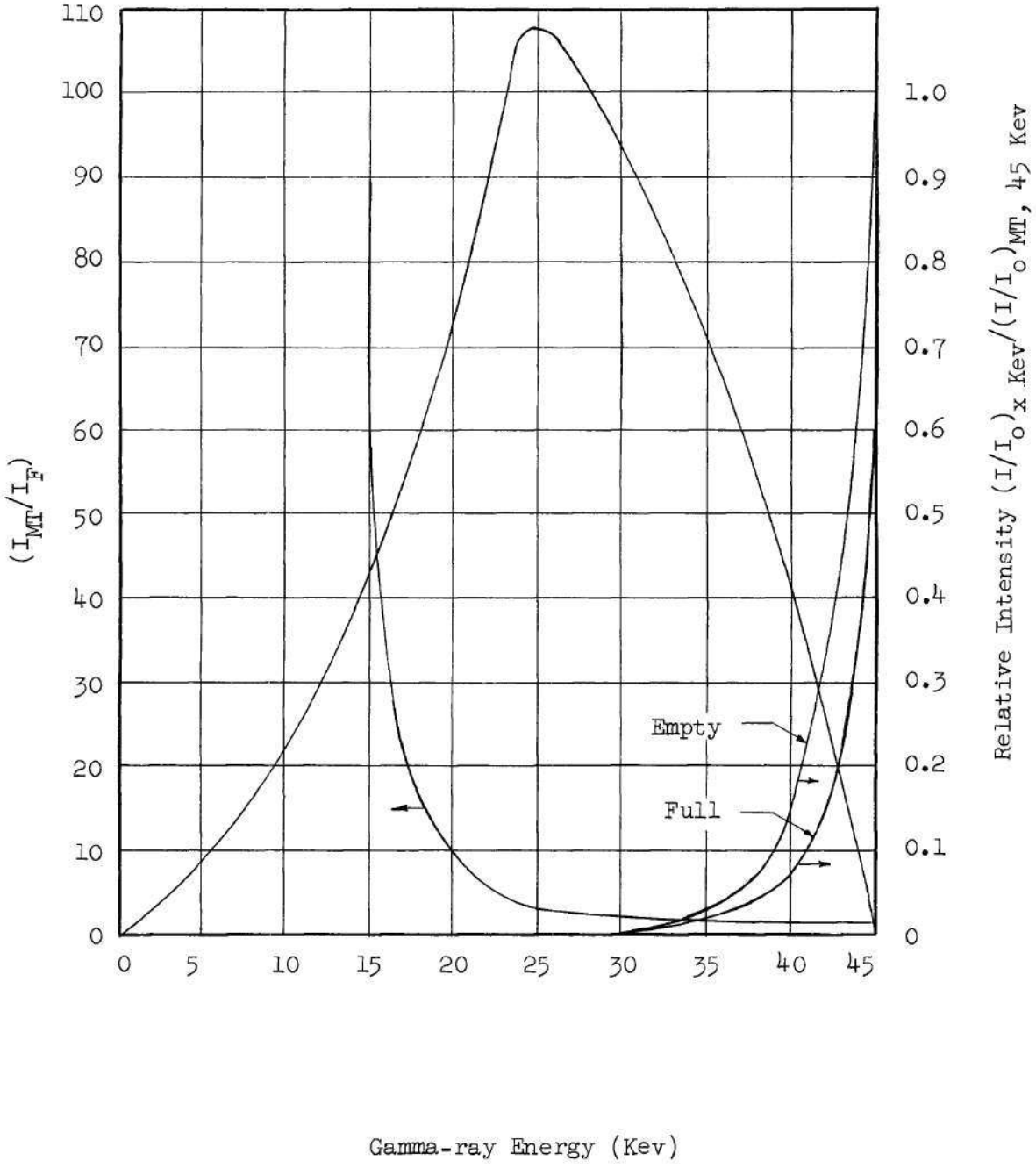

Figure 8. Relative Intensity versus Gamma-ray Energy.

1. Only the photons which have sufficient energy not to be attenuated by the pipe containing the liquid or vapor lie in the range between 30 Kev and 45 Kev.

2. The fractional change in intensity from the tube full of water to the tube full of steam is constant in the range between 30 Kev to 45 Kev.

Therefore, it may be concluded on the basis of these calculations that an X-ray tube which has the characteristic spectrum of gamma-ray energy may be considered as a monoenergetic gamma-ray source for the conditions that were previously specified.

The local void fraction α is defined as the ratio of chordal length of vapor to the cordal length of the tube, and is given by

$$\alpha = \frac{\ell n(I_{TP}/I_F)}{\ell n(I_{MT}/I_F)} \tag{4.204}$$

The average void fraction α_{avg} is given by

$$\alpha_{avg} = \frac{8}{\pi} \int_0^1 \alpha \sqrt{y(1-y)}\ dy \tag{4.205}$$

the fractional error in the local void fraction e is given by

$$e = \left[\frac{\Delta I_{TP}}{I_{TP}} \ \ell n \ \frac{I_{MT}}{I_F} + \frac{\Delta I_{MT}}{I_{MT}} \ \ell n \ \frac{I_{TP}}{I_F} + \frac{\Delta I_F}{I_F} \ \ell n \ \frac{I_{MT}}{I_{TP}} \right] \left[\frac{1}{\ell n \ \frac{I_{MT}}{I_F} \ \ell n \ \frac{I_{TP}}{I_F}} \right] \tag{4.206}$$

The error in the average void fraction e_{avg} is given by

$$e_{avg} = \frac{8}{\pi} \int_0^1 e \sqrt{y(1-y)}\ dy \qquad (4.207)$$

The derivations of equations (4.204), (4.205), (4.206) and (4.207) are given in Appendix C.

As it was shown previously a system of steam and water may be simulated by a system of lucite and air. The previous calculations may be confirmed experimentally by preparing mockups of possible two-phase flow patterns from lucite. The attenuation of the gamma beam from a 45 Kev peak X-ray tube may be measured, and the local void fraction α and the average void fraction α_{avg} can be calculated by equations (4.204) and (4.205). These calculated values of the void fraction may be compared with the predetermined actual values of the void fraction of the lucite mockup with reference to the statistical error involved in the counting as discussed in Appendix D and given by equations (4.206) and (4.207).

In Figure 9 (a) an overall view of the void fraction apparatus in position on the test section is shown. A Picker X-Ray tube Model PX-3B with a tungsten target was mounted in a carrage and shielded with one-eighth inch lead sheet. The carrage was mounted on rails and moved in a horizontal straight line perpendicular to the test section by a lead screw. The lead screw was attached to a Boston Gear Reducer. The Boston Gear Reducer was attached to a Master Speedranger variable speed gear reducer. This combination permitted variation of the traverse time across the tube from two minutes to eight minutes. The X-ray tube, carrage, and speed reducers were mounted on a table with adjustable legs.

Columniation of the gamma beam between the X-ray tube and the test section was accomplished by a hole of 3/32 inch diameter which was drilled

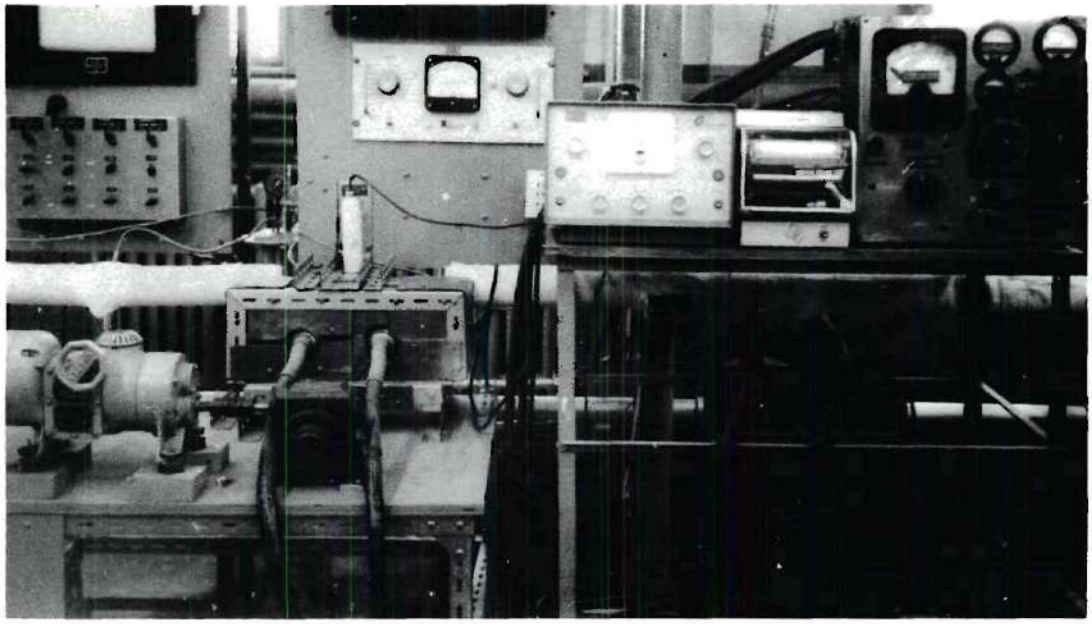

a. Overall View of the Void Fraction Apparatus

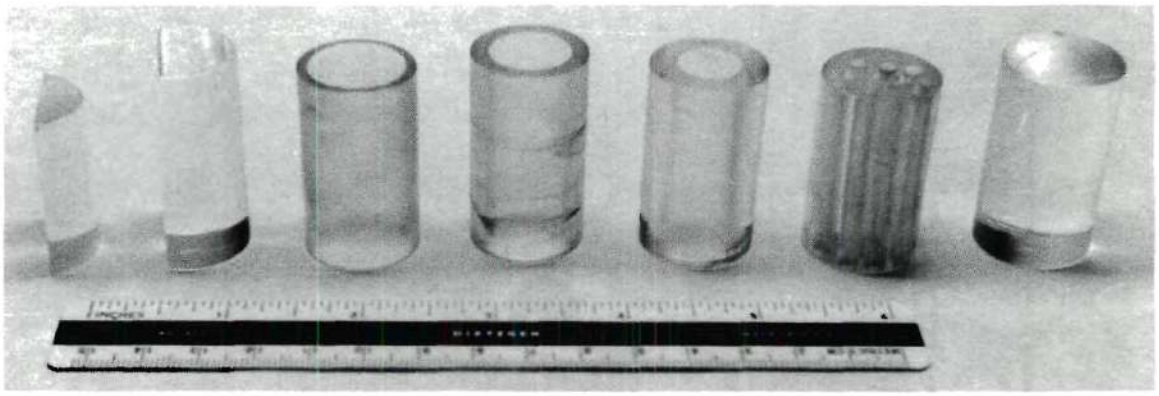

b. Lucite Mockups Numbers 1 through 7 from Left to Right

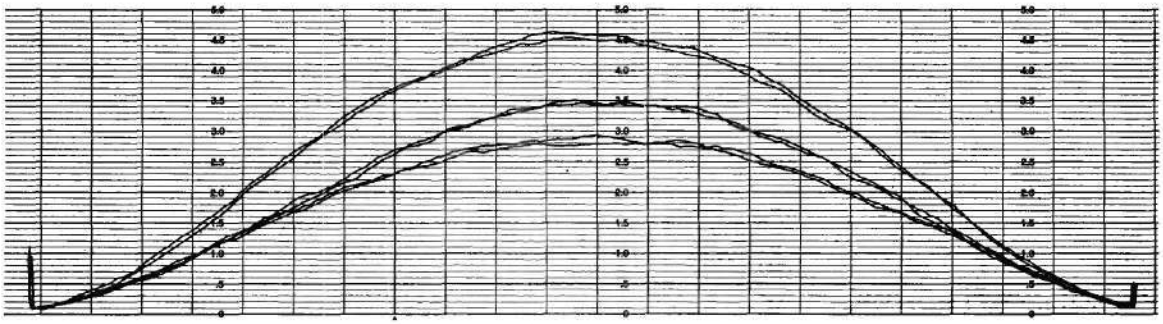

c. A Typical Composite Traverse – Mockup No. 6

Figure 9. Void Fraction Apparatus, Lucite Mockups, and a Typical Composite Traverse.

in a one-fourth inch thick lead sheet. The lead sheet was placed over the X-ray tube and aligned by measuring the count rate. Columniation between the top of the test section and a Nuclear Chicago Geiger - Mueller tube Type D-34 was accomplished by a one-sixteenth diameter hole drilled in a one-half inch thick sheet of lead, and was aligned by measuring the count rate. Both sheets of lead were mounted securely to the carrage. Columniation below the test section provided a parallel beam of radiation from the X-ray tube and reduced the possibility of scatter of the radiation. Columniation of the beam above the test section allowed the Geiger-Mueller tube to receive only the essentially parallel beam of radiation that could pass up the one-sixteenth inch diameter hole. Any radiation that hit the lead surrounding the hole was wholly attenuated.

The output from the Geiger-Mueller tube was measured by a Nuclear Chicago Analytical Count Rate Meter Model 1620A and recorded by a Texas Instruments Rectiriter strip chart recorder. The count rate meter measured the intensity of the radiation in counts per minute for six full scale ranges from 300 cpm to 100,000 cpm. The effective time constant for the tank circuit in the count rate meter could be selected for values 0.5, 2.0, 10.0 and 50.0 seconds. The plateau for the Geiger-Mueller tube was determined by the standard technique (69) of plotting the curve of intensity in counts per minute versus voltage on the Geiger-Mueller tube. The plateau is the region on the curve where the count rate is substantially constant with a change in voltage. The operating point was determined to be 1.0 Kv.

For a particular time constant and count rate, the fractional statistical error in the count rate is given by the following equation (70):

$$\frac{\Delta I}{I} = \frac{C}{\sqrt{2IC_t}} \qquad (4.208)$$

where $\Delta I/I$ is the fractional statistical error in the count rate I, C_t is the time constant in the tank circuit, and C is a constant which depends on the confidence limit. Table 1 gives the value of C and the corresponding confidence limit (71).

The schematic wiring diagram for the X-ray tube, transformer and control panel is given in Figure 10. Controls were provided to vary the peak voltage on the X-ray tube from 30 Kv to 55 Kv, and to vary the filament current from 1.0 to 50.0 milliamperes. For continuous operation

Table 1. Confidence Limits Corresponding to C

C	Confidence Limit	Reference Name
0.50	0.383	
0.6745	0.500	Probable Error
1.00	0.683	
1.65	0.900	Reliable Error
2.58	0.990	99% Error
3.00	0.997	99.7% Error

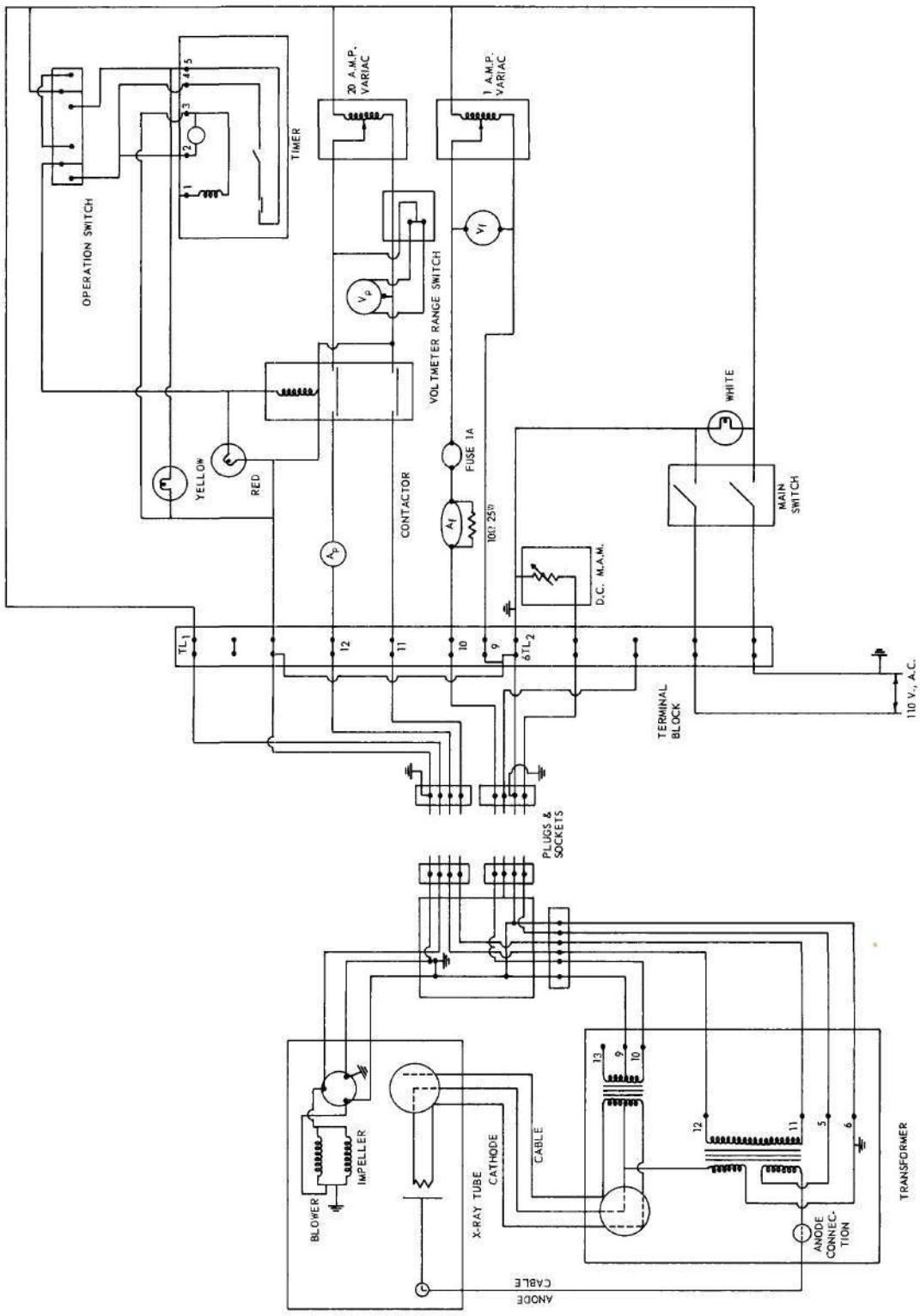

Figure 10. Wiring Diagram for X-ray Unit.

it was necessary to operate the filament current at 5.0 millamperes or less. A timer was also included to permit the operation of the tube for an interval of 0.1 second to 1.0 minutes. A General Electric 2.0 KVA Voltage Stabilizer was used to stabilize the line voltage to the control panel.

In Figure 9 (b) the lucite mockups are shown. From left to right, the first two mockups simulated stratified flow; the second three mockups simulated annular flow; the sixth mockup simulated bubble flow; the seventh mockup simulated all liquid flow. Table 2 gives the actual void fraction of the mockups.

To evaluate the void fraction by gamma ray attenuation, a 1.5 inch long section of 0.930 inch inside diameter test section was mounted horizontally so the vertical gamma beam from the X-ray tube would traverse in a plane perpendicular to the axis of the tube. The procedure which was followed to obtain the intensity in counts per minute versus tube diameter was as follows:

1. For a specified voltage and filament current on the X-ray tube, the full range scale reading was determined for the X-ray tube.

2. For a specified traverse time, the appropriate time constant for the count rate meter was determined.

3. Several traverses were each made of the 1.5 inch long test section containing no mockup (empty tube), containing mockup number seven (full tube), and then containing the six mockups which simulate the two-phase flow patterns.

For one mockup, the evaluation of the data obtained from the traverses of the tube were as follows.

1. Duplicate traverses of the empty tube were overlapped and examined for reproducibility with the aid of a light box. The reproducibility was found to be within the statistical error of the counting in all cases. A composite curve was obtained by tracing the individual curves on a separate length of recorder chart paper. Then a smoothed curve was drawn from the previously prepared composite curve. The procedure was repeated for the traverses of the full pipe and the traverses of the mockup.

2. The smoothed curves for the empty pipe, the full pipe, and the mockup were overlapped, aligned and traced on a separate length of recorder chart piper. Figure 9 (c) shows the overlapped composite curves for a typical traverse. Alignment of the individual traverse curves, composite curves, and smoothed curves was readily accomplished as the count rate increased rapidly over a very short distance when the gamma beam passed across the outer edge of the tube. Proper care was taken at the start of the traverse, since an extremely high count rate was obtained with only an air path between the Geiger-Mueller tube and the X-ray tube. The traverse was started with the gamma-beam off the tube. With the timer set on 0.1 second and the time constant set at 0.5 second, the X-ray tube was operated with the timer. For a 0.1 second interval of operation, the count rate meter was driven upscale, but not off scale, until the gamma beam touched the tube.

3. The distance on the smoothed curve which corresponded to the outside diameter of the pipe was measured. Thus knowing the wall thickness of the tube (0.035 inches), the corresponding length of the wall thickness on the smoothed curve was computed. The smoothed curve was

then divided into forty-nine equally spaced points based on the inside diameter of the tube; and the corresponding values of the intensity for the empty tube I_{MT}, for the full tube I_F, and for the two-phases mockup I_{TP} were read for each of the forty-nine points.

4. The forty-nine sets of values for I_{MT}, I_F and I_{TP} were evaluated using the Void Fraction computer program given in Appendix E for each mockup. The results from the computer program are the local void fraction α as computed by equation (4.204) as a function of the reduced tube diameter y; the error in the local void fraction e as computed by equations (4.206) and (4.208); the average void fraction α_{avg} as computed by equation (4.205); and the error in the average void fraction e_{avg} as computed by equation (4.207).

The optimum operating condition were experimentally determined for the peak voltage on the X-ray tube based on the requirements that, first there be a significant change in the count rate between the empty tube and the tube full of water and second that the count rate for a given time constant be sufficiently large to reduce the statistical error in counting to an acceptable value as given by equation (4.208). The optimum peak voltage was found to be 45.0 Kev, and the optimum time constant was found to be 10.0 seconds.

The optimum traverse time was experimentally determined based on the requirement that at each point on the tube, as the tube is traversed, the measured count rate was within the statistical error of the actual count rate for a given time constant. The optimum traverse time was found to be 5.7 minutes.

In Figure 11 a typical result of the traverse at the optimum

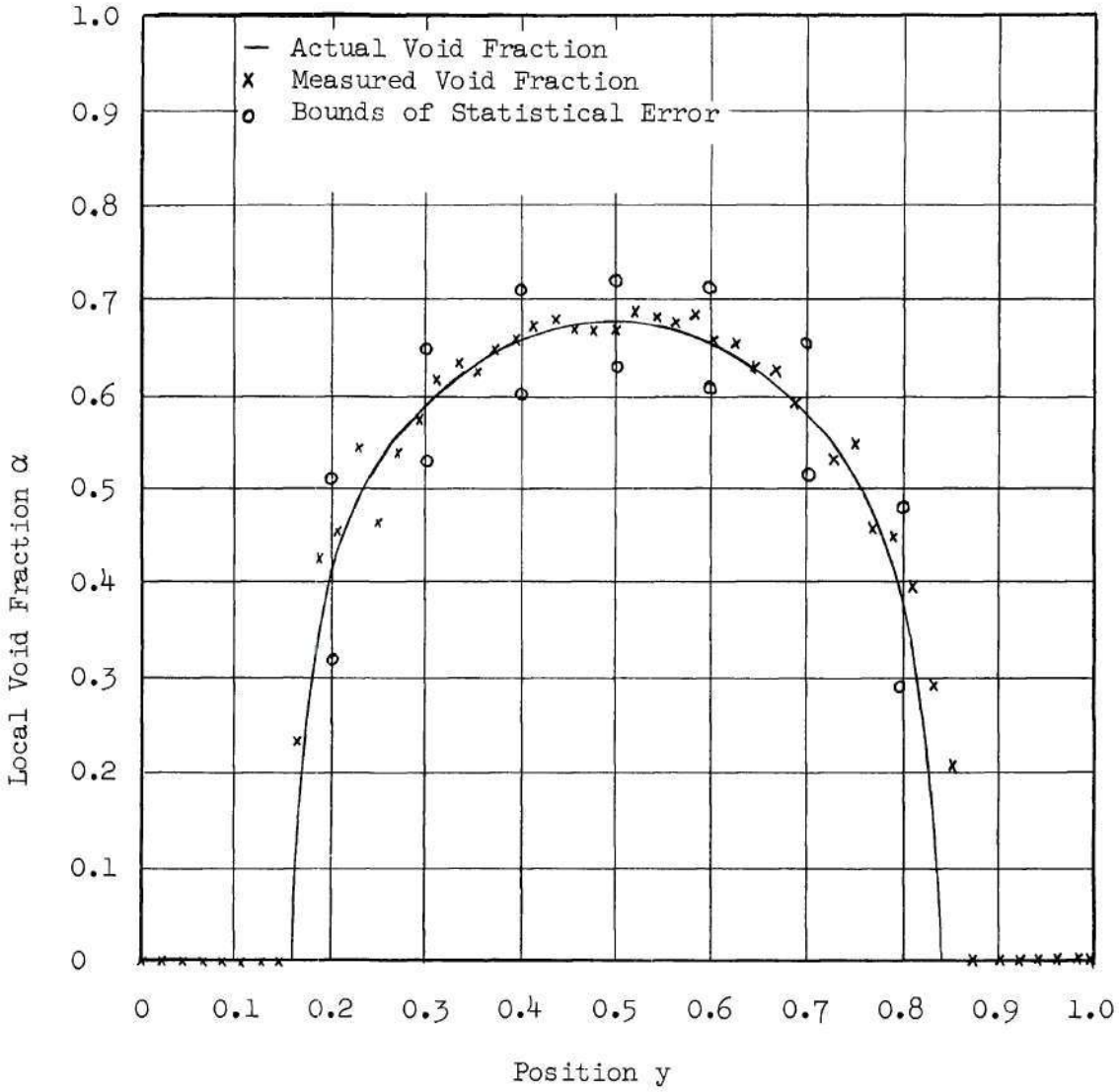

Figure 11. Comparison of Measured Local Void Fractions and Actual Void Fractions for Mockup 4.

operating conditions is shown. In Table 2 a comparison is made of the actual void fraction with the measured void fraction from the traverse at the optimum operating conditions. The actual void fraction was obtained by weighing the lucite mockup and measuring the characteristic dimensions accurately to compute the void fraction.

The value used in equation (4.208) for the constant "C" was the Probable Error i.e., C=0.6745, which corresponds to a confidence limit of 50 per cent. With reference to Table 2, it may be seen that the per cent deviation of the measured void fraction from the actual value of the void fraction is less than the per cent statistical error in the void fraction based on the Probable Error. Thus, when the void fraction measurement is applied to the test section with two-phase, steam-water flow, confidence may be placed in the measured void fraction that the error in the measured void fraction would lie with the statistical error as computed based on the Probable Error.

With reference to Figure 11, an indication of the flow pattern may be obtained from examining the plot of the local void fraction versus reduced tube diameter. For the case of annular flow, the local void fraction is zero until the vapor core is reached. The vapor core is then represented by the characteristically shaped curve in Figure 11. For stratified flow with the liquid filling slightly less than one-half the tube cross section, the local void fraction is equal to 1.0 until the liquid is reached, and then the local void fraction decreases as the center of the tube is approached. For the case of fog flow where the liquid and vapor are intimately mixed, the local void fraction would be constant. For the case of annular flow with liquid droplets in the vapor

Table 2. Results of Void Fraction Measurement

Mockup Number	Actual Void Fraction	Measured Void Fraction	Per Cent Deviation from Actual Void Fraction	Per Cent Statistical Error
1	0.6615	0.6796	2.7	15.5
2	0.2789	0.3046	9.2	35.1
3	0.6629	0.7049	6.3	13.2
4	0.4461	0.4693	5.2	12.0
5	0.2460	0.2238	9.0	16.2
6	0.2158	0.1738	19.5	23.5
		Average	8.7	19.3

core, the peak of the characteristic curve of Figure 11 would be flattened. In considering these possible flow types from the plot of the local void fraction versus reduced tube diameter from a horizontal traverse with a vertical gamma beam, it would be difficult to distinguish between a stratified flow with liquid occupying more than one-half the tube cross section, and an annular flow with liquid droplets entrained in the vapor core as the shape of both curves would be similar. To obtain an accurate description of the flow pattern, it would probably be necessary to traverse in both a horizontal and vertical direction and compare the results of both traverses. In this study traverses were made in a horizontal direction with a vertical gamma beam.

CHAPTER V

EXPERIMENTAL PROCEDURE

At the start of a series of test runs for a particular day the following procedure was used.

1. The Micromax temperature recorder was standardized to correct any small change in the dry cell voltage.

2. The Bristol recorder which measured the output from the pressure transducers was checked for zero reading at atmospheric pressure. The difference from the zero reading was usually less than ± 0.2 psi and could be attributed to the daily fluctuations in atmospheric pressure and laboratory temperature. The difference was noted, and this correction was included when the calibration correction was taken into account.

3. The zero and calibration procedure (69) for the Nuclear Chicago count rate meter was followed. The X-ray equipment was allowed to warm up for ten minutes. The test section had been previously drained; and then with the count rate meter and X-ray tube in order, several traverses of the empty test section were made. The temperature recorder was in operation at this time to measure the temperature.

4. The storage tank was filled with water and the water was recirculated through the heat exchanger and test section. The water was heated to approximately 200° F and maintained at this temperature while several traverses of the full pipe were made. The temperature was also recorded at this time. Appendix D gives the equations and their derivations to correct the intensity data from the empty pipe full of

air at room temperature and from the full pipe at approximately 200° F to the operating temperature with two-phase flow in the test section.

5. At this time single-phase pressure drop and flow rate data were obtained for use with the two-phase flow tests which were made the previous day. It was much less difficult to follow this procedure than to obtain single-phase flow data and then to attempt to obtain and maintain the corresponding flow rate and inlet pressure for two-phase flow.

Once the starting procedure was completed, several two-phase flow tests were made. The following procedure was used.

1. The water in the storage tank was heated from 200° F to 210° F. At this time the particular flow rate and inlet pressure were obtained. The inlet pressure is the pressure at the inlet of the test section, and it was monitored visually at the control panel (see Figure 4 (a)).

2. At this point the steam pressure in the heat exchanger was slowly increased. Correspondingly, the downstream control valve was slowly opened to maintain the flow rate constant, as flashing of the water was taking place across this valve.

3. Referring to Figure 12 (a), the flashing at the downstream control valve was transferred to the expansion section where a liquid core was formed. At this point a slight increase in steam pressure to the heat exchanger of the order of 0.5 to 1.5 psi caused the point of initial vaporization to shift from the expansion section to near the inlet of the test section. This slight increase in steam pressure had to be accomplished carefully as the pressure drop in the test section was increased by a factor of two or more as the point of initial vaporization moved toward the inlet of the test section. Figure 12 (b), (c)

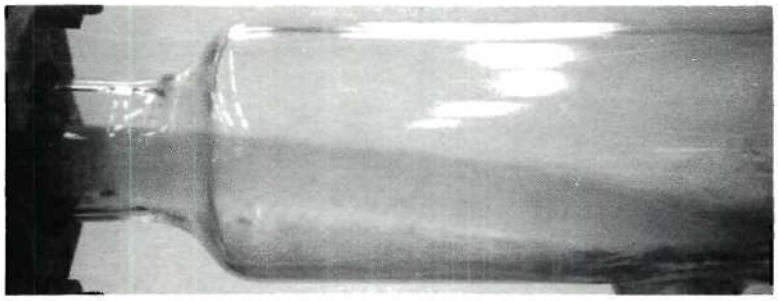

a. Point of Initial Vaporization in the Expansion Section

b. Point of Initial Vaporization Being Transfered Inside the Test Section

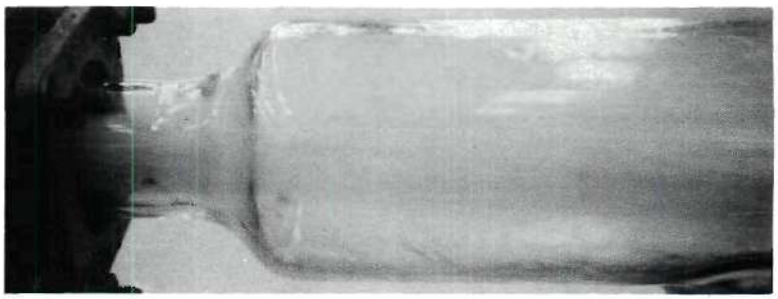

c. The Point of Initial Vaporization Near the Entrance of the Test Section

d. The Point of Initial Vaporization Near the Entrance of the Test Section

Figure 12. Obtaining Two-phase Flow in the Test Section.

and (d) show the point of initial vaporization moving from the exit of the test section to near the entrance of the test section. The formation of the annular flow can be seen in the sequence of pictures.

4. With the point of initial vaporization near the inlet of the test section steady state was obtained; and temperature measurements, pressure measurements, and traverses with the void fraction equipment were made.

After a series of runs was completed, temperature and pressure recorders were turned off. The steam flow to the heat exchanger was stopped, causing single-phase flow to occur in the test section. The pump was turned off and the system was drained. Atmospheric pressure in the laboratory was measured by a mercury barometer to ± 0.1 mm of Hg at the start and end of a series of runs which were made on a particular day. Also chart records for each run were removed and the recorders were prepared for another series of runs.

CHAPTER VI

DISCUSSION OF RESULTS

Experimental two-phase flow data for a total of twenty-eight runs are given in Table 7 and Figures 21 through 48 of Appendix A. The range of the variables was: mass flow rate - 445 to 864 lb_m/ft^2-sec; inlet pressures - 32.4 to 66.5 psia; corresponding inlet temperatures - 255 to 300° F; discharge pressures - 25.9 to 56.5 psia; and void fractions - 0.056 to 0.672.

The theoretical values of the liquid velocity, vapor velocity, quality, void fraction, and tube length as functions of temperature are given in Tables 8 through 34 of Appendix B. These values were obtained from the numerical solution of the Annular Flow equations for the boundary conditions of inlet temperature, saturation temperature corresponding to the measured outlet pressure, and mass flow of the twenty-eight experimental runs. The values reported in Tables 8 through 34 do not represent the numerical solution in its entirety, but are only representative values taken over the range of the solution. An example of the numerical solution in its entirety is given for one run in Table 37 of Appendix G and in Figures 14, 15 and 16. Comparisons are given in Table 3 and Table 4 of measured and theoretical values of both void fractions and tube lengths.

Experimental single-phase flow data are given in Table 6 of Appendix A. Twenty-eight runs were made at the corresponding mass flow rates and inlet pressures of the two-phase flow runs but for temperatures in

the range of 200° F and less. Single-phase flow results are given in Figure 13 in the form of a friction factor - Reynolds number plot.

Single-Phase Flow

In order to obtain a friction factor - Reynolds number relation for the test section, twenty-eight single-phase flow runs were made at mass flow rates and inlet pressures corresponding to mass flow rates and inlet pressures for the two-phase flow runs. The data are given in Table 6 of Appendix A for these twenty-eight tests runs which were made at temperatures of 200° F and less. The results of the pressure drop - flow rate measurements are plotted in Figure 13 as the Fanning Friction factor versus the Reynolds number. The smooth curve through the points is represented by the following equation

$$f = 0.00180 + (0.125)/(Re)^{0.32} \qquad (3.202)$$

Also shown on the figure is the accepted curve for smooth pipe given by McCabe and Smith (60).

It can be observed that the experimental curve is approximately 10 per cent higher than the accepted curve. Although it was necessary to have the liquid flow through a path which would not yield a uniform fully-developed turbulent velocity profile at the entrance to the test section, the data in Table 6 indicate this effect was not the cause of the higher values for the experimental friction factors, as the pressure drop from the entrance to the center of the tube was equal to the pressure drop from the center to the exit of the tube to within the accuracy of the measurements. Higher values for the friction factors were possibly the result of wall roughness.

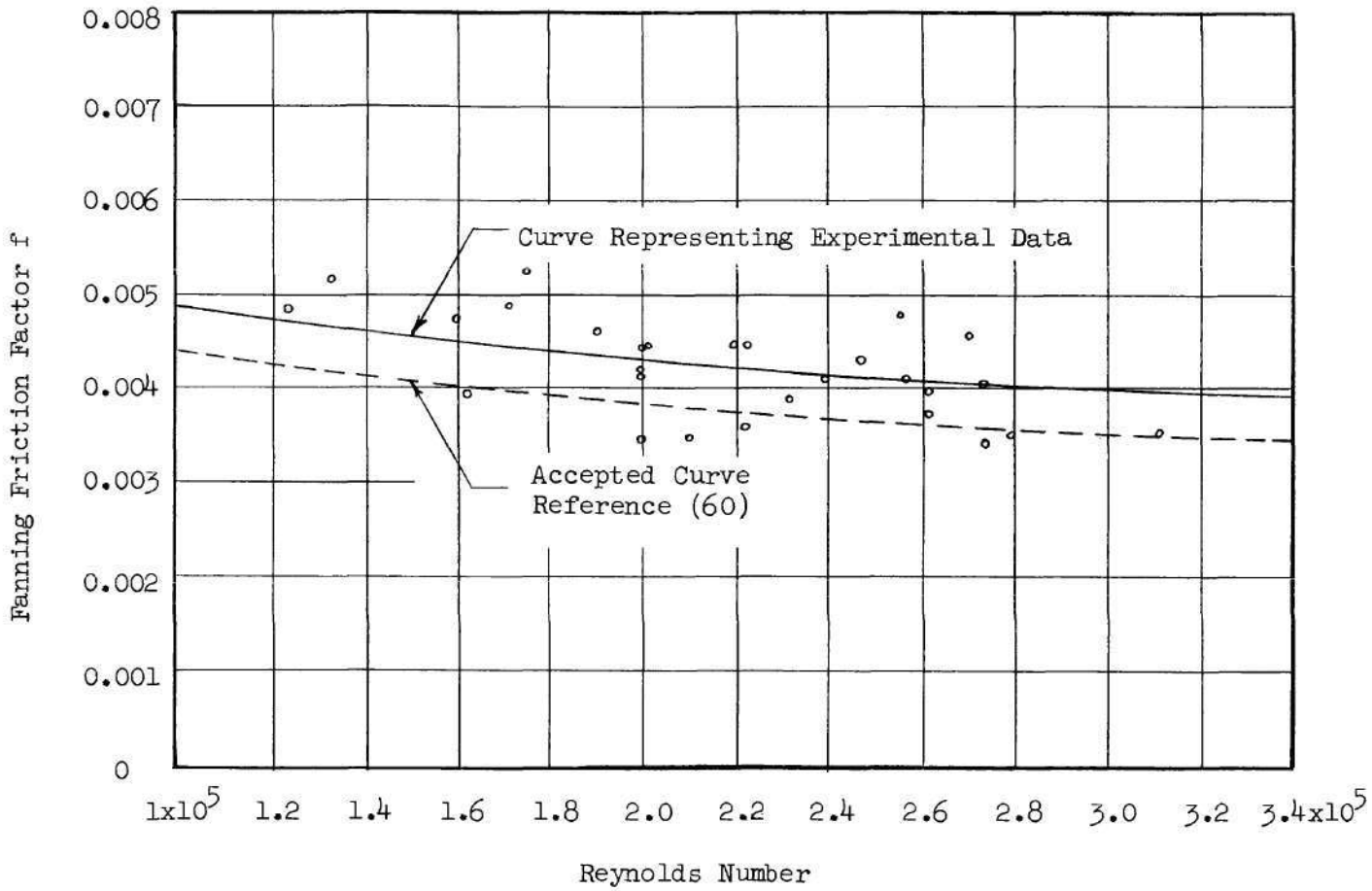

Figure 13. Friction Factor - Reynolds Number for All Liquid Flow the Test Section.

Two-Phase Flow

Selected values of the liquid velocity, vapor velocity, quality, void fraction and tube length as functions of temperature are given in Tables 8 through 34 of Appendix B. These values were obtained from the numerical solution of the Annular Flow equations. The boundary conditions for these solutions are the mass flow rates inlet temperatures and saturation temperatures corresponding to the measured outlet pressures of the twenty-eight experimental runs. The experimental data for these runs are given in Table 7 and Figures 21 through 48 of Appendix A. An example of the numerical solution in its entirety is given for one run in Table 37 of Appendix G and in Figures 14, 15, and 16.

Important results are summarized in Tables 3, 4, and 5. In Table 3 a comparison is made of measured tube lengths with computed tube lengths for equal pressure drops for runs where the computed void fraction was within the statistical error of the measured void fraction. In Table 4 a comparison is made of measured tube lengths with computed tube lengths for runs where the computed void fraction was not within the statistical error of the measured void fraction.

In Figures 17, 18, and 19, design charts are presented for rapid calculation of the two-phase flow parameters of mass flow rate, inlet pressure, outlet pressure, critical outlet pressure, L/D ratio and critical L/D ratio. These design charts were obtained from the numerical solution of the Annular Flow equation for even intervals of mass flow rate and inlet pressure.

Consideration of the Assumptions.--Five assumptions were made in the derivation of the Annular Flow equations as given in Chapter II. The

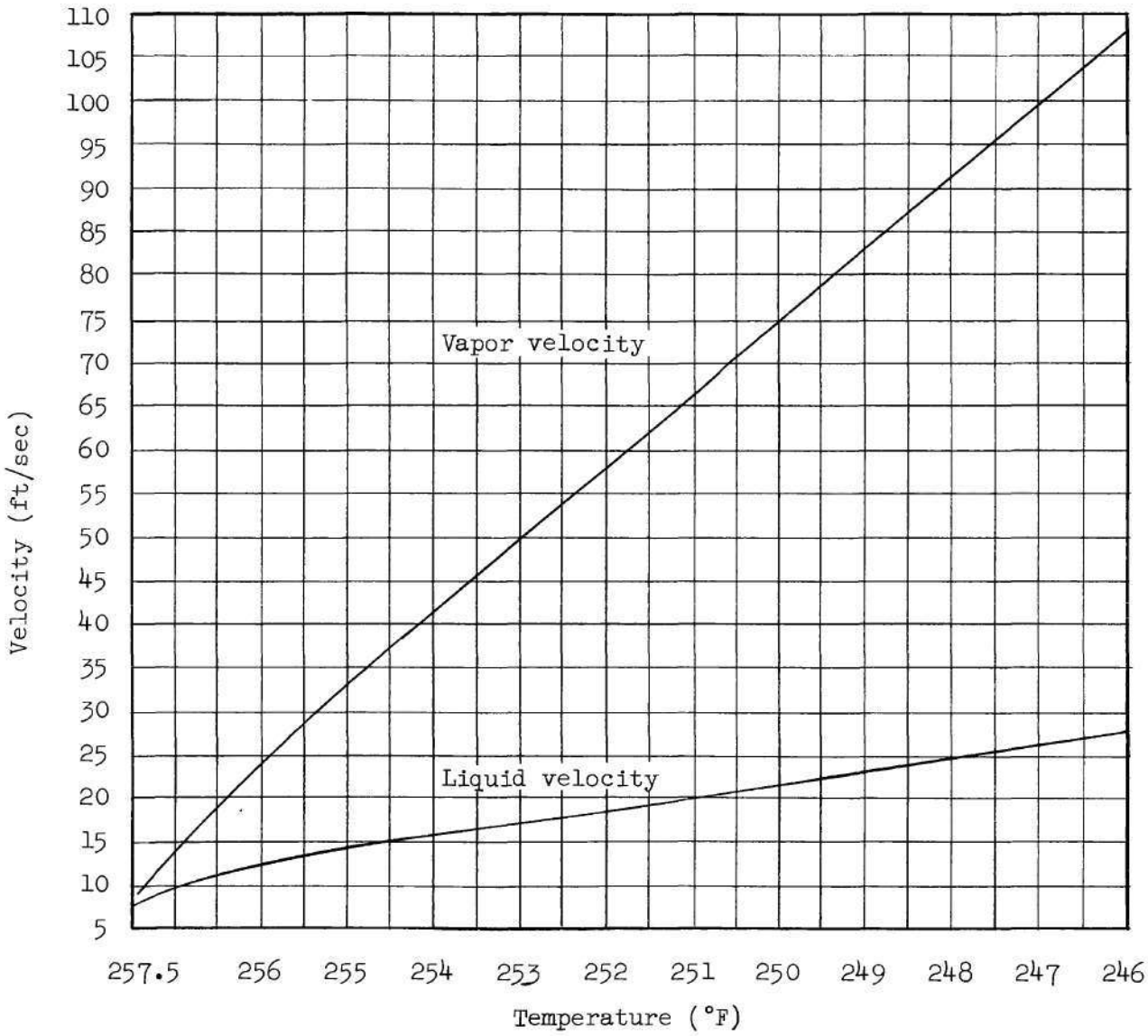

Figure 14. Liquid and Vapor Velocities as Functions of Temperature for Run 10222.

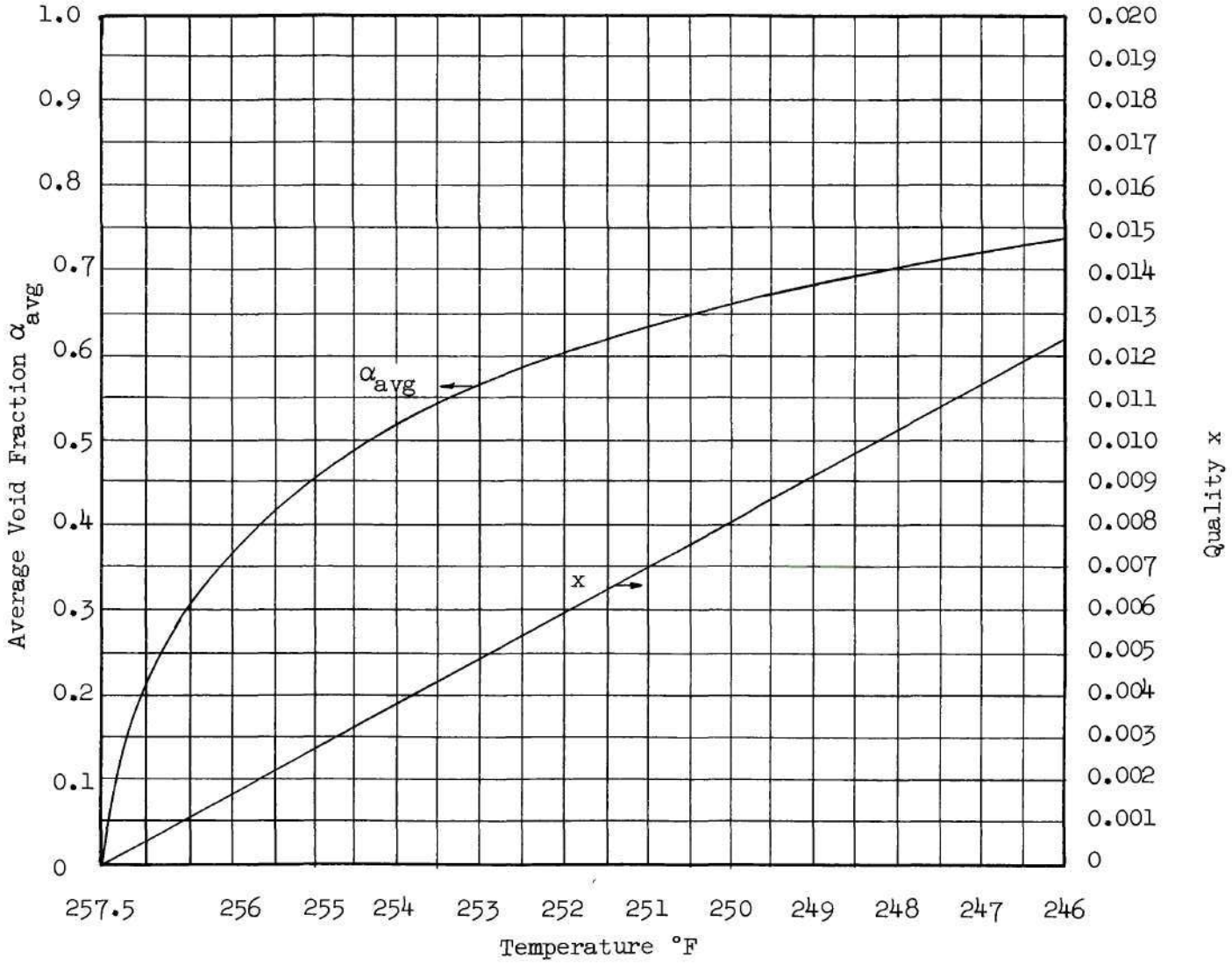

Figure 15. Quality and Void Fraction as Functions of Temperature for Run 10222.

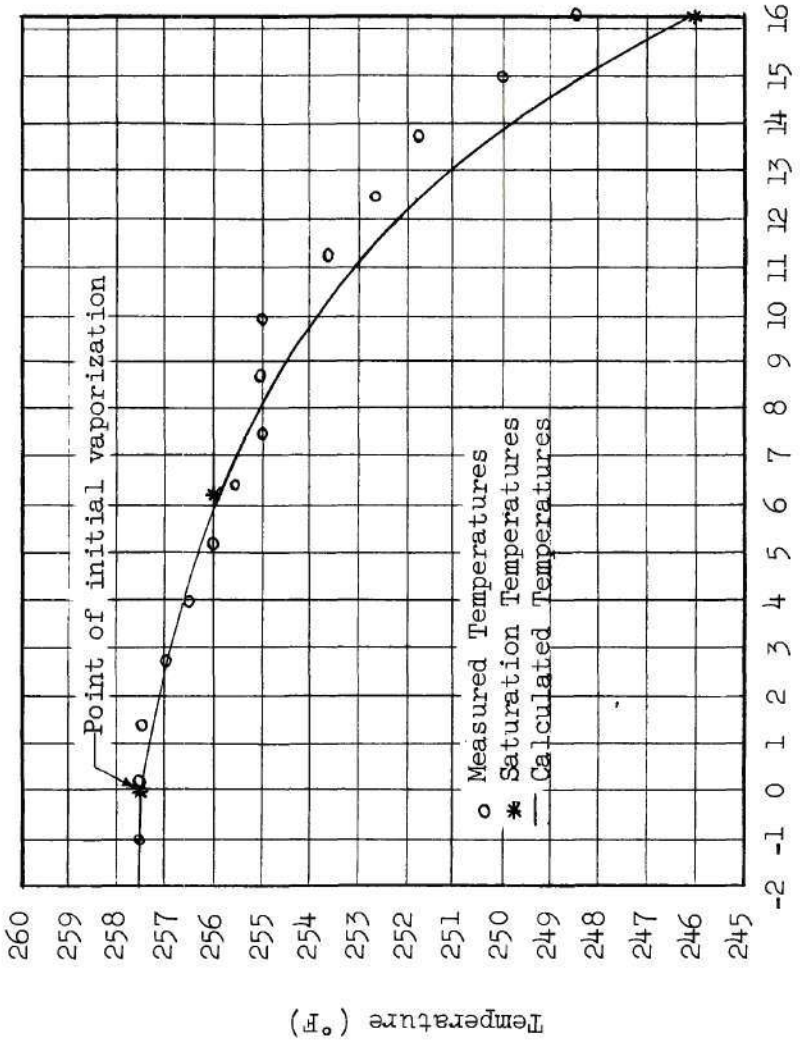

Figure 16. Temperature Distribution for Run 10222

first assumption (horizontal tube) and the second assumption (steady state) were accomplished by the design and operation of the experimental system. The third assumption of the equality of velocities whether based on continuity, momentum, or energy is not strictly true, but is probably not much in error in highly turbulent flow as experienced in these tests. The fourth assumption of constant temperature and pressure at any section normal to the flow and the fifth assumption of thermodynamic equilibrium will now be examined in detail.

The fourth and fifth assumptions would normally be expected to be approached unless the changes in temperature and pressure were so rapid that the rates of heat and mass transfer became controlling. When the rates of heat and mass transfer become controlling, these assumptions will not apply due to the appearance of temperature gradients in the liquid and vapor phases. Results will be given in the next section for the experimental runs where these assumptions apply and do not apply.

Comparison of Void Fractions and Tube Lengths.--In Table 3 comparisons are made of the computed void fractions with the measured void fractions and of the computed tube lengths with the measured tube lengths, for the runs where the measured temperatures approached saturation temperatures corresponding to the measured pressures. In these runs constant temperature was approached at the cross-section of the tube and thermodynamic equilibrium was approached at all stages of the expansion. Thus the assumptions of the Annular Flow equations were satisfied for these runs.

Comparing the void fractions computed by the Annular Flow equations with the measured values of the void fractions for these runs in Table 3, it is seen that the computed values of the void fraction lie

Table 3. Comparison of Measured Tube Lengths with Computed Tube Lengths for Runs where the Computed Void Fraction was within the Statistical Error of the Measured Void Fraction

Run Number	Mass Flow Rate (lb/ft^2-sec)	Inlet Pressure (psia)	Void Fraction			Length		Per Cent Deviation (Lm-Lc)(100)/Lm
			L	Measured	Calculated	Measured (feet) Lm	Calculated (feet) Lc	
3022	444.5	32.4	1	0.665±0.074	0.656	16.63	16.27	2.2
10222	444.5	33.9	1	0.672±0.100	0.606	16.67	16.30	2.2
10127	582.6	38.5	1	0.539±0.082	0.540	11.25	10.36	7.9
10131	582.6	46.9	1	0.632±0.073	0.570	17.00	17.90	-5.3
10224	582.6	49.6	1	0.430±0.079	0.558	19.42	20.25	-4.3
1028	582.6	54.9	1	0.608±0.091	0.592	19.42	21.70	-11.7
1037	582.6	54.6	2	0.429±0.084	0.357	19.42	22.17	-14.1
20227	729.6	57.4	1	0.494±0.087	0.461	13.38	13.72	-2.5
20215*	832.8	62.8	1	0.125±0.085	0.351	10.50	9.90	6.3
3037	709.8	64.3	2	0.304±0.085	0.297	19.40	19.90	-2.5
10215	729.6	65.2	1	0.394±0.097	0.404	16.00	15.87	0.8
10228	763.6	66.0	1	0.430±0.087	0.480	17.50	18.58	-6.2
10127	763.6	66.5	1	0.452±0.085	0.468	16.38	16.92	-3.3
						Average Per Cent Error		5.2

*Indicates Critical Flow Rate.

within the statistical error of the measured values. By this comparison it is concluded that the Annular Flow equations describe the complex two-phase flow phenomena to within the accuracy of the void fraction measurement.

Since the void fraction measurement is hindered by the statistical error inherent in the measurement, a comparison of the computed tube length with the measured tube length is given in Table 3 also. It is seen that the maximum positive deviation of the calculated value from the measured value is 7.9 per cent, the maximum negative deviation is -14.1% and the average deviation is ±5.2%. It should be noted that these deviations of the calculated values from the measured values are generally random which would indicate that at least part of the lack of agreement between the experimental measurements and the computed values could be due to experimental error.

In Table 4 comparisons are made of the computed void fractions with the measured void fractions and of the computed tube lengths with the measured tube lengths, for the runs where the measured temperatures were higher than the saturation temperatures corresponding to the measured pressures. In these runs there was a temperature gradient in the liquid annulus; and even though there could be equilibrium at the vapor-liquid interface, thermodynamic equilibrium was not attained at all stages in the expansion. Thus the assumptions which form the basis of the Annular Flow equations were not satisfied for these runs.

Comparing the void fractions computed by the Annular Flow equations with the measured values of the void fraction for these runs in Table 4, it is seen that the measured void fraction is less than the

Table 4. Comparison of Measured Tube Length with Computed Length for Runs where the Computed Void Fraction was Greater than the Measured Void Fraction

Run Number	Mass Flow Rate (lb/ft^2-sec)	Inlet Pressure (psia)	Void Fraction			Length		Per Cent Deviation (Lm-Lc)(100)/Lm
			L	Measured	Calculated	Measured (feet) Lm	Calculated (feet) Lc	
2036	554.0	32.6	2	0.123±0.050	0.342	10.25	7.44	27.4
1022	579.7	32.6	1	0.114±0.064	0.522	10.00	7.37	26.3
2022*	605.2	32.0	1	0.097±0.062	0.596	10.50	5.84	44.3
3036*	605.2	32.8	2	0.109±0.059	0.137	8.75	6.37	27.2
1033	557.1	39.5	2	0.189±0.113	0.429	16.00	13.13	17.9
20127*	637.7	38.3	1	0.373±0.081	0.524	10.63	8.19	22.9
1036*	637.7	38.8	2	0.060±0.042	0.412	12.13	8.14	32.8
20130	729.6	44.1	1	0.140±0.096	0.462	8.50	6.93	18.5
20224	729.6	45.8	1	0.101±0.062	0.496	10.50	7.66	27.0
10227	729.6	50.8	1	0.217±0.081	0.498	13.13	10.02	23.6
30224*	864.0	44.7	1	0.076±0.064	0.456	8.50	4.68	33.4
10130*	864.0	44.7	1	0.100±0.098	0.418	6.38	3.83	40.0
10213	729.6	52.3	1	0.226±0.062	0.607	16.00	13.14	17.9
10214*	848.5	54.5	1	0.056±0.050	0.488	10.00	5.64	43.6
30227*	848.5	52.3	1	0.132±0.096	0.421	9.50	6.77	40.3
							Average Per Cent Error	29.5

*Indicates Critical Flow Rate.

computed void fraction in all cases. The measured void fraction would be expected to be less than the computed void fraction, as a smaller fraction of the liquid had been vaporized as compared to the fraction that would have been vaporized had thermodynamic equilibrium been attained at the cross-section. Correspondingly the liquid velocity did not increase as rapidly as predicted by the Annular Flow equations as a result of the greater cross-sectional area for liquid flow and also as a result of the smaller interfacial shear forces. This would logically result in the measured tube length being greater than the calculated tube length for an equal pressure drop. That this was the case is illustrated in Table 4 where the per cent deviations of the computed values from the measured values of tube length are shown to be positive, the average per cent deviation being 29.5 per cent.

This phenomena of a temperature gradient in the liquid annulus of adiabatic two-phase flow of a pure fluid has also been observed by Hatch and Jacobs (17) for the two fluids trichloromonofluoromethane and hydrogen. Houghton (72) in a theoretical study showed that thermal equilibrium is not attained for two-phase flow in a channel with heat transfer, even with large void fractions. Anderson, Haselden, and Mantzouranis (73) also discuss temperature gradients in two-phase flow in a vertical long-tube evaporator.

It would be valuable if definite limits could be placed on the mass flow rate and inlet pressure to bound the regions in which the Annular Flow equations would hold. This is not presently possible due to the complex flow situation. If the results in Tables 3 and 4 are examined, it will be noticed that the mass flow rates are relatively

higher in Table 4 than the mass flow rates in Table 3. This is as expected since the liquid residence time is longer and the liquid film is thinner for the lower mass flow rates, thus permitting thermodynamic equilibrium to be approached more closely. In general, it may be concluded that if the Annular Flow equations are used for design purposes to compute the two-phase flow pressure drop for a given mass flow rate and tube length, the computed pressure drop will be accurate to at least ±10% if thermodynamic equilibrium is approached. If thermodynamic equilibrium is not approached the computed pressure drop will be of the order of 15 to 45 per cent greater than the actual pressure drop depending upon the departure from thermodynamic equilibrium at the tube cross-section. Thus, the use of the Annular Flow equations will give inherent over design rather than inherent under design.

Interface Velocity Relation.--In Chapter III, it was stated that the following equation

$$V_p = V_\ell \left[1 + 0.2\ (T_o - T)^2/81\right] \qquad (2.402)$$

was used to relate the interface velocity with liquid velocity and temperature. This equation is a modification of Linning's equation as discussed in Chapter III.

To determine the sensitivity of the solution of the Annular Flow equations to the relation for the interface velocity, the following two functions

$$V_p = V_\ell \qquad (6.201)$$

$$V_p = 1.2V_\ell \qquad (6.202)$$

were used to cover a range of possible values for the interface velocity. The Annular Flow equations were solved using equations (6.201) and (6.202) for the runs given in Table 3 to compare with the previously reported results obtained using equation (2.402). The average per cent deviation in comparing the computed tube lengths with the measured tube lengths using equation (6.202) was 7.1 per cent. The corresponding average per cent deviation using equation (6.201) was 14.6 per cent, and the previously reported results using equation (2.402) was 5.2 per cent. For all three equations, (2.402), (6.201) and (6.202), the computed void fractions were within the statistical error of the measured void fractions. From these considerations, it may be concluded that equation (2.402) more aptly describes the physical situation, but not significantly better than equations (6.201) and (6.202). Further attempts to improve the accuracy of the model by modification of equation (2.402) were not felt justified on the basis of the computer time which would have been required.

Recently, McManus (75) examined liquid distributions and surface characteristics in horizontal, annular, two-phase flow of air and water, but no results for the interface velocity were reported. Further work along these lines will be required before the character of the interface and its relative velocity can be fully described for two-phase flow with one or two components.

Comparison of Flow Models.--In Table 5 the pressure drops as computed by the Homogenous Flow model (14), the Martinelli-Nelson model (13) and the Annular Flow equations are compared. Both the Homogenous Flow model and Martinelli-Nelson model were described in detail in Chapter I. The

Table 5. Comparison of Pressure Drop fow Flow Models Based on Measured Tube Length for the Runs in Table 3.

Run Number	Pressure Drop						
	Measured (psi)	A. F. Eqns. (psi)	Per Cent Error	Homogenous (psi)	Per Cent Error	Martinelli (psi)	Per Cent Error
3022	6.5	6.66	-2.4	3.42	47.4	7.29	-12.2
10222	6.1	6.43	-4.9	3.43	43.7	6.86	-12.5
10127	4.8	5.22	-8.3	3.19	33.6	7.66	-59.6
10131	8.6	8.01	6.9	6.06	29.6	11.08	-28.8
10224	9.2	8.72	5.4	6.93	24.7	12.30	-33.7
1028	8.2	6.90	15.8	6.97	15.0	11.56	-40.9
1037	9.1	6.61	23.2	6.96	23.5	11.92	-31.0
20227	7.8	7.60	2.6	7.52	3.6	11.09	-36.2
20215	5.4	5.89	-9.2	7.71	-42.8	12.01	-122.3
3037	11.0	10.58	3.6	10.35	5.9	15.83	-44.0
10215	7.0	7.12	-1.4	9.04	-29.2	13.11	-87.4
10228	11.8	11.01	7.3	10.81	8.4	16.54	-40.2
10217	10.0	10.41	-4.0	10.13	1.3	15.59	-55.9
Average Per Cent Error			7.3		23.8		-46.5

conditions which were specified to compute the pressure drop for each run were the mass flow rate, inlet pressure and corresponding saturation temperature, and the measured length of tube from the point of initial vaporization to the exit. All three models require that there be thermodynamic equilibrium at all stages of the expansion and that there be constant temperature at the cross-section. Therefore, in order to obtain an objective comparison of the three models, the pressure drop was computed for the runs in which these basic assumptions were approached, i.e., the runs listed in Table 3.

As shown in Table 5, the Martinelli-Nelson model (13) predicts pressure drops which are consistently higher than the experimental pressure drops. Consistently high values resulted from the ratio $(\Delta P_{TPF}/\Delta P_o)$ being too large. $(\Delta P_{TPF}/\Delta P_o)$ is the ratio of the frictional pressure drop for two-phase flow to the frictional pressure drop for single phase flow with both flows at the same conditions of temperature and pressure. It is a function of the mean pressure of the system and the exit quality. The failure of the Martinelli-Nelson model to describe the pressure drop accurately was to be expected, since the model was based on results from isothermal two-component pressure drop data. The authors stated in their paper that the method was a tentative method for rapid calculation which was based upon a meager amount of data and required further experimental verification before it could be considered valid. The data on which the model was based covered a range of 18 psia to 3000 psia and exit qualities of 4 to 100 per cent. The accepted limit of accuracy of the Martinelli-Nelson model is ±40%, and it is seen that most of the pressure drop results as calculated by the Martinelli-Nelson model were

within this range, the average per cent error being 46.5 per cent.

The Homogenous Flow model was more successful in predicting the two-phase flow pressure drop, as can be seen in Table 5. The average per cent error for this model was 23.8 per cent.

The average per cent error for the Annular Flow equations was 7.3 per cent as compared to 23.8 per cent for the Homogenous Flow model and 46.5 per cent for the Martinelli-Nelson model. On the basis of these results, it is seen that the Homogenous Flow model and the Martinelli-Nelson model will give approximate results involving relatively simple calculations, while the Annular Flow equations will give results of the order of ± 10 per cent but involve complicated calculations. In order to eliminate these complicated calculations design charts for the system steam-water have been prepared from the numerical solution of the Annular Flow equations. These design charts are presented in the next section.

Design Charts.--In Figures 17, 18, and 19, design charts are presented for the system steam-water to permit the rapid computation of two-phase flow parameters. These design charts are based on the numerical solution of the Annular Flow equations for even intervals of mass flow rate and inlet pressure. The range of the charts is: inlet pressure - 30 to 150 psia, mass flow rate - 300 to 1000 lb_m/ft^2-sec, and L/D ratio - 25 to 1000.

In Figure 17 the pressure at any point in the tube is given as a function of the L/D ratio up to the critical L/D ratio, designated $(L/D)_c$, with mass flow rate as a parameter. In Figure 18, the mass flow rate is given as a function of $(L/D)_c$ with inlet pressure as a parameter. In

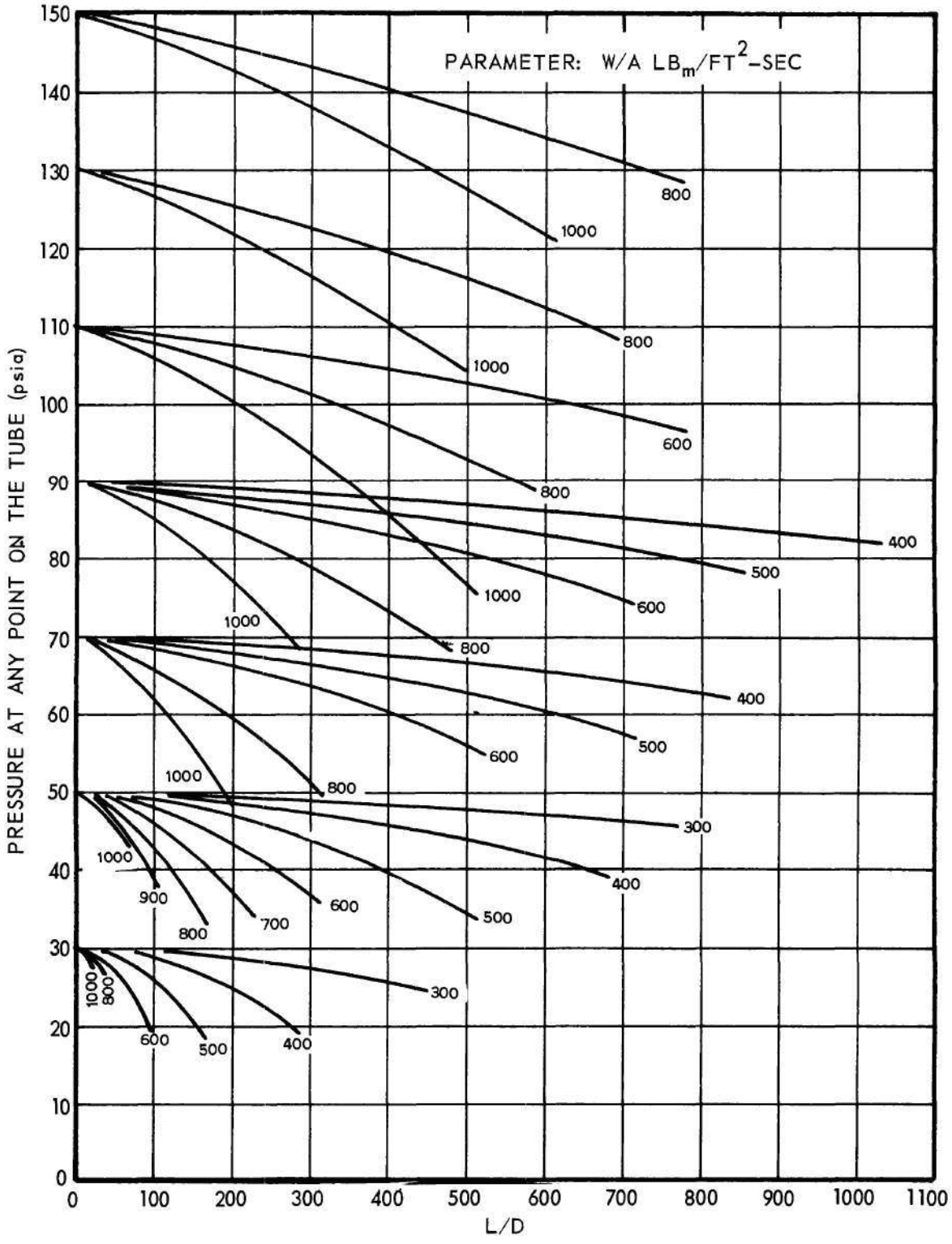

Figure 17. Pressure at any Point on the Tube versus L/D Ratio for the System Steam-Water.

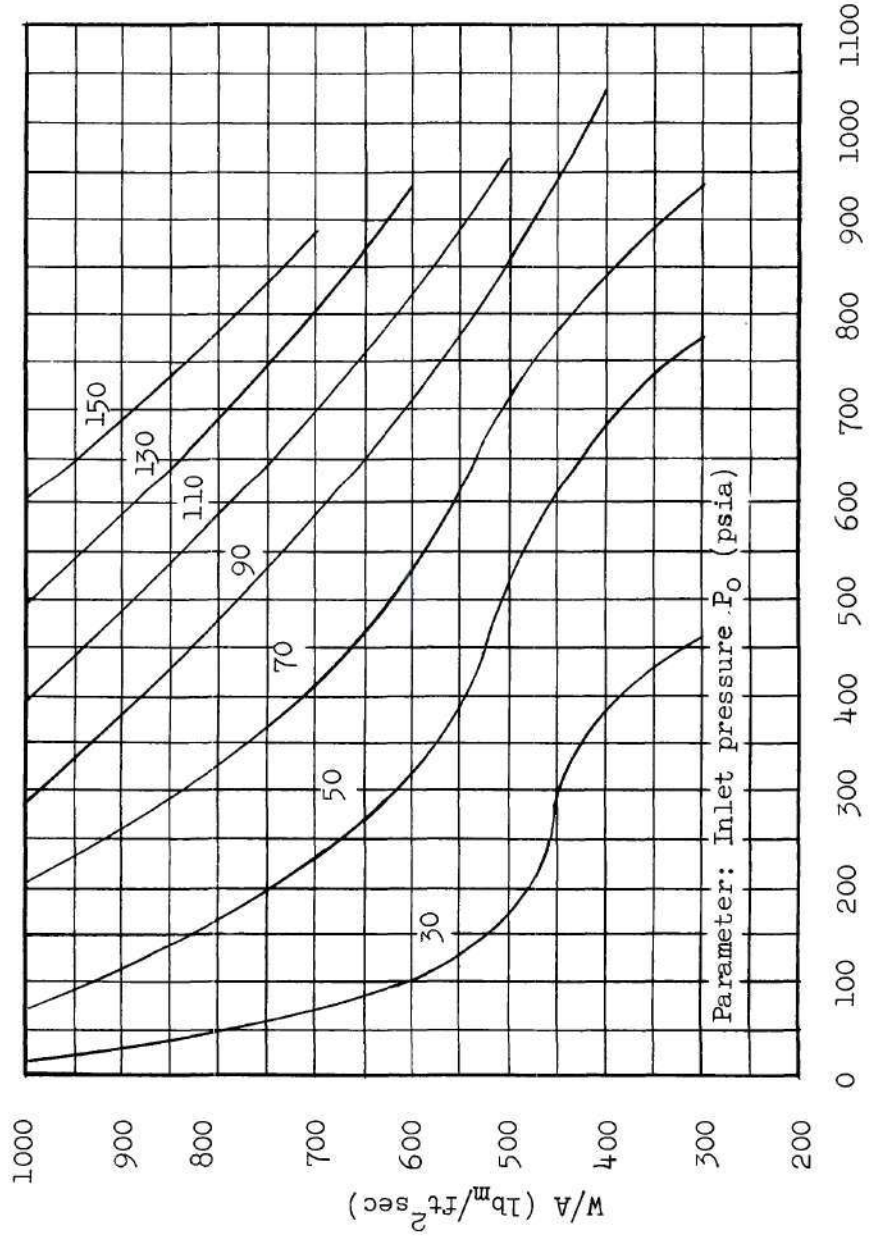

Figure 18. Mass Flow Rate versus $(L/D)_c$ for the System Steam-Water.

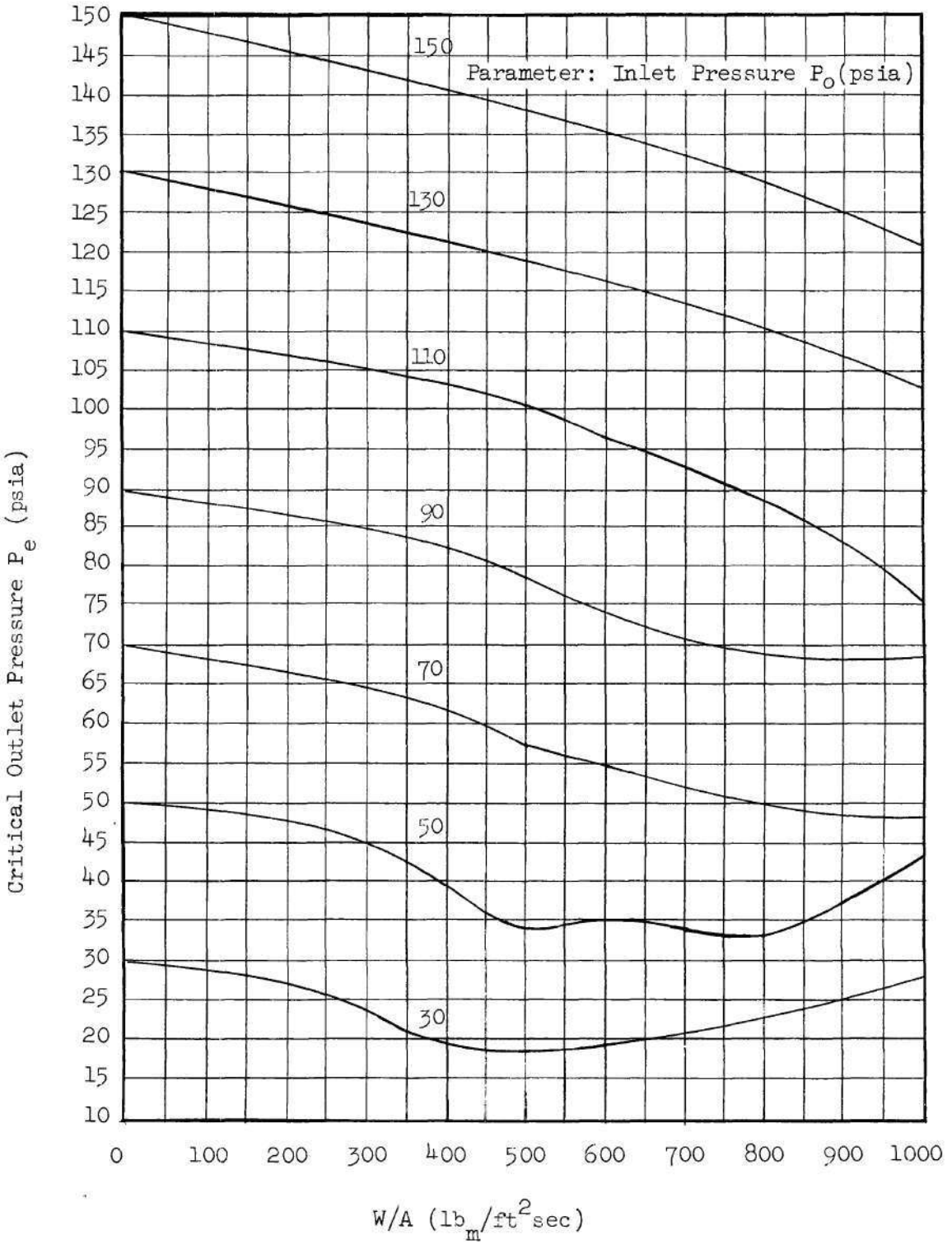

Figure 19. Critical Outlet Pressure versus Mass Flow Rate for the System Steam-Water.

Figure 19, the critical outlet pressure is given as a function of mass flow rate with inlet pressure as a parameter. The pressure drop up to the critical pressure drop may be estimated from Figure 17 for known values of the inlet pressure, mass flow rate and L/D ratio. The critical L/D ratio, $(L/D)_c$, may be estimated from Figure 18 for known values of the mass flow rate and inlet pressure, and the corresponding critical outlet pressure may be estimated from Figure 19.

It should be noted that the results presented in Figure 19 to determine the critical outlet pressure from the mass flow rate and inlet pressure are independent of any friction factor - Reynolds number relation. However, the results presented in Figure 18 to determine $(L/D)_c$ from the inlet pressure and mass flow rate are based on equation (3.202). If equation (3.202) does not describe the system, the computer program given in Appendix G can be used to compute the L/D ratio with the desired friction factor - Reynolds number relation substituted for equation (3.202).

In the derivation of the Annular Flow equations given in Chapter II, it was assumed that the quality was a function of temperature only, that is, the kinetic energy terms were neglected in the total energy equation, equation (2.312). This assumption was examined as it was possible to approximate the kinetic energy terms closely in the numerical solution of the equations. This was done by using the values of the velocities which were obtained in the preceding step in the total energy equation to compute the quality at the present step. The change in the velocities was small from step to step in the numerical solution and a good approximation to the kinetic energy terms was obtained. Due to the fact that the order of magnitude of the kinetic energy terms was much

less than the enthalpy terms, the result of including the kinetic energy terms in the total energy equation did not affect the solution of the equations for the range of the variables in this work. However, for the results which are given in the design charts, Figures 17, 18, and 19 this approximation to the kinetic energy terms was included.

Comparison with Previous Investigators.--Benjamin and Miller (14) reported pressure drop, flow rate, and equivalent length data for critical, two-phase flow of steam and water in cascade drain lines and found their experimental data were closely approximated by the Homogenous Flow model. A total of six runs were reported for a range of inlet pressures from 20.0 to 35.8 psia and mass flow rates from 157 to 286 lb_m/ft^2-sec. The average per cent deviation of the critical outlet pressures computed from the Annular Flow equations from the experimental critical outlet pressures was - 20.6 per cent. Isben (46) compared his data with that of Benjamin and Miller and found their data were significantly lower than the values which he observed.

Bottomley (19) reported one run for critical, two-phase flow of steam and water for an inlet pressure of 41.0 psia, outlet pressure of 22.0 psia and mass flow rate of 260 lb_m/ft^2-sec. The outlet pressure predicted by the Annular Flow equations was 35.5 psia which is 61.5 per cent higher than Bottomley's measured value. Isben (46) also reported that Bottomley's measured value was lower than the values he observed.

Burnell (29) reported nine critical two-phase flow runs for steam and water. For three of the nine runs at inlet pressures of 158, 114, and 52.4, the predicted critical outlet pressures from the Annular Flow equations were 57.2, 53.7 and 30.8 per cent higher, respectively, than the

experiment values. For the fourth run at an inlet pressure of 24.0 psia the predicted outlet pressure was 8.8 per cent less than the measured value. The inlet pressures for the other five runs were 14.3 psia and less. It was not possible to compare the experimental critical outlet pressures with the values predicted from the Annular Flow equations as the corresponding saturation temperatures were less than the lower limit of accuracy for the least squares polynomials fitted to the thermodynamic properties. Isben (46) found his data were within ± 10 per cent of Burnell's data in the exit pressure range of 6 to 15 psia, and 20 to 35 per cent lower in the exit pressure range from 24.5 to 58.5 psia.

Linning (27) reported twelve critical two-phase flow runs for steam and water in a one-eighth inch diameter tube for ranges of inlet pressures from 20.8 to 29.8 psia, mass flow rates from 266 to 485 lb_m/ft^2-sec and tube lengths from 7.2 to 30.0 inches. The average per cent deviation of the critical outlet pressure computed from the Annular Flow equations from the experimental values was ±21.4 per cent. Isben (46) found the data of Linning to be 40 to 50 per cent less than his experimental values.

Isben (46) reported data for critical, two-phase flow of steam and water in the range of critical outlet pressures from 4 to 43 psia and of exit qualities from 1.0 to 100.0 per cent. These data were obtained by mixing steam and water and flowing the mixture through three foot long test sections of 1/4, 1/2, 3/4, and 1 inch nominal diameter tubes. Also two annular test sections were used of 3/4 - 1/4 inch nominal diameters and 1 - 1/4 nominal diameters.

Isben found his data were correlated by a log-log plot of $(W/A)/P_c^{0.96}$

as a function of exit quality x. His correlation is shown in Figure 20. This correlation is supported by extensive data in the range for exit qualities more than 3 per cent, while only four data points were for exit qualities less than 3 per cent.

Results of the solution of the Annular Flow equations from the design charts are plotted on Figure 20. Unfortunately, only several points lie in the range of Isben's data. A smooth dotted curve is drawn through all of these points and indicate possibly the correlation curve in the low quality range is lower in this region than predicted by Isben.

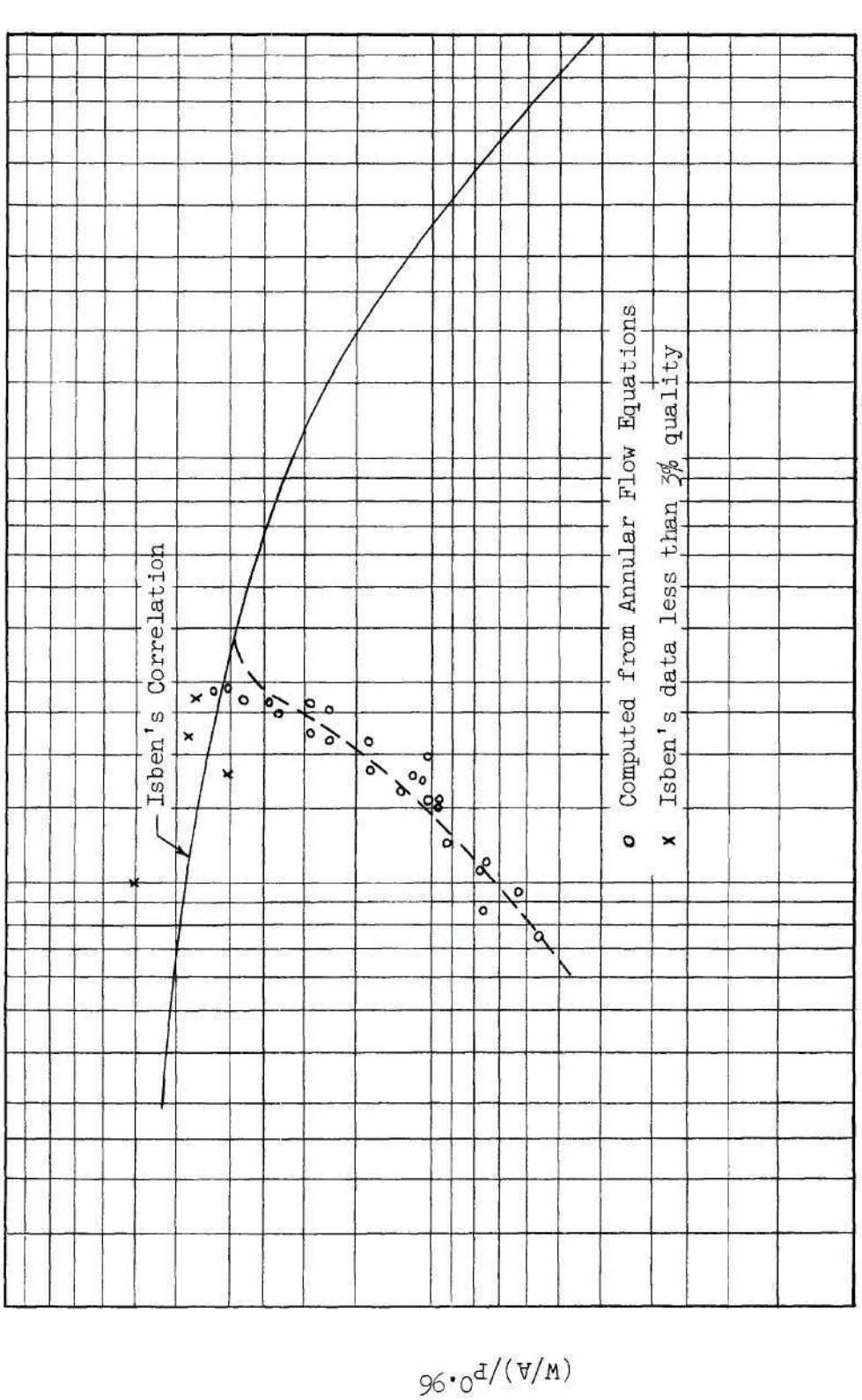

Figure 20. Empirical Correlation of Critical Flow Parameters.

CHAPTER VII

CONCLUSIONS AND RECOMMENDATIONS

The following conclusions are made on the basis of the results of this study:

1. The adiabatic, two-phase flow of steam and water in a horizontal tube from the point of initial vaporization to the exit of the tube was successfully described by the Annular Flow equations when the basic assumptions of thermodynamic equilibrium at all stages of the expansion and constant temperature across any section normal to the flow were approached. The accuracy in computing the two-phase flow pressure drop by the Annular Flow equations for a specified mass flow rate, inlet pressure and tube length was ± 10 per cent when these basic assumptions were met.

2. When the basic assumptions of thermodynamic equilibrium at all stages of the expansion and of constant temperature across any section normal to the flow were not approached, the pressure drop which was predicted from the Annular Flow equations was from 15 to 45 per cent greater than the measured pressure drop.

3. The solution of the Annular Flow equations required that only the initial conditions of mass flow rate and inlet pressure be known along with the tube length or outlet pressure. Further information concerning the flow variables at some point downstream from point of initial vaporization was not required to obtain a solution for the flow variables as a

function of distance along the tube. All previous flow models have required additional information about the flow variables at some point downstream from the point of initial vaporization or that a simplifying assumption be made to obtain a solution.

4. The use of an X-ray tube as a source of monoenergetic gamma radiation was developed for the measurement of the void fraction in two-phase steam-water flow. The accuracy of the measurement was established to be within the Probable Error.

The following recommendations are made for further research in this specific area of vaporizing two-phase flow which would provide fruitful results:

1. Modification of the Annular Flow equations to include rate equations for heat and mass transfer to describe the deviation from the basic assumptions of thermodynamic equilibrium at all stages in the expansion and constant temperature across any section normal to the flow. This would necessarily require a further description of the vapor-liquid interface. Studies could include both the adiabatic case for the total flow and heat transfer from the surroundings.

2. Basic studies to describe the critical flow phenomena in two-phase flow as a function of pressure, quality and mass flow rate.

A P P E N D I C E S

APPENDIX A

DATA FOR THE SINGLE PHASE FLOW RUNS AND THE TWO-PHASE FLOW RUNS

In Table 6 the experimental pressure drop-flow rate data is given for the twenty-eight single-phase flow runs.

In Table 7 the experimental pressure drop-flow rate data is given for the two-phase flow runs.

In Figure 21 through 48 for each of the twenty-eight two-phase flow runs, the measured temperatures and the saturation temperatures corresponding to the measured pressures are plotted against the test section length from the inlet (z = 0.0 ft) to the exit (z = 19.42 ft). The point of initial vaporization is indicated on each figure by an arrow. The point of initial vaporization was determined by the intersection of the curve drawn through the saturation temperatures corresponding to the measured pressures with the curve drawn through the measured temperature. The point on the test section where the void fraction was measured is designated on each figure as L-1 or L-2. Location L-1 was 3.17 feet from the exit of the test section and location L-2 was 8.17 feet from the exit of the test section. Also indicated on each figure is the inlet pressure P_o (taken at the point of initial vaporization) and corresponding saturation temperature T_o, and exit pressure P_e and corresponding saturation temperature T_e. Also designated on each figure is the two-phase flow pressure drop ΔP, and the length of the tube, L, from the point of initial vaporization to the exit.

Table 6. Single-Phase Flow Pressure Drop Data

Run Number	Mass Flow Rate (lb_m/ft^2-sec)	Measured Pressures (psia)			Temperature (°F)
		Entrance	Center	Exit	
3022	444.5	31.4	30.6	29.5	163
10222	444.5	33.7	32.9	31.9	154
2036	554.0	33.2	31.8	30.7	195
1022	579.7	33.3	31.9	30.5	195
2022	605.2	33.2	31.8	30.2	192
3036	605.2	33.6	32.1	30.6	196
1033	557.1	38.5	37.0	35.5	170
10127	582.6	39.6	38.0	36.6	152
20127	637.7	38.9	37.2	35.8	168
1036	637.7	38.4	37.1	35.8	175
10131	582.6	47.2	45.9	44.3	176
10224	582.6	47.2	46.3	44.7	154
20130	729.6	47.0	45.5	43.5	166
20224	729.6	47.6	45.8	43.7	190
10227	729.6	51.4	49.6	47.4	187
30224	864.0	47.0	45.0	42.2	193
10130	864.0	47.2	44.9	42.1	166
1028	582.6	55.4	54.1	52.3	160
1037	582.6	53.9	52.8	51.3	185
10213	729.6	54.8	53.0	51.0	172
20227	729.6	59.0	56.9	54.3	186
10214	848.4	55.6	53.7	51.1	174
30227	848.4	55.3	53.2	50.7	177
3037	709.8	66.0	64.2	62.0	185
10215	729.6	66.4	64.5	62.0	196
10228	763.6	69.7	67.8	65.3	170
10217	763.6	67.7	65.8	64.0	152
20215	832.8	66.1	63.6	60.9	177

Table 7. Two-Phase Flow Pressure Drop Data

Run Number	Mass Flow Rate (lb_m/ft^2-sec)	Measured Pressures (psia)				Remarks
		Entrance	Center	Exit	Expansion Section	
3022	444.5	32.6	31.5	25.9	21.8	
10222	444.5	34.0	33.2	27.8	25.3	
2036	554.0	33.5	32.4	28.7	25.5	
1022	579.7	33.5	32.5	29.1	27.0	
2022	605.2	32.7	31.7	28.2	24.0	critical flow
3036	605.2	34.6	33.1	29.6	26.6	critical flow
1033	557.1	39.6	38.5	32.9	28.7	
10127	582.6	39.3	38.2	33.7	30.8	
20127	637.7	39.3	38.1	33.7	28.2	critical flow
1036	637.7	39.7	38.2	34.1	29.6	critical flow
10131	582.6	47.2	45.9	38.3	34.3	
10224	582.6	49.8	48.4	40.4	39.0	
20130	729.6	46.2	44.5	40.2	33.5	
20224	729.6	46.9	45.6	41.0	38.6	
10227	729.6	51.9	50.8	44.9	40.1	
30224	864.0	47.0	45.1	40.9	38.9	critical flow
10130	864.0	48.4	46.0	41.8	37.6	critical flow
1028	582.6	55.0	53.9	46.7	44.7	
1037	582.6	54.6	53.2	45.5	41.7	
10213	729.6	54.9	49.3	43.0	36.8	
20227	729.6	58.4	57.1	49.6	47.3	
10214	848.4	56.2	54.5	49.3	46.0	critical flow
30227	848.4	55.0	53.4	48.4	46.2	critical flow
3037	709.8	64.5	63.0	53.3	51.4	
10215	729.6	65.2	64.1	58.2	57.8	
10228	763.6	66.5	64.9	54.2	49.6	
10217	763.6	67.0	65.8	55.0	50.4	
20215	832.8	64.1	62.7	57.4	56.2	critical flow

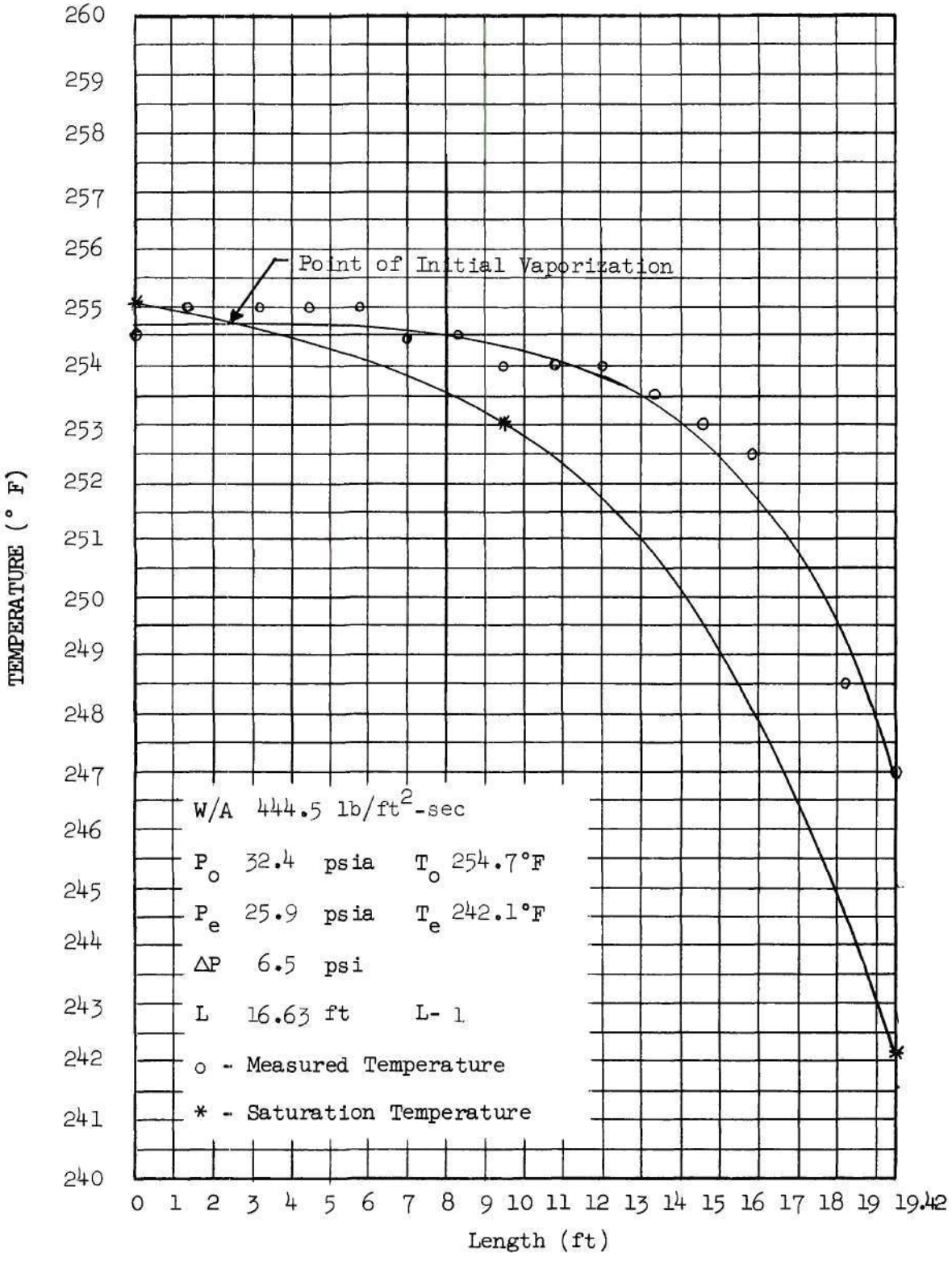

Figure 21. Temperature versus Length for Run 3022.

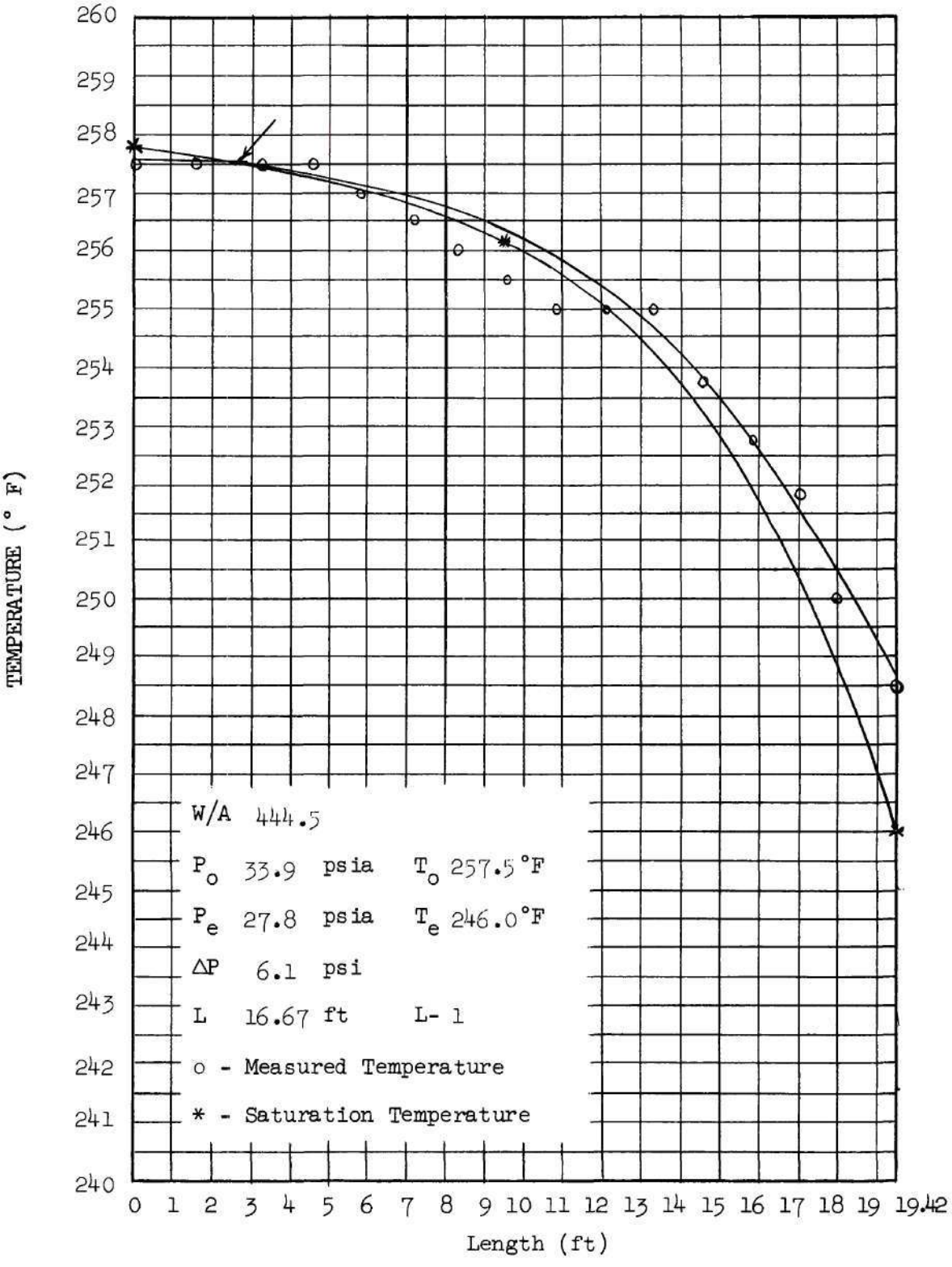

Figure 22. Temperature versus Length for Run 10222.

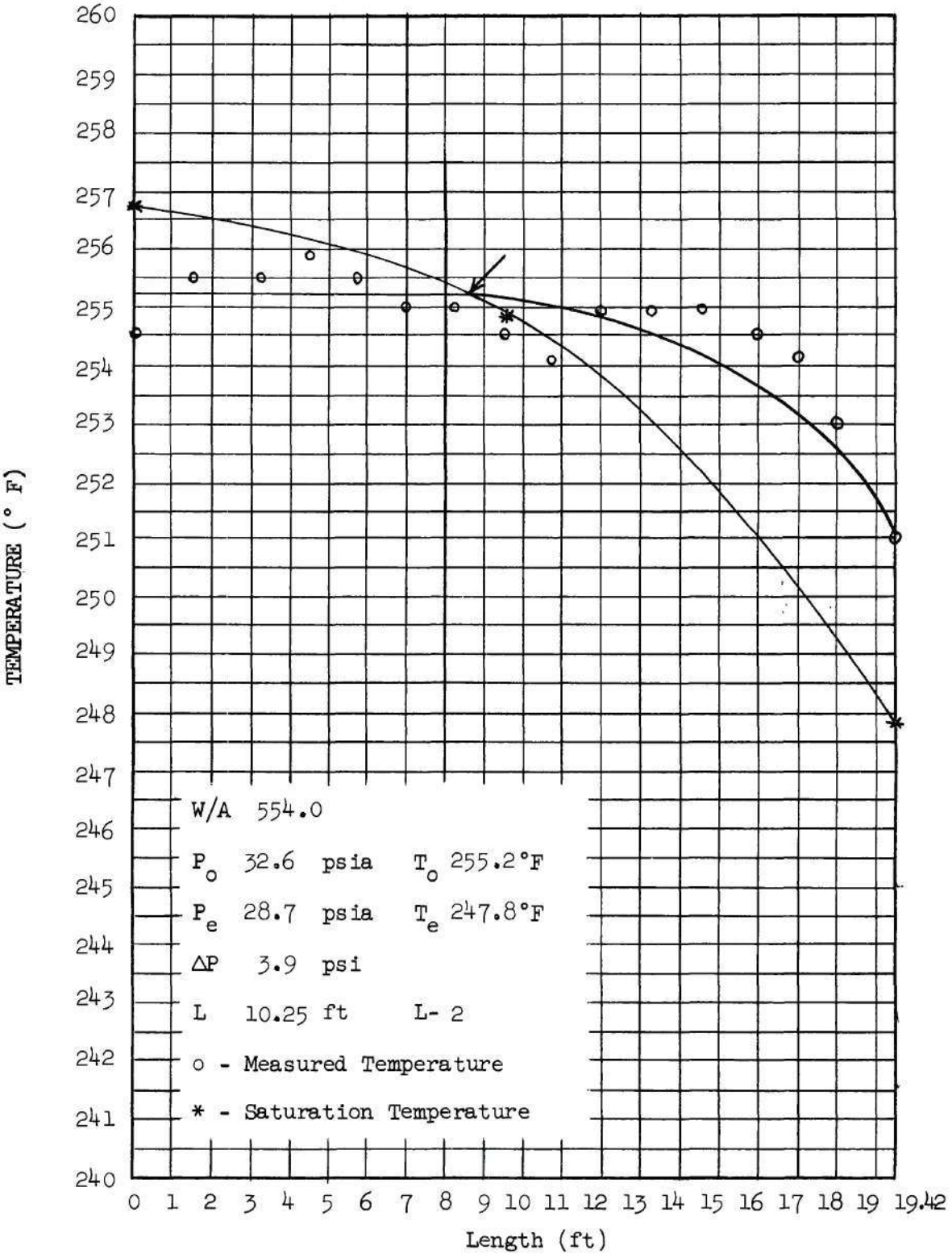

Figure 23. Temperature versus Length for Run 2036.

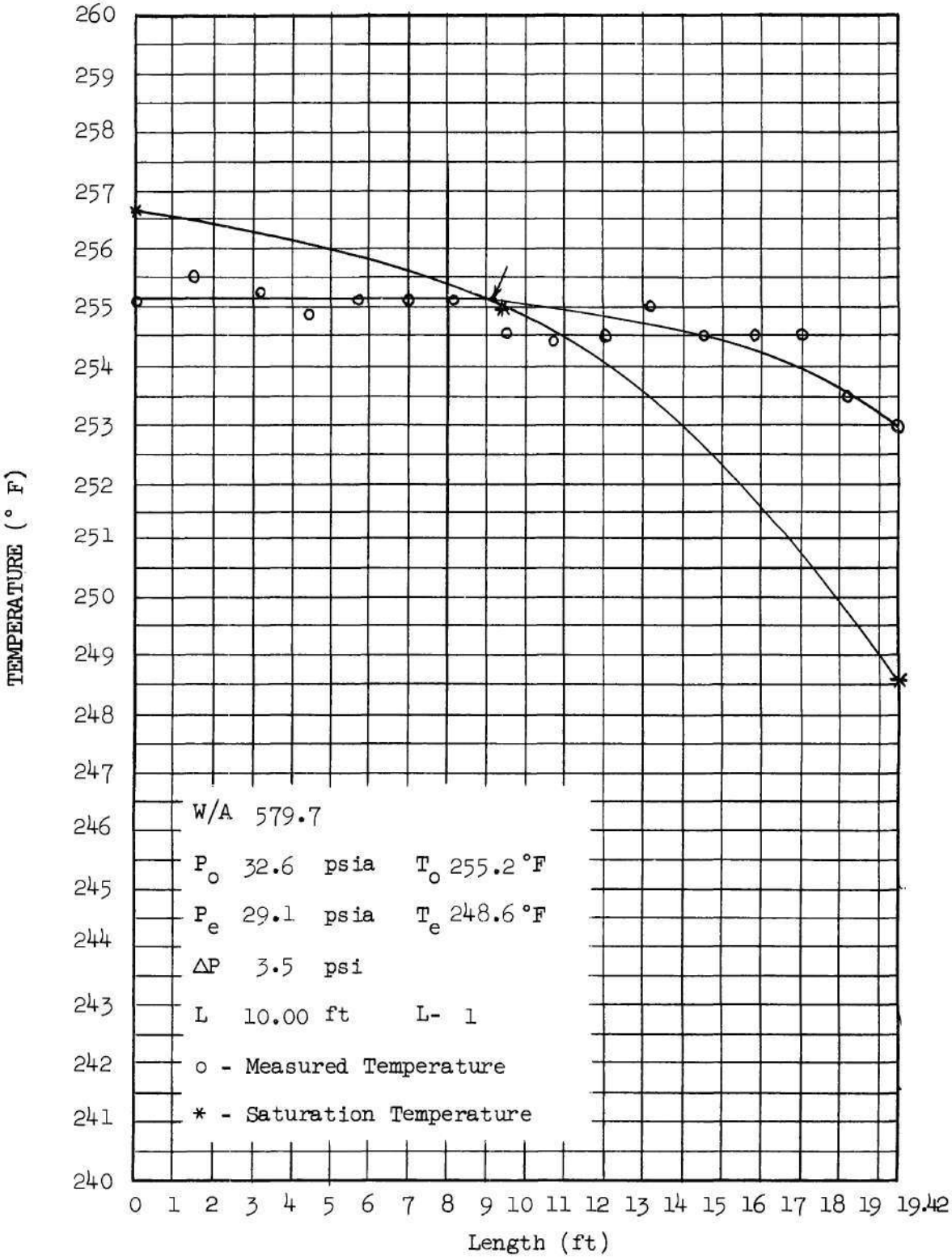

Figure 24. Temperature versus Length for Run 1022.

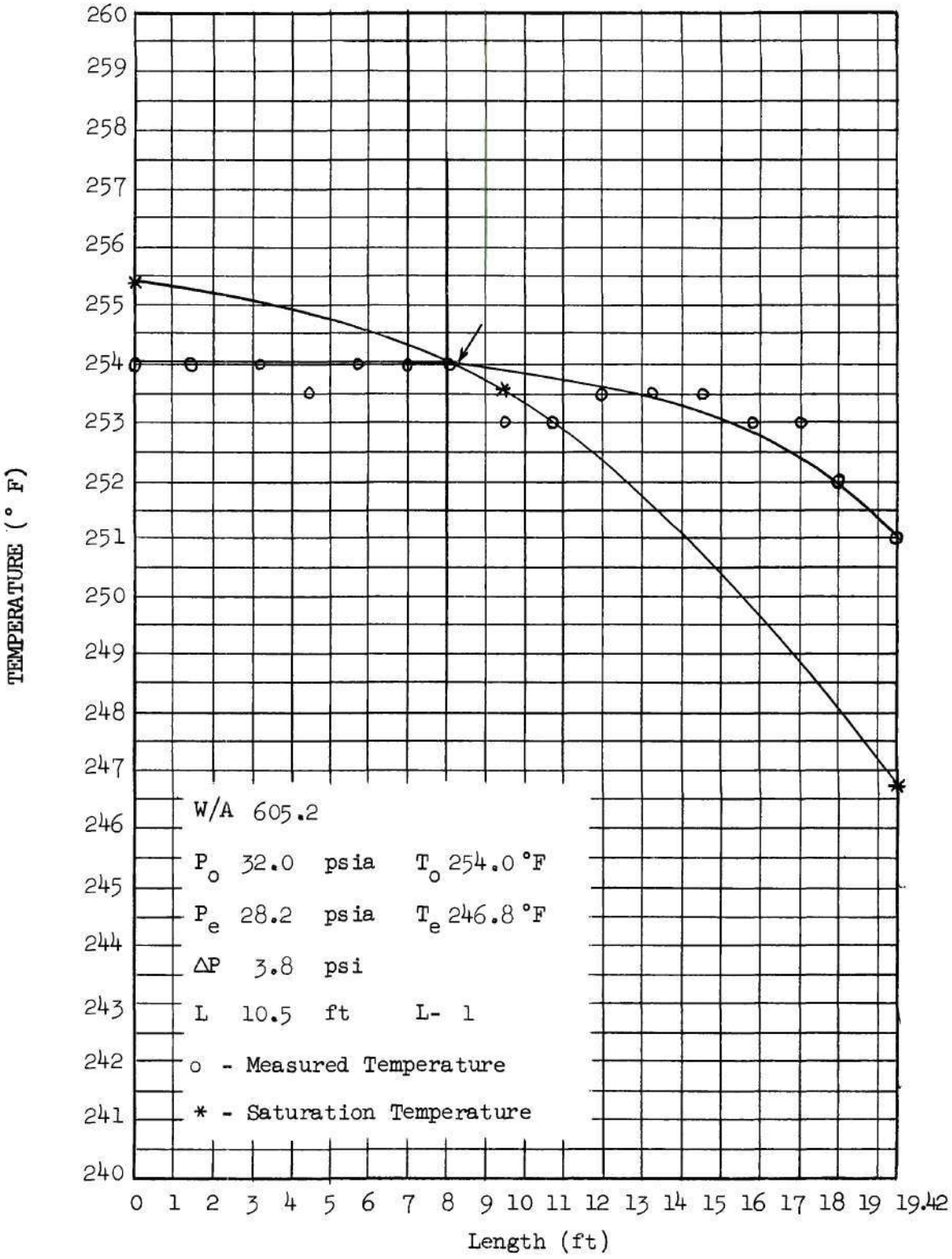

Figure 25. Temperature versus Length for Run 2022.

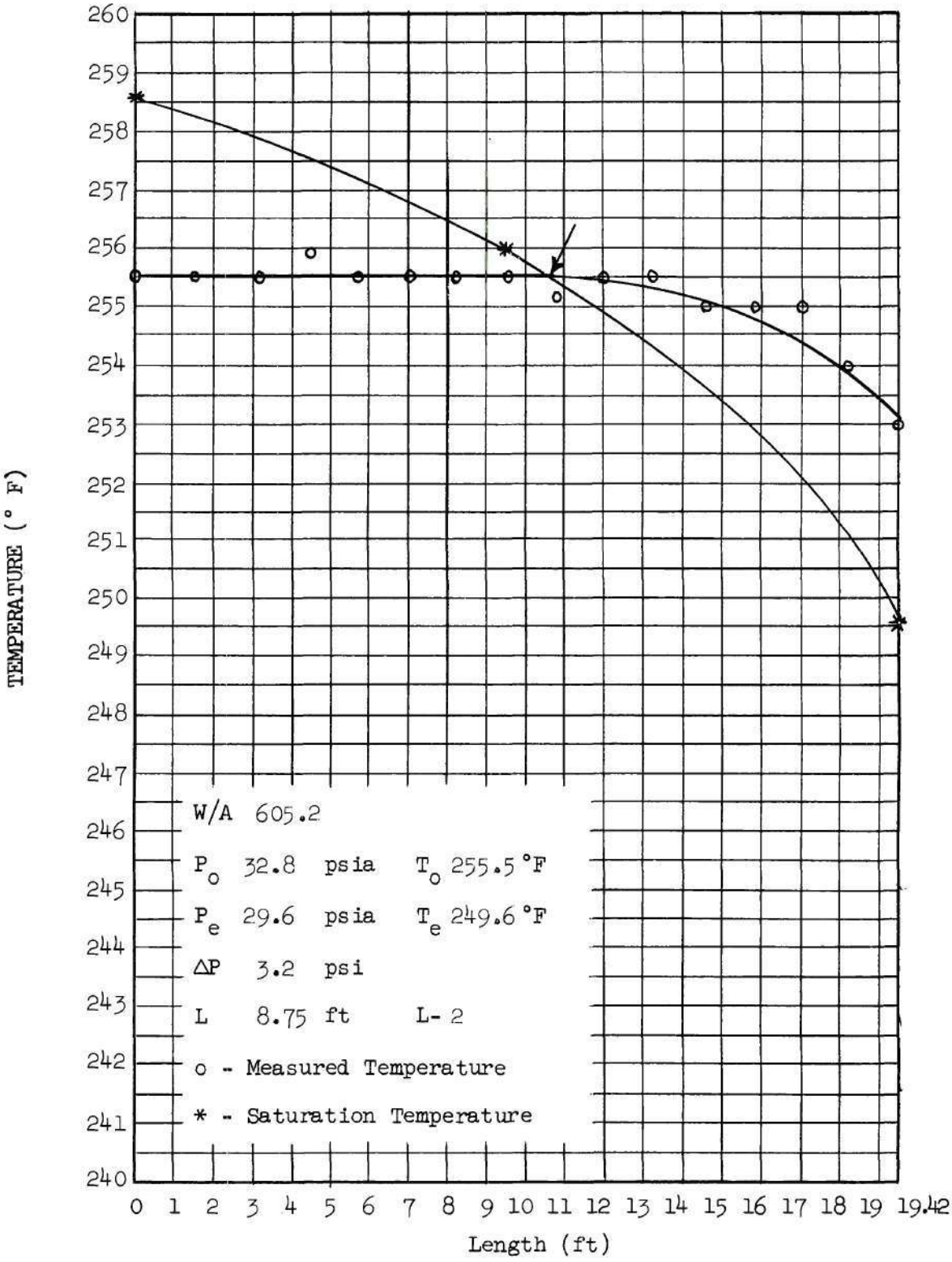

Figure 26. Temperature versus Length for Run 3036.

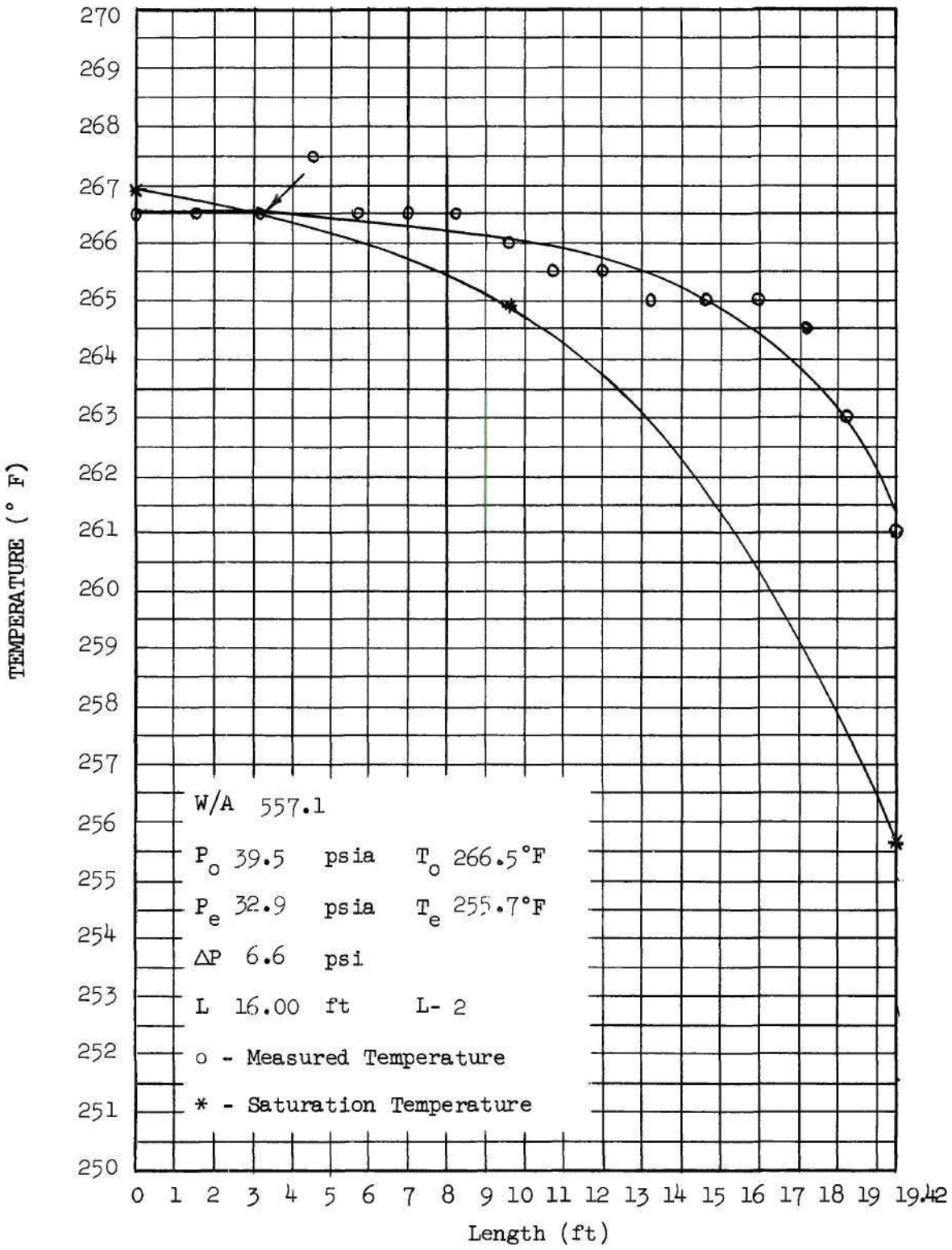

Figure 27. Temperature versus Length for Run 1033.

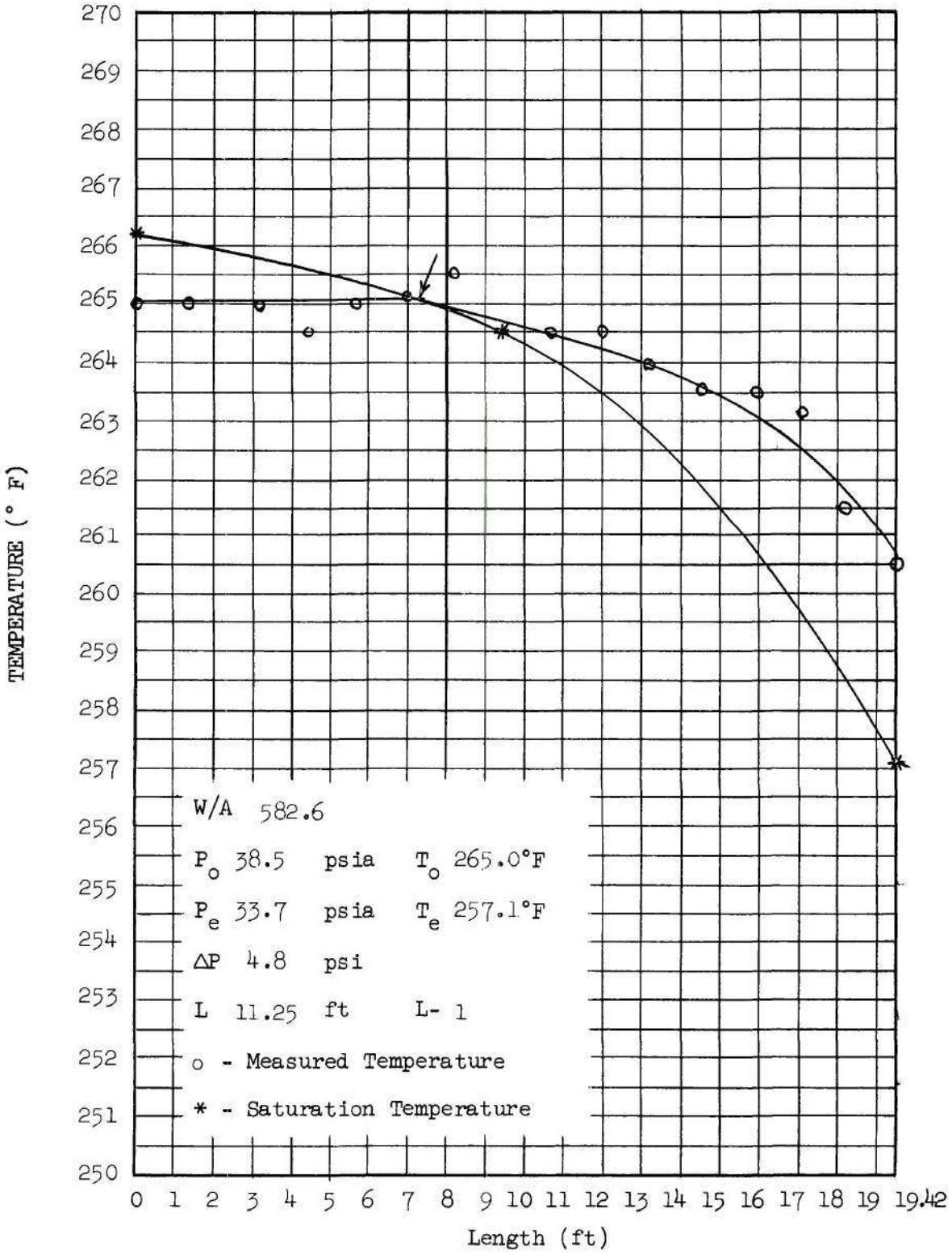

Figure 28. Temperature versus Length for Run 10127.

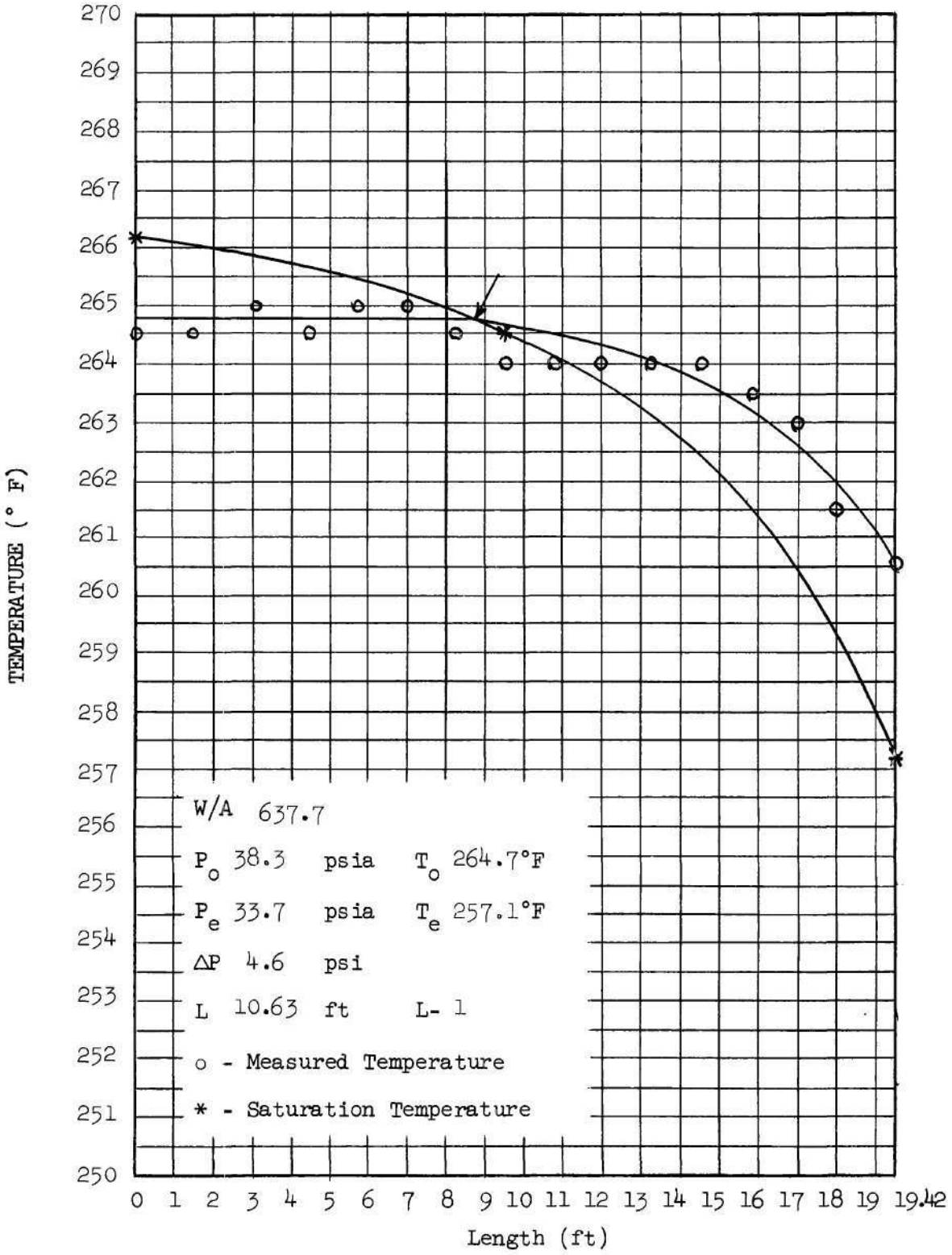

Figure 29. Temperature versus Length for Run 20127.

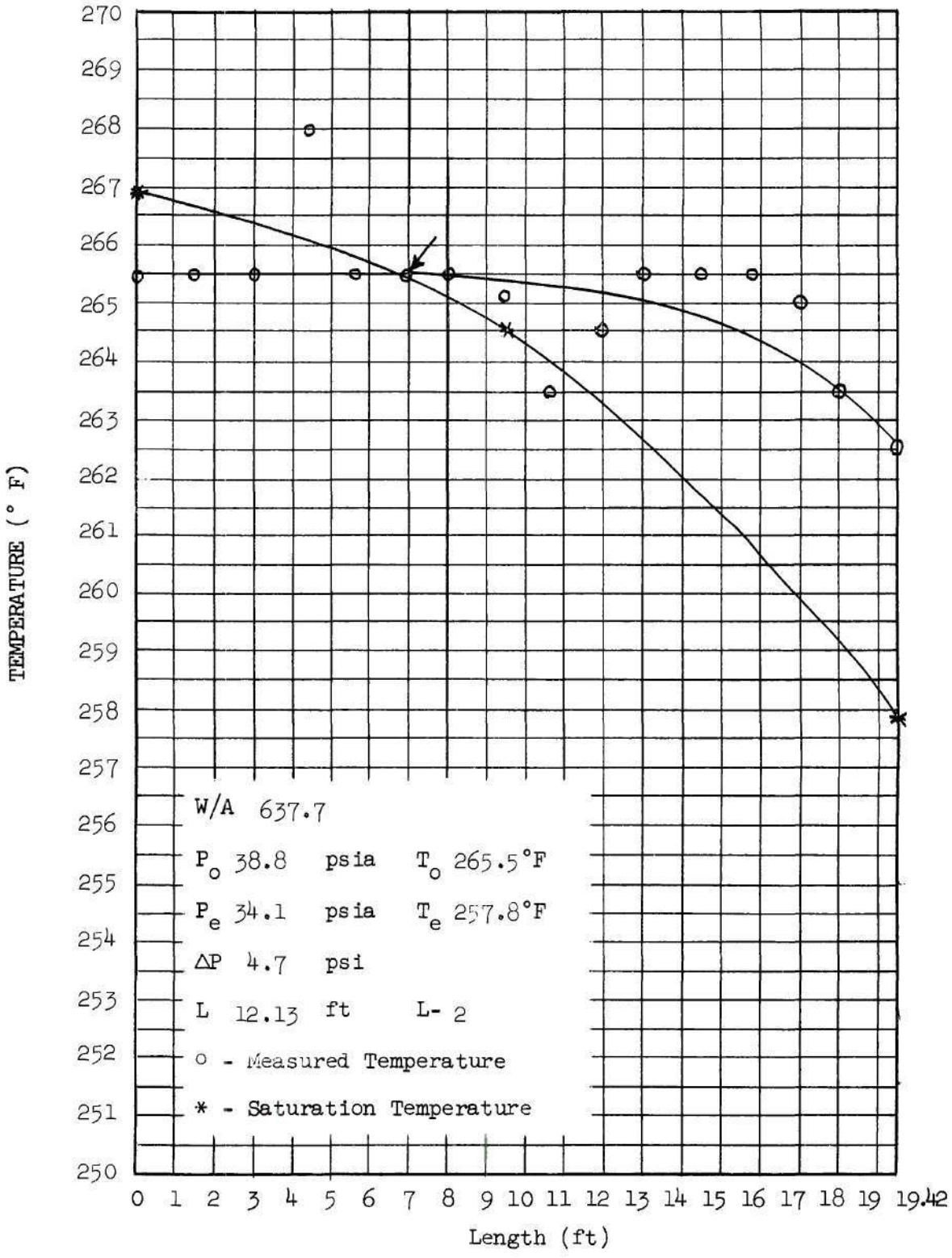

Figure 30. Temperature versus Length for Run 1036.

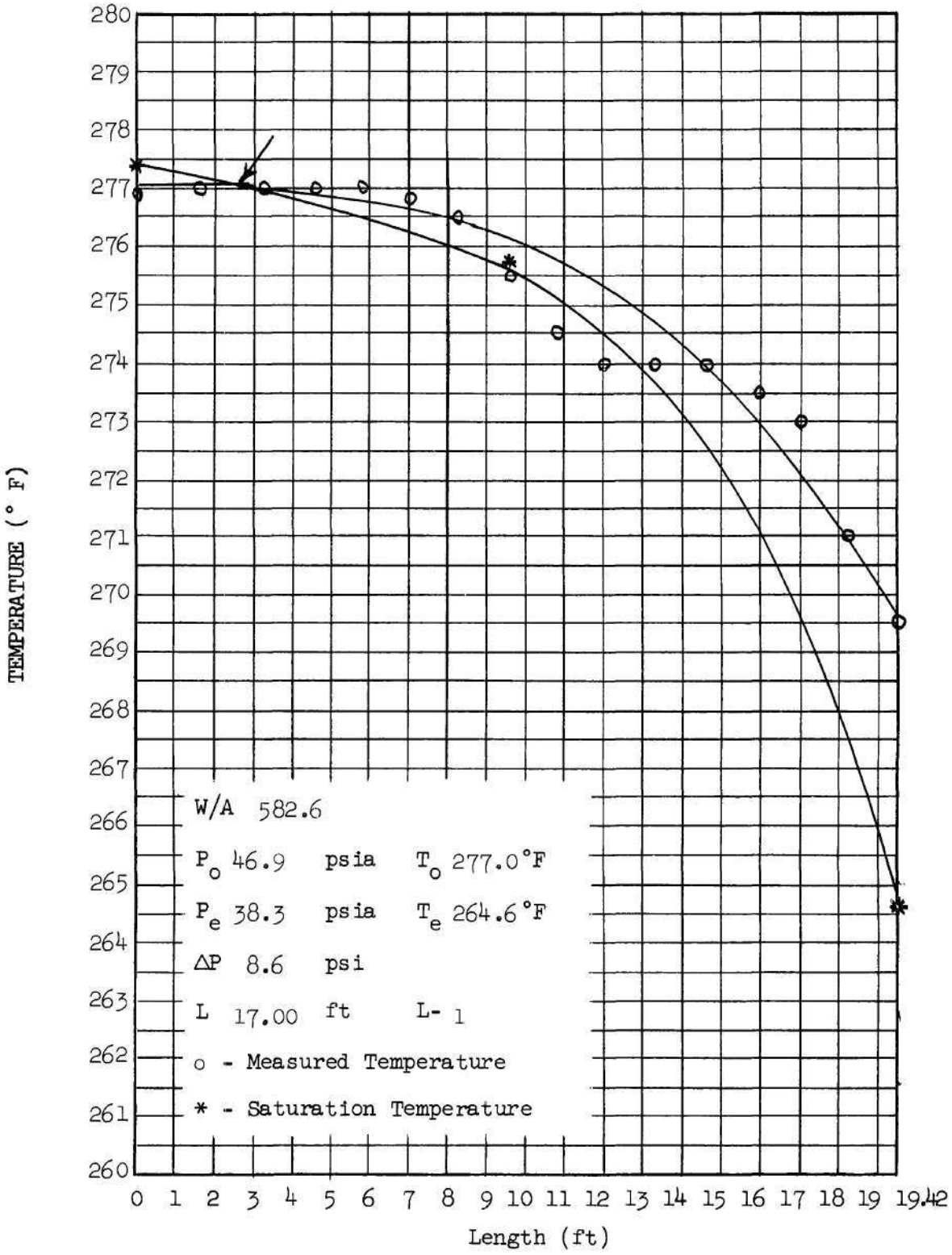

Figure 31. Temperature versus Length for Run 10131.

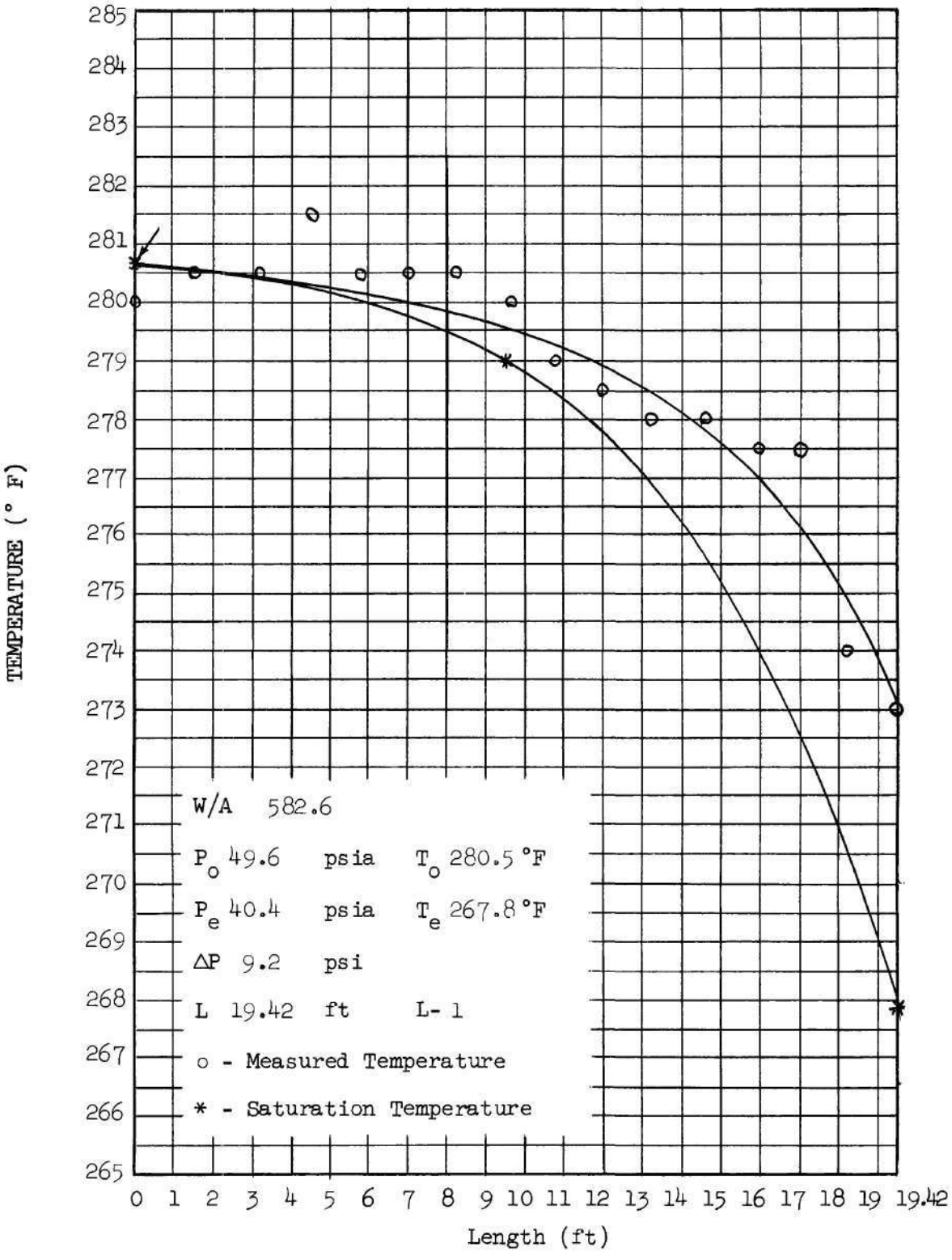

Figure 32. Temperature versus Length for Run 10224

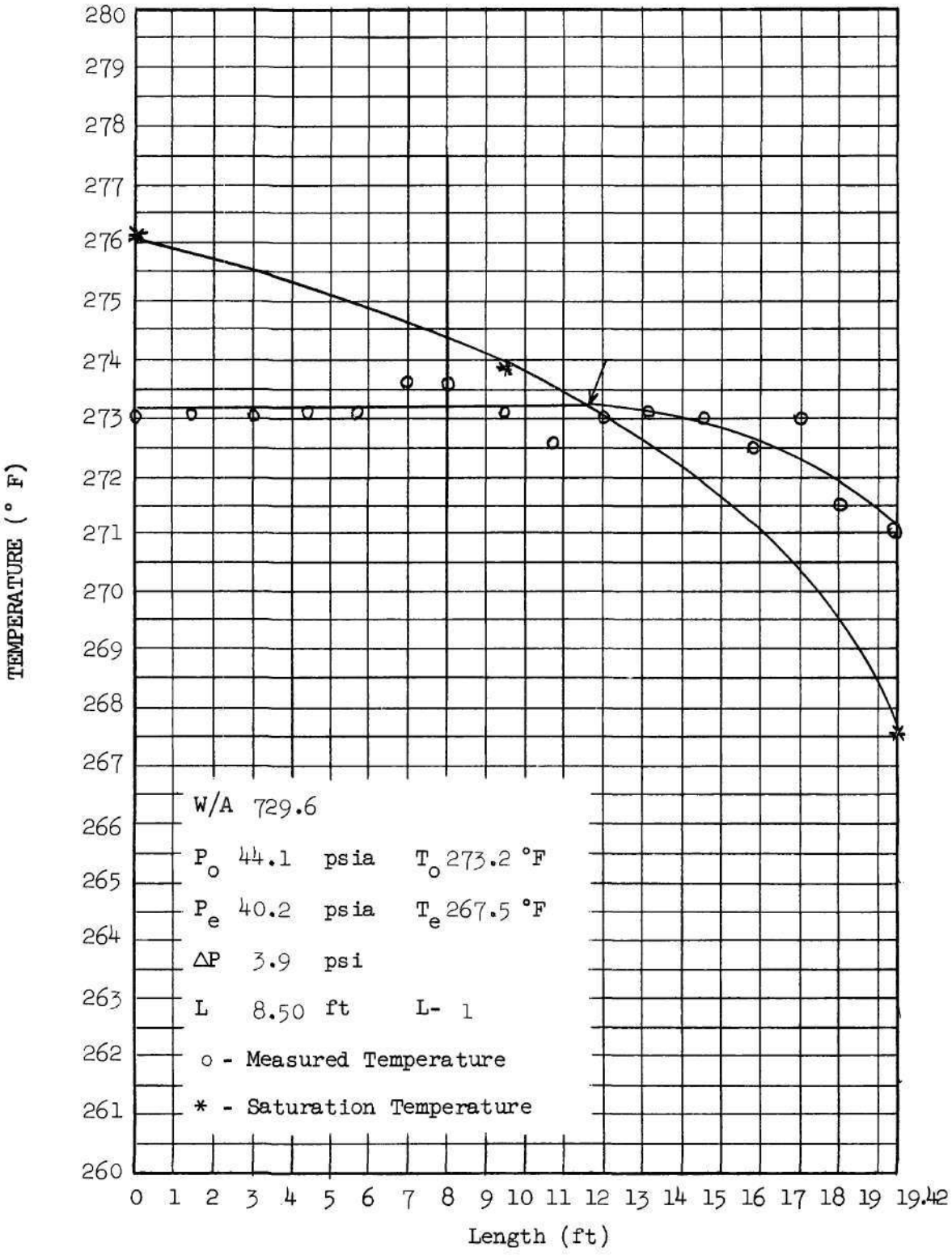

Figure 33. Temperature versus Length for Run 20130.

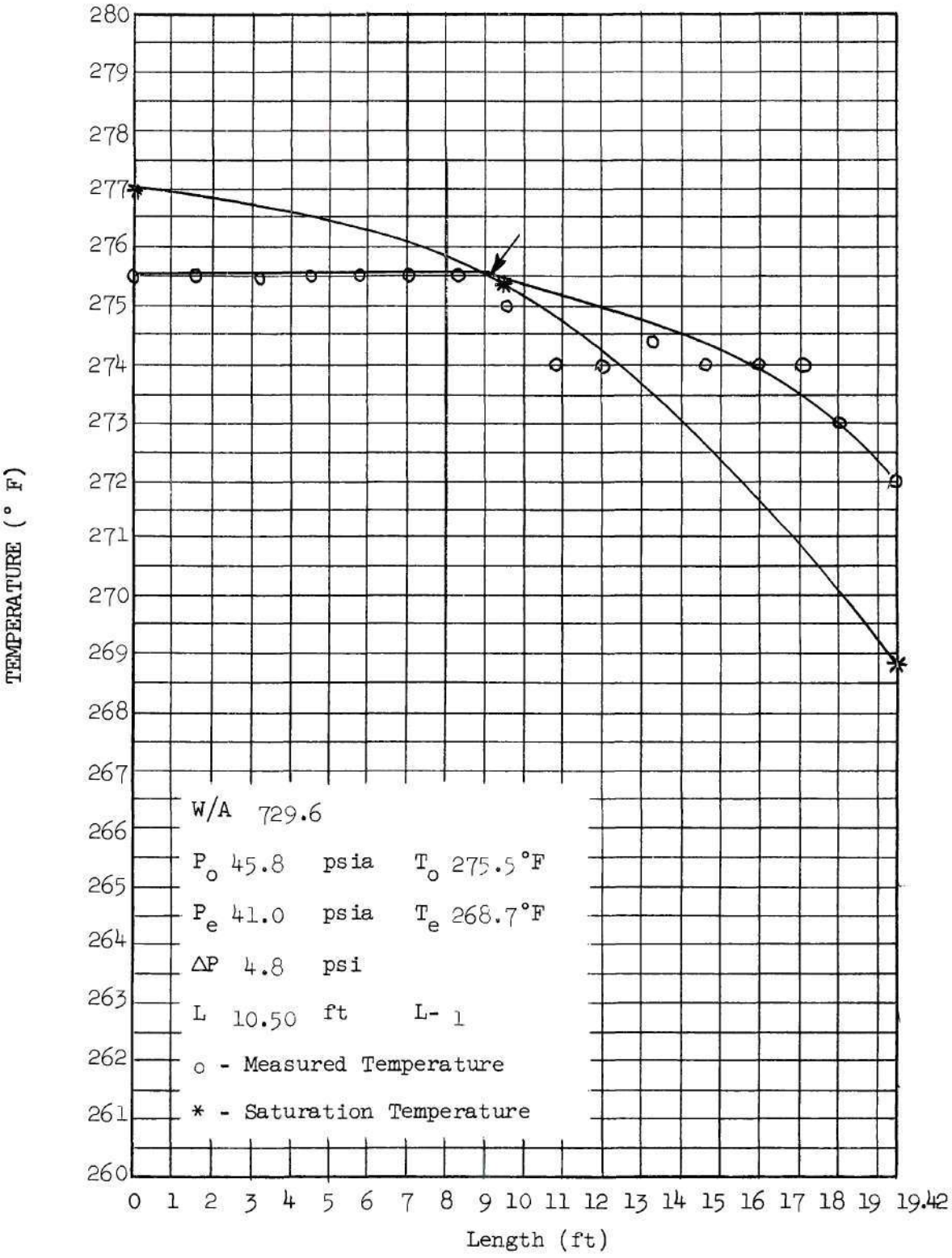

Figure 34. Temperature versus Length for Run 20224.

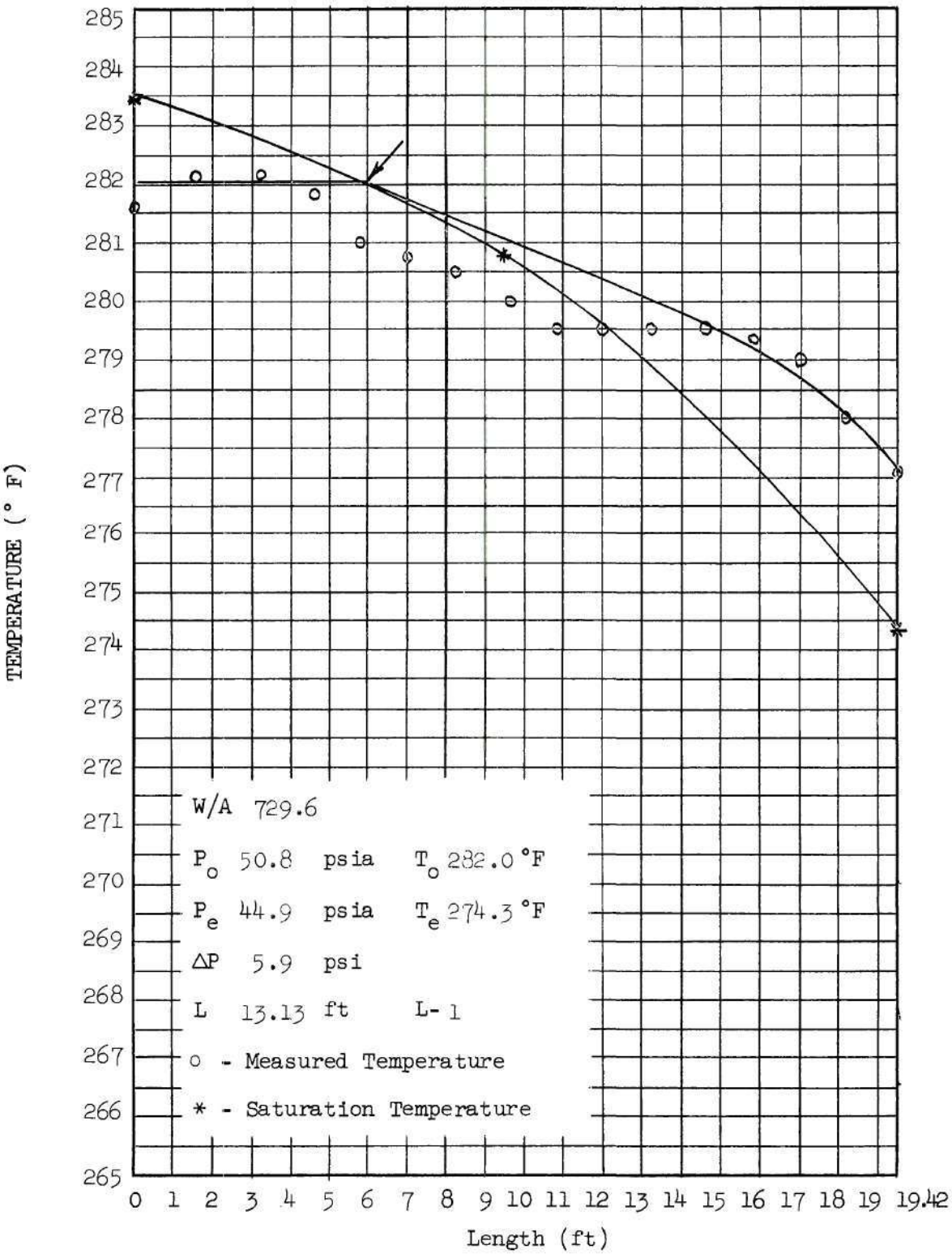

Figure 35. Temperature versus Length for Run 10227.

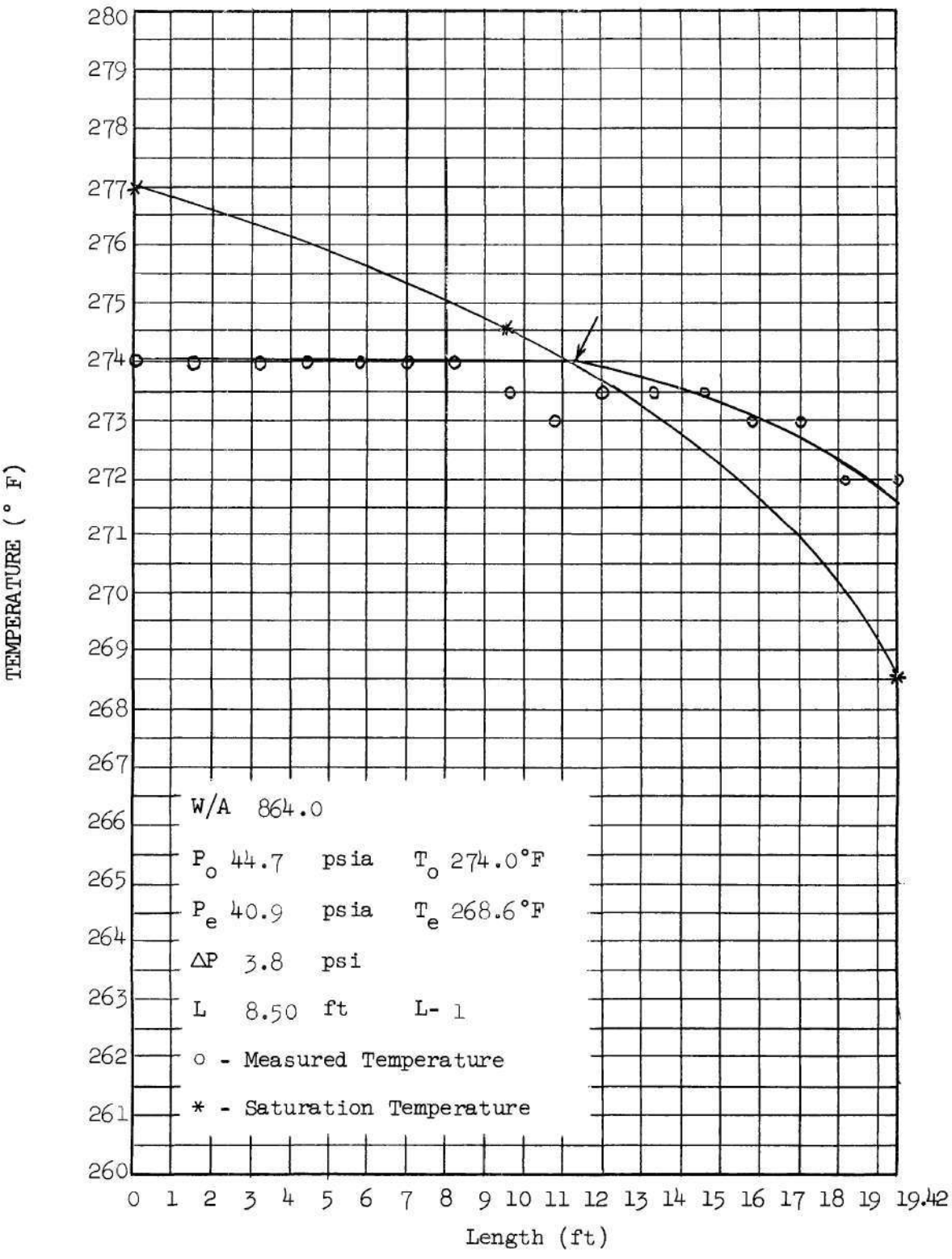

Figure 36. Temperature versus Length for Run 30224.

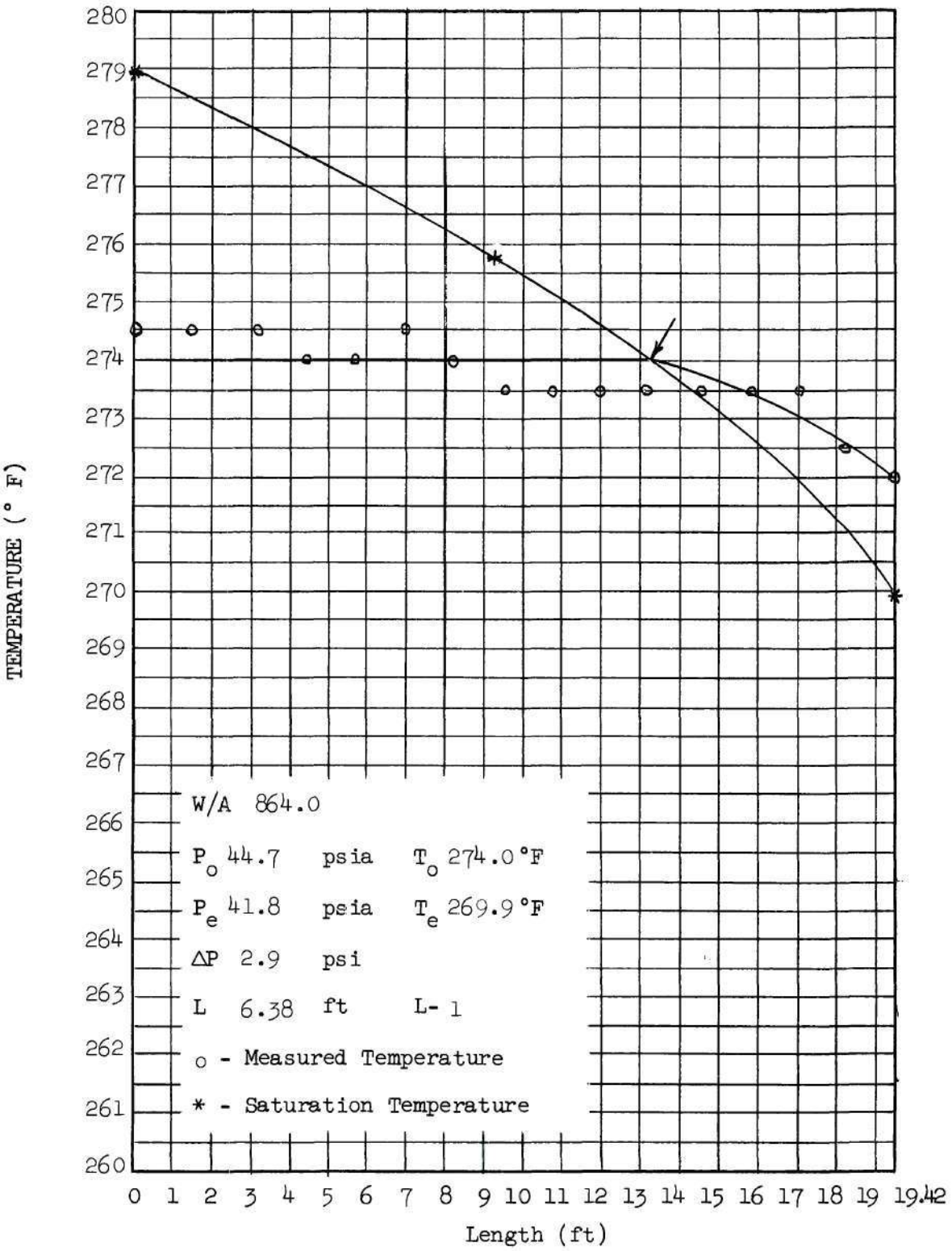

Figure 37. Temperature versus Length for Run 10130.

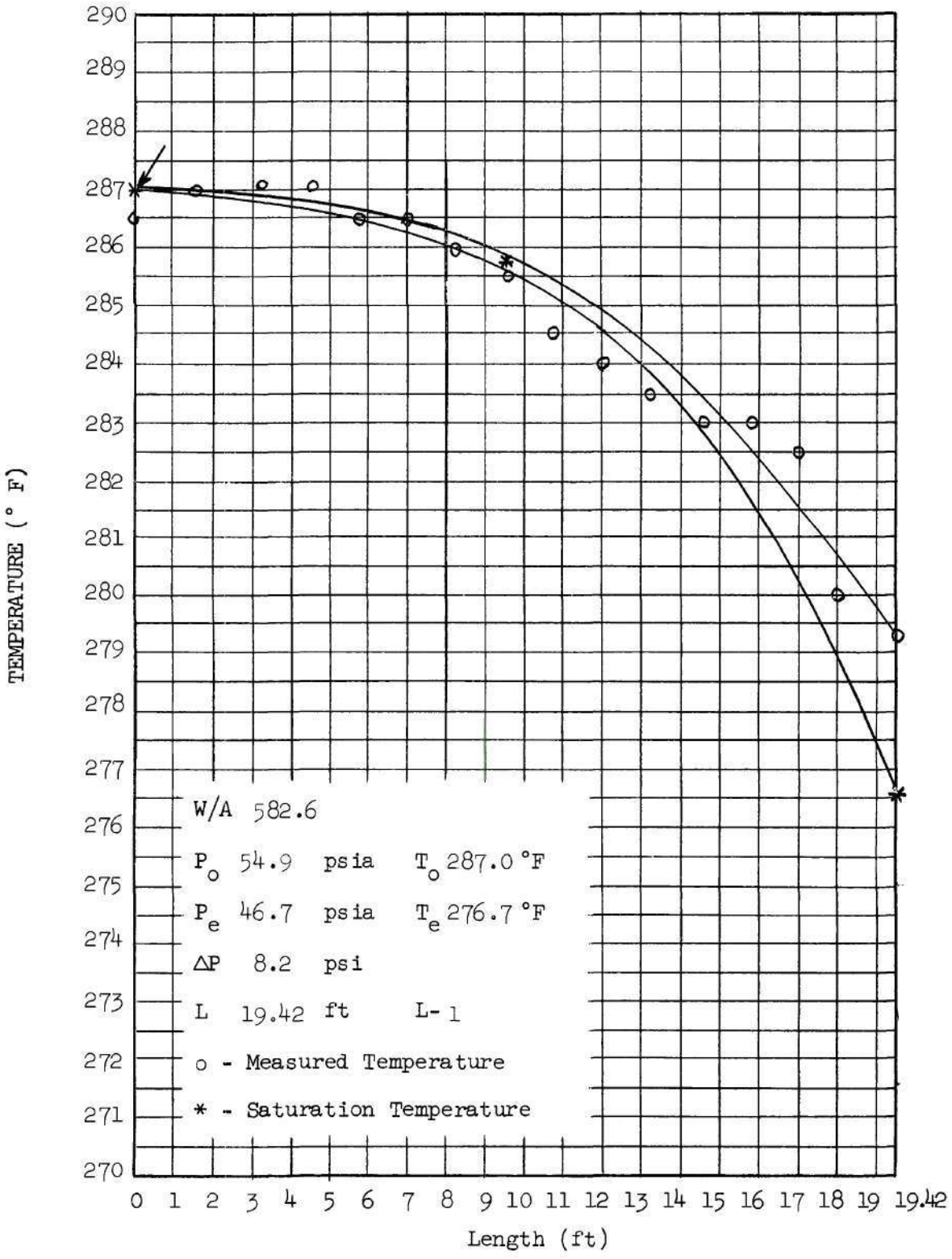

Figure 38. Temperature versus Length for Run 1028.

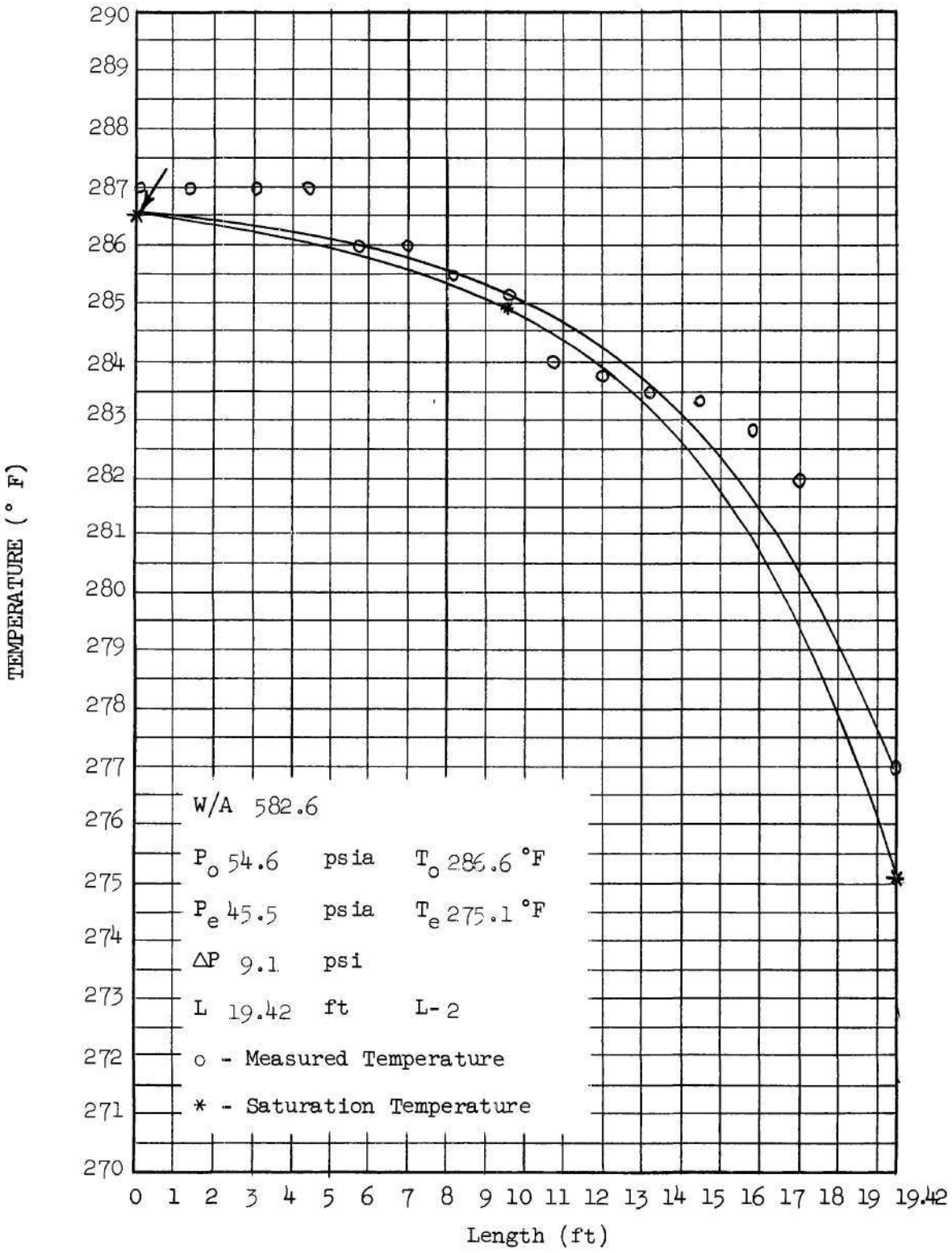

Figure 39. Temperature versus Length for Run 1037.

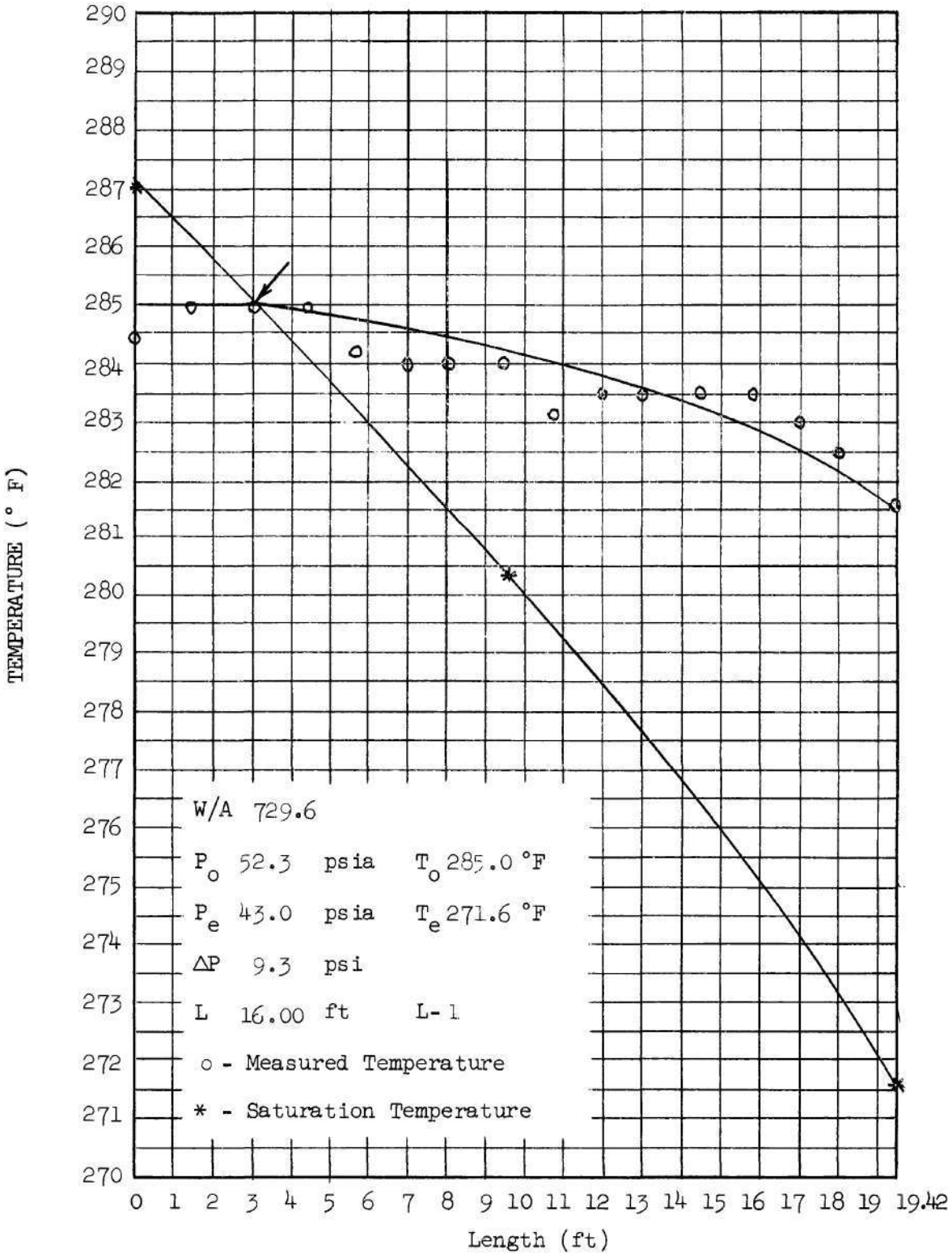

Figure 40. Temperature versus Length for Run 10213.

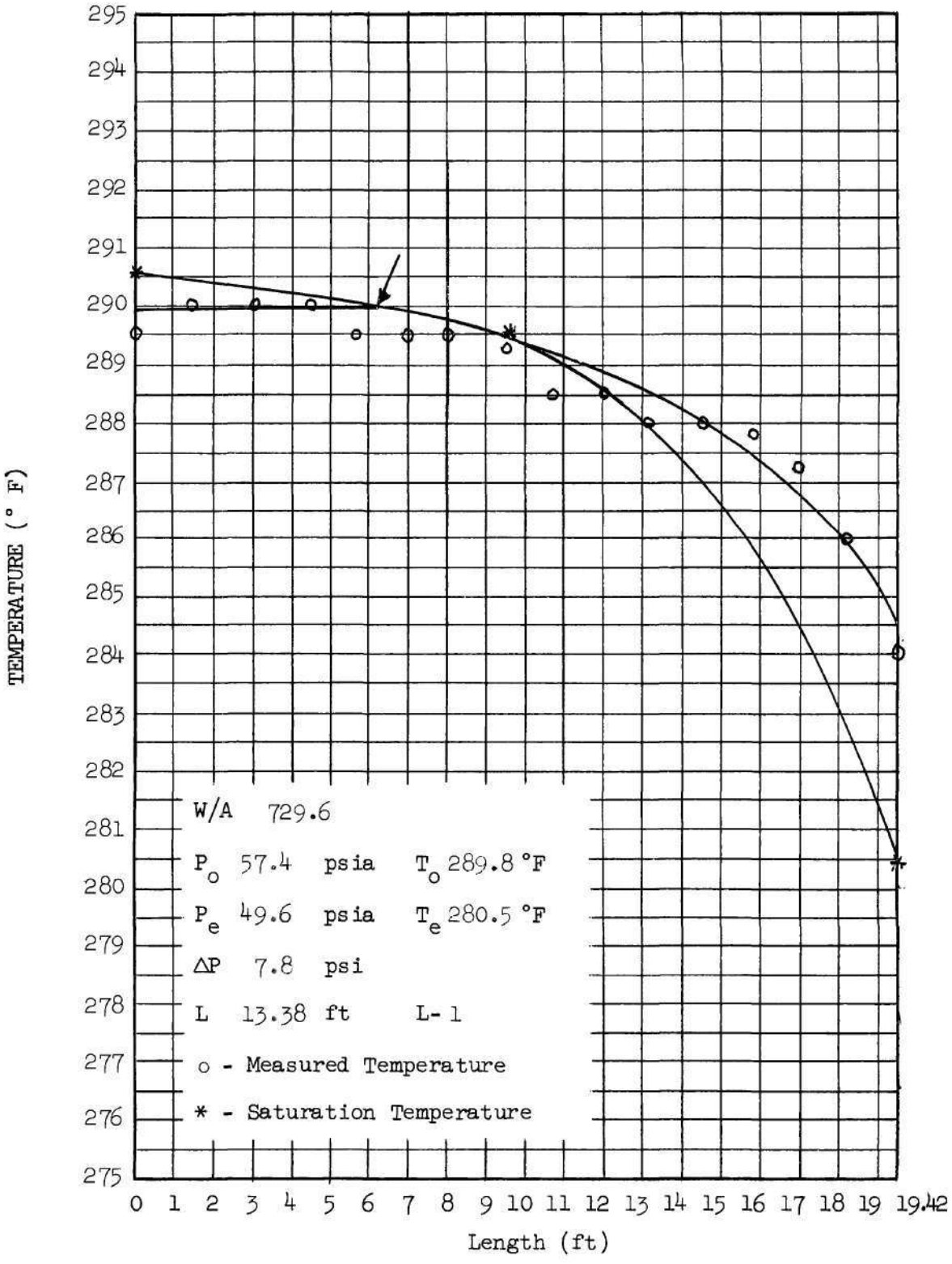

Figure 41. Temperature versus Length for Run 20227.

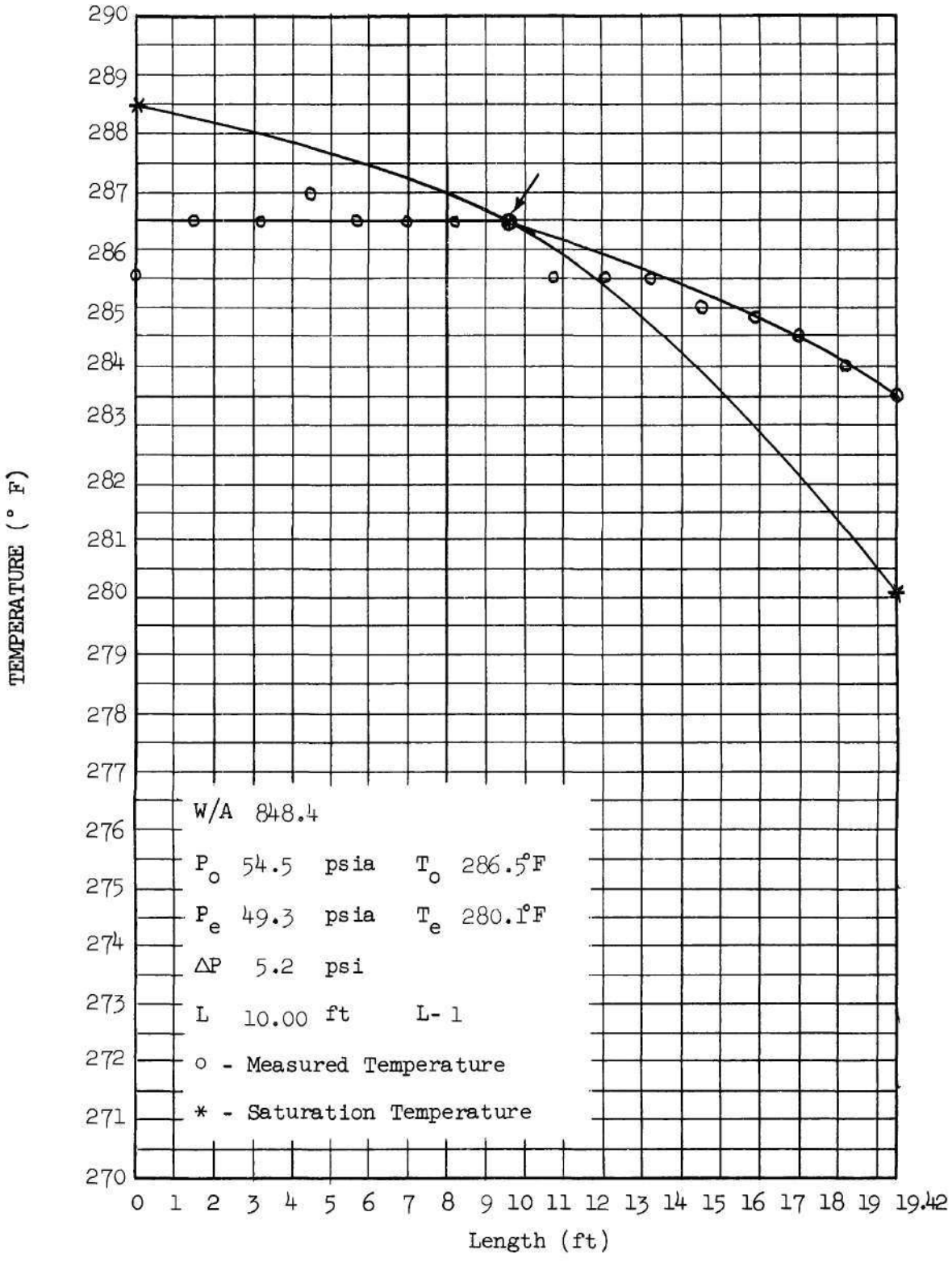

Figure 42. Temperature versus Length for Run 10214.

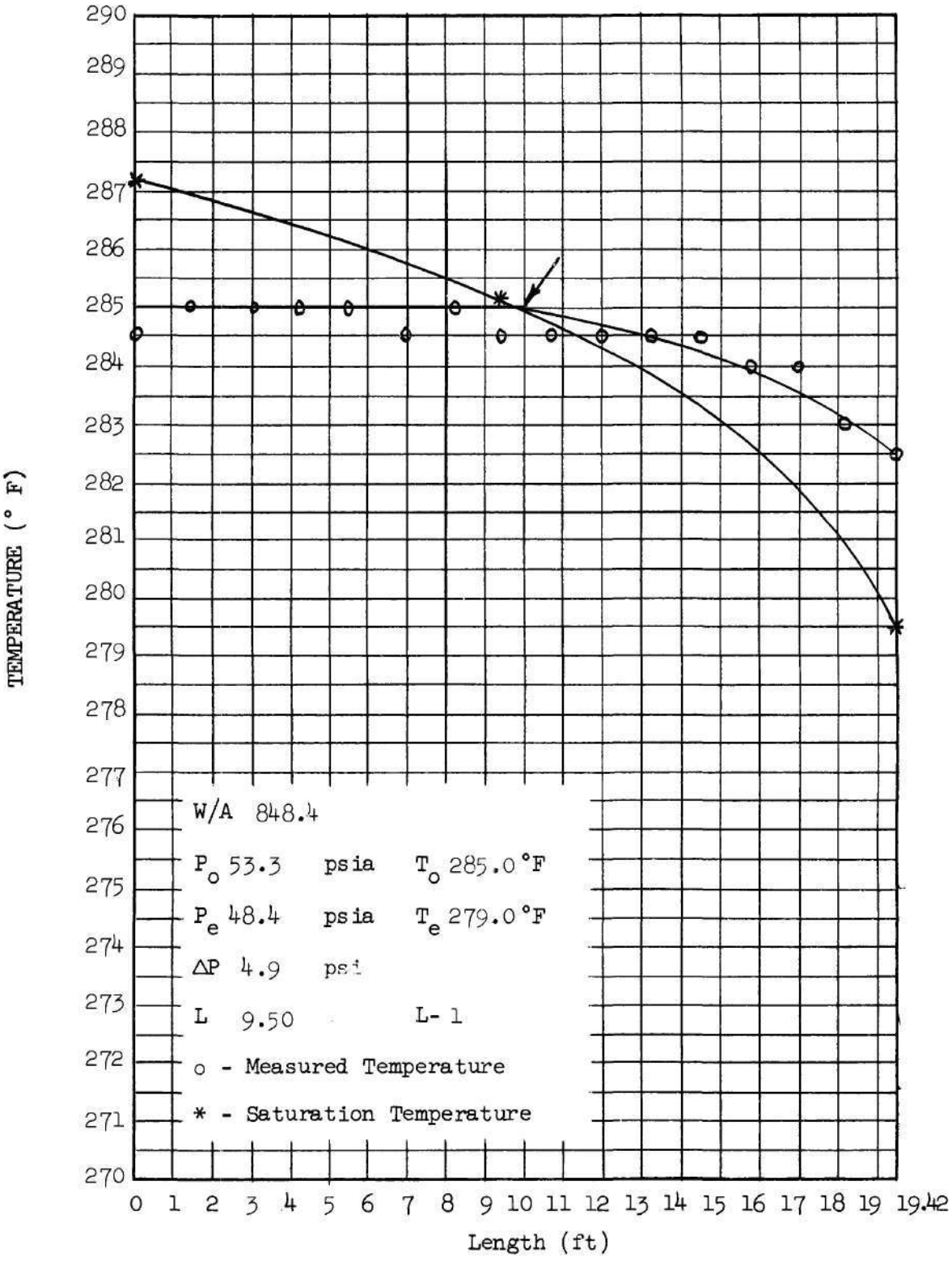

Figure 43. Temperature versus Length for Run 30227.

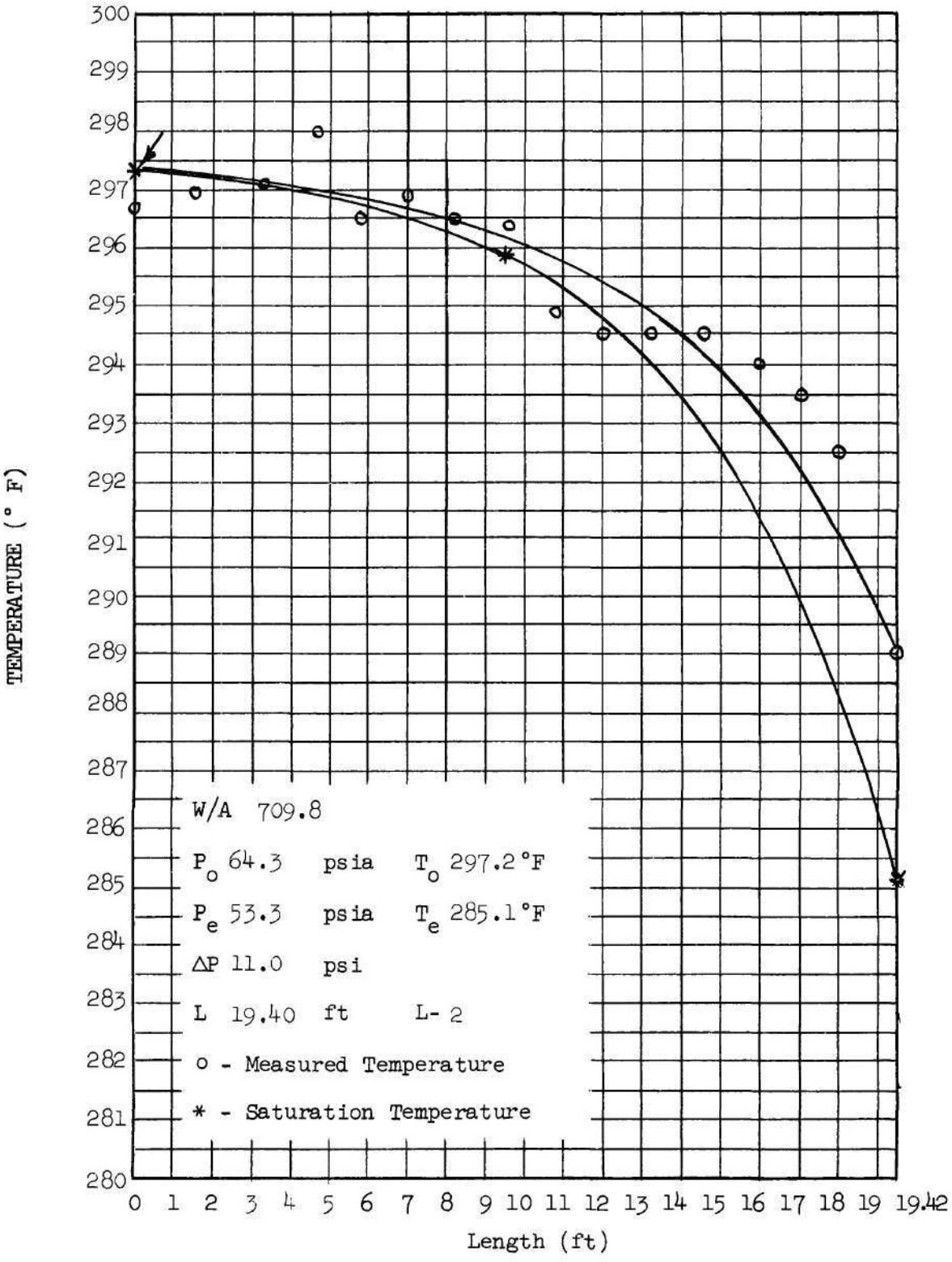

Figure 44. Temperature versus Length for Run 3037.

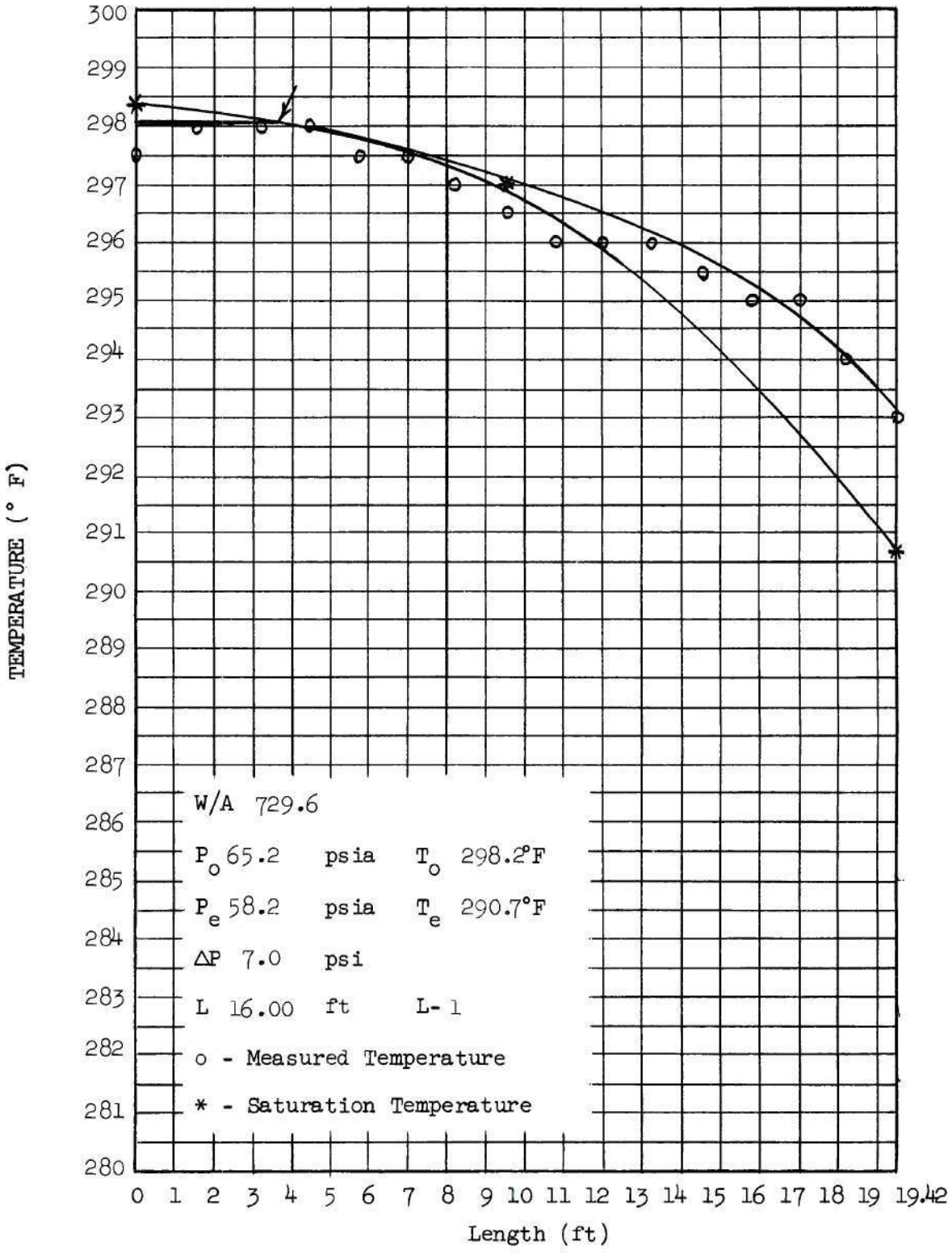

Figure 45. Temperature versus Length for Run 10215.

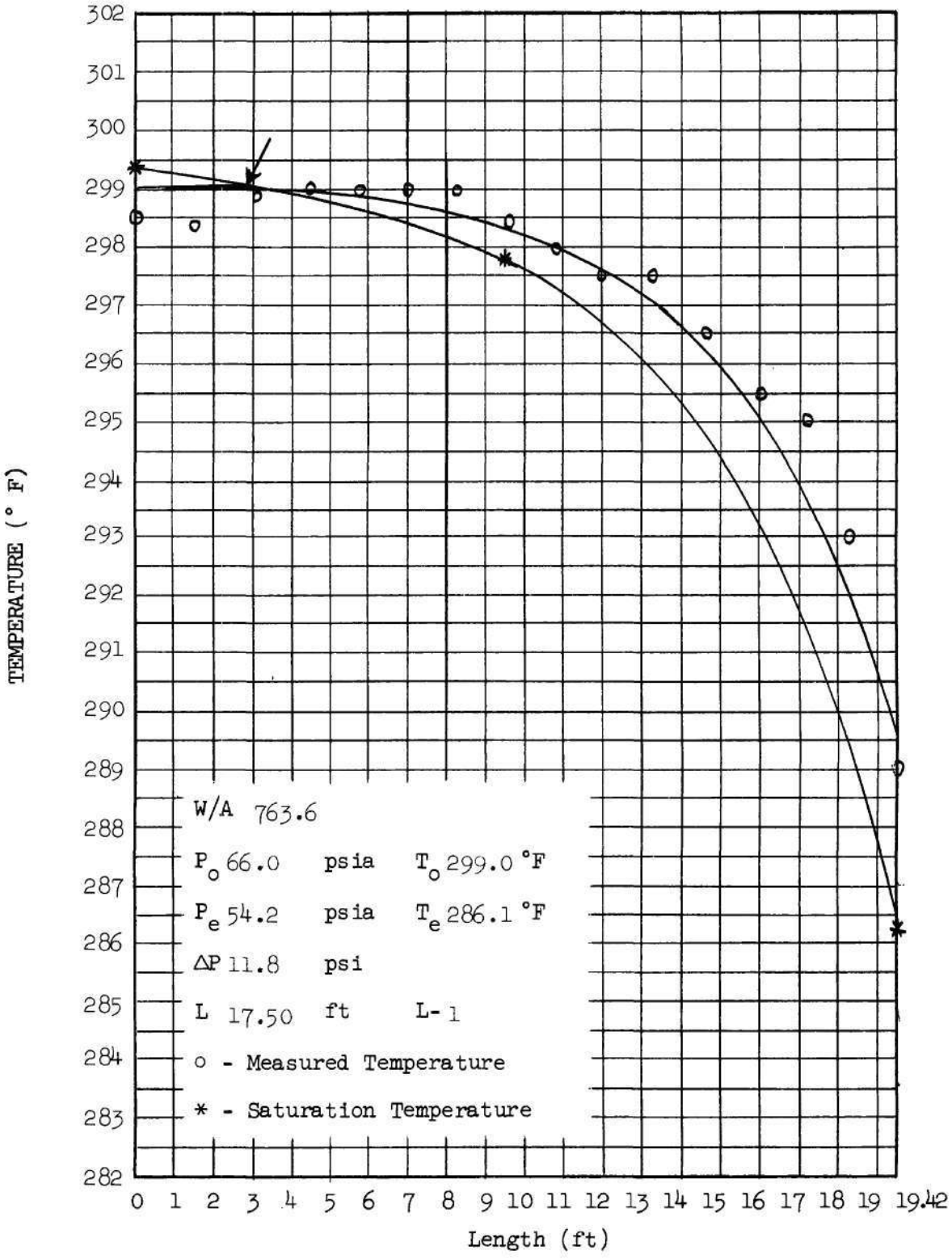

Figure 46. Temperature versus Length for Run 10228.

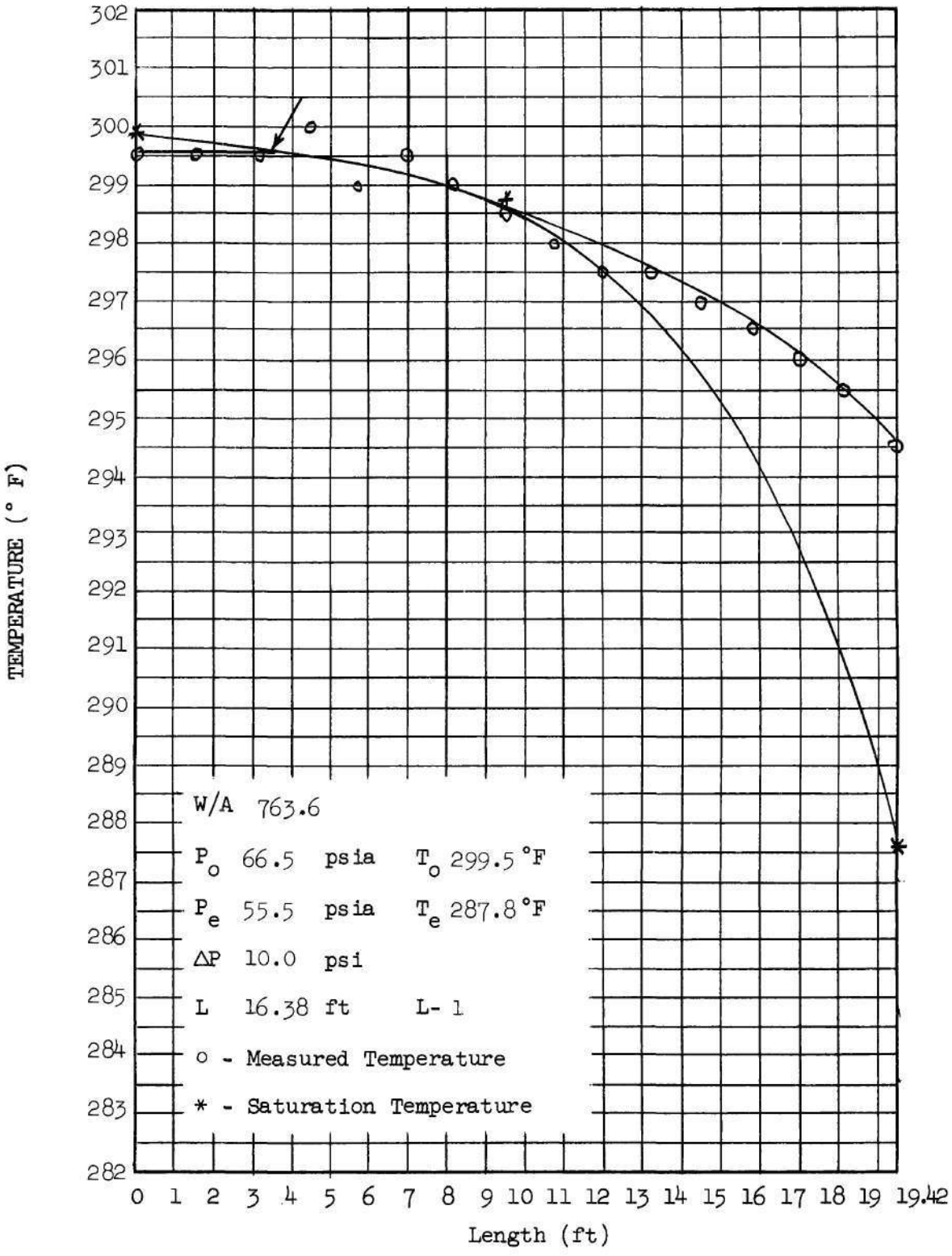

Figure 47. Temperature versus Length for Run 10217.

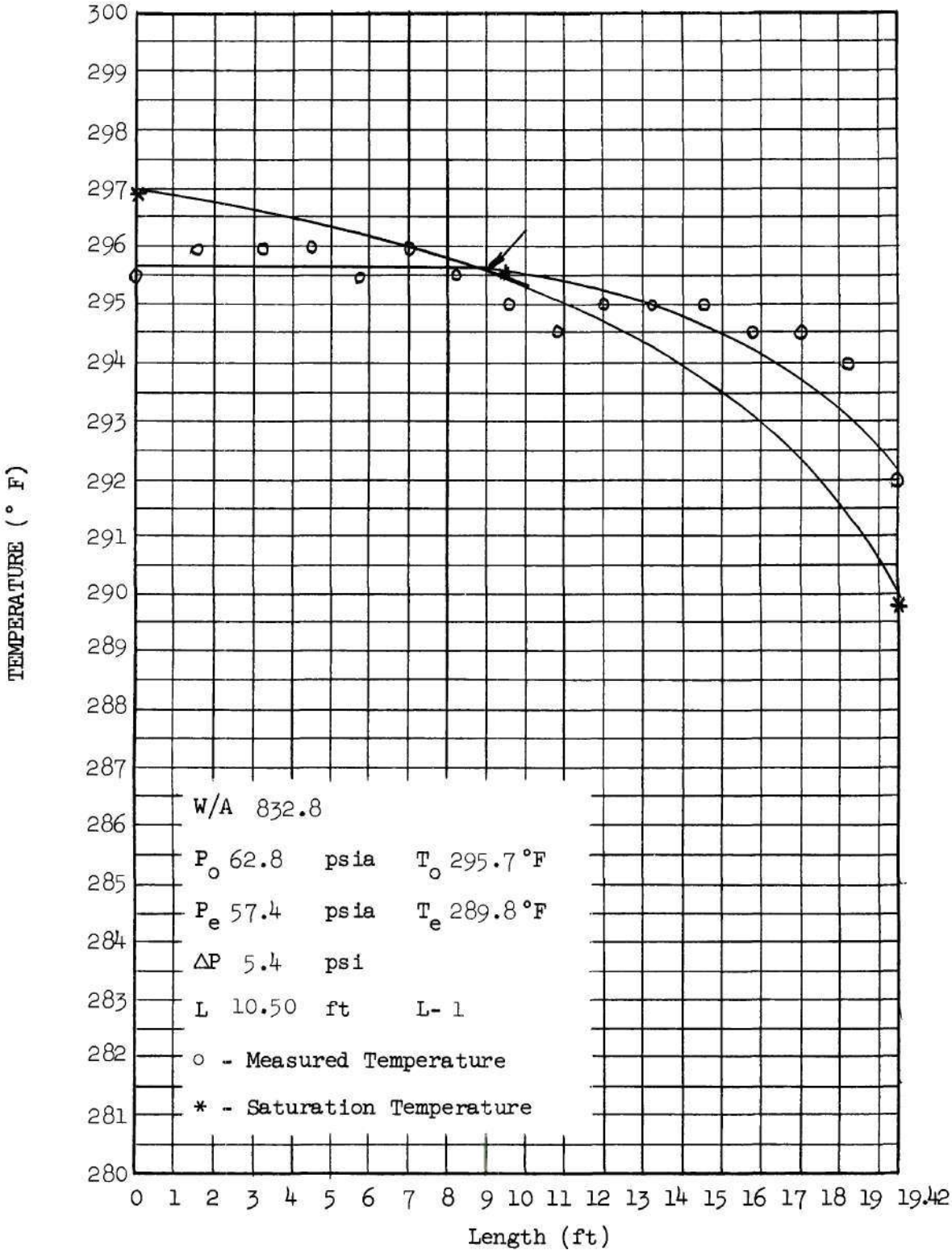

Figure 48. Temperature versus Length for Run 20215.

APPENDIX B

SELECTED VALUES OF THE NUMERICAL SOLUTION OF THE ANNULAR FLOW EQUATIONS FOR THE TWENTY-EIGHT TWO-PHASE FLOW RUNS

In Table 8 through 34 selected values from the numerical solution of the Annular Flow equations are given for twenty-seven of the twenty-eight two-phase flow runs i.e. excluding run 10222. The numerical solution is given in its entirety for run 10222 in Table 37 of Appendix G. The variables which are listed as a function of temperature are the liquid velocity V_ℓ, vapor velocity V_g, quality x, void fraction α_{avg}, and tube length z.

Table 8. Typical Values for the Variables of Run Number 3022

$W/A = 444.5\ lb_m/ft^2\text{-sec}$ $P_o = 32.4$ psia $\Delta P = 6.5$ psia $T_o = 254.7°$ F

$T_e = 242.1°$ F $(dV_\ell/dT)_{T_o} = -6.03673$ $\Delta T = 0.1$

Temperature °F	V_ℓ (ft/sec)	V_g (ft/sec)	x	α_{avg}	z(ft)
254.7	7.575	-	0	0	0
254.6	8.179	8.258	0.000108	0.07395	-
254.1	10.072	14.849	0.000647	0.24858	2.82
253.5	11.555	21.548	0.001295	0.34564	4.63
253.1	12.433	25.465	0.001726	0.39226	5.60
252.5	13.669	30.953	0.002372	0.44769	6.83
252.1	14.449	34.475	0.002802	0.47786	7.53
251.5	15.564	39.669	0.003448	0.51571	8.47
251.1	16.272	43.110	0.003877	0.53706	9.02
250.5	17.282	48.279	0.004521	0.56453	9.77
250.1	17.922	51.747	0.004950	0.58034	10.23
249.5	18.832	57.000	0.005593	0.60090	10.86
249.1	19.406	60.544	0.006021	0.61303	11.25
248.1	20.727	69.583	0.007090	0.63826	12.15
247.1	21.889	78.920	0.008157	0.65800	12.95
246.1	22.892	88.605	0.009223	0.67348	13.68
245.1	23.730	98.693	0.010287	0.68550	14.36
244.1	24.391	109.254	0.011348	0.69449	15.01
243.1	24.851	120.392	0.012408	0.70062	15.64
242.1	25.070	132.275	0.013572	0.70381	16.27

Table 9. Typical Values for the Variables of Run Number 2036

$W/A = 554.0\ lb_m/ft^2\text{-sec}$ $P_o = 32.6$ psia $\Delta P = 3.9$ psia $T_o = 255.2°$ F

$T_e = 247.8°$ F $(dV_\ell/dT)_{T_o} = -7.031$ $\Delta T = 0.2$

Temperature °F	V_ℓ (ft/sec)	V_g (ft/sec)	x	α_{avg}	z(ft)
255.2	9.442	-	0	0	0
255.0	10.849	11.652	0.000216	0.1298	-
254.8	12.082	13.866	0.000432	0.2189	1.37
254.4	14.051	18.571	0.000864	0.3288	2.21
254.0	15.564	23.359	0.001295	0.3944	2.84
253.6	16.842	28.038	0.001727	0.4407	3.36
253.2	17.977	32.617	0.002158	0.4763	3.81
252.8	19.010	37.132	0.002589	0.5051	4.20
252.4	19.961	41.610	0.003019	0.5290	4.56
252.0	20.844	46.076	0.003449	0.5492	4.89
251.6	21.666	50.546	0.003879	0.5666	5.19
251.2	22.734	55.033	0.004309	0.5817	5.47
250.8	23.150	59.547	0.004738	0.5949	5.74
250.4	23.820	64.098	0.005167	0.6065	6.00
250.0	24.444	68.692	0.005596	0.6168	6.24
249.6	25.026	73.338	0.006024	0.6259	6.47
249.2	25.566	78.040	0.006452	0.6340	6.70
248.8	26.065	82.804	0.006880	0.6413	6.92
248.4	26.524	87.637	0.007307	0.6477	7.13
248.0	26.945	95.096	0.007735	0.6534	7.34
247.8	27.140	94.026	0.007948	0.6561	7.44

Table 10. Typical Values for the Variables of Run Number 1022

$W/A = 579.7\ lb_m/ft^2\text{-sec}$ $P_o = 32.6$ psia $\Delta P = 3.5$ psia $T_o = 255.2°$ F

$T_e = 248.6°$ F $(dV_\ell/dT)_{T_o} = -7.409$ $\Delta T = 0.2$

Temperature °F	V_ℓ (ft/sec)	V_g (ft/sec)	x	α_{avg}	z (ft)
255.2	9.881	-	0	0	0
255.0	11.363	12.120	0.000216	0.1307	-
254.8	12.683	14.348	0.000432	0.2214	1.26
254.4	14.767	19.267	0.000864	0.3317	2.02
254.0	16.234	24.568	0.001295	0.3925	2.60
253.6	17.387	29.858	0.001727	0.4331	3.09
253.2	18.358	35.088	0.002158	0.4634	3.52
252.8	19.199	40.283	0.002589	0.4873	3.92
252.4	19.939	45.472	0.003019	0.5066	4.29
252.0	20.590	50.685	0.003449	0.5225	4.64
251.6	21.163	55.947	0.003879	0.5357	4.97
251.2	21.661	61.279	0.004309	0.5467	5.30
250.8	22.090	66.705	0.004738	0.5557	5.62
250.4	22.449	72.247	0.005167	0.5631	5.93
250.0	22.740	77.928	0.005596	0.5690	6.24
249.6	22.962	83.780	0.006024	0.5734	6.56
249.2	23.112	89.830	0.006452	0.5765	6.87
248.8	23.190	96.122	0.006880	0.5781	7.19
248.6	23.200	99.373	0.007094	0.5785	7.37

Table 11. Typical Values for the Variables of Run Number 2022

$W/A = 605.2\ lb_m/ft^2\text{-sec}$ $P_o = 32.0$ psia $\Delta P = 3.8$ psia $T_o = 254.0°F$

$T_e = 246.8°\ F$ $(dV_\ell/dT)_{T_o} = -7.9268$ $\Delta T = 0.2$

Temperature °F	V_ℓ (ft/sec)	V_g (ft/sec)	x	α_{avg}	z (ft)
254.0	10.309	-	0	0	0
253.8	11.894	12.596	0.000215	0.1336	-
253.6	13.336	14.836	0.000431	0.2274	1.13
253.2	15.810	19.465	0.000863	0.3488	1.80
252.8	17.708	24.450	0.001294	0.4189	2.28
252.4	19.216	29.555	0.001725	0.4648	2.66
252.0	20.484	34.669	0.002155	0.4983	2.99
251.6	21.589	39.776	0.002585	0.5243	3.29
251.2	22.574	44.883	0.003015	0.5453	3.55
250.8	23.461	50.000	0.003445	0.5628	3.81
250.4	24.266	55.142	0.003874	0.5776	4.04
250.0	24.999	60.317	0.004303	0.5902	4.26
249.6	25.667	65.540	0.004732	0.6011	4.48
249.2	26.275	70.815	0.005161	0.6106	4.69
248.8	26.827	76.153	0.005589	0.6188	4.89
248.4	27.326	81.563	0.006017	0.6260	5.08
248.0	27.774	87.053	0.006444	0.6323	5.27
247.6	28.172	92.631	0.006872	0.6377	5.46
247.2	28.521	98.308	0.007299	0.6424	5.65
246.8	28.821	104.092	0.007725	0.6463	5.84

ERRATUM

Page 146 was omitted from the original copy of this thesis and therefore from all copies.

Table 13. Typical Values for the Variables of Run Number 1033

$W/A = 557.1\ lb_m/ft^2\text{-sec}$ $P_o = 39.5$ psia $\Delta P = 6.6$ psia $T_o = 266.5°F$

$T_e = 255.7°F$ $(dV_\ell/dT)_{T_o} = -5.9425$ $\Delta T = 0.2$

Temperature °F	V_ℓ (ft/sec)	V_g (ft/sec)	x	α_{avg}	z (ft)
266.5	9.549	-	0	0	0
266.3	10.738	11.720	0.000218	0.1110	-
266.1	11.713	14.081	0.000437	0.1852	1.67
265.7	13.111	19.241	0.000874	0.2726	2.82
265.3	14.197	24.670	0.001311	0.3286	3.74
264.9	15.158	28.538	0.001747	0.3716	4.53
264.5	16.047	32.767	0.002183	0.4068	5.23
264.1	16.882	36.846	0.002619	0.4365	5.86
263.7	17.674	40.830	0.003054	0.4621	6.43
263.3	18.429	44.758	0.003490	0.4844	6.95
262.9	19.148	48.657	0.003924	0.5041	7.43
262.1	20.489	56.433	0.004793	0.5372	8.30
261.3	21.711	64.261	0.005661	0.5638	9.08
260.5	22.820	72.201	0.006527	0.5855	9.78
259.7	23.821	80.297	0.007392	0.6034	10.42
258.9	24.720	88.580	0.008256	0.6183	11.02
258.1	25.517	97.080	0.009119	0.6307	11.58
257.3	26.213	105.827	0.009980	0.6410	12.12
256.5	26.806	114.856	0.01084	0.6494	12.63
255.7	27.293	124.210	0.01170	0.6561	13.13

Table 14. Typical Values for the Variables of Run Number 10127

$W/A = 582.6\ lb_m/ft^2\text{-sec}$ $P_o = 38.5$ psia $\Delta P = 4.8$ psia $T_o = 265.0°F$

$T_e = 257.1°$ F $(dV_\ell/dT)_{T_o} = -6.4123$ $\Delta T = 0.2$

Temperature °F	V_ℓ (ft/sec)	V_g (ft/sec)	x	α_{avg}	z (ft)
265.0	9.978	-	0	0	0
264.8	11.260	12.155	0.000218	0.1141	-
264.6	12.354	14.433	0.000436	0.1928	1.5
264.2	13.965	19.543	0.000873	0.2864	2.49
263.8	15.160	24.607	0.001309	0.3430	3.28
263.4	16.175	29.422	0.001744	0.3847	3.95
263.0	17.083	34.054	0.002180	0.4177	4.55
262.6	17.912	38.573	0.002615	0.4450	5.09
262.2	18.672	43.027	0.003050	0.4680	5.59
261.8	19.381	47.452	0.003484	0.4877	6.05
261.4	20.033	51.876	0.003918	0.5047	6.49
261.0	20.634	56.319	0.004352	0.5195	6.90
260.6	21.187	60.800	0.004786	0.5323	7.29
260.2	21.690	65.332	0.005219	0.5434	7.67
259.8	22.146	69.932	0.005652	0.5531	8.04
259.4	22.554	74.612	0.006085	0.5615	8.39
259.0	22.912	79.387	0.006517	0.5686	8.74
258.6	23.220	84.275	0.006949	0.5746	9.08
258.2	23.475	89.292	0.007381	0.5795	9.42
257.4	23.821	99.804	0.008243	0.5861	10.10
257.1	23.887	103.952	0.008566	0.5875	10.36

Table 15. Typical Values for the Variables of Run Number 20127

$W/A = 637.7\ lb_m/ft^2\text{-sec}$ $P_o = 38.3$ psia $\Delta P = 4.6$ psia $T_o = 264.7°F$

$T_e = 257.1°F$ $(dV_\ell/dT)_{T_o} = -7.36253$ $\Delta T = 0.1$

Temperature °F	V_ℓ (ft/sec)	V_g (ft/sec)	x	α_{avg}	z (ft)
264.7	10.921	-	0	0	0
264.5	12.352	13.131	0.000218	0.1162	0.71
264.1	14.738	17.718	0.000654	0.2597	1.69
263.7	16.433	22.919	0.001090	0.3365	2.37
263.3	17.720	28.192	0.001526	0.3851	2.94
262.9	18.795	33.368	0.001961	0.4206	3.42
262.5	19.736	38.454	0.002397	0.4486	3.86
262.1	20.576	43.483	0.002831	0.4714	4.27
261.7	21.335	48.486	0.003266	0.4906	4.64
261.3	22.024	53.489	0.003700	0.5068	5.00
260.9	22.648	58.512	0.004134	0.5207	5.33
260.5	23.213	63.574	0.004568	0.5327	5.66
260.1	23.722	68.694	0.005001	0.5430	5.97
259.7	24.176	73.883	0.005434	0.5518	6.28
259.3	24.576	79.159	0.005867	0.5594	6.58
258.9	24.923	84.537	0.006299	0.5658	6.87
258.5	25.217	90.035	0.006731	0.5712	7.17
258.1	25.457	95.670	0.007163	0.5755	7.46
257.7	25.640	101.466	0.007594	0.5788	7.75
257.3	25.767	107.448	0.008025	0.5811	8.04
257.1	25.807	110.519	0.008241	0.5819	8.19

Table 16. Typical Values for the Variables of Run Number 1036

$W/A = 637.7\ lb_m/ft^2\text{-sec}$ $P_o = 38.8$ psia $\Delta P = 4.7$ psia $T_o = 265.5°F$

$T_e = 257.8°$ F $(dV_\ell/dT)_{T_o} = -7.687$ $\Delta T = 0.2$

Temperature °F	V_ℓ (ft/sec)	V_g (ft/sec)	x	α_{avg}	z (ft)
265.5	10.925	-	0	0	0
265.1	13.598	15.357	0.000436	0.1970	1.27
264.7	15.606	20.230	0.000873	0.3008	2.09
264.3	17.079	25.390	0.001309	0.3615	2.71
263.9	18.280	30.472	0.001745	0.4038	3.24
263.5	19.324	35.442	0.002181	0.4364	3.70
262.7	21.110	45.168	0.003051	0.4848	4.51
261.9	22.609	54.793	0.003920	0.5195	5.20
261.1	23.881	64.475	0.004788	0.5457	5.83
260.3	24.953	74.324	0.005655	0.5658	6.41
259.5	25.839	84.432	0.006520	0.5812	6.96
258.7	26.544	94.881	0.007385	0.5928	7.49
258.3	26.828	100.263	0.007816	0.5974	7.75
257.9	27.065	105.770	0.008248	0.6012	8.01
257.8	27.115	107.171	0.008356	0.6020	8.14

Table 17. Typical Values for the Variables of Run Number 10131

$W/A = 582.6\ lb_m/ft^2\text{-sec}$ $P_o = 46.9$ psia $\Delta P = 8.6$ psia $T_o = 277.0°F$

$T_e = 264.6°$ F $(dV_\ell/dT)_{T_o} = -5.3631$ $\Delta T = 0.2$

Temperature °F	V_ℓ (ft/sec)	V_g (ft/sec)	x	α_{avg}	z (ft)
277.0	10.040	-	0	0	0
276.8	11.113	12.235	0.000221	0.0968	-
276.6	11.948	14.824	0.000442	0.1602	1.84
276.2	13.079	20.467	0.000884	0.2333	3.19
275.8	13.967	25.485	0.001352	0.2825	4.33
275.4	14.767	29.987	0.001766	0.3218	5.33
275.0	15.516	34.159	0.002207	0.3550	6.22
274.6	16.230	38.121	0.002648	0.3837	7.04
274.2	16.912	41.947	0.003088	0.4090	7.79
273.8	17.568	45.687	0.003528	0.4314	8.48
273.4	18.199	49.374	0.003968	0.4515	9.12
273.0	18.806	53.031	0.004407	0.4695	9.72
272.2	19.952	60.319	0.005285	0.5006	10.82
271.4	21.011	67.642	0.006161	0.5264	11.81
270.6	21.986	75.055	0.007036	0.5480	12.71
269.4	23.299	86.421	0.008347	0.5743	13.93
268.6	24.080	94.202	0.009219	0.5886	14.68
267.4	25.113	106.223	0.010524	0.6063	15.72
266.6	25.713	114.504	0.011393	0.6160	16.37
265.4	26.477	127.383	0.012694	0.6278	17.30
264.6	26.891	136.322	0.01356	0.6341	17.90

Table 18. Typical Values for the Variables of Run Number 10224

$W/A = 582.6\ lb_m/ft^2\text{-sec}$ $P_o = 49.6$ psia $\Delta P = 9.2$ psia $T_o = 280.5°F$

$T_e = 267.8°$ F $(dV_\ell/dT)_{T_o} = -5.090$ $\Delta T = 0.2$

Temperature °F	V_ℓ (ft/sec)	V_g (ft/sec)	x	α_{avg}	z (ft)
280.5	10.059	-	0	0	0
280.3	11.077	12.281	0.000221	0.0922	-
280.1	11.842	15.025	0.000443	0.1511	1.95
279.7	12.858	20.869	0.000887	0.2187	3.42
278.9	14.405	30.394	0.001773	0.3035	5.79
277.7	16.402	42.098	0.003100	0.3895	8.56
276.9	17.611	49.294	0.003983	0.4321	10.07
276.1	18.738	56.340	0.004864	0.4670	11.40
275.3	19.785	63.368	0.005744	0.4958	12.58
274.9	20.280	66.899	0.006184	0.5085	13.13
274.5	20.757	70.449	0.006623	0.5201	13.65
274.1	21.215	74.024	0.007062	0.5307	14.15
273.3	22.077	81.264	0.007939	0.5496	15.09
272.9	22.482	84.935	0.008377	0.5580	15.54
272.1	23.242	92.390	0.009253	0.5731	16.39
271.3	23.937	100.012	0.010127	0.5860	17.18
270.5	24.570	107.818	0.010999	0.5972	17.94
269.7	25.141	115.821	0.011871	0.6068	18.66
268.9	25.653	124.037	0.012741	0.6152	19.35
268.1	26.105	132.488	0.013610	0.6223	20.01
267.8	26.258	135.726	0.01393	0.6243	20.25

Table 19. Typical Values for the Variables of Run Number 20130

$W/A = 729.6\ lb_m/ft^2\text{-sec}$ $P_o = 44.1$ psia $\Delta P = 3.9$ psia $T_o = 273.2°F$

$T_e = 267.5°F$ $(dV_\ell/dT)_{T_o} = -7.3696$ $\Delta T = 0.2$

Temperature °F	V_ℓ (ft/sec)	V_g (ft/sec)	x	α_{avg}	z (ft)
273.2	12.550	-	0	0	0
273.0	14.024	14.788	0.000220	0.1054	-
272.8	15.362	17.022	0.000440	0.1836	1.13
272.4	17.496	22.156	0.000880	0.2836	1.87
272.0	18.917	28.046	0.001320	0.3379	2.45
271.6	19.991	33.974	0.001759	0.3739	2.95
271.2	20.881	39.812	0.002198	0.4009	3.41
270.8	21.648	45.575	0.002637	0.4225	3.83
270.4	22.321	51.298	0.003076	0.4403	4.24
270.0	22.915	57.017	0.003514	0.4552	4.62
269.6	23.438	62.762	0.003952	0.4677	4.99
269.2	23.897	68.563	0.004390	0.4782	5.35
268.8	24.295	74.446	0.004827	0.4871	5.71
268.4	24.632	80.439	0.005264	0.4944	6.06
268.0	24.910	86.569	0.005700	0.5004	6.40
267.6	25.128	92.869	0.006137	0.5050	6.75
267.5	25.161	94.491	0.06246	0.5060	6.93

Table 20. Typical Values for the Variables of Run Number 20224

$W/A = 729.6\ lb_m/ft^2\text{-sec}$ $P_o = 45.8$ psia $\Delta P = 4.8$ psia $T_o = 275.5°F$

$T_e = 268.7°$ F $(dV_\ell/dT)_{T_o} = -7.1366$ $\Delta T = 0.2$

Temperature °F	V_ℓ (ft/sec)	V_g (ft/sec)	x	α_{avg}	z (ft)
275.5	12.565	-	0	0	0
275.3	13.992	14.786	0.000220	0.1023	-
275.1	15.281	17.011	0.000441	0.1783	1.17
274.7	17.352	22.029	0.000882	0.2768	1.95
274.3	18.806	27.601	0.001323	0.3332	2.56
273.9	19.950	33.151	0.001764	0.3718	3.09
273.5	20.924	38.582	0.002204	0.4014	3.56
273.1	21.785	43.915	0.002644	0.4255	3.99
272.7	22.560	49.182	0.003083	0.4456	4.39
272.3	23.264	54.413	0.003523	0.4627	4.77
271.9	23.907	59.636	0.003962	0.4775	5.13
271.5	24.493	64.871	0.004400	0.4903	5.47
271.1	25.027	70.137	0.004838	0.5015	5.80
270.7	25.512	75.450	0.005276	0.5113	6.13
270.3	25.948	80.826	0.005714	0.5198	6.44
269.9	26.338	86.281	0.006151	0.5272	6.75
269.5	26.681	91.829	0.006589	0.5336	7.05
269.1	26.977	97.489	0.007025	0.5390	7.36
268.7	27.226	103.274	0.07462	0.5436	7.66

Table 21. Typical Values for the Variables of Run Number 10227

$W/A = 729.6\ lb_m/ft^2\text{-sec}$ $P_o = 50.8$ psia $\Delta P = 5.9$ psia $T_o = 282.0°F$

$T_e = 274.3°\ F$ $(dV_\ell/dT)_{T_o} = -6.5211$ $\Delta T = 0.2$

Temperature °F	V_ℓ (ft/sec)	V_g (ft/sec)	x	α_{avg}	z (ft)
282.0	12.608	-	0	0	0
281.8	13.912	14.793	0.000222	0.0940	-
281.6	15.065	17.049	0.000444	0.1636	1.30
281.2	16.803	22.378	0.000888	0.2506	2.21
280.8	18.024	28.016	0.001332	0.3018	2.95
280.4	19.023	33.436	0.001776	0.3390	3.59
280.0	19.902	38.638	0.002219	0.3686	4.18
279.6	20.698	43.682	0.002662	0.3932	4.71
279.2	21.429	48.620	0.003105	0.4143	5.21
278.8	22.106	53.494	0.003547	0.4326	5.68
278.4	22.733	58.334	0.003989	0.4486	6.12
278.0	23.316	63.164	0.004431	0.4628	6.54
277.6	23.856	68.007	0.004872	0.4753	6.95
277.2	24.354	72.878	0.005313	0.4864	7.34
276.8	24.813	77.794	0.005754	0.4962	7.72
276.4	25.232	82.766	0.006194	0.5049	8.09
276.0	25.612	87.811	0.006634	0.5125	8.45
275.6	25.952	92.943	0.007074	0.5192	8.80
275.2	26.252	98.174	0.007513	0.5250	9.15
274.8	26.510	103.524	0.007952	0.5300	9.49
274.3	26.767	110.405	0.008546	0.5349	10.02

Table 22. Typical Values for the Variables of Run Number 30224

$W/A = 864.0\ lb_m/ft^2\text{-sec}$ $P_o = 44.7$ psia $\Delta P = 3.8$ psia $T_o = 274.0°F$

$T_e = 268.6°$ F $(dV_\ell/dT)_{T_o} = -9.051$ $\Delta T = 0.2$

Temperature °F	V_ℓ (ft/sec)	V_g (ft/sec)	x	α_{avg}	z (ft)
274.0	14.866	-	0	0	0
273.8	16.667	16.780	0.000220	0.1088	-
273.6	18.272	19.595	0.000440	0.1869	0.83
273.2	21.216	24.528	0.000881	0.3002	1.35
272.8	23.196	30.814	0.001321	0.3603	1.75
272.4	24.482	37.743	0.001761	0.3943	2.08
272.0	25.448	44.777	0.002200	0.4177	2.39
271.6	26.232	51.815	0.002640	0.4355	2.68
271.2	26.890	58.857	0.003078	0.4496	2.96
270.8	27.452	65.921	0.003517	0.4613	3.24
270.4	27.934	73.032	0.003955	0.4709	3.50
270.0	28.345	80.218	0.004393	0.4789	3.76
269.6	28.691	87.505	0.004831	0.4855	4.03
269.2	28.975	94.923	0.005268	0.4909	4.29
268.8	29.200	102.498	0.005705	0.4951	4.55
268.6	29.291	106.357	0.005924	0.4969	4.68

Table 23. Typical Values for the Variables of Run Number 10130

$W/A = 864.0\ lb_m/ft^2\text{-sec}$ $P_o = 44.7$ psia $\Delta P = 2.9$ psia $T_o = 274.0°F$

$T_e = 269.9°F$ $(dV_\ell/dT)_{T_o} = -9.051$ $\Delta T = 0.2$

Temperature °F	V_ℓ (ft/sec)	V_g (ft/sec)	x	α_{avg}	z (ft)
274.0	14.866	-	0	0	0
273.8	16.677	16.780	0.000220	0.1088	-
273.6	18.272	19.595	0.000440	0.1869	0.83
273.2	21.216	24.528	0.000881	0.3002	1.35
272.8	23.196	30.814	0.001321	0.3603	1.75
272.4	24.482	37.743	0.001761	0.3943	2.08
272.0	25.448	44.777	0.002200	0.4177	2.39
271.6	26.232	51.815	0.002640	0.4355	2.68
271.2	26.890	58.857	0.003078	0.4496	2.96
270.8	27.452	65.921	0.003517	0.4613	3.24
270.4	27.934	73.032	0.003955	0.4709	3.50
270.0	28.345	80.218	0.004393	0.4789	3.76
269.9	28.435	82.033	0.004502	0.4806	3.83

Table 24. Typical Values for the Variables of Run Number 1028

$W/A = 582.6\ lb_m/ft^2\text{-sec}$ $P_o = 54.9$ psia $\Delta P = 8.2$ psia $T_o = 287.0°F$

$T_e = 276.7°$ F $(dV_\ell/dT)_{T_o} = -5.037$ $\Delta T = 0.3$

Temperature °F	V_ℓ (ft/sec)	V_g (ft/sec)	x	α_{avg}	z (ft)
287.0	10.094	-	0	0	0
286.7	11.605	11.980	0.000335	0.1306	-
286.4	12.117	18.733	0.000670	0.1677	2.95
285.8	13.196	26.772	0.001339	0.2365	5.25
285.2	14.143	33.200	0.002008	0.2883	7.22
284.6	15.032	38.849	0.002676	0.3311	8.94
284.0	15.881	44.096	0.003344	0.3675	10.47
283.4	16.694	49.128	0.004010	0.3989	11.85
282.8	17.475	54.048	0.004343	0.4131	13.10
282.2	18.225	58.914	0.005341	0.4505	14.25
281.6	18.945	63.763	0.006006	0.4719	15.31
281.0	19.639	68.615	0.006669	0.4910	16.29
280.4	20.309	73.483	0.007332	0.5083	17.20
279.8	20.959	78.367	0.007995	0.5240	18.06
279.2	21.593	83.265	0.008656	0.5385	18.86
278.6	22.219	88.173	0.009317	0.5519	19.61
278.0	22.844	93.073	0.009977	0.5646	20.32
277.4	23.477	97.948	0.010636	0.5767	20.98
276.8	24.131	102.774	0.011295	0.5886	21.60
276.7	24.244	103.568	0.01139	0.5916	21.70

Table 25. Typical Values for the Variables of Run Number 1037

$W/A = 582.6\ lb_m/ft^2\text{-sec}$ $P_o = 54.6$ psia $\Delta P = 9.1$ psia $T_o = 286.6°F$

$T_e = 275.1°F$ $(dV_\ell/dT)_{T_o} = -4.64033$ $\Delta T = 0.2$

Temperature °F	V_ℓ (ft/sec)	V_g (ft/sec)	x	α_{avg}	z (ft)
286.6	10.092	-	0	0	0
286.4	11.020	12.392	0.000223	0.0845	-
286.2	11.671	15.454	0.000446	0.1358	2.16
285.8	12.523	21.632	0.000893	0.1951	3.84
285.4	13.218	26.744	0.001339	0.2380	5.32
285.0	13.860	31.163	0.001785	0.2737	6.65
284.6	14.471	35.161	0.002330	0.3048	7.86
284.2	15.058	38.894	0.002675	0.3324	8.97
283.8	15.627	42.457	0.003120	0.3571	10.00
283.4	16.177	45.909	0.003565	0.3794	10.96
282.6	17.228	52.629	0.004452	0.4180	12.70
281.8	18.212	59.252	0.005339	0.4502	14.25
281.0	19.131	65.882	0.006224	0.4773	15.64
280.2	19.985	72.583	0.007108	0.5003	16.92
279.4	20.776	79.388	0.007991	0.5199	18.09
278.6	21.506	86.327	0.008873	0.5368	19.18
277.8	22.175	93.421	0.009753	0.5514	20.21
277.0	22.784	100.684	0.010631	0.5640	21.17
276.6	23.067	104.388	0.011070	0.5696	21.64
276.2	23.336	108.139	0.011509	0.5748	22.09
275.1	23.998	118.737	0.012713	0.5873	22.17

Table 26. Typical Values for the Variables of Run Number 10213

$W/A = 729.6\ lb_m/ft^2\text{-sec}$ $P_o = 52.3$ psia $\Delta P = 9.3$ psia $T_o = 285.0°F$

$T_e = 271.6°F$ $(dV_\ell/dT)_{T_o} = -6.2554$ $\Delta T = 0.2$

Temperature °F	V_ℓ (ft/sec)	V_g (ft/sec)	x	α_{avg}	z (ft)
285.0	12.629	-	0	0	0
284.8	13.880	14.804	0.000223	0.0904	-
284.6	14.974	17.081	0.000446	0.1572	1.37
284.2	16.612	22.413	0.000891	0.2408	2.34
283.8	17.803	27.863	0.001337	0.2920	3.13
283.4	18.810	33.009	0.001782	0.3304	3.82
283.0	19.719	37.889	0.002226	0.3617	4.44
282.6	20.562	42.576	0.002671	0.3882	5.01
282.2	21.355	47.123	0.003115	0.4114	5.53
281.8	22.108	51.574	0.003558	0.4318	6.01
281.4	22.826	55.959	0.004002	0.4500	6.46
280.6	24.172	64.612	0.004888	0.4813	7.29
279.8	25.415	73.200	0.005772	0.5073	8.04
279.0	26.570	81.792	0.006655	0.5294	8.72
278.2	27.648	90.433	0.007537	0.5483	9.34
277.4	28.660	99.142	0.008418	0.5648	9.92
276.6	29.618	107.936	0.009297	0.5794	10.46
275.8	30.531	116.814	0.00175	0.5926	10.97
275.0	31.413	125.772	0.011052	0.6045	11.44
272.6	34.002	152.990	0.013674	0.6361	12.69
271.6	35.135	164.351	0.014763	0.6484	13.14

Table 27. Typical Values for the Variables of Run Number 20227

$W/A = 729.6\ lb_m/ft^2\text{-sec}$ $P_o = 57.4$ psia $\Delta P = 7.8$ psia $T_o = 289.8°F$

$T_e = 280.5°F$ $(dV_\ell/dT)_{T_o} = -5.8502$ $\Delta T = 0.2$

Temperature °F	V_ℓ (ft/sec)	V_g (ft/sec)	x	α_{avg}	z (ft)
289.8	12.662	-	0	0	0
289.6	13.832	14.831	0.000224	0.0848	-
289.4	14.829	17.208	0.000448	0.1467	1.47
289.0	16.224	23.010	0.000896	0.2205	2.56
288.6	17.223	28.738	0.001344	0.2663	3.47
288.2	18.076	34.035	0.001791	0.3013	4.28
287.8	18.848	39.004	0.002238	0.3304	5.02
287.4	19.564	43.746	0.002685	0.3553	5.71
287.0	20.236	48.333	0.003131	0.3771	6.34
286.6	20.869	52.821	0.003577	0.3964	6.94
286.2	21.468	57.245	0.004023	0.4137	7.50
285.8	22.035	61.632	0.004468	0.4291	8.04
285.0	23.076	70.385	0.005358	0.4556	9.04
284.6	23.552	74.784	0.005802	0.4670	9.51
284.2	23.998	79.213	0.006246	0.4772	9.96
283.8	24.416	83.685	0.006690	0.4865	10.40
283.0	25.162	92.799	0.007596	0.5024	11.25
282.6	25.490	97.464	0.008019	0.5091	11.66
281.8	26.051	107.060	0.008903	0.5203	12.45
281.0	26.480	117.105	0.009786	0.5287	13.23
280.5	26.657	123.681	0.01033	0.5326	13.72

Table 28. Typical Values for the Variables of Run Number 10214

$W/A = 848.4\ lb_m/ft^2\text{-sec}$ $P_o = 54.5$ psia $\Delta P = 5.2$ psia $T_o = 286.5°F$

$T_e = 280.1°F$ $(dV_\ell/dT)_{T_o} = -7.2597$ $\Delta T = 0.2$

Temperature °F	V_ℓ (ft/sec)	V_g (ft/sec)	x	α_{avg}	z (ft)
286.5	14.697	-	0	0	0
286.3	16.148	16.930	0.000223	0.0902	-
286.1	17.482	19.151	0.000446	0.1599	1.05
285.7	19.813	23.751	0.000893	0.2592	1.78
285.3	21.710	28.616	0.001339	0.3244	2.33
284.9	23.318	33.499	0.001785	0.3714	2.78
284.5	24.754	38.289	0.002230	0.4083	3.17
284.1	26.081	42.977	0.002675	0.4387	3.51
283.7	27.333	47.574	0.003120	0.4648	3.82
283.3	28.531	52.095	0.003564	0.4876	4.09
282.9	29.688	56.557	0.004008	0.5079	4.35
282.5	30.815	60.970	0.004452	0.5262	4.58
282.1	31.920	65.341	0.004895	0.5429	4.79
281.7	33.008	69.680	0.005339	0.5583	4.99
281.3	34.086	73.989	0.005781	0.5725	5.17
280.9	35.159	78.275	0.006224	0.5858	5.34
280.5	36.230	82.538	0.006666	0.5984	5.49
280.1	37.306	86.781	0.007108	0.6102	5.64

Table 29. Typical Values for the Variables of Run Number 30227

$W/A = 848.4\ lb_m/ft^2\text{-sec}$ $P_o = 52.3$ psia $\Delta P = 4.9$ psia $T_o = 285.0°F$

$T_e = 279.0°F$ $(dV_\ell/dT)_{T_o} = -7.4083$ $\Delta T = 0.2$

Temperature °F	V_ℓ (ft/sec)	V_g (ft/sec)	x	α_{avg}	z (ft)
285.0	14.685	-	0	0	0
284.8	16.166	16.930	0.000223	0.0919	-
284.6	17.530	19.167	0.000446	0.1629	1.03
284.2	19.780	24.268	0.000891	0.2586	1.73
283.8	21.279	30.399	0.001337	0.3113	2.29
283.4	22.385	36.680	0.001782	0.3457	2.78
283.0	23.293	42.874	0.002226	0.3717	3.22
283.6	24.076	48.973	0.002671	0.3925	3.63
282.2	24.767	55.002	0.003115	0.4098	4.02
281.8	25.383	60.995	0.003558	0.4245	4.40
281.4	25.935	66.985	0.004002	0.4371	4.76
281.0	26.430	72.994	0.004445	0.4480	5.11
280.6	26.870	79.053	0.004888	0.4574	5.45
280.2	27.259	85.180	0.005330	0.4655	5.79
279.8	27.599	91.399	0.005772	0.4725	6.12
279.4	27.889	97.735	0.006214	0.4783	6.45
279.0	28.131	104.210	0.006655	0.4831	6.77

Table 30. Typical Values for the Variables of Run Number 3037

$W/A = 709.8\ lb_m/ft^2\text{-sec}$ $P_o = 64.3$ psia $\Delta P = 11.0$ psia $T_o = 297.2°F$

$T_e = 285.1°F$ $(dV_\ell/dT)_{T_o} = -5.094$ $\Delta T = 0.2$

Temperature °F	V_ℓ (ft/sec)	V_g (ft/sec)	x	α_{avg}	z (ft)
297.2	12.369	-	0	0	0
297.0	13.388	14.567	0.000226	0.0764	-
296.8	14.196	17.264	0.000452	0.1292	1.74
296.4	15.245	23.652	0.000903	0.1897	3.09
296.0	16.036	29.392	0.001354	0.2302	4.27
295.6	16.740	34.476	0.001805	0.2630	5.34
295.2	17.397	39.115	0.002256	0.2913	6.32
294.8	18.021	43.456	0.002706	0.3163	7.22
294.0	19.195	51.593	0.003606	0.3590	8.86
293.2	20.288	59.333	0.004504	0.3944	10.32
292.4	21.308	66.895	0.005401	0.4241	11.63
292.0	21.794	70.650	0.005849	0.4394	12.24
291.2	22.719	78.150	0.006744	0.4610	13.39
290.4	23.588	85.680	0.007637	0.4815	14.45
289.6	24.406	93.264	0.008529	0.4996	15.43
288.8	25.181	100.913	0.009420	0.5156	16.35
288.0	25.922	108.627	0.010309	0.5301	17.21
287.2	26.641	116.388	0.011197	0.5434	18.02
286.4	27.349	124.166	0.012084	0.5558	18.78
285.6	28.066	131.921	0.012969	0.5677	19.49
285.1	28.528	136.631	0.013520	0.5752	19.90

Table 31. Typical Values for the Variables of Run Number 10215

W A = 729.6 lb_m ft^2-sec P_o = 65.2 psia ΔP = 7.0 psia T_o = 298.2°F

T_e = 290.7°F $(dV_\ell\ dT)_{T_o}$ = -5.41116 ΔT = 0.10

Temperature °F	V_ℓ (ft/sec	V_g (ft/sec)	x	α_{avg}	z (ft)
298.2	12.721	-	0	0	0
298.1	13.262	13.765	0.000113	0.0409	-
298.0	13.761	14.882	0.000226	0.0758	0.91
297.6	15.192	20.830	0.000678	0.1634	2.35
297.2	16.086	27.221	0.001130	0.2096	3.56
296.8	16.788	32.906	0.001582	0.2440	4.65
296.4	17.436	38.074	0.002033	0.2726	5.64
296.0	18.035	42.905	0.002484	0.2972	6.57
295.6	18.595	47.517	0.002935	0.3188	7.44
295.2	19.121	51.993	0.003385	0.3380	8.26
294.8	19.613	56.393	0.003835	0.3550	9.04
294.4	20.072	60.763	0.004284	0.3702	9.78
294.0	20.498	65.135	0.004734	0.3837	10.50
295.6	20.890	69.543	0.005182	0.3957	11.19
293.2	21.247	74.015	0.005631	0.4062	11.86
292.8	21.567	78.577	0.006079	0.4154	12.52
292.4	21.847	83.258	0.006527	0.4233	13.16
292.0	22.085	88.094	0.006975	0.4299	13.79
291.6	22.278	93.117	0.007422	0.4352	14.42
291.2	22.421	98.375	0.007869	0.4392	15.04
290.7	22.523	105.367	0.008538	0.4426	15.87

Table 32. Typical Values for the Variables of Run Number 10228

$W/A = 763.6\ lb_m/ft^2\text{-sec}$ $P_o = 66.0$ psia $\Delta P = 11.8$ psia $T_o = 299.0°F$
$T_e = 286.1°F$ $(dV_\ell/dT)_{T_o} = -5.414$ $\Delta T = 0.20$

Temperature °F	V_ℓ (ft/sec)	V_g (ft/sec)	x	α_{avg}	z (ft)
299.0	13.319	-	0	0	0
298.8	14.402	15.488	0.000226	0.0754	-
298.6	15.306	17.980	0.000452	0.1304	1.56
297.8	17.403	30.098	0.001357	0.2362	3.78
297.0	18.870	40.382	0.002261	0.2965	5.56
296.2	20.159	49.482	0.003163	0.3124	7.09
295.4	21.336	58.010	0.004063	0.3495	8.44
294.6	22.421	66.268	0.004962	0.4103	9.65
293.8	23.425	74.424	0.005860	0.4363	10.76
293.0	24.354	82.570	0.006757	0.4586	11.78
292.2	25.213	90.772	0.007652	0.4777	12.73
291.4	26.008	99.064	0.008546	0.4944	13.62
290.6	26.743	107.472	0.009438	0.5089	14.46
289.8	27.423	116.015	0.010329	0.5217	15.25
289.0	28.052	124.704	0.011219	0.5331	16.01
288.2	28.637	133.546	0.012108	0.5432	16.73
287.8	28.914	138.022	0.012551	0.5479	17.08
287.0	29.441	147.088	0.013438	0.5566	17.76
286.2	29.936	156.304	0.014323	0.5645	18.42
286.1	29.996	157.466	0.014433	0.5655	18.58

Table 33. Typical Values for the Variables of Run Number 10217

$W/A = 763.6\ lb_m/ft^2\text{-sec}$ $P_o = 66.5$ psia $\Delta P = 10.0$ psia $T_o = 299.5°F$

$T_e = 287.7°F$ $(dV_\ell/dT)_{T_o} = -5.4066$ $\Delta T = 0.20$

Temperature °F	V_ℓ (ft/sec)	V_g (ft/sec)	x	α_{avg}	z (ft)
299.5	13.323	-	0	0	0
299.3	14.404	15.410	0.000226	0.0753	-
299.1	15.294	17.991	0.000453	0.1294	1.57
298.3	17.384	30.033	0.001358	0.2351	3.81
297.5	18.865	40.170	0.002262	0.2961	5.60
296.7	20.182	49.082	0.003164	0.3429	7.14
295.9	21.399	57.381	0.004065	0.3812	8.49
295.1	22.542	65.362	0.004965	0.4133	9.69
294.3	23.623	73.175	0.005864	0.4409	10.78
293.5	24.654	80.900	0.006761	0.4650	11.78
292.7	25.647	88.575	0.007656	0.4864	12.69
291.9	26.615	96.207	0.008550	0.5058	13.53
291.1	27.574	103.791	0.009443	0.5236	14.30
290.3	28.543	111.299	0.010335	0.5404	15.01
289.5	29.544	118.687	0.011225	0.5565	15.67
288.7	30.609	125.900	0.012114	0.5725	16.26
288.3	31.176	129.419	0.012558	0.5806	16.54
287.9	31.774	132.870	0.013002	0.5888	16.80
287.7	32.087	134.565	0.013223	0.5929	16.92

Table 34. Typical Values for the Variables of Run Number 20215

$W/A = 832.8\ lb_m/ft^2\text{-sec}$ $P_o = 62.8$ psia $\Delta P = 5.4$ psia $T_o = 295.7°F$

$T_e = 289.8°F$ $(dV_\ell/dT)_{T_o} = -6.2681$ $\Delta T = 0.2$

Temperature °F	V_ℓ (ft/sec)	V_g (ft/sec)	x	α_{avg}	z (ft)
295.7	14.500	-	0	0	0
295.5	15.574	16.672	0.000225	0.07988	-
295.3	16.865	18.971	0.000451	0.1408	1.26
294.9	18.417	25.122	0.000902	0.2137	2.18
294.5	19.399	31.873	0.001352	0.2540	2.97
294.1	20.170	38.342	0.001802	0.2830	3.69
293.7	20.828	44.544	0.002252	0.3061	4.36
293.3	21.406	50.564	0.002702	0.3253	5.00
292.9	21.918	56.485	0.003151	0.3415	5.60
292.5	22.372	62.375	0.003600	0.3553	6.19
292.1	22.771	68.286	0.004049	0.3670	6.76
291.7	23.117	74.269	0.004497	0.3769	7.31
291.3	23.409	80.375	0.004945	0.3851	7.86
290.9	23.647	86.656	0.005392	0.3917	8.41
290.1	23.953	99.967	0.006286	0.4003	9.49
289.8	24.053	105.334	0.006621	0.40182	9.90

APPENDIX C

DERIVATION OF VOID FRACTION EQUATIONS

The attenuation of a monoenergetic beam of gamma radiation passing through a thin homogenous absorbing medium of uniform thickness is given by

$$I = I_o e^{-\sigma\rho t} \qquad (1.801)$$

where I = intensity of the radiation at thickness t (photons/cm^2sec)

I_o = intensity of the beam at t = o (photons/cm^2sec)

σ = mass attenuation coefficient (cm^2/gm)

t = absorbing medium thickness (cm)

ρ = density of the absorbing medium (gm/cm^2)

The following assumptions are made to obtain the relation for the local void fraction.

1. A monoenergetic beam of gamma radiation is used.

2. Equation (1.801) describes the attenuation of this monoenergetic beam of gamma radiation.

3. The beam of gamma radiation always passes through laminated layers of tube wall, water, and steam; or tube wall, lucite, and air. The beam is perpendicular to these laminated layers.

Richardson (38) discusses the case where the beam passes through laminated layers of material with the beam parallel to the laminated layers.

The attenuation of the beam through a chord of the tube when the tube is full of steam is given by

$$I_{MT} = I_o e^{-(\sigma_s \rho_s 2t_s + \sigma_w \rho_g m)} \qquad (C\text{-}1)$$

where I_{MT} = intensity of the beam having passed through the tube full of steam

I_0 = intensity of the beam incident on the tube

σ_s = mass attenuation coefficient of the tube

σ_w = mass attenuation coefficient of water

ρ_s = density of the tube material

ρ_g = density of steam

t_s = thickness of the tube wall

m = chordal length of the steam.

The attenuation of the beam through the same chord of the tube when the tube is full of water is given by

$$I_F = I_o e^{-(\sigma_s \rho_s 2t_s + \sigma_w \rho_\ell m)} \qquad (C\text{-}2)$$

where I_F = intensity of the beam having passed through the tube full of water

ρ_ℓ = density of water.

The attenuation of the beam through the same chord of the tube with the tube containing two-phase flow as shown in Figure 49 is given by

$$I_{TP} = I_o e^{-\left[\sigma_s \rho_s 2ts + \sigma_w \rho_g \ell + \sigma_w \rho_\ell (m-\ell)\right]} \qquad (C\text{-}3)$$

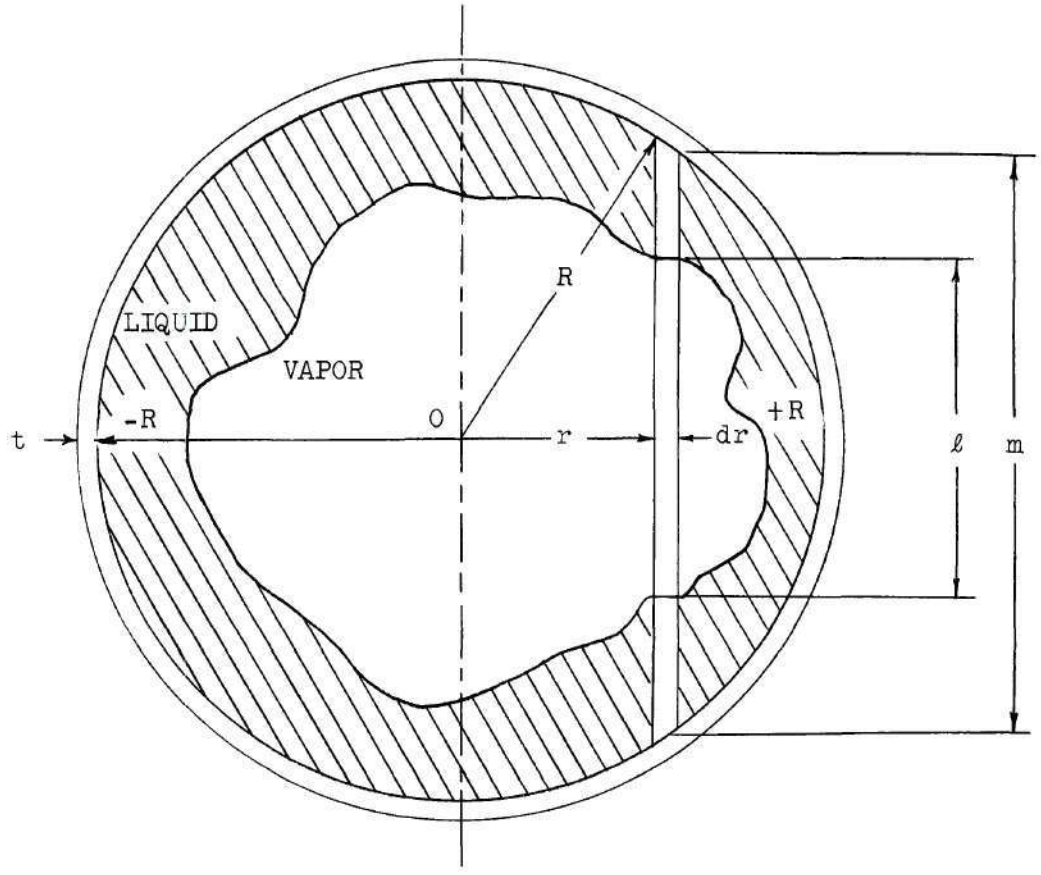

Figure 49. Representation of Cross-Section of Tube Containing Annular Flow.

where I_{TP} = intensity of the beam having passed through the tube containing two-phase flow.

If equation C-1 is divided by equation C-2, the result is

$$I_{MT}/I_F = e^{-\sigma_w \ell (\rho_g - \rho_\ell)} \qquad (C\text{-}4)$$

If equation C-3 is divided by equation C-2, the result is

$$I_{TP}/I_F = e^{-\sigma_w \ell (\rho_g - \rho_\ell)} \qquad (C\text{-}5)$$

The local void fraction is defined as the ratio of the chordal length of the steam to the chordal length of the tube i.e.,

$$\alpha = \frac{\ell}{m} \qquad (C\text{-}6)$$

Equation C-4 may be written as

$$-\sigma_w m (\rho_g - \rho_\ell) = \ell n (I_{MT}/I_F) \qquad (C\text{-}4)$$

Equation C-5 may be written as

$$-\sigma_w \ell (\rho_g - \rho_\ell) = \ell n (I_{TP}/I_F) \qquad (C\text{-}5)$$

The local void fraction may be expressed in terms of I_{TP}, I_{MT}, and I_F by dividing the logarithmic form of equation C-5 by the logarithmic form of equation C-4. The result is

$$\alpha = \frac{\ell n (I_{TP}/I_F)}{\ell n (I_{MT}/I_F)} \qquad (4.204)$$

The average void fraction is the ratio of the cross-sectional

area occupied by the steam to the cross-sectional area of the tube, and is given by

$$\alpha_{avg} = \frac{a_g}{A} = \frac{\int_{-R}^{R} \ell dr}{\pi R^2} \qquad (C\text{-}6)$$

ℓ can be expressed in terms of α by the following relations

$$\ell = \alpha \cdot m$$
$$m = 2\sqrt{R^2 - r^2}$$
$$\ell = 2\alpha\sqrt{R^2 - r^2}$$

Thus equation C-6 may be written as

$$\alpha_{avg} = \frac{1}{\pi R^2} \int_{-R}^{R} 2\alpha \sqrt{R^2 - r^2}\ dr$$

A convenient change of variables may be performed to shift the axis to the tube wall. Defining y by the following relation

$$y = \frac{r+R}{2R} \qquad (C\text{-}7)$$

the expression for α_{avg} becomes

$$\alpha_{avg} = \frac{8}{\pi} \int_{o}^{1} \alpha \sqrt{y(1-y)}\ dy \qquad (4.205)$$

In summary, if the intensities I_{MT}, I_{TP}, and I_F are known as a function of y, the local void fraction α may be evaluated by equation (4.204) as a function of y. It is then possible to evaluate the average void fraction by equation (4.205).

APPENDIX D

ERROR ANALYSIS OF THE VOID FRACTION MEASUREMENT

There are several sources of error in measuring the void fraction in two-phase flow. First, if the point of initial vaporization fluctuates around a point near the entrance of the test section, the void fraction will fluctuate at the point of measurement. This error is difficult to assess quantitatively, but observation at the expansion section showed a high frequency fluctuation in the liquid leaving the test section in a few cases. This high frequency fluctuation was not present in most cases, and the flow appeared to be steady. Even in those cases in which the fluctuations appeared, the measured void fraction is an accurate time average of the actual void fraction. Second, the location of the edges of the tube could introduce an error in evaluation of the void fraction. This difficulty was easily resolved as the count rate increased extremely rapidly when the edge of the tube was reached. This point has been previously discussed in Chapter IV. Third, the uncertainty in the location at which the gamma beam crossed the tube was one-sixteenth of an inch, and there was no difficulty in locating the position of the gamma beam on the tube to this magnitude. Fourth, the accuracy with which the intensity of the radiation can be measured must be considered.

There are several factors which will introduce error in the measurement of the intensity of the radiation. For a given detector and source, these factors are:

1. Background count.
2. Coincidence loss.
3. Statistical error in counting.
4. Accuracy of measuring and recording instruments.

The background count in the laboratory was of the order of 50 to 100 counts per minute depending on the proximity of other sources in the laboratory. It was possible to set the recording system on zero for a given background count, thus giving the reference of zero for the day's operations and nullifying the effect of background radiation.

The coincidence loss refers to the photons which were not counted while the Geiger-Mueller tube was discharged from the previous count. The intensity may be corrected for this "dead time" by the following relation

$$(I)_T = \frac{(I)_M}{1-\delta\cdot(I)_M} \qquad (D-1)$$

where $(I)_T$ = the true count rate

$(I)_M$ = the measured count rate

δ = the resolution time for the Geiger-Mueller tube and is equal to 200 microseconds.

The statistical error in the measurement of the intensity is given by equation (4.208). To access the error in the local void fraction α due to this statistical error in counting, the following analysis can be made. The local void fraction is given by

$$\alpha = \frac{\ell n\ (I_{TP}/I_F)}{\ell n\ (I_{MT}/I_F)} \qquad (4.204)$$

The fractional error in α can be expressed as

$$\frac{d\alpha}{\alpha} = \frac{\partial\alpha}{\partial I_{MT}} \cdot \frac{dI_{MT}}{\alpha} + \frac{\partial\alpha}{\partial I_F} \cdot \frac{dI_F}{\alpha} + \frac{\partial\alpha}{\partial I_{TP}} \frac{dI_{TP}}{\alpha} \qquad (D-2)$$

Partial differentation of equation (4.204) gives

$$\frac{\partial\alpha}{\partial I_{MT}} = - \frac{\ell n\ (I_{TP}/I_F)}{I_{MT}\left[\ell n(I_{MT}/I_F)\right]^2}$$

$$\frac{\partial\alpha}{\partial I_F} = \frac{\ell n\ (I_{TP}/I_{MT})}{I_F\left[\ell n\ (I_{MT}/I_F)\right]^2}$$

$$\frac{\partial\alpha}{\partial I_{TP}} = \frac{1}{I_{TP}\ \ell n(I_{MT}/I_F)}$$

If the positive values of above relations are substituted into equation D-2 an equation for the maximum error in α is obtained. This equation is

$$e = \frac{1}{\ell n\ \frac{I_{MT}}{I_F} \cdot \ell n\ \frac{I_{TP}}{I_F}} \left[\frac{\Delta I_{TP}}{I_{TP}}\ \ell n\ \frac{I_{MT}}{I_F} + \right. \qquad (4.206)$$

$$\left. \frac{\Delta I_{MT}}{I_{MT}}\ \ell n\ \frac{I_{TP}}{I_F} + \frac{\Delta I_F}{I_F}\ \ell n\ \frac{I_M}{I_{TP}} \right]$$

The error in the average void fraction may be ascertained by considering equation (4.205) written as

$$\alpha_{avg} = \frac{8}{\pi} \int_o^1 (\alpha \pm 3)\ \sqrt{y(1-y)}\ dy = \frac{8}{\pi} \int_o^1 \alpha\ \sqrt{y(1-y)}\ dy \qquad (D-3)$$

$$\pm\ \frac{8}{\pi} \int_o^1 e\ \sqrt{y(1-y)}\ dy$$

where the error in the average void fraction e_{avg} is

$$e_{avg} = \frac{8}{\pi} \int_0^1 e \sqrt{y(1-y)}\ dy \qquad (4.207)$$

The accuracy of the measuring and recording instrument i.e., the Nuclear Chicago count rate meter and the Texas Instruments Rectiriter recorder, is less than ± 1.0% of the full scale reading. Thus, the error which would be introduced by the measuring and recording system is considerably less than the normal 10 to 20 per cent error due to the statistical error in counting.

The temperature corrections of the intensities will now be considered. These are the corrections which arise when the empty tube is traversed at room temperature, the full tube is traversed at approximately 200°F and the tube containing two-phase flow is traversed at the operating temperature. The following relations will be used:
For the tube containing steam at the operating temperature T;

$$I_{MT,T} = I_o e^{-(\sigma_s \rho_{g,T} 2t_{s,T} + \sigma_w \rho_{g,T} m)} \qquad (D-4)$$

For the tube containing air at room temperature T_1,

$$I_{MT,T_1} = I_o e^{-(\sigma_s \rho_{s,T_1} 2t_{s,T_1} + \sigma_{air} \rho_{air,T_1} m)} \qquad (D-5)$$

For the tube containing water at temperature T_2,

$$I_{F,T_2} = I_o e^{-(\sigma_s \rho_{s,T_2} 2t_{s,T_2} + \sigma_w \rho_{\ell,T_2} m)} \qquad (D-6)$$

For the tube containing water at temperature T,

$$I_{F,T} = I_o e^{-(\sigma_s \rho_{s,T}\, 2t_{s,T} + \sigma_w \rho_{\ell,T}\, m)} \qquad (D\text{-}7)$$

For the tube containing two-phase flow at temperature T,

$$I_{TP,T} = I_o e^{-\left[\sigma_s \rho_{s,T}\, 2t_{s,T} + \sigma_w \rho_{\ell,T}(m-\ell) + \sigma_w \rho_{g,T}\, \ell\right]} \qquad (D\text{-}8)$$

If equation D-4 is divided by equation D-7, the result is

$$(I_{MT}/I_F)_T = e^{\sigma_w m(\rho_{\ell,T}-\rho_{g,T})} \qquad (D\text{-}9)$$

If equation D-5 is divided by equation D-6, the result is

$$(I_{MT,T_1}/I_{F,T_2}) = e^{\left[2\sigma_s(\rho_{s,T_2}-\rho_{s,T_1})+\sigma_w m(\rho_{\ell,T_2}-\rho_{air,T_1})\right]} \qquad (D\text{-}10)$$

where σ_{air} is taken equal to σ_w.

If the logarithmic forms of equations D-9 and D-10 are combined, the result is

$$\ell n \left(\frac{I_{MT}}{I_F}\right)_T = \ell n \frac{I_{MT,T_1}}{I_{F,T_2}} + \sigma_w m \left[(\rho_{\ell,T}-\rho_{\ell,T_2}) + (\rho_{air,T_1}-\rho_{g,T})\right]$$

where the term involving the change in density and thickness of the tube is neglected as this term is small compared to the other terms. If the definition of y from Appendix C is used, the equation above can be written as

$$\ell n \left(\frac{I_{MT}}{I_F}\right)_T = \ell n \frac{I_{MT,T_1}}{I_{F,T_2}} + 2\sigma_w D \sqrt{y(1-y)} \left[(\rho_{\ell,T} - \rho_{\ell,T_2}) + (\rho_{air,T_1} - \rho_{g,T})\right] \qquad (D-11)$$

If equations D-6, D-7 and D-8 are combined in a way similar to that used to obtain equation D-11, the result is,

$$\ell n \left(\frac{I_{TP}}{I_F}\right)_T = \ell n \frac{I_{TP,T}}{I_{F,T_2}} + 2\sigma_w D \sqrt{y(1-y)} (\rho_{\ell,T} - \rho_{\ell,T_2}) \qquad (D-12)$$

If equations D-4, D-5 and D-8 are combined in a way similar to that used to obtain equation D-11, the result is,

$$\ell n \left(\frac{I_{MT}}{I_{TP}}\right)_T = \ell n \frac{I_{MT,T_1}}{I_{TP,T}} + 2\sigma_w D \sqrt{y(1-y)} (\rho_{air,T_1} - \rho_{g,T}) \qquad (D-13)$$

Using the data from Figure 7 and knowing the diameter of the tube to be 0.930 in, the value of $2\sigma_w D$ was calculated and found to be 0.02119 ft^3/lb_M.

The correction due to temperature variation affects the calculated value of the void fraction by 10 per cent or less.

APPENDIX E

THE VOID FRACTION COMPUTER PROGRAM

A program to analyze the data from the void fraction measurement was written in ALGOL for the Burroughs 220 Electronic Data Processing System. A further description of the programming language and the computer is given in Chapter III. The input data to the computer were the run number, date, the temperature of the two-phase flow, the temperature with the tube full of water, the temperature with the tube empty, and the forty-nine sets of values for I_{MT}, I_{TP}, and I_F which were obtained from the recorder chart records of the traverses. These sets of intensities were numbered for x starting at the tube edge (x = 0.0) and going to the opposite tube edge (x = 49.0)

Referring to the computer program, the following calculations were made with the input data:

1. The density of the liquid and vapor were calculated from the least square polynomials for the specific volume as given in Chapter III.

2. From the values of x, the corresponding values of y were computed.

3. The correction for coincidence loss was made for each individual intensity measurement by equation D-1.

4. The values of the left hand side of equations D-11, D-12, and D-13 were computed.

5. The local void fraction was computed by equation (4.204).

6. The values of the errors in the intensities I_{MT}, I_{TP}, and I_F were computed by equation (4.208).

7. The per cent error in the local void fraction was computed by equation (4.206).

8. The average void fraction was computed by equation (4.205).

9. The error in the average void fraction was computed by equation (4.207).

The output of the computer program was the following

1. The run number, data, and temperatures.

2. The average void fraction, the statistical error in the average void fraction, and the per cent error in the average void fraction.

3. The computed values of y and the corresponding values of the local void fraction, error in the local void fraction, and the per cent error in the local void fraction.

An example of the output for a typical run, run number 10213 is given following the computer program in Table 35. Also Figure 50 shows the results for this particular run. Table 36 gives the ALGOL symbols corresponding to the symbols used in the text.

```
0200                    BAC-220 STANDARD VERSION   2/1/62
0200    COMMENT VOID FRACTION COMPUTER PROGRAM                                  $
0200    INTEGER J,RUNNO,DATE                                                    $  3
0200    ARRAY   X(50),IM(50),I(50),IT(50),Y(50),IMT(50),IL(50),ITP(50),LNTPF(50
0200    ),LNMTF(50),LNMTTP(50),A(50),DIMT(50),DIF(50),DITP(50),PE(50),F(50),E(5
0200    0),G(50)                                                                $  4
0200    TRANS.. READ($$DATA1)                                                   $  5
0204            DWTTP    =   (1.0)/( (1.6834591**-8).(TTP).(TTP)  -  (2.2433702
0207    **-7).(TTP)  +   1.6004569**-2  )                                       $  11
0217            DWTFL   = (1.0) / (  (1.6834591**-8).(TFL).(TFL)  - (2.2433702*
0220    *-7).(TFL)   +   1.6004569**-2  )                                       $  12
0230            DSTTP   =  (1.0) / ( (9.0089112**-8).(TTP).(TTP).(TTP).(TTP)  -
0235    (1.1194411**-4).(TTP).(TTP).(TTP)  +  (5.2583948**-2).(TTP).(TTP)     -
0246    (11.150526).(TTP)   +   912.01727  )                                    $  13
0256            DSTMT    =  (1.0) / ( (9.0089112**-8).(TMT).(TMT).(TMT).(TMT) -
0261    (1.1194411**-4).(TMT).(TMT).(TMT)  +  (5.2583948**-2).(TMT).(TMT)     -
0272    (11.150526).(TMT)    +   912.01727  )                                   $  14
0282            FOR J = (1,1,49)                                                $  6
0293    BEGIN   Y(J) =   X(J) / 48.0                                            $  7
```

```
0299            IMT(J)    =  IM(J) / ( 1.0  - ( IM(J)/ 150.0 ) )                $  8
0309            IL(J)     =  I(J)  / ( 1.0  - ( I(J) / 150.0 ) )                $  9
0319            ITP(J)    =  IT(J) / ( 1.0  - ( IT(J)/ 150.0 ) )                $  10
0329            LNTPF(J)    =   LOG( ITP(J) / IL(J) )  + (0.02119)(  DWTTP     -
0338    DWTFL ). SQRT( Y(J)( 1.0 - Y(J) ) )                                     $  15
0350            LNMTF(J)    =   LOG(  IMT(J) / IL(J)  ) +  (0.02119)(  ( (DSTMT)
0356    -(DSTTP) ) + ( (DWTTP) - (DWTFL) )  ). SQRT( Y(J)( 1.0 - Y(J) ) )       $  16
0375            LNMTTP(J)   =   LOG( IMT(J) / ITP(J) )  + (0.02119)(   DSTMT  -
0384    DSTTP   ).SQRT(  Y(J)( 1.0 - Y(J) )  )                                  $  17
0396            IF  I(J)   EQL   IT(J)                                          $
0396    BEGIN   A(J)  =  0.00                                                   $
0404            GO TO  JFK                                  END                 $
0405            A(J)   =    LNTPF(J) / LNMTF(J)                                 $  18
0410    JFK..   DIMT(J)  = ( (0.6745).(IMT(J)) )/ SQRT( (666.66667). IMT(J) )   $  19
0424            DIF(J)   = ( (0.6745).(IL(J) ) )/ SQRT( (666.66667). IL(J)  )   $  20
0438            DITP(J)  = ( (0.6745).(ITP(J)) )/ SQRT( (666.66667). ITP(J) )   $  21
0452            IF  I(J)  EQL  IT(J)                                            $
0452    BEGIN   PE(J)  =  0.00                                                  $
0460            GO TO  NEXT                                 END                 $
```

```
0461            PE(J)=(   (   ( DITP(J)•LNMTF(J) )/( ITP(J) )    +   ( DIMT(J)•LNTP
0469    F(J) )/( IMT(J) )    +   ( DIF(J)•LNMTTP(J) )/( IL(J) )    )(100•0)    )/( LN
0482    MTF(J)•LNTPF(J) )                                                          $   22
0487    NEXT••  F(J)    =     A(J) • SQRT( Y(J)( 1•0 - Y(J) ) )                    $   23
0496            E(J)    =   ( PE(J)•A(J) )/(100•0)                                $   24
0502            G(J)    =     E(J) • SQRT( Y(J)( 1•0 - Y(J) ) )                   $   25
0511                                                      END                     $   26
0512            AAVG  = ((1•0)/((3•14159)(18•0)))(  F(1) + F(49) +  2•0( F(3)+F
0512    (5) + F(7) + F(9) + F(11) + F(13) + F(15) + F(17) + F(19) + F(21) + F(2
0512    3) + F(25) + F(27) + F(29) + F(31) + F(33) + F(35) + F(37) + F(39) +F(4
0535    1) + F(43) + F(45) + F(47) )  +  4•0( F(2) + F(4) + F(6) + F(8) + F(10)
0535    + F(12) + F(14) + F(16) + F(18) + F(20) + F(22) + F(24) + F(26) + F(28)
0535    + F(30) + F(32) + F(34) + F(36) + F(38) + F(40) + F(42) + F(44) + F(46)
0562    ) )                                                                        $   27
0566            EAAVG  =  (  (1•0)/(3•14159)(18•0)  )( G(1) + G(49)+2•0( G(3) +
0566    G(5) + G(7) + G(9) + G(11)+ G(13) + G(15) + G(17) + G(19) + G(21) + G(2
0566    3) + G(25) + G(27) + G(29) + G(31) + G(33) + G(35) + G(37) + G(39) +G(4
0589    1) + G(43) + G(45) + G(47) )  +  4•0( G(2) + G(4) + G(6) + G(8) + G(10)
0589    + G(12) + G(14) + G(16) + G(18) + G(20) + G(22) + G(24) + G(26) + G(28)
```

```
0616      + G(30) + G(32) + G(34) + G(36) + G(38) + G(40) + G(42)+G(44)+G(46) ))$  28
0620              PEAAVG  =  ( (EAAVG)(100.0) ) / (AAVG)                          $  29
0625              WRITE($$INFO,FMT1)                                             $  30
0633              WRITE($$AVG,FMT2)                                              $  31
0641              WRITE($$FMT3)                                                  $  32
0645              WRITE($$YAPE,FMT4)                                             $  33
0653              GO TO TRANS                                                    $  34
0654      INPUT   DATA1(RUNNO,DATE,TTP,TFL,TMT,FOR J=(1,1,49)$(X(J),IM(J),I(J),IT
0695      (J) ) )                                                                $  35
0702      OUTPUT  INFO( RUNNO ,DATE,TTP,TFL,TMT )                                $  36
0721      OUTPUT  AVG( AAVG,EAAVG,PEAAVG)                                        $  37
0734      OUTPUT  YAPE( FOR J=(1,1,49)$(Y(J),A(J),E(J),PE(J) ) )                 $  38
0767      FORMAT  FMT1(B3,*RUN NO*,I5,B5,*DATE*,I6,B5,*TEMPERATURE TWO PHASE*,X7.
0767      1,B5,*TEMPERATURE FULL*,X7.1,B5,*TEMPERATURE MT*,X7.1,W3)              $  39
0795      FORMAT  FMT2(B3,*AVERAGE VOID FRACTION=*,X8.6,B3,*STATISTICAL ERROR IN
0795      A =*,X8.6,B3,*PERCENT ERROR IN A =*,X7.2,W4)                           $  40
0819      FORMAT  FMT3(B5,*POSITION Y*,B5,*VOID FRACTION A*,B5,*ST. ERROR IN A*,B
0819      5,*PERCENT ERROR IN A*,W4)                                             $  41
0840      FORMAT  FMT4(B5,X9.6,B8,X8.6,B14,X8.6,B12,X7.2,W0)                     $  42
```

```
0851                FINISH                                          $  43
COMPILED PROGRAM ENDS AT 0852
PROGRAM VARIABLES BEGIN AT 3434
```

TABLE 35. MEASURED LOCAL VOID FRACTION FOR RUN 10213

RUN NUMBER 10213

TTP = 283.0 OF TFL = 160.0 OF TMT = 146.0 OF

AVERAGE VOID FRACTION (AAVG) = 0.226378

STATISTICAL ERROR IN AAVG (EAAVG) = 0.062466

PERCENT ERROR IN AAVG (PEAAVG) = 27.59

POSITION Y	VOID FRACTION A	STATISTICAL ERROR IN A	PERCENT ERROR IN A
0.000000	0.000000	0.000000	0.00
0.020833	0.000000	0.000000	0.00
0.041666	0.000000	0.000000	0.00
0.062500	0.000000	0.000000	0.00
0.083333	0.000000	0.000000	0.00
0.104166	0.000000	0.000000	0.00
0.125000	0.000000	0.000000	0.00
0.145833	0.000000	0.000000	0.00
0.166666	0.011621	0.131733	1133.48
0.187500	0.087474	0.113009	129.19
0.208333	0.114098	0.103912	91.07
0.229166	0.186061	0.087340	46.94
0.250000	0.224438	0.083892	37.37
0.270833	0.216027	0.081674	37.80
0.291666	0.236952	0.078274	33.03
0.312500	0.255241	0.075234	29.47
0.333333	0.253192	0.072192	28.51
0.354166	0.255446	0.072993	28.57
0.375000	0.251239	0.072094	28.69

(CONTINUED)

TABLE 35. (CONTINUED)

POSITION Y	VOID FRACTION A	STATISTICAL ERROR IN A	PERCENT ERROR IN A
0.395833	0.267738	0.071280	26.62
0.416666	0.290525	0.068297	23.50
0.437500	0.319910	0.064930	20.29
0.458333	0.348316	0.063645	18.27
0.479166	0.341998	0.062970	18.41
0.500000	0.354997	0.062873	17.71
0.520833	0.362405	0.064164	17.70
0.541666	0.361097	0.065358	18.09
0.562500	0.344755	0.066143	19.18
0.583333	0.355597	0.067637	19.02
0.604166	0.348849	0.070356	20.16
0.625000	0.362210	0.071641	19.77
0.645833	0.350384	0.072776	20.77
0.666666	0.308327	0.075437	24.46
0.687500	0.342131	0.075771	22.14
0.708333	0.324900	0.077887	23.97
0.729166	0.326098	0.082146	25.19
0.750000	0.327413	0.084091	25.68
0.770833	0.329900	0.089036	26.98
0.791666	0.288188	0.099586	34.55
0.812500	0.212698	0.112488	52.88
0.833333	0.209356	0.117829	56.28
0.854166	0.000000	0.000000	0.00
0.875000	0.000000	0.000000	0.00
0.895833	0.000000	0.000000	0.00
0.916666	0.000000	0.000000	0.00
0.937500	0.000000	0.000000	0.00
0.958333	0.000000	0.000000	0.00
0.979166	0.000000	0.000000	0.00
1.000000	0.000000	0.000000	0.00

Table 36. Nomenclature for Void Fraction Computer Program

SYMBOLS			
ALBOL	TEXT		
A	α	local void fraction as defined by equation (4.204)	dimensionless
AAVG	α_{avg}	average void fraction as defined by equation (4.205)	dimensionless
DIF	ΔI_F	statistical error in I_F as defined by equation (4.208)	counts/min
DIMT	ΔI_{MT}	statistical error in I_{MT} as defined by equation (4.208)	counts/min
DITP	ΔI_{TP}	statistical error in I_{TP} as defined by equation (4.208)	counts/min
DSTMT	ρ_{g,T_1}	density of steam at T_1	lb/ft^3
DSTTP	$\rho_{g,T}$	density of steam at T	lb/ft^3
DWTFL	ρ_{ℓ,T_2}	density of water at T_2	lb/ft^3
DWTTP	$\rho_{\ell,T}$	density of water at T	lb/ft^3
E	e	error in α as defined by equation (4.206)	dimensionless
EAAVG	e_{avg}	error in α_{avg} as defined by equation (4.207)	dimensionless
F	$\alpha\sqrt{y(1-y)}$	function as defined by equation (4.205)	dimensionless
G	$e\sqrt{y(1-y)}$	function as defined by equation (4.207)	dimensionless
I	I_F	measured intensity from the	counts/min
IL	$(I_F)_T$	measured intensity from the full pipe corrected for coincidence loss, equation (IV-1)	counts/min
IM	I_{MT}	measured intensity from the empty pipe	counts/min

IMT	$(I_{MT})_T$	measured intensity from the empty pipe corrected for coincidence loss, equation (IV-1)	counts/min
IT	I_{TP}	measured intensity from pipe containing two-phase flow	counts/min
ITP	$(I_{TP})_T$	measured intensity from pipe containing two-phase flow, corrected for coincidence loss, equation (IV-1)	counts/min
LNMTF	$\ell n(I_{MT}/I_F)_T$	function defined by equation (IV-11)	dimensionless
LNTPF	$\ell n(I_{TP}/I_F)_T$	function defined by equation (IV-12)	dimensionless
LNMTTP	$\ell n(I_{MT}/I_F)_T$	function defined by equation (IV-13)	dimensionless
PE	$100 \cdot e$	per cent error in local void fraction	dimensionless
PEAAVG	$100 \cdot e_{avg}$	per cent error in average void fraction	dimensionless
TFL	T_2	temperature of water for traverse of the full tube	°F
TMT	T_1	temperature of air for traverse of the empty tube	°F
TTP	T	temperature of two-phase flow	°F
X	x	location on composite plot of intensities variable defined by equation (III-7)	dimensionless

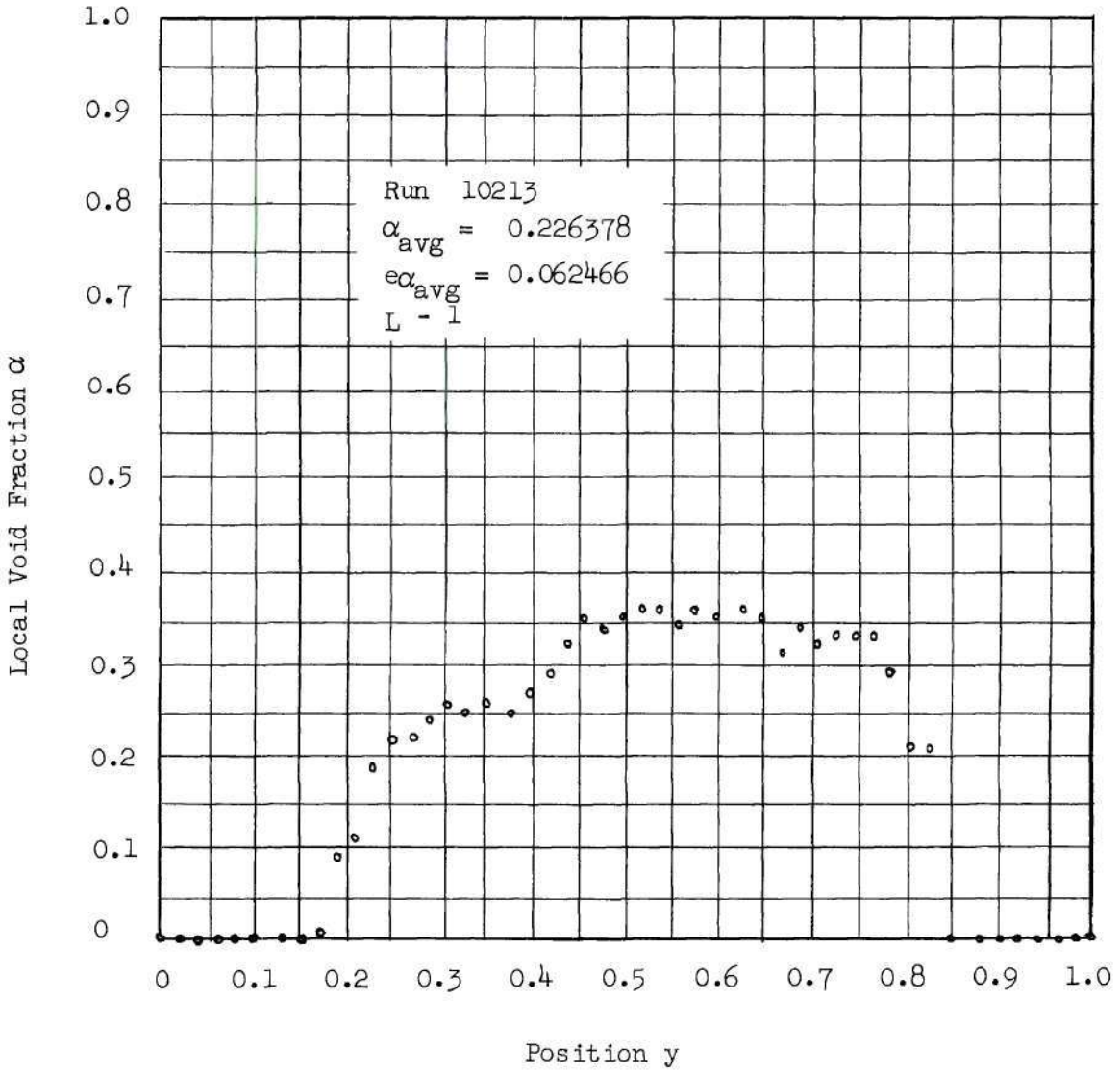

Figure 50. Measured Local Void Fraction for Run Number 10213.

APPENDIX F

EVALUATION OF HEAT TRANSFER FOR THE TEST SECTION

Calculations are made to establish the validity of the following statements.

1. The heat loss from the test section is sufficiently small to justify the assumption of adiabatic conditions.

2. The temperature drop across the test section tube wall is sufficiently small and the heat transfer by axial conduction is sufficiently small to justify the assumption that the outside wall temperature is equal to the liquid temperature at the cross-section.

Considering statement one, the rate of heat transfer from the test section, insulated with one inch of 85% magnesia, is given by

$$q = U_i A_i \Delta T \qquad \text{(F-1)}$$

where q = the rate of heat transfer, BTU/hr

ΔT = the temperature difference between the fluid and the surroundings, °F

U_i = the overall heat transfer coefficient, based on the inside tube area, BTU/hr ft^2 °F

A_i = area of the tube based on the inside diameter

$$A_i = \pi D_i L \qquad \text{(F-2)}$$

where D_i = inside diameter of the tube = 0.930 inches

L = tube length = 19.42 ft.

$$U_i = \frac{1}{\frac{1}{h_i} + \frac{D_i t_s}{\overline{D}_s K_s} + \frac{D_i t_m}{D_m K_m}} \qquad (F\text{-}3)$$

where $\overline{D}_s$ = logarithmic mean diameter of the tube wall

$\overline{D}_m$ = logarithmic mean diameter of the insulation

K_m = thermal conductivity of the insulation = 0.112 BTU/hr ft^2°F/ft

K_s = thermal conductivity of the tube = 9.77 BTU/hr ft^2°F/ft

t_s = wall thickness of the tube = 0.035 inches

t_m = thickness of the insulation = 1.0 inches

h_i = heat transfer coefficient of the liquid film and assumed to be given by the Nusselt relation (74)

$$\frac{h_i D_i}{K} = 0.023\ (Re)^{0.8}\ (Pr)^{1/3} \qquad (F\text{-}4)$$

where K = thermal conductivity of water at 300°F = 0.394 BTU/hr ft^2°F/ft

Re = Reynolds number = 5×10^5 as an average

Pr = Prandtl number = 1.17 for water at 300°F

The highest operating temperature was 300°F and the ambient temperature in the laboratory was 70°F on the average. If the preceding equations are evaluated at these temperatures, an estimate of the maximum heat loss from the test section will be obtained. The results are:

h_i = 4470 BTU/hr ft^2°F

$D_i t_s / \overline{D}_s K_s$ = 0.000284 hr ft^2°F/BTU

$D_i t_m / \overline{D}_m K_m$ = 0.480 hr ft^2°F/BTU

U_i = 2.08 BTU/hr ft^2°F

$A_i = 4.73\ ft^2$

$\Delta T = 230°F$

$q_{max} = 2265\ BTU/hr$

The change in the liquid temperature will be calculated to determine for the effect of this heat loss on the liquid flowing in the tube. For an average flow rate of 3.0 lb_m/sec, the change in temperature is given by

$$\Delta t = q_{max}/WC_p \qquad (F\text{-}5)$$

If the proper substitutions are made, the result is

$$\Delta t = 0.209°F$$

Thus the heat loss from the twenty-foot test section results in the maximum of a quarter of a degree change in liquid temperature at 300°F. This heat loss is sufficiently small to justify the assumption of adiabatic flow.

Considering statement two, the temperature drop across the tube wall Δt_w, is proportional to the total temperature drop. This may be expressed as

$$\Delta t_w = \frac{D_i t_s / \overline{D}_s \; K_s}{1/U_i} \qquad (F\text{-}6)$$

Solving equation F-6, the result is

$$\Delta t_w = 0.1596°F$$

Thus, the temperature drop across the tube wall is less than 0.2°F.

To consider axial heat transfer along the test section, an energy balance may be written on a differential length of the tube, dz. At steady state the heat transferred to the control volume is equal to the heat transferred from the control volume or

$$q \text{ cond, in} + q_w = q_{atms} + q \text{ cond, out}$$

where q_{atms} = heat transferred from the tube through the insulation

q_w = heat transferred from the water to the tube

$q_{cond,in}$ = heat transferred by conductions into the control volume

$q_{cond,out}$ = heat transferred by conductions from the control volume

By Fouriers Law, the preceding equation may be written as

$$-KA \frac{dT}{dz} + q_w = q_{atms} + \left[-KA \frac{dT}{dz} + \frac{d}{dz}\left(-KA \frac{dT}{dz}\right) dz\right]$$

If the above relation is simplified, the result is,

$$-KA\left(\frac{d^2T}{dz^2}\right) \Delta z = q_w - q_{atms} \qquad \text{(F-7)}$$

where $q_w - q_{atms}$ is the amount of heat transferred by conduction along the tube wall. It is necessary to evaluate d^2T/dz^2, and this may be done by expressing d^2T/dz^2 in the following difference form.

$$\frac{d^2T}{dz^2} \doteq \frac{T_{i+2} - 2T_{i+1} + T_i}{(\Delta z)^2} \qquad \text{(F-8)}$$

If data from Figure 17 is used, $T_{i+2} = 254.0°F$, $T_{i+1} = 253.0°F$, $T_i = 248.5°F$, and $\Delta z = 3.75$ ft, and equation F-8 gives

$$\frac{d^2T}{dz^2} \doteq -0.248°F/ft^2$$

If equation F-7 is evaluated, the result is

$$q_w - q_{atms} = 0.00670 \text{ BTU/hr} \qquad \text{(F-9)}$$

The following relation gives the per cent of the maximum amount of heat lost to the surroundings that is transferred by axial conduction.

$$\frac{q_w - q_{atms}}{q_{max}} \times 100$$

If the above relation is solved using equation (F-9) and the value for q_{max} which was obtained previously, the per cent of heat lost to the surroundings that was transferred axially is 2.95×10^{-4} per cent.

It is seen that the temperature drop across the tube wall is approximately 0.2°F, and the per cent of the heat lost to the surroundings that is transferred axially is 2.95×10^{-4} per cent. Thus, the temperature drop across the test section tube wall is sufficiently small and the heat transfer by axial conduction is sufficiently small to justify the assumption that the outside wall temperature is equal to the liquid temperature at the cross-section.

APPENDIX G

DESCRIPTION OF THE COMPUTER SOLUTION AND THE COMPUTER PROGRAM

Description.--The computer solution of the Annular Flow equations was written in ALGOL (63) to be used with the Burroughs Algebraic Compiler. The digital computer was the Burroughs 220 Electronic Data Processing System located at the Rich Electronic Computer Center on the campus of the Georgia Institute of Technology. The compiler reads the ALGOL program on the Line Printer, an IBM 407 printer. The output from the program is also printed on the Line Printer.

The input data for the program are the mass flow rate per unit area (W/A) in lb. per ft.^{2}-sec.; inlet temperature T_o, outlet temperature T_e, and the interval, ΔT, for the numerical method in degrees Fahrenheit. An example of the output is given in Table 37 after the computer program. The output includes the L/D ratio, pressure, liquid velocity, vapor velocity, maximum liquid velocity, minimum liquid velocity, Reynolds number, quality, void fraction, and relative velocity factor as functions of temperature. Also the values of the initial slope and the change in the initial slope are given.

The steps to obtain the solution for specified input data are:

1. The initial liquid velocity and the initial value of F from equation (3.201) are calculated where

$$F = \frac{D(1-\alpha_{avg})}{2f\ W(1-x)V_\ell} \left(\frac{dF_w}{dT}\right)_T \qquad (3.201)$$

and F at T_o is given by

$$F_o = - \frac{DA}{2fW} \left(\frac{dP}{dT}\right)_{T_o}$$

2. The solution is started using equation (2.403) at $T_1 = T_o + \Delta T$

$$V_{\ell,1} = V_o + \left(\frac{dV_\ell}{dT}\right)_{T_o} (\Delta T) \qquad (2.403)$$

3. At T_1 the thermodynamic properties, x, V_g, V_p, $V_{\ell,max}$, $V_{\ell,min}$, relative velocity factor k, void fraction α_{avg}, and $(dV_\ell/dT)T_1$ are evaluated. The solution is then continued by the method of Runge-Kutta to $T_2 = T_o + 2\Delta T$ where all of the previously mentioned variables are calculated, and the L/D ratio evaluated by Simpson's Rule. Then prior to proceding with the next step the solution is examined to insure the physical requirements are met.

As previously mentioned, the physical requirements are that the liquid velocity does not exceed the maximum liquid velocity; and the vapor velocity, the liquid velocity and the relative velocity factor are each increasing with temperature. If any of these physical requirements are not met as the solution proceeds stepping an amount ΔT, control is transferred from the solution loop to a sequence of logic statements that adjust the initial slope and start the solution again at T_o. Figure 2 shows various values of the initial slope that did not satisfy the physical requirements of the problem, and also the specific value of the slope that did satisfy the physical requirements of the problem.

For an interval ΔT which the numerical solution approaches the true solution of the differential equation, it may be said that specifying an initial slope defines a particular solution of the differential equation. This is true, but it does not guarantee that this particular solution, as determined by the initial slope, satisfies the physical requirements placed on the solution. It also may be said that there may be a range of initial slopes that will satisfy the physical requirements placed on the solution. This is also true, but this range of initial slope is so narrow that if the maximum and minimum values of the initial slope in this range were used no significant difference could be detected in the two solutions. If the results given in Figure 2 are considered, the initial slope is being changed in the sixth significant figure, and for an interval $\Delta T = 0.1°F$ the liquid velocity, $V_{\ell,1} \doteq 7.5$ ft./sec., is being changed in the seventh significant figure. This is approaching the limit of the computer as the computer only carries eight significant figures. It was desired to have the most accurate solution possible, and difficulty was encountered in choosing an interval which required the initial slope to be specified to more than eight significant figures. In cases where this happened a logic statement was included to increase the size of the interval and start the solution over with the new interval.

The Computer Program.--The program consist of a sequence of statements which are written in a "language," ALGOL, that approximates scientific notations and mathematical notation, and is written in the order that one might specify to be performed on a desk calculator. The steps in the program are, first an "ARRAY" statement requesting allocation of

memory space to be reserved for various variables. Second, a "READ" statement is made to have the specified data read into the machine. Third, is the body of the program where the instructions for the actual calculations are performed. Fourth, the "WRITE" statements are made to have the results of the calculations as specified in the "OUTPUT" statements printed on the Line Printer according to the instructions in the "FORMAT" statements. Fifth, the statement "FINISH" is made to signify conclusion of the program. With these facts in mind the program may be examined for specific details in the calculations. In Table 37, the computer solution is given in its entirety for run 10222. The nomenclature for the computer program is given in Table 38.

```
0200                    BAC-220 STANDARD VERSION   2/1/62
0200      COMMENT SOLUTION OF ANNULAR TWO-PHASE FLOW EQUATIONS FOR GIVEN          001
0200              VALUES OF MASS FLOW RATE IN LB/FTFTSEC , INLET TEMPERATURE
0200              IN OF , OUTLET TEMPERATURE IN OF AND INTERVAL DT              $ 002
0200      INTEGER I,S,J,RUNNO,R,E,M                                             $ 003
0200      ARRAY   T(140), Z(140), VEL(140,2), VEG(140), VELM(140),               004
0200              VELS(140), RE(140), X(140), A(140), RVEL(140), F(140),         005
0200              HL(2), DELTAH(2), DDELTAH(2), DHL(2), DX(2), VG(2), VL(2),     006
0200                    DP(2), DHG(2), VEP(2), DVEL(2), DFW(2), VISL(2),         007
0200              VEGS(2), FFACTOR(2), P(140), LOD(140)                         $ 008
0200      TRANS.. READ($$DATA)                                                  $ 009
0204      INPUT   DATA( WOA, INTEMP, OUTEMP, DT, DERO, DDERO  )                 $ 010
0226              COSO  =  1.0                                                  $ 011
0228              CON  =   81.0                                                 $ 014
0230              D  =  0.930                                                   $ 16
0232              W = WOA(0.0047173)                                            $
0235              T(1) =  INTEMP                                                $ 017
0237              VL(1)  =  (1.6834591**-8)(INTEMP)(INTEMP)  - (2.2433702**-7)(IN 019
0240      TEMP)  +    1.6004569**-2                                             $ 020
```

```
0246            VEL(1,2)  =  (WOA).VL(1)                                          $ 021
0249          P(1)  =  (2.1002138**-8)(INTEMP)(INTEMP)(INTEMP)(INTEMP)      -    022
0254     (7.7171229**-6)(INTEMP)(INTEMP)(INTEMP)+ (1.6371444**-3)(INTEMP)(INTEMP 023
0260     )  - (0.16258768)(INTEMP)   +   6.6913990                               $ 024
0271            HL(1)  =  (1.4895535**-4)(INTEMP)(INTEMP)  + (0.94243237)(INTEM 025
0274     P)  - 26.480936                                                         $ 026
0280            DHL(1)  = (2.0)(1.4895535**-4)(INTEMP)  +  0.94243237           $ 027
0285            DELTAH(1)  = -(6.7723173**-4)(INTEMP)(INTEMP) -(0.34243090)(INT 028
0288     EMP)  +  1073.5792                                                      $ 029
0294            VISL(1) = -(10.041969)  +  (0.24975186).T(1)                      030
0297            -(0.16055983**-2).T(1).T(1)  +  (0.42085671**-5).T(1).T(1).T(1) 031
0308            -(0.39703004**-8).T(1).T(1).T(1).T(1)                           $ 032
0318            RE(1) = (0.930/12.0)(VEL(1,2))/(VL(1))(VISL(1))(6.72**-5)       $ 033
0329            DP( 1 ) = (4.0)(2.1002138**-8).T( 1 ).T( 1 ).T( 1 )   -   (7.71 034
0334     71229**-6)(3.0).T( 1 ).T( 1 )+(1.6371444**-3)(2.0).T( 1 )-0.16258768   $ 035
0347            DFW(1) = -(0.0047173).DP(1).(144.0)                             $ 036
0353            FFACTOR( 1 ) =  0.00180  + (0.125)/ (RE( 1 ))*0.320             $ 037
0363            F( 1 ) =  (32.174)(0.930/12.0).DFW( 1 )/(2.0).FFACTOR( 1 ).W.VE 038
0366     L(1,2)                                                                  $ 039
```

```
0376     IKE..   DUM1  =  VEL(1,2)                                                    $ 043
0378             M  =  2                                                             $ 044
0380     EAR..   DVEL(1)  =  DERO                                                    $ 045
0382             VEG(1)  =  VEL(1,2)                                                 $
0384             VEGJ  =  VEL(1,2)                                                   $
0386             VEGK  =  VEL(1,2)                                                   $
0388             VELM(1)  =  VEL(1,2)                                                $
0390             VELS(1)  =  VEL(1,2)                                                $
0392            RVEL(1)=  1.0                                                        $ 040
0394             A(1)  =  0.0                                                        $
0395             X(1) = 0.0                                                          $ 041
0396             Z(1) = 0.0                                                          $ 042
0397             VEL(2,M)    =  VEL(1,M)    +  DVEL(1).DT                         $ 046
0406             I  =  1                                                             $ 047
0408     PETE..  T(I+1)  =  INTEMP  +  (DT)(I)                                       $ 048
0415             HL( 1+1 )  =  (1.4895535**-4).T(I+1).T(I+1)  +  (0.94243237).T( 049
0415     I+1)  -   26.480936                                                         $ 050
0425             DELTAH( 1+1 ) = -(6.7723173**-4).T(I+1).T(I+1) - (0.34243090).T 051
0425     (I+1)    +  1073.5792                                                       $ 052
```

```
0435            X(I+1) = (HL(1) - HL(1+1) )/ (DELTAH(1+1) )                    $  17
0441            DDELTAH(1+1)  =  -(2.0)(6.7723173**-4)T(I+1) - 0.34243090      $ 054
0449            DHL(1+1) = (2.0)(1.4895535**-4).T(I+1) + 0.94243237            $ 055
0455            DX(1+1) = -( DHL(1+1) + X(I+1).DDELTAH(1+1) )/ (DELTAH(1+1))   $ 056
0464            VG(1+1) = (9.0089112**-8).T(I+1).T(I+1).T(I+1).T(I+1)  -  (1.11 057
0470    94411**-4).T(I+1).T(I+1).T(I+1)  +  (5.2583948**-2).T(I+1).T(I+1)  -  ( 058
0481    11.150526).T(I+1)  +  912.01727                                        $ 059
0487            VL(1+1)  = (1.6834591**-8).T(I+1).T(I+1) - (2.2433702**-7).T(I+ 060
0487    1)  +  1.6004569**-2                                                   $ 061
0497            DP(1+1) = (4.0)(2.1002138**-8).T(I+1).T(I+1).T(I+1)  -  (7.71 062
0503    71229**-6)(3.0).T(I+1).T(I+1)+(1.6371444**-3)(2.0).T(I+1)-0.16258768   $ 063
0516            DHG(1+1) = -(2.0)(5.3013464**-4).T(I+1) + 0.60103002           $ 064
0524            VEG(I+1)  = ( W.X(I+1).VG(1+1).VEL(I+1,M))/( ( 0.0047173  )  . 065
0535    VEL(I+1,M)-  W.( 1.0 - X(I+1))VL(1+1)  )                               $ 066
0556            VEP(1+1)  =VEL(I+1,M).( 1.0  + (  ( (0.2)(  INTEMP             - 067
0564    T(I+1) )( INTEMP - T(I+1) ) ) / ( CON  )    )  )                       $ 068
0575            DVEL(  1+1     )  =  ((-1.0)/(VEL(I+1,M )  )  ) (  (777.98)(32. 069
0584    174).DHL( 1+1      )  +  ((777.98)(32.174).DELTAH(  1+1     ).DX( 1+1) 070
0593          )/( 1.0  - X(  I+1     ) )  + ( ( (DX( 1+1      ).( VEG( I+1  ) 071
```

```
0602     -VEL(I+1,M)) ( VEG(I+1)  -VEL(I+1,M) ) )   /                                ( 072
0623     (2.0).X( I+1      ) )   +   (144.0)(32.174).VG( 1+1      ).DP(1+1      ) 073
0637     -        (777.98)(32.174).DHG( 1+1      ) )(X(I+1  )    )/( ( 1.0 - X( 074
0646      I+1      ) ).(((VEG( I+1      ).(COSO))/(VEP( 1+1)     )) - 1.0) )))$ 075
0660             VEGS(1+1)  =(  W.X(I+1).VG(1+1) )/(0.0047173        )          $ 076
0667             VELS(I+1)  =( W.(1.0 - X(I+1) ).VL(1+1) )/(0.0047173        ) $ 077
0675             P(I+1) =  (2.1002138**-8).T(I+1).T(I+1).T(I+1).T(I+1) - (7.7171 078
0681     229**-6).T(I+1).T(I+1).T(I+1) +(1.6371444**-3).T(I+1).T(I+1) -(0.162587 079
0692     68).T(I+1) + 6.6913990                                                  $ 080
0698             VISL(1+1) = -(10.041969)  +  (0.24975186).T(I+1)                  081
0702     -(0.16055983**-2).T(I+1).T(I+1) + (0.42085671**-5).T(I+1).T(I+1).T(I+1) 082
0713             -(0.39703004**-8).T(I+1).T(I+1).T(I+1).T(I+1)                   $ 083
0723             RVEL(I+1)  = (VEG(I+1))/(VEL(I+1,M))                            $ 084
0735             A(I+1) =( W.X(I+1).VG(1+1) )/(0.0047173)(VEG(I+1) )             $ 085
0747             DFW(1+1) = (  (777.98)(32.174)( VEP(1+1)  - (COSO).VEG(I+1) )   086
0751     ( DELTAH(1+1).DX(1+1)  +  (1.0 - X(I+1)).DHL(1+1) )                     + 087
0762     ( VEP(1+1) -COSO.VEL(I+1,M)  )( X(I+1).DHG(1+1)(777.98)(32.174)         - 088
0777     (VEG(I+1)-VEL(I+1,M))(VEG(I+1)-VEL(I+1,M)).DX(1+1)/ (2.0)  )            + 089
0803     (COSO.VEL(I+1,M) .VEG(I+1)/(W) - ( ( X(I+1).VG(1+1) + ( 1.0 - X(I+1) ). 090
```

```
0824      VL(I+1) ).                                                                    091
0825      VEP(I+1)/(0.0047173) ) )(144.0)(32.174)(0.0047173).DP(I+1)                ) 092
0833      (W)/( (32.174)(VEL(I+1,M))( VEP(I+1) - (COSO)VEG(I+1) ) )                 $ 093
0851                RE(I+1) = (0.930/12.0)(VEL(I+1,M))/(VL(I+1)).(VISL(I+1))(6.7     094
0859      2**-5)                                                                    $ 095
0869                FFACTOR(I+1) =  0.00180  + (0.125)/ (RE(I+1))*0.320             $ 096
0880                VELM(I+1)  = VEGS(I+1)  +  VELS(I+1)                           $ 097
0884                F(I+1) =  (32.174)(0.930/12.0).DFW(I+1)/(2.0).FFACTOR(I+1).W.VE 098
0887      L(I+1,M).(( 1.0 - X(I+1) )/( 1.0 - A(I+1) ) )                            $ 099
0914                A1  =  DVEL(I+1).DT                                            $ 100
0917                TJ  =  INTEMP  +  DT/2.0   +  (DT)(I)                          $ 101
0928                VELJ  =  VEL(I+1,M)       +  A1 / 2.0                          $ 102
0939                HLJ =  (1.4895535**-4)(TJ)(TJ) + (0.94243237)(TJ) - 26.480936 $ 103
0948                DELTAHJ = -(6.7723173**-4)(TJ)(TJ) -(0.34243090)(TJ)+1073.5792$ 104
0957                XJ =(HL(1) - HLJ)/(DELTAHJ)                                    $
0962                DDELTAHJ  =  -(2.0)(6.7723173**-4)(TJ)  - 0.34243090           $ 106
0969                DHLJ  = (2.0)(1.4895535**-4)(TJ) + 0.94243237                  $ 107
0974                DXJ =  - ( DHLJ + XJ.DDELTAHJ )/(DELTAHJ)                      $ 108
0982                VGJ =  (9.0089112**-8)(TJ)(TJ)(TJ)(TJ) - (1.1194411**-4)(TJ)(TJ 109
```

```
0987      )(TJ) + (5.2583948**-2)(TJ)(TJ) - (11.150526)(TJ) +  912.01727          $ 110
1004              VLJ = (1.6834591**-8)(TJ)(TJ)-(2.2433702**-7)(TJ)  + 1.6004569* 111
1004      *-2                                                                    $ 112
1013              DPJ = (4.0)(2.1002138**-8)(TJ)(TJ)(TJ) - (7.7171229**-6)(3.0)(T 113
1018      J)(TJ)  + (1.6371444**-3)(2.0)(TJ)  - 0.16258768                       $ 114
1031              DHGJ = -(2.0)(5.3013464**-4)(TJ)  +  0.60103002                $ 115
1038              VEGJ =  (W.XJ.VGJ.VELJ)/( (0.0047173).VELJ -W.(1.0 - XJ).VLJ )$ 116
1056              VEPJ =  VELJ.( 1.0  + (0.2)( INTEMP - TJ )( INTEMP - TJ )/( CON 117
1063       ) )                                                                   $ 118
1068              DVELJ =  ((-1.0)/(VELJ))(  (777.98)(32.174).DHLJ  + ((777.98)(3 119
1075      2.174).DELTAHJ.DXJ) / ( 1.0  -  XJ )  +  ( ( ( DXJ.(VEGJ - VELJ)(VEGJ - 120
1095      VELJ ) ) / ( (2.0).XJ )  + (144.0)(32.174).VGJ.DPJ   -  (777.98)(32.174 121
1109      ).DHGJ ) ( XJ ) / ( ( 1.0 - XJ ).  ( ( VEGJ.(COSO) ) / ( VEPJ ) - 1.0 ) 122
1124      ) ) )                                                                 $ 123
1132              A2  = (DVELJ)(DT)                                             $ 124
1135              TK =  INTEMP  +  DT        + (DT)(I)                          $ 125
1142              VELK  =  VEL(I+1,M)+ 2.0(A2)  -  A1                           $ 126
1153              HLK  =   (1.4895535**-4)(TK)(TK) + (0.94243237)(TK) -26.480936$ 127
1162              DELTAHK = -(6.7723173**-4)(TK)(TK) -(0.34243090)(TK)+1073.5792$ 129
```

```
1171            DHLK   = (2.0)(1.4895535**-4)(TK) + 0.94243237                    $ 130
1176            XK =(HL(1) - HLK)/(DELTAHK)                                       $
1181            DDELTAHK   =  -(2.0)(6.7723173**-4)(TK)  - 0.34243090             $ 132
1188            DXK =  - ( DHLK + XK.DDELTAHK )/(DELTAHK)                         $ 134
1196            VGK =  (9.0089112**-8)(TK)(TK)(TK)(TK) - (1.1194411**-4)(TK)(TK 135
1201    )(TK) + (5.2583948**-2)(TK)(TK) - (11.150526)(TK) +  912.01727            $ 136
1218            VLK = (1.6834591**-8)(TK)(TK)-(2.2433702**-7)(TK)  + 1.6004569* 137
1218    *-2                                                                       $ 138
1227            DPK = (4.0)(2.1002138**-8)(TK)(TK)(TK) - (7.7171229**-6)(3.0)(T 139
1232    K)(TK)  + (1.6371444**-3)(2.0)(TK)  - 0.16258768                          $ 140
1245            DHGK = -(2.0)(5.3013464**-4)(TK)  +  0.60103002                   $ 141
1252            VEGK =  (W.XK.VGK.VELK)/( (0.0047173).VELK -W.(1.0-XK).VLK  )     $ 142
1270            VEPK = VELK.(1.0 + (0.2)(INTEMP - TK)(INTEMP - TK)/( CON ) )      $ 143
1282            DVELK =((-1.0)/(VELK))( (777.98)(32.174).DHLK +((777.98)(32.174 144
1289    ).DELTAHK.DXK)/(1.0- XK)  + ( ( (DXK.(VEGK -VELK)(VEGK -VELK) )/((2.0). 145
1313    XK)  + (144.0)(32.174).VGK.DPK  - (777.98)(32.174).DHGK )( XK )/( (1.0- 146
1332    XK).(((VEGK.(COSO))/(VEPK) - 1.0) ) ) )           )                       $ 147
1346            A3=  (DVELK)(DT)                                                  $ 148
1349            IF  VEL(I+1,M)   GTR   VELM(I+1)                                  $ 149
```

```
1349            GO  TO  JOE                                                    $ 150
1362            IF  VEG(I+1)   LEQ   VEG(I)                                    $ 151
1362            GO  TO  JOE                                                    $ 152
1369            IF   RVEL(I+1)   LEQ   RVEL(I)                                 $ 153
1369            GO   TO   JOE                                                  $ 154
1376            IF  VEL(I+1,M)  LSS  VEL(I,M)                                  $ 155
1376    BEGIN   IF  DDERO   GEQ    -0.0000001                                  $ 157
1376            GO  TO  SKIT                                                   $ 158
1399            GO  TO  SAL                              END                   $ 159
1400            E = MOD( (I+1), 2 )                                            $ 160
1406            IF E EQL  1                                                    $ 161
1406    BEGIN   SUM1 = 0.0                                                     $ 162
1412            SUM2 = 0.0                                                     $ 163
1413            FOR J = ( 2 , 2 , I )                                          $ 164
1424    BEGIN   SUM1 = SUM1 + F(J)                                             $ 165
1429            SUM2 = SUM2 + F(J+1)                          END              $ 166
1434            Z(I+1) = (DT/3.0)( F(1) - F(I+1) + 4.0(SUM1) + 2.0(SUM2) )     $ 167
1449            LOD(I+1)  =  Z(I+1)/(D/12.0)                      END          $ 167A
1458            IF  T(I+1)   GEQ   OUTEMP                                      $ 168
```

```
1458     BEGIN   I = I+1                                                    $ 169
1467             IF  I  EQL  139                                           $
1467             GO  TO  SKIT                                              $
1473             VEL(I+1,M)  =  VEL(I,M)  +  ( A1 + (4.0)(A2) + A3 )/(6.0) $ 170
1493             GO TO  PETE                                               $ 171
1494                                                        END            $ 172
1494             GO  TO  SKIT                                              $ 173
1495     SAL..   IF  VEL(I+1,M)  GEQ  DUM1                                 $ 174
1506     BEGIN   DUM1  =  VEL(I+1,M)                                       $ 175
1514             DERO  =  DERO  +  DDERO                                   $ 176
1517             GO  TO  EAR                                    END        $ 177
1518     JOE..   DERO  =  DERO  -  DDERO                                   $ 178
1521             IF  DDERO   GEQ    -0.0000001                             $
1521             GO  TO  SKIT                                              $ 158
1527             DDERO  =DDERO/10.0                                        $ 179
1531             GO  TO  EAR                                               $ 180
1532     SKIT..  DPC  = P(1)  -  P(I+1)                                    $ 181
1536             WRITE($$INFO,FMT1)                                        $ 184
1544     OUTPUT  INFO(WOA)                                                 $
```

```
1551     FORMAT  FMT1(B5,*MASS FLOW RATE*,X7.1,B1,*LB/FTFTSEC*,W3)                $
1563             WRITE($$COMP,FMT2)                                              $ 189
1571     OUTPUT  COMP(P(1),INTEMP,P(I+1),T(I+1) )                                $
1589     FORMAT  FMT2(B5,*INLET PRESSURE*,X6.2,B1,*PSIA*,B5,*INLET TEMP*,X7.2,
1589     B1, *OF*,B5,*OUTLET PRESSURE*,X6.2,B1,*PSIA*,B5,*OUTLET TEMP*,X7.2,
1589     B1, *OF*,W4)                                                            $
1621             WRITE($$LEN,FMTX)                                               $
1629     OUTPUT  LEN(DPC)                                                        $
1636     FORMAT  FMTX(B5,*PRESSURE DROP*,X7.2,B1,*PSIA*,W4)                      $
1646             WRITE($$FMT3)                                                   $ 197
1650     FORMAT  FMT3(B4,*TEMP OF*,B3,*LENGTH FT*,B3,*PRESSURE*,B3,
1650     *LIQUID VELOCITY FPS*,B3,*VAPOR VELOCITY FPS*,B3,*VELM*,B3,*VELS*,B3,
1650     *REYNOLDS NO*,W4)                                                       $
1680             WRITE($$RESULTS,FMT4)                                           $ 200
1688     OUTPUT  RESULTS( FOR S= (1,1,I+1)$(T(S),  Z(S),P(S),VEL(S,M),VEG(S),
1730     VELM(S),VELS(S),RE(S)  )  )                                             $
1745     FORMAT  FMT4(   X6.2,B4,X6.2,B4,X8.3,B4,X8.3,B4 ,X8.3,B4,X5.1,B2,X5.1,
1745     B2,X10.1,W0)                                                            $
1763             WRITE($$FMT5)                                                   $ 205
```

```
1767     FORMAT  FMT5(B4,*TEMP OF*,B3,*LENGTH FT*,B3,*QUALITY LBV/LBT*,B3,*VOID  206
1767     FRACTION*,B2,*RELATIVE VELOCITY FACTOR*,W4)                          $ 207
1791             WRITE($$ANSWERS,FMT6)                                       $ 208
1799     OUTPUT  ANSWERS( FOR R = (1,1,(I+1))$(T(R),  Z(R),X(R),A(R),RVEL(R) ))$
1839     FORMAT  FMT6(B4,X6.2,B5,X6.2,B6,X8.6,B11,X8.6,B9,X7.3,W0)            $ 210
1852             WRITE($$CONST,FMT7)                                         $ 211
1860     OUTPUT  CONST( DT,                    DERO,  DDERO  )               $ 212
1873     FORMAT  FMT7(*DT=*,X5.2,B5,
1873                     *DERO=*,X13.8,B5,*DDERO=*,X10.8,W4)                 $ 214
1886             IF  I  EQL  139                                             $
1891     BEGIN   WRITE($$NOTE)                                               $
1895     FORMAT  NOTE(*STORAGE CAPACITY WAS EXCEEDED*,W4)                     $
1904             GO  TO  TRANS                              END              $
1905             IF  DERO  GTR  0.1                                          $
1905     BEGIN   DERO  = -0.5                                                $
1912             DDERO  =  -0.1                                              $
1914             GO  TO  IKE                          END                    $
1915             GO TO TRANS                                                 $ 220
1916             FINISH                                                      $ 221
```

```
COMPILED PROGRAM ENDS AT 1917
PROGRAM VARIABLES BEGIN AT 2209
```

TABLE 37. EXAMPLE OF THE NUMERICAL SOLUTION OF THE ANNULAR FLOW EQUATIONS FOR RUN 10222

MASS FLOW RATE 444.5 LB/FTFT-SEC

INLET TEMPERATURE 257.5 OF OUTLET TEMPERATURE 246.0 OF

TEMPERATURE (OF)	LENGTH (FT)	PRESSURE (PSIA)	LIQUID VELOCITY (FPS)	VAPOR VELOCITY (FPS)	VELM (FPS)	VELS (FPS)	REYNOLDS NUMBER
257.50		33.953	7.586	7.586	7.5	7.5	232120.5
257.40		33.895	8.136	8.649	8.1	7.5	248860.1
257.30	1.24	33.837	8.619	9.780	8.7	7.5	263496.7
257.20		33.779	9.022	11.058	9.3	7.5	275705.6
257.10	2.19	33.721	9.357	12.415	9.9	7.5	285815.1
257.00		33.664	9.650	13.753	10.5	7.5	294620.1
256.90	3.00	33.606	9.917	15.037	11.1	7.5	302631.3
256.80		33.549	10.167	16.262	11.7	7.5	310129.6
256.70	3.73	33.491	10.406	17.434	12.3	7.5	317268.7
256.60		33.434	10.637	18.558	12.9	7.5	324145.9
256.50	4.39	33.377	10.861	19.640	13.5	7.5	330819.6
256.40		33.320	11.079	20.686	14.1	7.5	337332.4
256.30	4.99	33.263	11.294	21.701	14.7	7.5	343709.1
256.20		33.206	11.505	22.690	15.3	7.5	349973.1
256.10	5.55	33.149	11.713	23.655	15.9	7.5	356138.1
256.00		33.092	11.919	24.601	16.5	7.5	362216.5
255.90	6.06	33.035	12.122	25.528	17.1	7.5	368213.5
255.80		32.979	12.322	26.440	17.7	7.5	374142.8
255.70	6.55	32.922	12.521	27.340	18.3	7.5	380002.2

(CONTINUED)

TABLE 37. (CONTINUED)

TEMPERATURE (OF)	LENGTH (FT)	PRESSURE (PSIA)	LIQUID VELOCITY (FPS)	VAPOR VELOCITY (FPS)	VELM (FPS)	VELS (FPS)	REYNOLDS NUMBER
255.60		32.866	12.718	28.227	19.0	7.5	385801.9
255.50	7.00	32.809	12.913	29.104	19.6	7.5	391539.1
255.40		32.753	13.107	29.971	20.2	7.5	397223.0
255.30	7.43	32.696	13.299	30.831	20.8	7.5	402853.3
255.20		32.640	13.489	31.684	21.4	7.5	408431.7
255.10	7.84	32.584	13.678	32.531	22.1	7.5	413959.1
255.00		32.528	13.865	33.372	22.7	7.5	419437.4
254.90	8.22	32.472	14.051	34.209	23.3	7.5	424870.0
254.80		32.416	14.236	35.041	24.0	7.5	430255.7
254.70	8.58	32.361	14.420	35.871	24.6	7.5	435595.4
254.60		32.305	14.602	36.696	25.2	7.5	440889.8
254.50	8.93	32.249	14.782	37.520	25.9	7.5	446142.1
254.40		32.194	14.962	38.340	26.5	7.5	451347.8
254.30	9.26	32.138	15.140	39.159	27.1	7.5	456512.7
254.20		32.083	15.317	39.977	27.8	7.5	461635.2
254.10	9.57	32.027	15.493	40.793	28.4	7.5	466718.1
254.00		31.972	15.668	41.608	29.1	7.5	471754.8
253.90	9.87	31.917	15.841	42.422	29.7	7.5	476757.5
253.80		31.862	16.013	43.236	30.4	7.5	481715.1
253.70	10.16	31.807	16.184	44.049	31.0	7.5	486636.1
253.60		31.752	16.354	44.862	31.7	7.5	491514.5
253.50	10.43	31.697	16.523	45.674	32.3	7.5	496357.2
253.40		31.642	16.691	46.487	33.0	7.5	501162.0
253.30	10.70	31.588	16.857	47.300	33.6	7.5	505928.6

(CONTINUED)

TABLE 37. (CONTINUED)

TEMPERATURE (OF)	LENGTH (FT)	PRESSURE (PSIA)	LIQUID VELOCITY (FPS)	VAPOR VELOCITY (FPS)	VELM (FPS)	VELS (FPS)	REYNOLDS NUMBER
253.20		31.533	17.023	48.114	34.3	7.5	510658.0
253.10	10.95	31.478	17.188	48.927	35.0	7.5	515351.7
253.00		31.424	17.351	49.741	35.6	7.5	520007.1
252.90	11.20	31.370	17.513	50.556	36.3	7.5	524629.9
252.80		31.315	17.675	51.372	30.0	7.5	523214.1
252.70	11.44	31.261	17.835	52.187	37.6	7.5	533767.7
252.60		31.207	17.995	53.005	38.3	7.5	538285.7
252.50	11.67	31.153	18.153	53.822	39.0	7.5	542771.8
252.40		31.099	18.311	54.641	39.7	7.5	547223.4
252.30	11.89	31.045	18.467	55.460	40.3	7.5	551646.8
252.20		30.991	18.623	56.282	41.0	7.5	556036.3
252.10	12.10	30.937	18.778	57.103	41.7	7.5	560397.6
252.00		30.883	18.932	57.926	42.4	7.5	564727.7
251.90	12.31	30.830	19.085	58.751	43.1	7.5	569026.5
251.80		30.776	19.238	59.575	43.8	7.5	573301.8
251.70	12.51	30.723	19.389	60.402	44.5	7.5	577545.9
251.60		30.669	19.540	61.229	45.1	7.5	581764.8
251.50	12.70	30.616	19.690	62.059	45.8	7.5	585956.1
251.40		30.563	19.840	62.888	46.5	7.5	590123.2
251.30	12.89	30.510	19.989	63.720	47.2	7.5	594265.1
251.20		30.456	20.137	64.552	47.9	7.5	598386.0
251.10	13.07	30.403	20.284	65.386	48.6	7.5	602480.8
251.00		30.350	20.431	66.221	49.3	7.5	606555.7
250.90	13.25	30.298	20.577	67.058	50.0	7.5	610610.0

(CONTINUED)

TABLE 37. (CONTINUED)

TEMPERATURE (OF)	LENGTH (FT)	PRESSURE (PSIA)	LIQUID VELOCITY (FPS)	VAPOR VELOCITY (FPS)	VELM (FPS)	VELS (FPS)	REYNOLDS NUMBER
250.80		30.245	20.723	67.894	50.8	7.5	614647.0
250.70	13.42	30.142	20.862	68.734	51.5	7.5	613653.5
250.60		30.139	21.013	69.573	52.2	7.5	622660.2
250.50	13.59	30.087	21.158	70.415	52.9	7.5	626639.2
250.40		30.034	21.302	71.257	53.6	7.5	630607.1
250.30	13.75	29.982	21.446	72.100	54.3	7.5	634555.0
250.20		29.930	21.589	72.945	55.1	7.4	638493.6
250.10	13.91	29.877	21.732	73.791	55.8	7.4	642416.9
250.00		29.825	21.875	74.637	56.5	7.4	646334.1
249.90	14.06	29.773	22.018	75.485	57.2	7.4	650235.6
249.80		29.721	22.160	76.336	58.0	7.4	654133.8
249.70	14.21	29.669	22.303	77.185	58.7	7.4	658020.1
249.60		29.617	22.445	78.036	59.4	7.4	661906.7
249.50	14.35	29.565	22.587	78.888	60.2	7.4	665783.0
249.40		29.513	22.730	79.740	60.9	7.4	669658.2
249.30	14.49	29.462	22.872	80.594	61.6	7.4	673531.0
249.20		29.410	23.015	81.449	62.4	7.4	677404.0
249.10	14.63	29.359	23.157	82.304	63.1	7.4	681277.8
249.00		29.307	23.300	83.160	63.9	7.4	685154.0
248.90	14.76	29.256	23.444	84.017	64.6	7.4	689035.2
248.80		29.204	23.587	84.875	65.4	7.4	692922.1
248.70	14.89	29.153	23.731	85.732	66.1	7.4	696816.9
248.60		29.102	23.876	86.591	66.9	7.4	700721.0
248.50	15.02	29.051	24.021	87.450	67.6	7.4	704636.6

(CONTINUED)

TABLE 37. (CONTINUED)

TEMPERATURE (OF)	LENGTH (FT)	PRESSURE (PSIA)	LIQUID VELOCITY (FPS)	VAPOR VELOCITY (FPS)	VELM (FPS)	VELS (FPS)	REYNOLDS NUMBER
248.40		29.000	24.166	88.310	68.4	7.4	708565.6
248.30	15.14	28.949	24.312	89.169	69.2	7.4	712509.1
248.20		28.898	24.459	90.029	69.9	7.4	716469.2
248.10	15.26	28.847	24.607	90.891	70.7	7.4	720448.9
248.00		28.797	24.756	91.750	71.5	7.4	724448.6
247.90	15.37	28.746	24.905	92.611	72.2	7.4	728472.1
247.80		28.695	25.056	93.473	73.0	7.4	732521.0
247.70	15.49	28.645	25.207	94.333	73.8	7.4	736597.1
247.60		28.594	25.360	95.193	74.6	7.4	740703.0
247.50	15.59	28.544	25.514	96.054	75.4	7.4	744841.3
247.40		28.494	25.670	96.914	76.1	7.4	749013.6
247.30	15.70	28.443	25.826	97.775	76.9	7.4	753224.2
247.20		28.393	25.985	98.633	77.7	7.4	757473.3
247.10	15.80	28.343	26.145	99.493	78.5	7.4	761765.1
247.00		28.293	26.306	100.351	79.3	7.4	766102.0
246.90	15.90	28.243	26.470	101.209	80.1	7.4	770488.1
246.80		28.193	26.635	102.066	80.9	7.4	774923.6
246.70	15.99	28.144	26.803	102.922	81.7	7.4	779414.7
246.60		28.094	26.972	103.778	82.5	7.4	783961.5
246.50	16.08	28.044	27.144	104.632	83.3	7.4	788568.8
246.40		27.995	27.318	105.485	84.1	7.4	793239.0
246.30	16.17	27.945	27.494	106.338	84.9	7.4	797977.2
246.20		27.896	27.674	107.188	85.7	7.4	802784.7
246.10	16.26	27.846	27.856	108.037	86.5	7.4	807666.9
246.00		27.797	28.040	108.886	87.4	7.4	812626.5
245.90	16.34	27.748	28.228	109.732	88.2	7.4	817668.7

(CONTINUED)

TABLE 37. (CONTINUED)

TEMPERATURE (OF)	LENGTH (FT)	QUALITY	VOID FRACTION	RELATIVE VELOCITY FACTOR
257.50		0.000000	0.000000	1.000
257.40		0.000108	0.067833	1.063
257.30	1.24	0.000216	0.120157	1.134
257.20		0.000325	0.159629	1.225
257.10	2.19	0.000433	0.189853	1.326
257.00		0.000541	0.214544	1.425
256.90	3.00	0.000649	0.235807	1.516
256.80		0.000758	0.254740	1.599
256.70	3.73	0.000866	0.271959	1.675
256.60		0.000974	0.287843	1.744
256.50	4.39	0.001082	0.302640	1.808
256.40		0.001190	0.316523	1.867
256.30	4.99	0.001298	0.329617	1.921
256.20		0.001407	0.342021	1.972
256.10	5.55	0.001515	0.353810	2.019
256.00		0.001623	0.365043	2.063
255.90	6.06	0.001731	0.375773	2.105
255.80		0.001839	0.386042	2.145
255.70	6.55	0.001947	0.395884	2.183
255.60		0.002055	0.405330	2.219
255.50	7.00	0.002163	0.414409	2.253
255.40		0.002271	0.423145	2.286
255.30	7.43	0.002379	0.431558	2.318
255.20		0.002487	0.439669	2.348
255.10	7.84	0.002595	0.447494	2.378

(CONTINUED)

TABLE 37. (CONTINUED)

TEMPERATURE (OF)	LENGTH (FT)	QUALITY	VOID FRACTION	RELATIVE VELOCITY FACTOR
255.00		0.002703	0.455049	2.406
254.90	8.22	0.002810	0.462349	2.434
254.80		0.002918	0.469408	2.461
254.70	8.58	0.003026	0.476237	2.487
254.60		0.003134	0.482849	2.513
254.50	8.93	0.003242	0.489253	2.538
254.40		0.003350	0.495459	2.562
254.30	9.26	0.003457	0.501478	2.586
254.20		0.003565	0.507316	2.609
254.10	9.57	0.003673	0.512983	2.632
254.00		0.003781	0.518486	2.655
253.90	9.87	0.003888	0.523832	2.677
253.80		0.003996	0.529028	2.699
253.70	10.16	0.004104	0.534080	2.721
253.60	.	0.004211	0.538995	2.743
253.50	10.43	0.004319	0.543777	2.764
253.40		0.004426	0.548432	2.785
253.30	10.70	0.004534	0.552966	2.805
253.20		0.004642	0.557383	2.826
253.10	10.95	0.004749	0.561688	2.846
253.00		0.004857	0.565885	2.866
252.90	11.20	0.004964	0.569978	2.886
252.80		0.005072	0.573972	2.906
252.70	11.44	0.005179	0.577870	2.926
252.60		0.005287	0.581676	2.945

(CONTINUED)

TABLE 37. (CONTINUED)

TEMPERATURE (OF)	LENGTH (FT)	QUALITY	VOID FRACTION	RELATIVE VELOCITY FACTOR
252.50	11.67	0.005394	0.585394	2.964
252.40		0.005501	0.589025	2.984
252.30	11.89	0.005609	0.592575	3.003
252.20		0.005716	0.596046	3.022
252.10	12.10	0.005823	0.599440	3.040
252.00		0.005931	0.602761	3.059
251.90	12.31	0.006038	0.606012	3.078
251.80		0.006145	0.609194	3.096
251.70	12.51	0.006253	0.612311	3.115
251.60		0.006360	0.615364	3.133
251.50	12.70	0.006467	0.618356	3.151
251.40		0.006574	0.621290	3.169
251.30	12.89	0.006682	0.624167	3.187
251.20		0.006789	0.626990	3.205
251.10	13.07	0.006896	0.629760	3.223
251.00		0.007003	0.632479	3.241
250.90	13.25	0.007110	0.635150	3.258
250.80		0.007217	0.637774	3.276
250.70	13.42	0.007324	0.640353	3.293
250.60		0.007432	0.642888	3.310
250.50	13.59	0.007539	0.645381	3.328
250.40		0.007646	0.647834	3.345
250.30	13.75	0.007753	0.650248	3.361
250.20		0.007860	0.652625	3.378
250.10	13.91	0.007967	0.654967	3.395

(CONTINUED)

TABLE 37. (CONTINUED)

TEMPERATURE (OF)	LENGTH (FT)	QUALITY	VOID FRACTION	RELATIVE VELOCITY FACTOR
250.00		0.008074	0.657274	3.411
249.90	14.06	0.008181	0.659548	3.428
249.80		0.008287	0.661790	3.444
249.70	14.21	0.008394	0.664002	3.460
249.60		0.008501	0.666185	3.476
249.50	14.35	0.008608	0.668340	3.492
249.40		0.008715	0.670468	3.508
249.30	14.49	0.008822	0.672572	3.523
249.20		0.008929	0.674650	3.538
249.10	14.63	0.009035	0.676706	3.554
249.00		0.009142	0.678740	3.569
248.90	14.76	0.009249	0.680753	3.583
248.80		0.009356	0.682746	3.598
248.70	14.89	0.009462	0.684720	3.612
248.60		0.009569	0.686677	3.626
248.50	15.02	0.009676	0.688617	3.640
248.40		0.009782	0.690540	3.654
248.30	15.14	0.009889	0.692449	3.667
248.20		0.009996	0.694345	3.680
248.10	15.26	0.010102	0.696227	3.693
248.00		0.010209	0.698097	3.706
247.90	15.37	0.010316	0.699957	3.718
247.80		0.010422	0.701806	3.730
247.70	15.49	0.010529	0.703645	3.742
247.60		0.010635	0.705477	3.753

(CONTINUED)

TABLE 37. (CONTINUED)

TEMPERATURE (OF)	LENGTH (FT)	QUALITY	VOID FRACTION	RELATIVE VELOCITY FACTOR
247.50	15.59	0.010742	0.707300	3.764
247.40		0.010848	0.709117	3.775
247.30	15.70	0.010955	0.710928	3.785
247.20		0.011061	0.712734	3.795
247.10	15.80	0.011168	0.714536	3.805
247.00		0.011274	0.716334	3.814
246.90	15.90	0.011380	0.718129	3.823
246.80		0.011487	0.719923	3.831
246.70	15.99	0.011593	0.721715	3.839
246.60		0.011699	0.723506	3.847
246.50	16.08	0.011806	0.725298	3.854
246.40		0.011912	0.727091	3.861
246.30	16.17	0.012018	0.728886	3.867
246.20		0.012125	0.730683	3.873
246.10	16.26	0.012231	0.732483	3.878
246.00		0.012337	0.734287	3.883
245.90	16.34	0.012443	0.736095	3.887

DT= -.10 DERO= -5.50747000 DDERO=-.00001

Table 38. Nomenclature for Annular Flow Equations Computer Program

ALGOL	TEXT	DEFINITION	UNITS
A	α	void fraction	dimensionless
A1	b_1	relation defined in equation (2.401)	ft/sec
A2	b_2	relation defined in equation (2.401)	ft/sec
A3	b_3	relation defined in equation (2.401)	ft/sec
AR	A	area	ft^2
COSO	cos θ	slope of the two-phase interface	dimensionless
D	D	pipe diameter	in
DDELTAH	$d(\Delta H/dT)$	derivative of enthalpy of vaporization	BTU/lb_m-°F
DDERO		change in initial slope of V_ℓ versus T curve	ft/sec °F
DELTAH	H	enthalpy of vaporization	BTU/lb_m
DERO	$(dV_\ell/dT)_{T_o}$	initial slope of V_ℓ versus T curve	ft/sec-°F
DFW	dF_w/dT	derivative of wall shear force	lb_f/°F
DHG	dH/dT	derivative of the enthalpy of the vapor	BTU/lb_m-°F
DHL	dh/dT	derivative of the enthalpy of the liquid	BTU/lb_m-°F
DP	dP/dT	derivative of the pressure	lb_f/in^2-°F
DPC	ΔP	total pressure drop	lb_f/in^2
DT	ΔT	interval	°F
DVEL	dV_ℓ/dT	derivative of liquid velocity	ft/sec-°F

DX	dx/dT	derivative of quality	lb_v/lb_t-°F
F	F	function as defined by equation (4.501)	ft/°F
FFACTOR	f	friction factor	dimensionless
HL	h	enthalpy of liquid	BTU/lb_m
INTEMP	T_o	inlet temperature	°F
LOD	L/D	length to diameter ratio	dimensionless
OUTEMP	T_e	outlet temperature	°F
P	P	pressure	lb_f/in^2
RE	Re	Reynolds number	dimensionless
RVEL	k	relative velocity factor	dimensionless
T	T	temperature	°F
VEG	V_g	velocity of vapor	ft/sec
VEGS	V_g^*	superficial vapor velocity	ft/sec
VEL	V_ℓ	velocity of liquid	ft/sec
VELM	$V_{\ell,max}$	maximum liquid velocity	ft/sec
VELS	V_ℓ^*	superficial liquid velocity	ft/sec
VEP	V_p	velocity of the interface	ft/sec
VG	v_g	specific volume of the vapor	ft^3/lb_m
VISL	μ_ℓ	viscosity of the liquid	centipoise$\cdot 10^{-1}$
VL	v_ℓ	specific volume of the liquid	ft^3/lb_m
W	W	mass flow rate	lb_m/sec
WOA	W/A	mass flow rate per unit area	lb_m/ft^2-sec
X	x	quality	lb_v/lb_t
Z	z	pipe length	ft

J as the last letter of one of the above variables indicates the evaluation of the variable to compute b_2 for equation (2.401).

K as the last letter of one of the above variable indicates the evaluation of the variable to compute b_3 for equation (2.401).

LOGIC STATEMENTS

EQL = equal to

GEQ $\geq$ greater than or equal to

GTR > greater than

LEQ $\leq$ less than or equal to

LSS < less than

BIBLIOGRAPHY

1. Barbet, E., "Evaporation in the Sugar Industry," Bulletin de L'Association des chimistes de Sucrerie et de Distillerie de France et des Colinies, 38, 111 (1914).

2. Bozeman, H. C., "Finding Multiphase Flow Answers," Oil and Gas Journal, 32, 133 (1961).

3. Isben, H. S., R. H. Moen, and D. R. Mosher, Two Phase Pressure Drops, Report No. AECU - 2994, U. S. Atomic Energy Commission, November, 1954.

4. Ward, H. C., M. J. Goglia, J. M. Spurlock, and T. L. Gossage, Performance of a JP-4 Aircraft Fuel System -- A Comparison of Analytic Predictions with Experimental Results for Two-Phase Flow, Wright Air Development Center, Report No. 55-422, part 3 (ASTIA Document No. AD - 130, 905) March, 1957.

5. Gresham, W. A., P. A. Foster, and R. J. Kyle, Review of the Literature on Two-Phase (Gas-Liquid) Fluid Flow in Pipes, WADC Report No. 55 - 422, part 1 (ASTIA Document No. AD - 95,752) June, 1955.

6. Ward, H. C., J. E. Rhodes, W. T. Ziegler, and L. W. Ross, Analytical Investigation of Two-Phase Vapor-Liquid Ratio Measuring Systems and Two-Phase Flow Literature Survey Supplement, WADC Report No. 59 - 230, August, 1959.

7. Bennett, J. A. R., Two-Phase Flow in Gas-Liquid Systems: A Literature Survey, Atomic Energy Research Establishment Report No. AERE CERI - 2497, March, 1958.

8. Charvonia, D. A., Review of the Published Literature Pertaining to the Annular, Two-Phase Flow of Liquid and Gaseous Media in a Pipe, Armed Services Technical Information Agency Document AD - 208,040: Project Squid Technical Report PUR - 32 - R, December, 1958.

9. Rodabaugh, Rowena, Two-Phase Flow and Acoustic Phenomena in Gases and Liquids: Literature Search No. 177, Jet Propulsion Laboratory, California Institute of Technology, June, 1960.

10. Jens, W. H. and G. Leppert, "Recent Developments in Boiling Research," Journal of the American Society of Naval Engineers, 67, 137, 437 (1955).

11. Shell Pipeline Company, Two-Phase Flow Literature, Unpublished report.

12. Ambrose, W. T., Literature Survey of Flow Patterns Associated with Two-Phase Flow, Report No. HW - 52, 927, U. S. Atomic Energy Commission, October 8, 1957.

13. Martinelli, R. C. and D. B. Nelson, "Predictions of Pressure Drop During Forced Circulation Boiling of Water," Transactions of the American Society of Mechanical Engineers, 70, 695 (1948).

14. Benjamin, M. W., and J. G. Miller, "Flow of Flashing Mixture of Water and Steam Through Pipes," Transactions of the American Society of Mechanical Engineers, 64, 657 (1942).

15. Lockhart, R. W., and R. C. Martinelli, "Proposed Correlation of Data for Isothermal Two-Phase Two-Component Flow in Pipes," Chemical Engineering Progress, 45, No. 1, 39-48 (1949).

16. Davis, W. J., "The Effect of the Froude Number in Estimating Vertical Two-Phase Gas-Liquid Friction Losses," paper presented at the Forty-Sixth National Meeting of American Institute of Chemical Engineers, February 4-7, 1961.

17. Hatch, M. R., and R. B. Jacobs, "Prediction of Pressure Drop in Two-Phase Single-Component Fluid Flow," Journal of the American Institute of Chemical Engineers, 8, No. 1, 18-25 (1962).

18. Buthod, A. P., "Thermodynamics of Two-Phase Flow in Furnace Tubes and Transfer Lines," paper presented at the Fifty-Fourth Annual Meeting of American Institute of Chemical Engineers, Dec. 2-7, 1961.

19. Bottomley, W. T., "Flow of Boiling Water Through Orifices and Pipes," Transactions of the North East Coast Institute of Engineers and Shipbuilders, 53, 65-100 (1936-1937).

20. Dusinberre, G. M., Discussion of "The Flow of a Flashing Mixture of Water and Steam through Pipes," by M. W. Benjamin and J. G. Miller, Transactions of the American Society of Mechanical Engineers, 64, 666 (1942).

21. Bridge, T. E., "How to Design the Piping for Conveying Flashing Hot Water," Heating, Piping and Air Conditioning, 21, 69, 92, 98 (Mar., Apr., May, 1949).

22. Allen, W. F., Jr., "Flow of Flashing Mixture of Water and Steam Through Pipes and Valves," Transactions of the American Society of Mechanical Engineers, 73, 257 - 265 (April, 1951).

23. Bergelin, O. P., et al., "Co-current Gas-Liquid Flow II, Flow in Vertical Tubes," Heat Transfer and Fluid Mechanics Institute, Berkeley, California meeting (published by the American Society of Mechanical Engineers), 19 - 28 (1949).

24. Davidson, W. F., et al., "Studies of Heat Transmission Through Boiler Tubing at Pressures from 500 to 3300 pounds," Transactions of the American Society of Mechanical Engineers, 65, 553-591 (1943).

25. Schneider, F. N., P. D. White, and R. L. Huntington, "Horizontal Two-Phase Oil and Gas Flow," Pipe Line Industry, (October, 1954).

26. Isben, op. cit., p. 76.

27. Linning, D. L., The Adiabatic Flow of Evaporating Fluids in Pipes, University of Glasgow, Scotland, Ph. D. Thesis (1951).

28. Bolstad, M. M. and R. C. Jordan, "Theory and Use of the Capillary Tube Expansion Device," Refrigeration Engineering, 56, 519 (1948).

29. Burnell, J. G., "Flow of Boiling Water Through Nozzles, Orifices, and Pipes," Engineering, 164, 572 (1947).

30. Martinelli, R. C., M. K. Boelter, et al., "Isothermal Pressure Drop for Two-Phase Two-Component Flow in a Horizontal Pipe," Transactions of the American Society of Mechanical Engineers, 66, 139 - 51 (1944).

31. Glovier, G. W., and M. M. Omer, "The Horizontal Pipeline Flow of Air-Water Mixtures," paper presented at the Joint Chemical Engineering Congress, Cleveland, Ohio (May 7-10, 1961).

32. Krasiakova, L. U., "Some Characteristics of Movements of Two-Phase Mixtures in Horizontal Pipe," Zhurnal Technicheskoi Fiziki, 22 No. 4, 656 (1952).

33. Johnson, G. E., III, Evaluation of the Concentration Method for Determining the V/L Ratio in Two-Phase Fluid Flow, Georgia Institute of Technology, M. S. Thesis (1961).

34. Dengler, C. E., and J. N. Addoms, "Heat Transfer Mechanism for Vaporization of Water in a Vertical Tube," Chemical Engineering Symposium Series: "Heat Transfer - Louisville," 52, No. 18, 95 (1956).

35. Isben, H. S., N. C. Sher, and K. C. Eddy, "Void Fractions in Two-Phase Steam-Water Flow," Journal of the American Institute of Chemical Engineers, 3, 136 (1957).

36. Isben, H. S., et al., "Void Fractions in Two-Phase Flow," Journal of American Institute of Chemical Engineers, 5, 427 (1959).

37. Marchaterre, J. F., The Effect of Pressure on Boiling Density in Multiple Rectangular Channels, Michigan College of Mining and Technology, M. S. Thesis, (AEC Report ANL - 5522) Feb. 1956.

38. Richardson, B. L., Some Problems in Horizontal Two-Phase Two-Component Flow, Report No. ANL - 5949, U. S. Atomic Energy Commission, Dec. 1958.

39. Cook, W. H., Boiling Density in Vertical Rectangular Multichannel Sections with Natural Circulation, Illinois Institute of Technology Ph. D. Thesis (AEC Report No. ANL - 5621) 1956.

40. Hooker, H. H., and G. F. Popper, A Gamma-Ray Attenuation Method for Void Fraction Determination in Experimental Boiling Heat Transfer Test Facilities, Report No. ANL - 5766, U. S. Atomic Energy Commission, Nov. 1958.

41. Petrick, M., Two-Phase Air-Water Flow Phenomena, Report No. ANL - 5787, U. S. Atomic Energy Commission, March 1958.

42. Schwartz, K., "Investigation of the Density Distribution, Water and Steam Velocities as Well as the Pressure Loss in Vertical and Horizontal Upflow Boiler Tubes," Report No. AEC - tr - 2314, U. S. Atomic Energy Commission (1954).

43. Zmola, P. C., and R. V. Bailey, "Power Removal from Boiling Nuclear Reactors," Transactions of the American Society of Mechanical Engineers, 78, 881 - 92 (1956).

44. Shapiro, A. H., The Dynamics and Thermodynamics of Compressible Fluid Flow, New York: The Ronald Press Company, 1953, p. 47.

45. Karplus, H. B., Acoustic Properties of Steam as a Measure of Droplet Content, Report No. AECU - 4123, U. S. Atomic Energy Commission, Nov. 1959.

46. Isben, H. S., J. E. Moy, and A. J. R. Da Cruz, "Two-Phase, Steam-Water Critical Flow," Journal of the American Institute of Chemical Engineers, 3, No. 3, 361 (1957).

47. Waters, E. D., Methods for Investigating Critical Discharge Phenomena with Saturated Water, Report No. HW - 56, 964, U. S. Atomic Energy Commission, August 29, 1958.

48. Harvey, B. F., and A. S. Foust, "Two-Phase One-Dimensional Flow Equations and Their Application to Flow in Evaporator Tubes," Chemical Engineering Progress Symposium Series: Heat Transfer-Atlantic City, 49, No. 5, 91 (1953).

49. Schweppe, J. L., and A. S. Foust, "Effect of Forced Circulation Rate on Boiling - Heat Transfer in a Short Vertical Tube," Chemical Engineering Program Symposium Series: Heat Transfer - Atlantic City, 49, No. 5, 77 (1953).

50. Stein, R. P., et al., "Pressure Drop and Heat Transfer to Nonboiling and Boiling Water in Turbulent Flow in an Internally Heated Annulus," Chemical Engineering Progress Symposium Series: Nuclear Engineering, Part I, 50, No. 11, 115, (1954).

51. Steitz, W. G., "The Critical and Two-Phase Flow of Steam," Journal of Engineering for Power, Transactions of the American Society of Mechanical Engineers, 3, 145 (April, 1961).

52. Keenan, J. H., and F. G. Keyes, Thermodynamic Properties of Steam, New York: John Wiley and Sons, Inc., (1956).

53. Bennett, J. A. R., op. cit., p. 20.

54. Shapiro, A. H., op. cit., p. 17

55. Ibid., p. 26.

56. Ibid., p. 39.

57. Jensen, A. P., and R. M. Price, Jr., Least Square Polynomial Curve Fitting PL05, a pamphlet from the Rich Electronic Computer Center, Georgia Institute of Technology, Atlanta, Georgia, April 14, 1958.

58. Kuntz, K. S., Numerical Analysis, New York: McGraw Hill Book Company, Inc., 1957, Chapter 7.

59. International Critical Tables, New York: McGraw Hill Book Company Inc., 1929, 5, p. 10.

60. McCabe, W. L., and J. C. Smith, Unit Operations of Chemical Engineering, New York: McGraw Hill Book Company, Inc., 1956, p. 67.

61. Kuntz, K. S., op. cit., p. 146.

62. Ibid., p. 183.

63. A Reference Manual: Burroughs Algebraic Compiler, Burroughs Corporation, Detroit 32, Michigan.

64. Marchaterre, J. F., Personal Communication.

65. Semat, Henry, Introduction to Atomic and Nuclear Physics, New York: Rinehart and Company, Inc., 1956, p. 135.

66. Grodstein, G. W., X-ray Attenuation Coefficients from 10 Kev to 100 Mev, National Bureau of Standards Circular-583, U. S. Department of Commerce (1957), p. 21.

67. Clark, G. L., Applied X-Rays, New York: McGraw Hill Book Company, Inc., 1955, p. 164.

68. Grodstein, G. W., op. cit., p. 32.

69. Operation and Maintenance Manual: Model 1620 Analytical Count-Rate Meter, Nuclear Chicago Corporation, 223 West Erie Street, Chicago 10, Illinois, March 1955.

70. Ibid., p. 16.

71. Kuyper, A. C., "The Statistics of Radioactive Measurement," Journal of Chemical Education 36, 128 (1959).

72. Houghton, Gerald, "An Analysis of Vapor Void Profiles in Heated Channels," Nuclear Science and Engineering, 12, 390-397 (1962).

73. Anderson, G. H., G. G. Haselden, and B. G. Mantzouranis, "Two-Phase (Gas-Liquid) Flow Phenomena - III: The Calculation of Heat Transfer in a Vertical Long - Tube Evaporator," Chemical Engineering Science, 16, 222 - 230 (1961).

74. McCabe, N. L. and J. C. Smith, op. cit., p. 441.

75. McManus, H. N., Jr., "An Experimental Investigation of Liquid Distribution and Surface Character in Horizontal Annular Two-Phase Flow," OOR Project No. 2117, Contract DA-30-115-992, (Sibley School of Mechanical Engineering, Cornell University) October, 1959.

VITA

Ralph Webster Pike, Jr. was born in Tampa, Florida, on November 10, 1935. He attended elementary schools in Miami, Florida, and secondary schools in Orlando, Florida, graduating from Wm. R. Boone High School in June, 1953. He attended Orlando Junior College, Orlando, Florida, and graduated from the Georgia Institute of Technology, Atlanta, Georgia, in June, 1958 with a B. Ch. E. degree.

He has been employed in the summer by the following companies while an undergraduate and graduate student: American Viscose Corporation, Marcus Hook, Pennsylvania; Humble Oil and Refining Company, Houston, Texas; Swift and Company, Bartow, Florida; and Georgia Institute of Technology, Atlanta, Georgia.

He is a member of Sigma Xi and Tau Beta Pi honorary fraternities and Pi Kappa Alpha social fraternity. He was the recipient of the Dow Chemical Company Fellowship for the academic years 1959-1960 and 1960-1961. He holds the rank of Second Lieutenant in the United States Army Reserve.

In August, 1958, he married the former Patricia Layne Jennings of Orlando, Florida.